AD-A152 118 THE EFFECT OF LOAD FACTOR ON AIRCRAFT HANDLING QUALITIES(U) AIR FORCE INST OF TECH WRIGHT-PATTERSON AFB OH SCHOOL OF ENGINEERING J R RIEMER 10 AUG 84 1/4

UNCLASSIFIED AFIT/GAE/AA/84J-2 F/G 20/4 NL

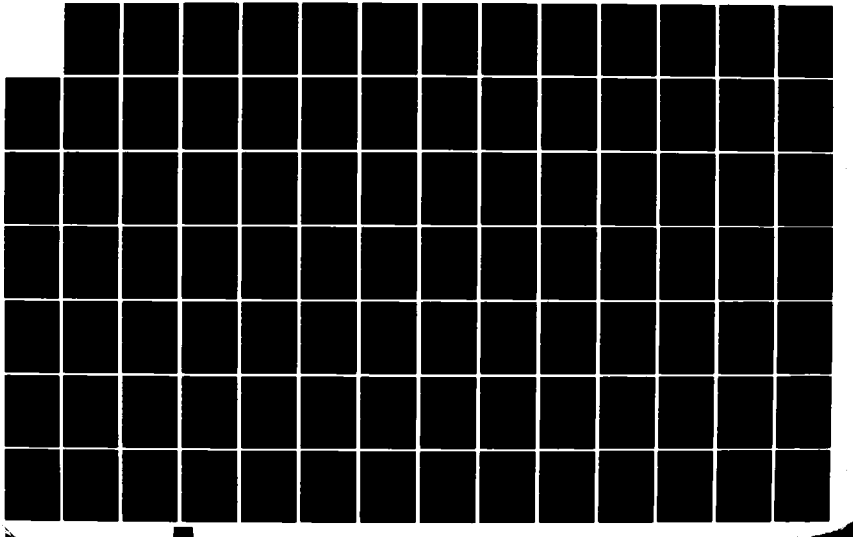

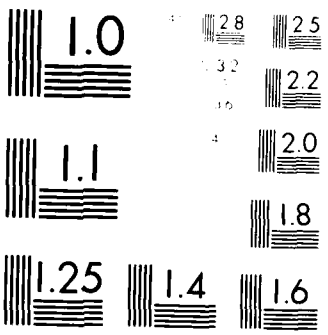
1.0
2.8
2.5
3.2
2.2
1.1
2.0
1.8
1.25
1.4
1.6

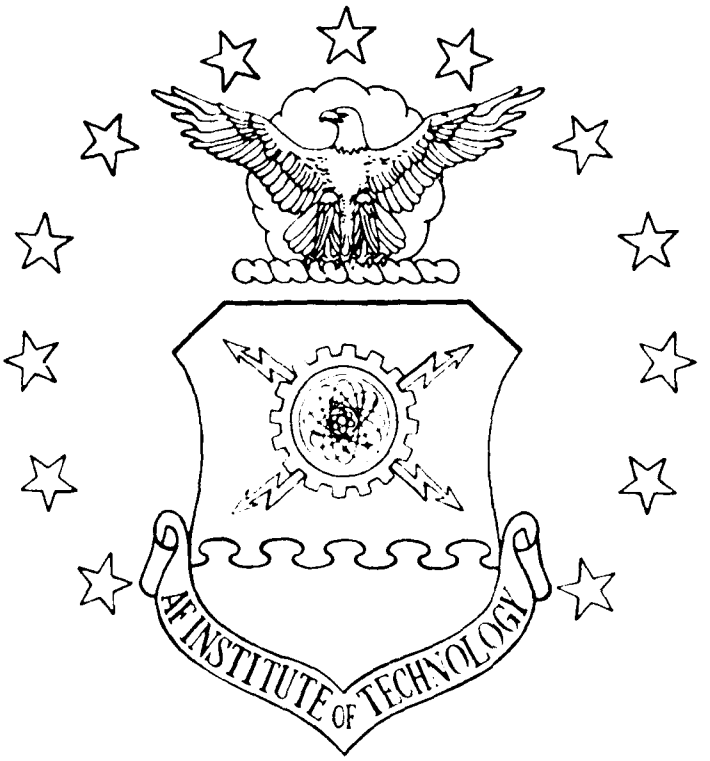

THE EFFECT OF LOAD FACTOR ON AIRCRAFT HANDLING QUALITIES

THESIS

AFIT/GAE/AA/84J-2 JEFFREY R. RIEMER
CAPT USAF

DEPARTMENT OF THE AIR FORCE
AIR UNIVERSITY
AIR FORCE INSTITUTE OF TECHNOLOGY

Wright-Patterson Air Force Base, Ohio

AFIT/GAE/AA/84J-2

THE EFFECT OF LOAD FACTOR ON AIRCRAFT HANDLING QUALITIES

THESIS

AFIT/GAE/AA/84J-2 JEFFREY R. RIEMER
CAPT USAF

UNCLASSIFIED

SECURITY CLASSIFICATION OF THIS PAGE

REPORT DOCUMENTATION PAGE

1a REPORT SECURITY CLASSIFICATION UNCLASSIFIED	1b RESTRICTIVE MARKINGS None
2a SECURITY CLASSIFICATION AUTHORITY	3 DISTRIBUTION/AVAILABILITY OF REPORT Unlimited
2b DECLASSIFICATION/DOWNGRADING SCHEDULE	
4 PERFORMING ORGANIZATION REPORT NUMBER(S) AFIT/GAE/AA/84D-2	5 MONITORING ORGANIZATION REPORT NUMBER(S)
6a NAME OF PERFORMING ORGANIZATION Air Force Institute of Technology	6b OFFICE SYMBOL (If applicable) ENY	7a NAME OF MONITORING ORGANIZATION
6c ADDRESS (City, State and ZIP Code) Wright-Patterson AFB Dayton, Ohio 45433		7b ADDRESS (City, State and ZIP Code)
8a NAME OF FUNDING/SPONSORING ORGANIZATION USAF Test Pilot School	8b OFFICE SYMBOL (If applicable) TENC	9 PROCUREMENT INSTRUMENT IDENTIFICATION NUMBER
8c ADDRESS (City, State and ZIP Code) USAFTPS/TENC, Stop 209 Edwards AFB CA 93523-5000		10 SOURCE OF FUNDING NOS PROGRAM ELEMENT NO / PROJECT NO / TASK NO / WORK UNIT NO
11 TITLE (Include Security Classification) The Effect of Load Factor on Aircraft Handling Qualities		
12 PERSONAL AUTHOR(S) Capt Jeffrey R. Riemer		
13a TYPE OF REPORT MS - Thesis	13b TIME COVERED FROM Jun 82 TO Aug 84	14 DATE OF REPORT (Yr, Mo, Day) 84 Aug 10	15 PAGE COUNT 370
16 SUPPLEMENTARY NOTATION Prepared in conjunction with the Joint AFIT/TPS Program		
17 COSATI CODES FIELD / GROUP / SUB GR	18 SUBJECT TERMS (Continue on reverse if necessary and identify by block number) Handling Qualities, Simulation, Load Factor, A-7D, Equations of Motion, Flight Test, Flight Controls	

19 ABSTRACT (Continue on reverse if necessary and identify by block number)

This report documents the results of a limited simulation and flight test of the A-7D to determine the effect of load factor on aircraft handling qualities. The test condition was 15,000 feet indicated pressure altitude, 0.6 indicated Mach number, at load factors ranging from 1 to 3G's for the mechanical and fully augmented flight control configurations. The equations of motion were developed to include turning flight. The equations were linearized and put into first order form $\dot{x} = A\bar{x} + B\bar{u}$. Eigenvalues/eigenvectors, Argand diagrams, Bode plots, and time histories were used to predict the effect of load factor on aircraft handling qualities with respect to MIL-F-8785C. Linear systems analysis was useful in predicting aircraft response for ballet and impulse inputs. As load factor increased the longitudinal and lateral modes became kinematically coupled. Load factor destabilized the phugoid mode. Load factor had little effect on short period dynamics, but caused the parameter n/α to increase. The fully augmented aircraft resulted in the flying qualities degrading from level one to level two. The dutch roll mode [illegible] improved with an (illegible)

20 DISTRIBUTION/AVAILABILITY OF ABSTRACT UNCLASSIFIED/UNLIMITED [X] SAME AS RPT [ ] DTIC USERS [ ]	21 ABSTRACT SECURITY CLASSIFICATION UNCLASSIFIED
22a NAME OF RESPONSIBLE INDIVIDUAL Captain Jeffrey R. Riemer	22b TELEPHONE NUMBER (Include Area Code) 805-277-2434	22c OFFICE SYMBOL USAFTPS/TENC

DD FORM 1473, 83 APR EDITION OF 1 JAN 73 IS OBSOLETE

SECURITY CLASSIFICATION OF THIS PAGE

19. (Continued)

AFIT/GAE/AA/84J-2

THE EFFECT OF LOAD FACTOR ON AIRCRAFT HANDLING QUALITIES

THESIS

Presented to the Faculty of the School of Engineering

of the Air Force Institute of Technology

Air University

In Partial Fulfillment of the

Requirements for the Degree of

Master of Science

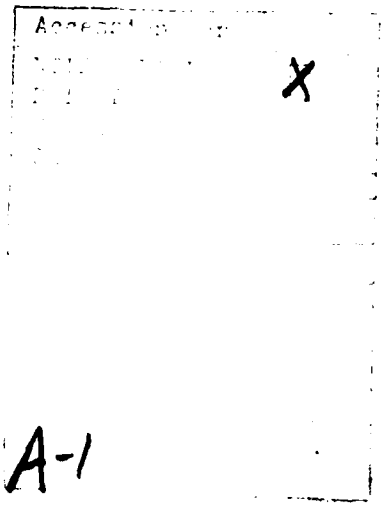

by

Jeffrey R. Riemer

CAPT USAF

Graduate Aeronautical Engineering

August 1984

Table of Contents

List of Figures

List of Tables

Preface

This thesis addresses the subject of loaded flying qualities. The effect of load factor on the various response modes is analyzed using linear systems analysis, and flight test was used to verify and supplement the analysis.

The work on this thesis was accomplished through the Joint Air Force Institute of Technology/Test Pilot School (AFIT/TPS) Program. The AFIT portion provided the theoretical background for the analysis, and the TPS portion tied the theoretical knowledge to practical application in the form of flight test.

I wish to express my gratitude to my thesis advisors Dr. Robert A. Calico and Major (Dr.) James T. Silverthorn, whose guidance and patience were invaluable. Thanks is also given to the Air Force Test Pilot School for sponsoring the project, and to my typist Mrs Pam Staley for typing all these equations and symbols. Most of all I want to thank my wife, Denise, and son, Richard, for their support and understanding which made the completion of this program possible.

Jeffrey R. Riemer

Symbol	Description	Units
[illegible]	[illegible]	[illegible]
A	system plant matrix	--
A_x	$m\cos\alpha_e\cos\beta_e$	slug
A_x'	$A_x - (C_x/C_y)A_y$	slug
A_y	$m\sin\beta_e$	slug
A_z	$m\sin\alpha_e\cos\beta_e$	slug
A_z'	$A_z - (C_z/C_y)A_y$	slug
AFIT	Air Force Institute of Technology	--
b	wing span	ft
B_x	$-mV_e\sin\alpha_e\cos\beta_e - X_{\dot{\alpha}}$	lb-sec
B_z	$mV_e\cos\alpha_e\cos\beta_e + Z_{\dot{\alpha}}$	lb-sec
c	wing chord or chord of an airfoil	ft
$\bar{c}$	length of the mac	ft
C	side force	lb
C_D	airplane total drag coefficient	dimensionless
C_{D_V}	$V_e\partial C_D/\partial V$	dimensionless
C_{D_α}	$\partial C_D/\partial\alpha$	per rad
$C_{D_{\delta_e}}$	$\partial C_D/\partial\delta_e$	per rad
C_ℓ	rolling moment coefficient	dimensionless
C_{ℓ_p}	$\frac{2V}{b}(\partial C_\ell/\partial p)$	per rad

C_{ℓ_β}	$\partial C_\ell / \partial \beta$	per rad
$C_{\ell_{\delta_a}}$	$\partial C_\ell / \partial \delta_a$	per rad
$C_{\ell_{\delta_r}}$	$\partial C_\ell / \partial \delta_r$	per rad
C_L	airplane lift coefficient	dimensionless
C_{L_q}	$\frac{2V_e}{\bar{c}} (\partial C_L / \partial q)$	per rad
C_{L_V}	$V_e \partial C_L / \partial V$	dimensionless
C_{L_α}	$\partial C_L / \partial \alpha$	per rad
$C_{L_{\dot{\alpha}}}$	$\frac{2V_e}{\bar{c}} \partial C_L / \partial \alpha$	per rad
$C_{L_{\delta_e}}$	$\partial C_L / \partial \delta_e$	per rad
C_m	pitching moment coefficient	dimensionless
C_{m_q}	$\frac{2V_e}{\bar{c}} (\partial C_m / \partial q)$	per rad
C_{m_V}	$V_e (\partial C_m / \partial V)$	dimensionless
C_{m_α}	$\partial C_m / \partial \alpha$	per rad
$C_{m_{\dot{\alpha}}}$	$\frac{2V_e}{\bar{c}} \partial C_m / \partial \alpha$	per rad

Abbreviation or Symbol	Definition	Units
$C_{m_{\delta_e}}$	$\partial C_m/\partial \delta_e$	per rad
C_n	yawing moment coefficient	dimensionless
C_{n_p}	$\frac{2V_e}{b}(\partial C_n/\partial p)$	per rad
C_{n_r}	$\frac{\partial V_e}{b}(\partial C_n/\partial r)$	per rad
C_{n_β}	$\partial C_n/\partial \beta$	per rad
$C_{n_{\delta_a}}$	$\partial C_n/\partial \delta_a$	per rad
$C_{n_{\delta_r}}$	$\partial C_n/\partial \delta_r$	per rad
C_T	thrust coefficient	dimensionless
C_{T_V}	$V_e \partial C_T/\partial V$	dimensionless
C_X	$mV_e \cos\alpha_e \cos\beta_e$	lb-sec
C_Y	$mV_e \cos\beta_e$	lb-sec
C_y	side force coefficient	dimensionless
C_{y_p}	$\frac{2V_e}{b}(\partial C_Y/\partial p)$	per rad
C_{y_r}	$\frac{2V_e}{b}(\partial C_{y/\mu r})$	per rad
$C_{y\beta}$	$\partial C_y/\partial \beta$	per rad
$C_{y_{\delta_a}}$	$\partial C_y/\partial \delta_a$	per rad

Abbreviation or Symbol	Definition	Units
$C_{Y_{\delta_r}}$	$\partial C_Y/\partial \delta_r$	per rad
C_Z	$-mV_e \sin\alpha_e \sin\beta_e$	lb-sec
cg	center of gravity	pct MAC
D	drag	lb
D_e	equilibrium drag	lb
D_V	$1/2\ \rho V_e S\ (2C_D + V\partial C_{D/\partial V})$	slug/sec
D_X	$X_V - mq_e \sin\alpha_e \cos\beta_e + mr_e \sin\beta_e$	slug/sec
$D_{X'}$	$D_X - (C_X/C_Y)D_Y$	slug/sec
$D_{X''}$	$(B_Z/(A_{X'}B_Z - A_{Z'}B_X))(D_{X'} - (B_X/B_Z)D_{Z'})$	1/sec
D_Y	$-mr_e \cos\alpha_e \cos\beta_e + mp_e \sin\alpha_e \cos\beta_e$	slug/sec
D_Z	$Z_V - mp_e \sin\beta_e + mq_e \cos\alpha_e \cos\beta_e$	slug/sec
$D_{Z'}$	$D_Z - (C_Z/C_Y)D_Y$	slug/sec
$D_{Z''}$	$(A_{X'}/(B_Z A_{X'} - B_X A_{Z'}))(D_{Z'} - (A_{Z'}/A_{X'})D_{X'})$	slug/lb-sec^2
D_α	$\partial D/\partial \alpha$	lb
D_{δ_e}	$1/2\ \rho V_e^2 S C_{D\delta_e}$	lb
d/dt or .	time rate of change	--
E_X	$X_\alpha - mq_e V_e \cos\alpha_e \cos\beta_e$	lb
$E_{X'}$	$E_X - (C_X/C_Y)E_Y$	lb
$E_{X''}$	$(B_Z/(A_{Z'}B_Z - A_{Z'}B_X))(E_{X'} - (B_X/B_Z)E_{Z'})$	ft/sec^2
E_Y	$mr_e V_e \sin\alpha_e \cos\beta_e + mp_e V_e \cos\alpha_e \cos\beta_e$	lb

Abbreviation or Symbol	Definition	Units
E_Z	$Z_\alpha - mq_e V_e \sin\alpha_e \cos\beta_e$	lb
$E_{Z'}$	$E_Z - (C_Z/C_Y)E_Y$	lb
$E_{Z''}$	$(A_{X'}/(B_Z A_{X'} - B_X A_{Z'}))(E_{Z'} - (A_{Z'}/A_{X'})E_{X'})$	1/sec
f_1, f_2, f_3	coordinate axes	--
$\bar{F}$	force vector	lb
$\bar{F}_A$	aerodynamic force vector	lb
F_{AX}, F_{AY}, F_{AZ}	aerodynamic force components	lb
F_{AX_B}	aerodynamic force component in the X direction written in the body axes reference frame	lb
F_B	body axes reference frame	--
F_E	earth fixed reference frame	--
F_{EC}	earth centered reference frame	--
F_g	intermediate reference frame	--
$\bar{F}_G$	gravitational force vector	lb
F_h	intermediate reference frame	--
F_{GX}, F_{GY}, F_{GZ}	gravitational force components	--
F_I	inertial reference frame	--
F_S	stability axes reference frame	--
$\bar{F}_T$	thrust force vector	lb
F_{TX}, F_{TY}, F_{TZ}	thrust force components	lb
F_V	vehicle carried reference frame	--

Abbreviation or Symbol	Definition	Units
F_W	wind reference frame	--
F_x	intermediate reference frame	--
F_X	$X_q - mV_e \sin\alpha_e \cos\beta_e$	slug ft/sec
$F_{X'}$	$(B_Z/(A_X B_Z - A_Z B_X))(F_X - (B_X/B_Z)F_Z)$	ft/sec
g	acceleration due to gravity	32.17405 ft/sec^2
GW	gross weight	lb
G_X	$-mg\cos\theta_e$	lb
$G_{X'}$	$G_X - (C_X/C_Y)G_Y$	lb
$G_{X''}$	$(B_Z/(A_X B_Z - A_Z B_X)(G_{X'} - (B_X/B_Z)G_{Z'})$	ft/sec^2
G_Y	$-mg\sin\Phi_e \sin\theta_e$	lb
G_Z	$-mg\cos\Phi_e \sin\theta_e$	lb
$G_{Z'}$	$G_Z - (C_Z/C_Y)G_Y$	lb
$G_{Z''}$	$(A_{X'}/(B_Z A_{X'} - B_X A_{Z'}))(G_{Z'} - (A_{Z'}/A_{X'})G_{X'})$	1/sec
$\bar{H}$	angular momentum vector	slug-ft^2/sec
H_c	pressure altitude	ft
H_X	$mq_e V_e \sin\alpha_e \sin\beta_e + mr_e V_e \cos\beta_e$	lb
$H_{X'}$	$H_X - (C_X/C_Y)H_Y$	lb
$H_{X''}$	$(B_Z/(A_X B_Z - A_Z B_X)(H_{X'} - (B_X/B_Z)H_{Z'})$	ft/sec^2
H_Y	$Y_\beta + mr_e V_e \cos\alpha_e \sin\beta_e - mp_e V_e \sin\alpha_e \sin\beta_e$	lb
H_Z	$-mp_e V_e \cos\beta_e - mq_e V_e \cos\alpha_e \sin\beta_e$	lb
$H_{Z'}$	$H_Z - (C_Z/C_Y)H_Y$	lb

Abbreviation or Symbol	Definition	Units
$H_{Z''}$	$(A_{X'}/(B_Z A_{X'} - B_X A_{Z'}))(H_{Z'} - (A_{Z'}/A_{X'})H_{X'})$	per sec
IMN	indicated mach number	--
I_X, I_Y, I_Z	moments of inertia	slug-ft^2
I_{XX}, I_{YY}, I_{ZZ}	moments of inertia	slug-ft^2
I_{XY}, I_{XZ}, I_{YZ}	products of inertia	slug-ft^2
I1	$I_X I_Z - I_{ZX}^2$	slug^2-ft^4
I2	$(I_Z(I_Y - I_Z) - I_{ZX}^2)/I1$	dimensionless
I3	$(I_{ZX} I_Z + I_{ZX}(I_X - I_Y)/I1$	dimensionless
I4	$(I_X(I_X - I_Y) + I_{ZX}^2)/I1$	dimensionless
I5	$(I_{ZX}(I_Y - I_Z) - I_{ZX} I_X)/I1$	dimensionless
J_Y	$Y_p + mV_e \sin\alpha_e \cos\beta_e$	lb-sec
K_{ARI}	aileron rudder interconnect gain	--
K_T	trim constant	rad/inch
K_X	$mV_e \sin\beta_e$	slug-ft/sec
$K_{X'}$	$K_X - (C_X/C_Y)K_Y$	slug-ft/sec
$K_{X''}$	$(B_Z/(A_{X'} B_Z - A_{Z'} B_X))(K_{X'} - (B_X/B_Z)K_{Z'})$	ft/sec
K_Y	$Y_r - mV_e \cos\alpha_e \cos\beta_e$	slug-ft/sec
$K_{Z'}$	$-(C_Z/C_Y)K_Y$	slug-ft/sec
$K_{Z''}$	$(A_{X'}/(B_Z A_{X'} - B_X A_{Z'}))(K_{Z'} - (A_{Z'}/A_{X'})K_{X'})$	dimensionless
KCAS	knots calibrated airspeed	--
KIAS	knots indicated airspeed	--

[illegible]	[illegible]	[illegible]
[illegible]	[illegible]	
[illegible]	[illegible]	
L	airplane lift	lb
L	rolling moment	ft-lb
L_e	equilibrium airplane lift	lb
L_{fW}	transformation matrix from F_W to F_f reference frame	--
L_{gr}	transformation matrix from F_Y to F_g reference frame	--
L_{hg}	transformation matrix from F_g to F_h reference frame	--
L_p	$1/4\ \rho V_e S b^2 C_{\ell_p}$	ft^2 slug/sec
$I_{p'}$	$(L_p I_Z + N_p I_{ZX})/II$	1/sec
L_q	$1/4\ \rho V_e S \bar{c} C_{\ell_q}$	slug-ft/sec
L_r	$1/4\ \rho V_e S b^2 C_{\ell_r}$	ft^2-slug/sec
$L_{r'}$	$(L_r I_Z + N_r I_{ZX})/II$	1/sec
L_V	$1/2\ \rho V_e S(2C_L + VbC_{L_{\dot{\alpha}}}/2V)$	[illegible]
L_α	$1/2\ \rho V_e^2 S C_{L_\alpha}$	lb
$L_{\dot{\alpha}}$	$1/4\ \rho V_e S c C_{L_{\dot{\alpha}}}$	slug-ft/sec
L_β	$1/2\ \rho V_e^2 S b C_{\ell_\beta}$	ft-lb
$L_{\beta'}$	$(L_\beta I_Z + N_\beta I_{XZ})/I$	1/sec^2
[illegible]	[illegible]	ft-lb

Abbreviation or Symbol	Definition	Units
$I_{\delta a'}$	$(I_{\delta a} I_Z + N_{\delta a} I_{ZX})/II$	$1/sec^2$
$I_{\delta e}$	$1/2\ \rho V_e^2 SC_{I_{\delta e}}$	lb
$I_{\delta r}$	$1/2\ \rho V_e^2 SbC_{\ell_{\delta r}}$	ft-lb
$I_{\delta r'}$	$(I_{\delta r} I_Z + N_{\delta r} I_{ZX})/II$	$1/sec^2$
I_{Bf}	transformation matrix from F_f to F_B reference frame	--
I_{BW}	transformation matrix from F_W to F_B reference frame	--
I_{BV}	transformation matrix from F_V to F_B reference frame	--
I_E	leading edge	--
I_{EEC}	transformation matrix from F_{EC} to F_E reference frame	--
I_{EX}	transformation matrix from F_X to F_E reference frame	--
I_{VEC}	transformation matrix from F_{EC} to F_V reference frame	--
I_{wh}	transformation matrix from F_h to F_w reference frame	--
I_{wv}	transformation matrix from F_v to F_w reference frame	--
I_{XEC}	transformation matrix from F_{EC} to F_X reference frame	--
m	mass	slugs
M	flight or free stream Mach number	dimensionless
M	pitching moment	ft-lb
M_q	$1/4\ \rho V_e S\bar{c}^2 C_{m_q}$	slug-ft^2/sec
$M_{\dot{\alpha}}$	$1/2\ \rho V_e S\bar{c}^2 (2C_{m_{\dot{\alpha}}} + C_{m_{\delta V}})$	slug ft/sec

[illegible]	[illegible]	[illegible]
$M_{\dot{\alpha}}$	[illegible]	[illegible]
$M_{\dot{\beta}}$	[illegible] $C_{m_{\dot{\alpha}}}$	[illegible]
$M_{\delta e}$	$1/2\ \rho V_e^2 S\bar{c} C_{\delta e}$	ft-lb
$M_{\delta T}$	$1/2\ \rho V_e^2 S\bar{c} C_{m_{\delta T}}$	ft-lb
MAC	mean aerodynamic chord	ft
MGC	mean geometric chord	ft
MIL	military	--
MIL SPEC	military specification	--
n	load factor, g's	dimensionless
N	yawing moment	ft-lb
N_e	equilibrium yawing moment	ft-lb
N_P	$1/4\ \rho V_e S b^2 C_{n_p}$	ft^2-slug/sec
$N_{P'}$	$(N_P I_X + L_P I_{ZX})/I1$	$1/sec^2$
N_r	$1/4\ \rho V_e S b^2 C_{n_r}$	ft^2-slug/sec
$N_{r'}$	$(N_r I_X + L_r I_{ZX})/I1$	$1/sec^2$
N_β	$1/2\ \rho V_e^2 S b C_{n_\beta}$	ft-lb
$N_{\beta'}$	$(N_\beta I_X + L_\beta I_{ZX})/I1$	$1/sec^2$
$N_{\delta a}$	$1/2\ \rho V_e^2 S b C_{n_{\delta a}}$	ft-lb
$N_{\delta a'}$	$(N_{\delta a} I_X + L_{\delta a} I_{ZX})/I1$	$1/sec^2$
$N_{\delta r}$	$1/2\ \rho V_e^2 S b C_{n_{\delta r}}$	ft-lb

Abbreviation or Symbol	Definition	Units
$N_{\delta r}'$	$(N_{\delta r} I_X + L_{\delta r} I_{ZX})/11$	$1/sec^2$
NM	nautical miles	--
p	roll rate (body axes)	rad/sec
P_e	equilibrium roll rate	rad/sec
P_w	roll rate (wind axes)	rad/sec
P	linear momentum	slug-ft/sec
pct	percent	--
q	pitch rate (body axes)	rad/sec
q_e	equilibrium pitch rate	rad/sec
q_w	pitch rate (wind axes)	rad/sec
$\bar{q}$	dynamic pressure $(1/2\ \rho V_e^2)$	lb/ft^2
Q_X'	$-(C_X/C_Y)Q_Y$	lb
Q_X''	$(B_Z/(A_X'B_Z - A_Z'B_X))(Q_X' - (B_X/B_Z)Q_Z')$	ft/sec^2
Q_Y	$mg\cos\phi_e\cos\theta_e$	lb
Q_Z	$-mg\sin\phi_e\cos\theta_e$	lb
Q_Z'	$Q_Z - (C_Z/C_Y)Q_Y$	lb
Q_Z''	$(A_X'/(B_ZA_X' - B_XA_Z'))(Q_Z' - (A_Z'/A_X')Q_X')$	1/sec
r	yaw rate (body axes)	rad/sec
r_e	equilibrium yaw rate	rad/sec
r_w	yaw rate (wind axes)	rad/sec
rad	radian, radians	dimensionless
rpm	revolutions per minute	--

Abbreviation or Symbol	Definition	Units
$\bar{R}$	radius vector	ft
$R_{X'}$	$-(C_X/C_Y)R_Y$	lb
$R_{X''}$	$(B_Z/(A_{X'}B_Z - A_{Z'}B_X))(R_{X'} - (B_X/B_Z)R_{Z'})$	ft/sec^2
R_Y	$Y_{\delta r}$	lb
$R_{Z'}$	$-(C_Z/C_Y)R_Y$	lb
$R_{Z''}$	$(A_{X'}/(B_ZA_{X'} - B_XA_{Z'}))(R_{Z'} - (A_{Z'}/A_{X'})R_{X'})$	1/sec
S	wing area	ft^2
S_t	tail area	ft^2
$S_{X'}$	$-(C_X/C_Y)S_Y$	ft/sec^2
$S_{X''}$	$(B_Z/(A_{X'}B_Z - A_{Z'}B_X))(S_{X'} - (B_X/B_Z)S_{Z'})$	ft/sec^2
S_Y	$Y_{\delta a}$	lb
$S_{Z'}$	$-(C_Z/C_Y)S_Y$	lb
$S_{Z''}$	$(A_{X'}/(B_ZA_{X'} - B_XA_{Z'}))(S_{Z'} - (A_{Z'}/A_{X'})S_{X'})$	1/sec
SAS	stability augmentation system	--
sec	second, seconds	--
SL	sea level	--
S/N	serial number	--
t	time	sec
T	period of damped cyclic motion	sec
T	thrust	lb
T_e	equilibrium thrust	lb
TED	trailing edge down	--

Abbreviation or Symbol	Definition	Units
TEU	trailing edge up	--
T_X, T_Y, T_Z	thrust components	lb
TPS	Test Pilot School	--
T_V	$1/2\ \rho V_e SC_{T_V}$	slug/sec
T_X	$T_{\delta_T} \cos\alpha_T$	lb
$T_{X'}$	$(B_Z/(A_{X'}B_Z - A_{Z'}B_X))(T_X - (B_X/B_Z)T_Z)$	ft/sec^2
T_Z	$-T_{\delta_T} \sin\alpha_T$	lb
$T_{Z'}$	$(A_{X'}/(B_Z A_{X'} - B_X A_{Z'}))(T_Z - (A_{Z'}/A_{X'})T_X)$	1/sec
$T_{1/2}$	time to damp to 1/2 amplitude	sec
T_{δ_T}	$1/2\ \rho V_e^2 SC_{T_{\delta_T}}$	lb
u	perturbed velocity along X body axis; $V\cos\beta\cos\alpha$	ft/sec
U_o	steady state velocity along X body axis	ft/sec
UHF	ultra high frequency	--
UHT	unit horizontal tail	--
USAF	United States Air Force	--
USAFTPS	United States Air Force Test Pilot School	--
v	perturbed velocity along Y body axis	ft/sec
V	velocity in general, also true velocity wind axes	ft/sec
V_e	equilibrium velocity along wind axes	ft/sec
$\bar{V}_{cm/I}$	velocity of center of mass with respect to inertial space	ft/sec

Abbreviation or Symbol	Definition	Units
V_S	stall speed	ft/sec, kt
w	perturbed velocity along the body Z axis ($V\cos\beta\sin\alpha$)	ft/sec
wrt	with respect to	--
W	airplane gross weight	lb
W_f	fuel flow	lb/hr
W_X	$L_{\delta e}\sin\alpha_e - D_{\delta e}\cos\alpha_e$	lb
$W_{X'}$	$(B_Z/(A_X B_Z - A_Z B_X))(W_X - (B_X/B_Z)W_Z)$	ft/sec^2
W_Z	$-L_{\delta e}\cos\alpha_e - D_{\delta e}\sin\alpha_e$	lb
$W_{Z'}$	$(A_{X'}/(B_Z A_{X'} - B_X A_{Z'}))(W_Z - (A_{Z'}/A_{X'})W_X)$	1/sec
X_1, X_2, X_3	axes	--
X_B, Y_B, Z_B	axes	--
X_E, Y_E, Z_E	axes	--
X_{EC}, Y_{EC}, Z_{EC}	axes	--
X_I, Y_I, Z_I	axes	--
X_S, Y_S, Z_S	axes	--
X_V, Y_V, Z_V	axes	--
X_W, Y_W, Z_W	axes	--
X	force along X axis	lb
X_q	$L_q\sin\alpha_e$	slug-ft/sec
X_V	$-D_V\cos\alpha_e + L_V\sin\alpha_e + T_V\cos\alpha_T$	slug/sec
X_α	$D_e\sin\alpha_e - D_\alpha\cos\alpha_e + L_e\cos\alpha_e + L_\alpha\sin\alpha_e$	lb

Symbol	Definition	Units
[illegible]	[illegible]	[illegible]
[illegible]	[illegible]	lb
X_{δ_T}	$T_{\delta_T}\cos\alpha_T$	lb
Y	force along y axis	lb
Y_p	$1/4\ \rho V_e SbC_{y_p}$	lb-sec
Y_r	$1/4\ \rho V_e SbC_{y_r}$	lb-sec
Y_β	$1/2\ \rho V_e^2 SC_{y_\beta}$	lb
$Y_{\delta a}$	$1/2\ \rho V_e^2 SC_{y_{\delta a}}$	lb
$Y_{\delta r}$	$1/2\ \rho V_e^2 SC_{y_{\delta r}}$	lb
Z	force along Z axis	lb
Z_q	$-L_q\cos\alpha_e$	slug ft/sec
Z_V	$-D_V\sin\alpha_e - L_V\cos\alpha_e - T_V\cos\alpha_T$	slug/sec
Z_α	$-D_e\cos\alpha_e + L_e\sin\alpha_e - L_\alpha\cos\alpha_e - D_\alpha\sin\alpha_e$	lb
$Z_{\dot{\alpha}}$	$L_{\dot{\alpha}}\cos\alpha_e$	slug ft/sec
Z_{δ_e}	$-L_{\delta_e}\cos\alpha_e - T_{\delta_e}\sin\alpha_e$	lb
Z_{δ_T}	$-T_{\delta_T}\sin\alpha_T$	lb
α	angle of attack	rad, deg
α_e	equilibrium angle of attack	rad, deg
α_T	tail angle of attack	rad, deg

Abbreviation or Symbol	Definition	Units
α_T	inclination of thrust vector with body X axis	rad, deg
β	sideslip angle	
β_e	equilibrium sideslip angle	rad, deg
δ_a	total aileron and spoiler deflection	rad, deg
δ_{1+3}	CAS aileron variables (δ_1, δ_2, δ_3)	--
δ_{ac}	commanded aileron to control actuator	rad
$\delta_{am_{1+3}}$	mechanical aileron variables	--
δ_{ap}	aileron force input from the pilot	lb
δ_{aCAS}	total CAS aileron input	rad
δ_c	control deflection in general	rad, deg
δ_e	total elevator deflection	rad, deg
$\delta_{e_{1,2}}$	CAS elevator variables	rad, deg
δ_{ec}	commanded elevator to control actuator	rad
$\delta_{em_{1,2}}$	mechanical elevator variables	--
δ_{ep}	elevator force input from pilot	lb
δ_{eCAS}	total CAS elevator input	rad
δ_p	rudder pedal deflection	rad, deg
δ_r	total rudder deflection	rad, deg
$\delta_{r_{1+11}}$	CAS rudder variables	--

Abbreviation or Symbol	Definition	Units
δ_{rc}	commanded rudder to control actuator	rad
δ_{rm}	mechanical rudder variable	rad
δ_{rp}	rudder force input from pilot	lb
δ_T	throttle deflection	rad, deg
ε	downwash angle	rad, deg
ζ	damping ratio	--
θ	pitch angle	rad, deg
θ_e	equilibrium pitch angle	rad, deg
θ_w	pitch angle wind axes	rad, deg
$\ddot{\theta}$	pitch acceleration	rad/sec^2
λ	eigenvalue	--
λ	longitude	deg
λ_E	angle between $\hat{X}_l$ and $\hat{Z}_E$	rad, deg
μ	latitude	deg
μ_{E_l}	angle between $\hat{X}_{EC}$ and $\hat{X}_l$	rad, deg
μ	angle between $\hat{X}_I$ and $\hat{X}_{EC}$	rad, deg
ρ	air density	lb-sec^2/ft^4, slug/ft^3
ϕ	bank angle	rad, deg
Φ_e	equilibrium bank angle	rad, deg
Φ_w	bank angle wind axes	rad, deg
Φ/β	phi to beta ratio	--
ψ	yaw angle	rad, deg

Abbreviation or Symbol	Definition	Units
ψ_e	equilibrium yaw angle	rad, deg
ψ_w	yaw angle wind axes	rad, deg
ω	frequency	rad/sec
ω_d	damped frequency	rad/sec
ω_{DR}	dutch roll frequency	rad/sec
ω_n	natural frequency	rad/sec
ω_{ph}	phugoid frequency	rad/sec
ω_{sp}	short period frequency	rad/sec
$\bar{\omega}$	angular velocity vector	rad/sec
$\bar{\omega}_{E/I}$	angular velocity of F_E wrt F_I	rad/sec
$\bar{\omega}_{EC/E}$	angular velocity of F_{EC} wrt F_E	rad/sec
$\bar{\omega}_{V/EC}$	angular velocity of F_V wrt F_{EC}	rad/sec
$\bar{\omega}_{V/I}$	angular velocity of F_V wrt F_I	rad/sec

Abstract

This report documents the results of a limited simulation and flight test of the A-7D to determine the effect of load factor on aircraft handling qualities. The test condition was 15,000 feet indicated pressure altitude, 0.6 indicated Mach number, at load factors ranging from 1 to 3G's for the mechanical and fully augmented flight control configurations. The equations of motion were developed to include turning flight. The equations were linearized and put into first order form $\dot{\bar{x}} = A\bar{x} + B\bar{u}$. Eigenvalues/eigenvectors, Argand diagrams, Bode plots, and time histories were used to predict the effect of load factor on aircraft handling qualities with respect to MIL-F-8785C. Linear systems analysis was useful in predicting aircraft response for doublet and impulse inputs. As load factor increased the longitudinal and lateral modes became kinematically coupled. Load factor destablized the phugoid mode. Load factor had little affect on short period dynamics, but caused the parameter n/α to increase for the fully augmented aircraft resulted in the flying qualities degrading from level one to level two. The dutch roll mode dynamics improved with an increase in load factor. The roll mode time constant increased with load factor; however, remained within level one criteria. Linear systems analysis was determined invalid for step roll inputs. Frequency response analysis showed the affect of pole/zero movement as load factor increased. Flight test results verified the trends predicted by analysis. In addition, flight test revealed that cross coupling between the longitudinal and lateral modes was aggravated by rapidily removing step roll inputs. The appendices contain plots as well as detailed

information on reference frames, equations of motion development, A-7D flight control system modeling, and computer programs used in this study.

THE EFFECT OF LOAD FACTOR ON AIRCRAFT HANDLING QUALITIES

I. Introduction

This thesis presents the results of a limited flying qualities evaluation of the A-7D, at load factors from 1 to 3 G's, and a flight condition of 15,000 feet indicated pressure altitude (H_{ic}) at Ø.6 indicated mach number (IMN).

Background

Military Specification for Flying Qualities of Piloted Airplanes MIL-F-8785C [Ref 1] is used by the United States Air Force Test Pilot School (USAFTPS) as a guideline for evaluating open loop handling qualities of various aircraft. MIL-F-8785C was republished in November 1980. This new version replaced the old version MIL-F-8785B, and two paragraphs were changed which affected the Test Pilot School (TPS) curriculum. Paragraph 3.3.4 "Roll Control Effectiveness" added the requirement for rolls to be initiated from wings level flight and from steady bank angles. This expanded the MIL-F-8785B requirement for rolls initiated from zero roll rate. The background document for MIL-F-8785C [Ref 2] states the MIL-F-8785B requirement always applied the [illegible] applicable to velocity-vector-load factor (v-h-n) flight [illegible], the application of these requirements at other than 1G [illegible] overlooked. Paragraph 3.3.4.1.2 "Roll Performance in Flight Phase GA" adds requirements for [illegible] roll at load factors greater than [illegible] maximum [illegible].

[illegible]

While performing step roll inputs at other than 1G, longitudinal as well as lateral-directional oscillations were observed during the roll, even though no longitudinal inputs had been made. Furthermore, the sideslip oscillations were greater than initially anticipated. This raised the question -- What effect may load factor have on aircraft handling qualities, and can the effect, if any, be predicted analytically?

Purpose

The primary purpose of this thesis is to investigate the effect load factor has on aircraft handling qualities, and determine if linear systems analysis can analytically predict the effect. The A-7D was selected as the aircraft to analyze for several reasons: First it is one of the TPS curriculum aircraft with telemetry capability; second, it has a sophisticated flight control system with selectable augmentation which allowed analysis of non-augmented and fully augmented cases; finally, the aerodynamic and flight control data was available for modelling purposes.

Objectives

The specific objectives of this limited evaluation were to:

1. Analyze the effect of load factor on aircraft dynamics/handling qualities.

2. Determine how well analytical tools (e.g. eigenvalues, eigenvectors, frequency response plots, computer models) can predict aircraft handling qualities based on compliance with MIL-F-8785C.

3. Compare analytical results with flight test results to determine the validity of using linear systems analysis to predict handling qualities at other than 1G.

Approach

The primary analytical methods used for determining the effect of load factor on aircraft handling qualities were linear systems analysis techniques. Flight test provided the source of verification and qualitative comments.

After a general set of equations of motion were derived to include turning flight, they were linearized and written in the familiar first order linear state variable differential equation form.

$$\dot{\bar{x}} = A\bar{x} + B\bar{u} \tag{1.1}$$

where $\bar{x}$ represents the state variable vector, and $\bar{u}$ represents the input vector. The A and B matrices represent the aircraft, and control matrices respectively. The original set of equations were expanded to include the A-7D's mechanical and augmented flight control systems.

Analysis of this system of equations was accomplished using eigenvalues/eigenvectors, argand diagrams, Bode plots, and time histories. In addition, parameters required by MIL-F-8785C, such as ω_n, ζ, n/α, etc. were extracted to determine MIL SPEC compliance.

Flight test was used to determine the validity of the analytical findings, and to qualitatively comment on the effect of load factor on handling qualities.

Assumptions

For the equations of motion development a flat non rotating earth, fixed in space, i.e., inertia frame was used. The aircraft was assumed to be a rigid body of fixed mass with the thrust vector lying in the plane of symmetry. The xz plane was the plane of symmetry and the flow about the aircraft was steady, except that $\dot{u}$ stability derivatives were

included in the equations of motion. Perturbations from the equilibrium condition remained relatively small with the products and squares of the perturbation variables being negligible. Atmospheric properties were considered constant during perturbations from the equilibrium condition.

Sign Convention

The following sign convention is used:

1. Forces, moments, and rates are positive with respect to a right handed coordinate system with the x-axis out the aircraft nose, the y-axis out the right wing, and the z-axis out the bottom of the aircraft (Figure 1-1).

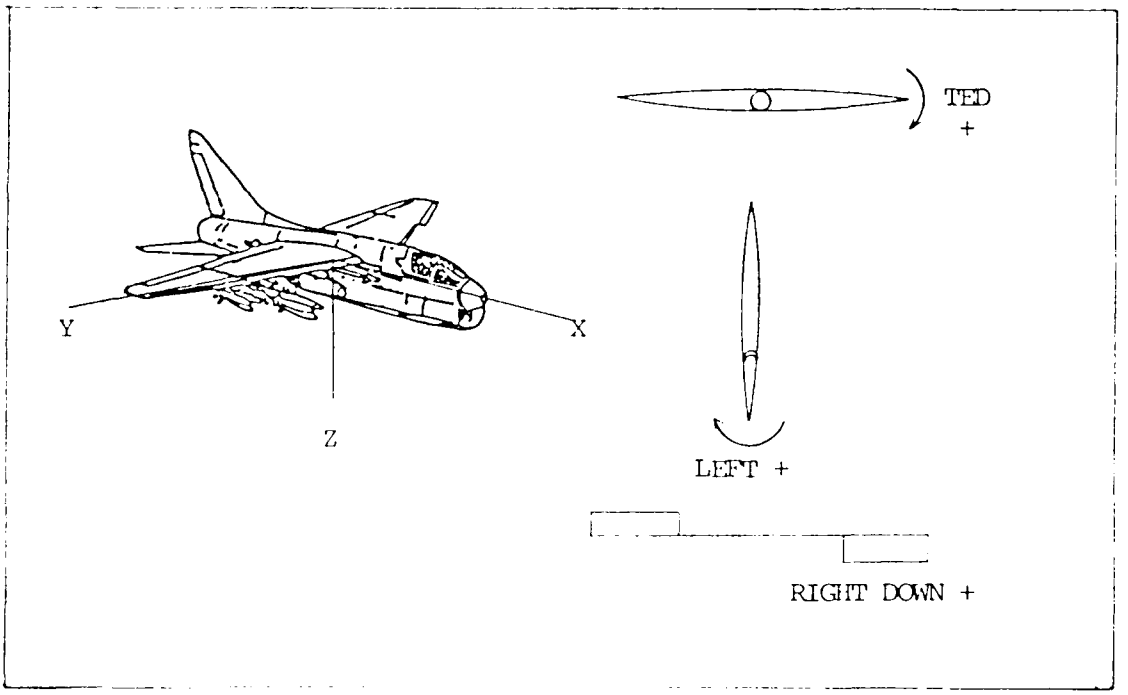

Figure 1-1. Sign Convention

2. Elevator (Unit Horizontal Tail (UHT)) trailing edge down is considered a positive deflection (NASA standard).

3. Rudder trailing edge left is considered a positive deflection (NASA standard).

4. Right aileron trailing edge down is considered a positive deflection [Ref 3:300].

Presentation

This thesis is composed of six chapters. Chapter II summarizes the general equations development, presents the aircraft parameters and stability derivatives for various load factors, and summarizes the additional equations required to model the flight control system. In addition, the A and B matrices for various load factors, and flight control configurations are presented. Chapter III presents the analytical predictions of the effect of load factor on the handling qualities. Chapter IV discusses and presents the results of the flight test portion of the study. Chapter V compares the analytical and flight test results, and Chapter VI gives the conclusions and recommendations.

II. Development of Equations

Introduction

This chapter summarizes the general equations of motion development, presents the aircraft parameters and stability derivatives for the load factors considered, and summarizes the additional equations required to model the flight control system. To supplement this chapter, Appendix A contains a detailed explanation of reference frames; Appendix B contains a very detailed derivation of the equations of motion for level turning flight which can be simplified for straight and level unaccelerated flight; Appendix C contains an explanation of the A-7D's flight control system along with the derivation of the additional state equations required to include the flight control system in the computer model.

Equations of Motion

The sum of the external forces are equal to the time rate of change of the linear momentum, and the sum of the applied moments is equal to the time rate of change of the angular momentum. Yes, Newtons Second Law was the starting point for this development. The standard assumptions that the earth is fixed in space, the aircraft is a rigid body, and the aircraft's mass remains constant were made, which are valid assumptions for this purpose. The equations were derived in body axes to allow direct comparison with flight test data. This is because the flight test instrumentation system measures body axes as opposed to stability axes angular rates. Furthermore, flight control feedbacks are also body axes quantities. Grouping the three force, moment, and kinematic equations developed in Appendix A into the following set allows the motion of the aircraft to be described.

Forces

$$X: \quad T_{\cos\alpha_T} + F_{AX_B} - mg \sin\theta = m(\dot{u} + qw - rv) \tag{2.1}$$

$$Y: \quad F_{AY_B} + mg \sin\phi \cos\theta = m(\dot{v} + ru - pw) \tag{2.2}$$

$$Z: \quad -T \sin\alpha_T + F_{AZ_B} + mg \cos\phi \cos\theta = m(\dot{w} + pv - qu) \tag{2.3}$$

Moments

$$L = \dot{p} I_{xx} - \dot{r} I_{xz} + qr(I_{zz} - I_{yy}) - pq I_{xz} \tag{2.4}$$

$$M = \dot{q} I_{yy} + pr(I_{xx} - I_{zz}) + I_{xz}(p^2 - r^2) \tag{2.5}$$

$$N = \dot{r} I_{zz} - \dot{p} I_{zx} + pq(I_{yy} - I_{xx}) + qr I_{xz} \tag{2.6}$$

Kinematics

$$\dot{\phi} = p + q \sin\phi \tan\theta + r \cos\phi \tan\theta \tag{2.7}$$

$$\dot{\theta} = q \cos\phi - r \sin\phi \tag{2.8}$$

$$\dot{\psi} = [\, q \sin\phi + r \cos\phi \,] \sec \tag{2.9}$$

Note: since none of the equations depend on ψ, the $\dot{\psi}$ equation can be omitted.

To correlate the force equations with variables used in the A-7D Aerodynamic Data report [Ref 4], and those measured from flight test, they were written in terms of V, α, β, L, D, Y, p, q, r, ϕ, and θ, as detailed in Appendix B.

where

V = free stream true velocity

α = angle of attack

β = angle of sideslip

L = lift

D = drag

Y = side force

p, q, r = body axes rates

ϕ = bank angle

θ = pitch angle

which yield

X Force Equation:

$$-D\cos\alpha + T\cos\alpha_T = m\left[\dot{V}\cos\alpha\cos\beta - V\dot{\alpha}\sin\alpha\cos\beta - V\dot{\beta}\cos\alpha\sin\beta + q(V\sin\alpha\cos\beta) - r(V\sin\beta) + g\sin\theta\right] \quad (2.10)$$

Y Force Equation:

$$Y = m\left[\dot{V}\sin\beta + V\dot{\beta}\cos\beta + r(V\cos\alpha\cos\beta) - p(V\sin\alpha\cos\beta) - g\sin\phi\cos\theta\right] \quad (2.11)$$

Z Force Equation:

$$-D\sin\alpha - L\cos\alpha - T\sin\alpha_T = m\left[\dot{V}\sin\alpha\cos\beta + V\dot{\alpha}\cos\alpha\cos\beta - V\dot{\beta}\sin\alpha\sin\beta + p(V\sin\beta) - q(V\cos\alpha\cos\beta) - g\cos\phi\cos\theta\right] \quad (2.12)$$

Linearization. At this point there are several approaches that can be taken to solve this system of equations. Numerical integration techniques can be employed to solve the non linear set of differential equations, or the equations can be linearized for a small disturbance about an equilibrium condition of interest. The linearization method was chosen for this problem, and the details of this process are contained in Appendix B. The linearized coupled body axes equations of motion valid for steady level turns, and straight and level flight are summarized below:

X-Force Equation:

$$\left[m\cos\alpha_e\cos\beta_e\right]\Delta\dot{V} + \left[-mV_e\sin\alpha_e\cos\beta_e - L_{\dot{\alpha}}\sin\alpha_e\right]\Delta\dot{\alpha} + \left[mV_e\cos\alpha_e\sin\beta_e\right]\Delta\dot{\beta}$$

$$= \left[(D_V\cos\alpha_e + L_V\sin\alpha_e + T_V\cos\alpha_T) - mq_e\sin\alpha_e\cos\beta_e + mr_e\sin\beta_e\right]\Delta V$$

$$+ \left[(D_e\sin\alpha_e - D_\alpha\cos\alpha_e + L_e\cos\alpha_e + L_\alpha\sin\alpha_e) - mq_eV_e\cos\alpha_e\cos\beta_e\right]\Delta\alpha$$

$$+ \left[L_q\sin\alpha_e - mV_e\sin\alpha_e\cos\beta_e\right]\Delta q + \left[-mg\cos\theta_e\right]\Delta\theta$$

$$+ \left[mq_eV_e\sin\alpha_e\sin\beta_e + mr_eV_e\cos\beta_e\right]\Delta\beta + \left[mV_e\sin\beta_e\right]\Delta r$$

$$+ \left[L_{\delta_e}\sin\alpha_e - D_{\delta_e}\cos\alpha_e\right]\delta_e + \left[T_{\delta_T}\cos\alpha_T\right]\delta_T \qquad (2.13)$$

Y Force Equation:

$$\left[m\sin\beta_e\right]\Delta\dot{V} + \left[mV_e\cos\beta_e\right]\Delta\dot{\beta} = \left[-mr_e\cos\alpha_e\cos\beta_e + mp_e\sin\alpha_e\cos\beta_e\right]\Delta V$$

$$+ \left[mr_eV_e\sin\alpha_e\cos\beta_e + mp_eV_e\cos\alpha_e\cos\beta_e\right]\Delta\alpha + \left[-mg\sin\phi_e\sin\theta_e\right]\Delta\theta$$

$$+ \left[Y_\beta + mr_eV_e\cos\alpha_e\sin\beta_e - mp_eV_e\sin\alpha_e\sin\beta_e\right]\Delta\beta + \left[Y_p + mV_e\sin\alpha_e\cos\beta_e\right]\Delta p$$

$$+ \left[Y_r - mV_e\cos\alpha_e\cos\beta_e\right]\Delta r + \left[mg\cos\phi_e\cos\theta_e\right]\Delta\phi + \left[Y_{\delta_r}\right]\delta_r + \left[Y_{\delta_a}\right]\delta_a$$

(2.14)

Z Force Equation:

$$\left[m\sin\alpha_e\cos\beta_e\right]\Delta\dot{V} + \left[mV_e\cos\alpha_e\cos\beta_e + L_{\dot{\alpha}}\cos\alpha_e\right]\Delta\dot{\alpha} + \left[-mV_e\sin\alpha_e\sin\beta_e\right]\Delta\dot{\beta}$$

$$= \left[(-D_V\sin\alpha_e - L_V\cos\alpha_e - T_V\sin\alpha_T) - mp_e\sin\beta_e + mq_e\cos\alpha_e\cos\beta_e\right]\Delta V$$

$$+ \left[(-D_e\cos\alpha_e + L_e\sin\alpha_e - L_\alpha\cos\alpha_e - D_\alpha\sin\alpha_e) - mr_eV_e\sin\alpha_e\cos\beta_e\right]\Delta\alpha$$

$$+ \left[-L_q \cos\alpha_e + mV_e \cos\alpha_e \cos\beta_e\right] \Delta q + \left[-mg\cos\Phi_e \sin\theta_e\right] \Delta\theta$$

$$+ \left[-mp_e V_e \cos\beta_e - mq_e V_e \cos\alpha_e \sin\beta_e\right] \Delta\beta + \left[-mV_e \sin\beta_e\right] \Delta p + \left[-mg\sin\Phi_e \cos\theta_e\right] \Delta\Phi$$

$$+ \left[-L_{\delta_e} \cos\alpha_e - D_{\delta_e} \sin\alpha_e\right] \delta_e - T_{\delta_T} \sin\alpha_T \delta_T \qquad (2.15)$$

L Moment Equation: (Rolling Moment)

$$I_x \dot{\Delta p} - I_{xz} \dot{\Delta r} = \left[r_e(I_y - I_z) + p_e I_{xz}\right] \Delta q + \left[L_\beta\right] \Delta\beta + \left[L_\beta + q_e I_{xz}\right] \Delta p$$

$$+ \left[L_r + q_e(I_y - I_z)\right] \Delta r + L_{\delta_r} \delta_r + L_{\delta_a} \delta_a \qquad (2.16)$$

M Moment Equation: (Pitching Moment)

$$I_y \dot{\Delta q} - M_{\dot{\alpha}} \dot{\Delta\alpha} = M_V \Delta v + M_\alpha \Delta\alpha + M_q \Delta q + \left[r_e(I_z - I_x) - 2p_e I_{xz}\right] \Delta p$$

$$+ \left[p_e(I_z - I_x) + 2r_e I_{xz}\right] \Delta r + M_{\delta_e} \delta_e + M_{\delta_t} \delta_t \qquad (2.17)$$

N Moment Equation: (Yawing Moment)

$$I_z \dot{\Delta r} - I_{zx} \dot{\Delta p} = \left[p_e(I_x - I_y) - r_e I_{xz}\right] \Delta q + N_\beta \Delta\beta + \left[q_e(I_x - I_y) + N_p\right] \Delta p$$

$$+ \left[-q_e I_{xz} + N_r\right] \Delta r + N_{\delta_r} \delta_r + N_{\delta_a} \delta_a \qquad (2.18)$$

$\dot{\Phi}$ Equation:

$$\dot{\Delta\Phi} = \left[r_e \cos\Phi_e \sec^2\theta_e + q_e \sin\Phi_e \sec^2\theta_e\right] \Delta\theta + \left[\sin\Phi_e \tan\theta_e\right] \Delta q$$

$$+ \Delta p + \left[\cos\Phi_e \tan\theta_e\right] \Delta r + \left[q_e \cos\Phi_e \tan\theta_e - r_e \sin\Phi_e \tan\theta_e\right] \Delta\Phi \qquad (2.19)$$

$\dot{\theta}$ Equation:

$$\dot{\Delta\theta} = \left[\cos\Phi_e\right] \Delta q + \left[-\sin\Phi_e\right] \Delta r + \left[-q_e \sin\Phi_e - r_e \cos\Phi_e\right] \Delta\Phi \qquad (2.20)$$

First Order Form. Writing these equations in the familiar

$$\dot{\bar{x}} = A\bar{x} + B\bar{u} \tag{1.1}$$

state variable form allows for convenient modern control system analysis. The state vector $\bar{x}$, and the input vector $\bar{u}$ are defined as follows; where the Δ's preceding each perturbation variable has been omitted.

$$\bar{x} = \begin{bmatrix} V \\ \alpha \\ q \\ \theta \\ \beta \\ p \\ r \\ \phi \end{bmatrix} \qquad \bar{u} = \begin{bmatrix} \delta_e \\ \delta_r \\ \delta_a \\ \delta_t \end{bmatrix} \tag{2.21}$$

The δ_t element in the input vector is included at this point to keep the development general, however, the final form will assume a constant thrust setting and it will be dropped.

Since all eight of these equations are coupled for turning flight, the coefficients of the state and input variables are extremely complex; therefore, a notation was developed to simplify the equations. The definition of each symbol used is presented in the "List of Symbols", and the details of manipulating the equations into first order form are given in Appendix B. The first order form of the equations using the simplified notation are listed below:

$$\Delta\dot{V} = D_x''\Delta V + E_x''\Delta\alpha + F_x'\Delta q + C_x''\Delta\theta + H_x''\Delta\beta + J_x''\Delta p + K_x''\Delta r$$
$$+ Q_x''\Delta\phi + W_x'\delta_e + T_x'\delta_T + R_x''\delta_r + S_x''\delta_a \qquad (2.22)$$

$$\Delta\dot{\alpha} = D_z''\Delta V + E_z''\Delta\alpha + F_z'\Delta q + G_z''\Delta\theta + H_z''\Delta\beta + J_z''\Delta p + K_z''\Delta r$$
$$+ Q_z''\Delta\phi + W_z'\delta_e + T_z'\delta_T + R_z''\delta_r + S_z''\delta_a \qquad (2.23)$$

$$\Delta\dot{q} = \frac{1}{I_y}\Big[\left[M_V + M_\alpha^{\cdot}D_z''\right]\Delta V + \left[M_\alpha + M_\alpha^{\cdot}E_z''\right]\Delta\alpha + \left[M_q + M_\alpha^{\cdot}F_z'\right]\Delta q$$
$$+ \left[M_\alpha^{\cdot}G_z''\right]\Delta\theta + \left[M_\alpha^{\cdot}H_z''\right]\Delta\beta + \left[r_e(I_z - I_x) - 2p_eI_{xz} + M_\alpha^{\cdot}J_z''\right]\Delta p$$
$$+ \left[p_e(I_z - I_x) + 2r_eI_{xz} + M_\alpha K_z''\right]\Delta r + \left[M_\alpha Q_z''\right]\Delta\phi$$
$$+ \left[M_{\delta_e} + M_\alpha^{\cdot}W_z'\right]\delta_e + \left[M_{\delta_T} + M_\alpha^{\cdot}T_z'\right]\delta_T + \left[M_\alpha^{\cdot}R_z''\right]\delta_r$$
$$+ \left[M_\alpha^{\cdot}S_z''\right]\delta_a\Big] \qquad (2.24)$$

$$\Delta\dot{\theta} = \left[\cos\phi_e\right]\Delta q + \left[-\sin\phi_e\right]\Delta r + \left[-q_e\sin\phi_e - r_e\cos\phi_e\right]\Delta\phi \qquad (2.25)$$

$$\Delta\dot{\beta} = \frac{1}{C_y}\Big[\left[D_y - A_yD_x''\right]\Delta V + \left[E_y - A_yE_x''\right]\Delta\alpha + \left[-A_yF_x'\right]\Delta q$$
$$+ \left[G_y - A_yG_x''\right]\Delta\theta + \left[H_y - A_yH_x''\right]\Delta\beta + \left[J_y - A_yJ_x''\right]\Delta p$$
$$+ \left[K_y - A_yK_x''\right]\Delta r + \left[Q_y - A_yQ_x''\right]\Delta\phi + \left[-A_yW_x'\right]\delta_e$$
$$+ \left[-A_yT_x'\right]\delta_T + \left[R_y - A_yR_x''\right]\delta_r + \left[S_y - A_yS_x''\right]\delta_a\Big] \qquad (2.26)$$

$$\Delta\dot{p} = \left[r_e(I2) + p_e(I3)\right]\Delta q + L_\beta'\Delta\beta + \left[L_p' + q_e(I3)\right]\Delta p$$
$$\left[L_r' + q_e(I2)\right]\Delta r + L_{\delta_r}'\delta_r + L_{\delta_a}'\delta_a \qquad (2.27)$$

$$\Delta\dot{r} = \left[p_e(I4) + r_e(I5)\right]\Delta q + N_\beta'\Delta\beta + \left[N_p' + q_e(I4)\right]\Delta p$$
$$+ \left[N_r' + q_e(I5)\right]\Delta r + N_{\delta_r}'\delta_r + N_{\delta_a}'\delta_a \qquad (2.28)$$

$$\Delta\dot{\phi} = \left[r_e\cos\phi_e\sec^2\theta_e + q_e\sin\phi_e\sec^2\theta\right]\Delta\theta + \left[\sin\phi_e\tan\theta_e\right]\Delta q$$
$$+ \Delta p + \left[\cos\phi_e\tan\theta_e\right]\Delta r + \left[q_e\cos\phi_e\tan\theta_e - r_e\sin\phi_e\tan\theta_e\right]\Delta\phi \qquad (2.29)$$

This system of equations can be used for any conventional airplane to describe its motion during perturbations from straight and level or steady level turning flight. The A-7D was used in this problem and the information required to evaluate these equations is provided in the next section.

A-7D Parameters and Data Package Handling

The A-7D fixed parameters for this model at the specified flight condition are presented in Table 2-1.

Table 2-1

Flight Condition and Geometeric Parameters

Item	Symbol	Value
Altitude	H_c, h	15000
Mach	M, INM	0.6
Density	ρ	.001496
True Airspeed	V	634.7
Dynamic Pressure	$\bar{q}$	301.3
Weight	W	25338
Gravity	g	32.1725
Mass	m	787.57
Center of Gravity	cg	28.71
Wing Area	S	375
Wing Span	b	38.73
Mean Aerodynamic Chord	$\bar{c}$	10.84
Moments of Inertia	I_{x_s}	15365
	I_{y_s}	69528
	I_{z_s}	79005
Product of Inertia	I_{xz_s}	-1664

The A-7 Aerodynamic Data report [Ref 4] and the A-7D Estimated Flying Qualities report [Ref 5] were the primary sources for the aerodynamic and stability derivative data required. The data were in stability axes and several of the derivatives (such as C_{ℓ_r}, C_{ℓ_p}, C_{n_p}) varied with angle of attack. Several steps as outlined below were required to convert this data to body axes for each of the load factors of interest.

First it was necessary to obtain 1G data at the 15,000 ft, 0.6M flight condition. This data was stored on diskette for later access using Data Creator (Appendix D). A program called Delta Alpha Solver calculated the change in angle of attack and UHT (δ_e) as a function of load factor. Since these calculations were done in stability axes, this program also changes the stability axes load factors and bank angles to body axes (Appendix D). The results of these calculations are listed in Table 2-2.

TABLE 2-2

DELTA ALPHA SOLVER RESULTS

DELTA ALPHA (DEG)	DELTA STABILATOR (DEG)	STABILITY AXIS		BODY AXIS	
		LOAD FACTOR (G)	BANK ANGLE (DEG)	LOAD FACTOR (G)	BANK ANGLE (DEG)
0	0	1	0	1.00	0
1.56	-0.88	1.5	48.2	1.49	48.5
3.11	-1.74	2	60	1.97	60.6
4.66	-2.59	2.5	66.4	2.44	67.5
6.22	-3.44	3	70.5	2.90	72.1

Note: The delta alpha and delta stabilator values are referenced to 1G: $\alpha_o = 4.36$ $\delta_{e_o} = 4.17$.

The program uses these body axes bank angles to calculate equilibrium rates (p_e, q_e, r_e).

With the equilibrium angles of attack determined at each load factor, the data package was re-entered to obtain those stability derivatives affected by angle of attack and those values were stored on diskette using Data Creator. The non-dimensional parameters obtained are given in Table 2-3.

Table 2-3

Non Dimensional Aerodynamic and Stability Derivative Parameters

(15,000 ft, 0.6M, 26,718 MAC, 25,338 lb)

Parameters	Trim Points					
	1		2		3	
	Axes		Axes		Axes	
	Stability	Body	Stability	Body	Stability	Body
Longitudinal						
C_L	.1142	-	.4466	-	.6727	-
C_{L_V}	.0241	-	.0241	-	.0241	-
C_{L_α}	4.4464	-	4.4464	-	4.4464	-
$C_{L_{\dot{\alpha}}}$	0	-	0	-	0	-
C_{L_q}	1.956	-	1.956	-	1.956	-
$C_{L_{\delta e}}$	.5959	-	.5959	-	.5959	-
C_{L_0}	.0335	-	.0335	-	.0475	-
C_{D_V}	6.483 E-03	-	6.483 E-03	-	6.483 E-03	-
C_{D_α}	.1901	-	.4433	-	.6802	-
$C_{D_{\delta e}}$	0	-	0	-	0	-
C_{m_V}	6.43 E-03	6.43 E-03	6.43 E-03	6.43 E-03	6.43 E-03	6.43 E-03
C_{m_α}	-.4584	-.4584	-.4584	-.4584	-.4584	-.4584
$C_{m_{\dot{\alpha}}}$	-.77	-.77	-.77	-.77	-.77	-.77
C_{m_q}	-3.95	-3.95	-3.95	-3.95	-3.95	-3.95
$C_{m_{\delta e}}$	-.9053	-.9053	-.9053	-.9053	-.9053	-.9053
C_{m_0}	0	0	0	0	0	0

Table 2-3 (Continued)

Non Dimensional Aerodynamic and Stability Derivative Parameters

(15,000 ft, 0.6M, 28,718 MAC, 25,338 lb)

Parameters	Load Factor 1 Axes		2 Axes		3 Axes	
	Stability	Body	Stability	Body	Stability	Body
Lateral-Directional						
C_{Y_β}	-.7162	-.7162	-.7162	-.7162	-.7162	-.7162
C_{Y_p}	.1364	.1094	.2179	.1747	.1413	.0870
C_{Y_r}	.3364	.3277	.3364	.3440	.2628	.3039
$C_{Y_{\delta_r}}$	.2005	.2005	.2005	.2005	.2005	.2005
$C_{Y_{\delta_a}}$	0	0	0	0	0	0
C_{ℓ_β}	-.0905	-.0972	-.1020	-.1119	-.0988	-.1155
C_{ℓ_p}	-.273	-.2812	-.2938	-.3106	-.2344	-.2675
C_{ℓ_r}	.1077	.1095	.1490	.1504	.1662	.1810
$C_{\ell_{\delta_r}}$	.0241	.0310	.0213	.0330	8.20 E-03	.0249
$C_{\ell_{\delta_a}}$	-.0642	-.0649	-.0642	-.0654	-.0519	-.0532
C_{n_β}	.0917	.0846	.0831	.0891	.1003	.0805
C_{n_p}	-2.24 E-03	-4.84 E-04	-.0222	-.0208	-4.0 E-03	.0106
C_{n_r}	-.3042	-.2960	-.3213	-.3045	-.3469	-.3138
$C_{n_{\delta_r}}$	-.0917	-.0886	-.0917	-.0882	-.0917	-.0886
$C_{n_{\delta_a}}$	.0123	7.38 E-03	.0137	5.24 E-03	.0117	1.97 E-03

Finally, the program Augmented AMAT BMAT/Ver 2 (Appendix D) is used to calculate the individual elements of the A and B matrices. To accomplish this, several intermediate steps are performed. The remaining equilibrium values are calculated (Table 2-4), the stability derivatives are dimensionalized and X, Z body axes derivatives are calculated (Table 2-5).

Table 2-4

BODY AXES EQUILIBRIUM VALUES
(15,000 ft, 0.6M, 28.71% MAC, 25,338 lb)

LOAD FACTOR (G)	ANGLE OF ATTACK (DEG)	SIDESLIP ANGLE (DEG)	BANK ANGLE (DEG)	ROLL RATE (DEG/SEC)	PITCH RATE (DEG/SEC)	YAW RATE (DES/SEC)	ELEVATOR DEFLECTION (DEG)	RUDDER DEFLECTION (DEG)	AILERON DEFLECTION (DEG)
1	4.36	0	0	0	0	0	-4.17	0	0
1.5	5.915	-.04	49.495	-.335	2.419	2.14	-5.048	-.243	.104
2	7.47	-.047	60.639	-.654	4.347	2.445	-5.907	-.277	.206
2.5	9.025	-.052	67.481	-1.044	6.071	2.517	-6.759	.294	.339
3	10.579	-.057	72.099	-1.508	7.684	2.482	-7.608	-.315	.466

NOTE: LOAD FACTOR IS IN STABILITY AXES

Table 2.5

Dimensional Body Axis Aerodynamic and Stability Derivatives

[... ft, ... MM, 2...71 MSC, 25,3... ft

Parameter	Level Flight		
Unconditional			
X_u	25334.10	50879.59	[illegible]
X_w	164.46	164.34	[illegible]
X_q	501755	501755	[illegible]
$X_{\dot{w}}$	0	0	
Z_u	1887.42	1887.42	[illegible]
Z_w	67335.37	67335.37	[illegible]
Z_q	2356.00	3785.43	[illegible]
$Z_{\dot{w}}$	8.67	13.17	[illegible]
M_u	21706.87	50092.29	[illegible]
$M_{\dot{w}}$	0	0	
M_w	12.41	12.41	12.41
M_q	-561491	-561491	-561491
$M_{\dot{q}}$	-8054.17	-8054.17	-8054.17
M_{T_u}	-41316.83	-41316.83	-41316.83
M_{T_w}	-1108886	-1108886	[illegible]
$M_{T_{\dot{w}}}$			
X_{T_u}	-2.22	-4.31	[illegible]
X_{T_w}	419430.57	[illegible]	[illegible]
$X_{T_{\dot{w}}}$	0	0	
X_{T_q}	143.49	245.39	[illegible]
Z_{T_u}	[illegible]	[illegible]	[illegible]
Z_{T_w}			
Z_{T_q}	-884.89	-1664.66	[illegible]
$Z_{T_{\dot{w}}}$	-502377	-501175	[illegible]
M_{T_u}	0	0	
M_{T_w}	-1881.96	-1871.41	[illegible]
M_{T_q}	[illegible]	[illegible]	[illegible]
$M_{T_{\dot{w}}}$		0	

Table 2-5 Continued

Body Axes Aerodynamic and Stability Derivative Expressions

	Term Number		
	1	2	3
Derivative Expression Coefficient			
$Y_{\dot{v}}$	-809929	-809929	-8074.4
$Y_{\dot{p}}$	377.19	602.15	293.87
$Y_{\dot{r}}$	1129.67	1186.07	1047.65
$Y_{\dot{\delta}_r}$	22656.05	22656.05	22656.05
$Y_{\dot{\delta}_a}$	0	0	0
Y_v	-425427	-469674	-5956.29
Y_p	-37544.15	-41474.58	-5713.42
Y_r	14615.18	20082.56	24173.01
Y_{δ_r}	135675	144601	208964
Y_{δ_a}	-264244	-280379	-[illegible]
$N_{\dot{v}}$	570645	642471	56[illegible]
$N_{\dot{p}}$	-64.69	-[illegible]	-[illegible]
$N_{\dot{r}}$	-39527.15	-[illegible]	-41[illegible]
N_v	-[illegible]	-[illegible]	-[illegible]
N_p	[illegible]	[illegible]	[illegible]

With all the required numbers available the A and B matrices are produced for the desired load factors 1, 2, and 3G's in Tables 2-6, 2-7, and 2-8 respectively.

Table 2-6

BASIC A AND B MATRICES 1G

A-MATRIX

-.011	4.60561	0	-32.1725	0	0	0	0
-1.7E-04	-1.00849	.99822	0	0	0	0	0
2E-04	-7.95895	-.70965	0	0	0	0	0
0	0	1	0	0	0	0	0
0	0	0	0	-.1619	.07678	-.99485	.05054
0	0	0	0	-26.74221	-2.44543	.84871	0
0	0	0	0	3.61883	-.09983	-.46702	0
0	0	0	0	0	1	.01624	0

B-MATRIX

0	0	0
-.13471	0	0
-15.93334	0	0
0	0	0
0	.04532	0
0	7.81296001	-18.4286
0	-4.65753	.45114
0	0	0

Table 2-7

BASIC A AND B MATRICES 2G

A-MATRIX

-.01629	-47.41174	0	-31.89824	27.72112	.13277	-1.00682	-3.60219
-2.1E-04	-1.01135	.99822	3.33E-03	5.86E-03	7.8E-04	2.1E-04	-.04344
2E-04	-7.95962	-.70965	-3.9E-04	-6.8E-04	.03987	-6.56E-03	5.03E-03
0	0	.4903	0	0	0	-.87155	-.09705
-7E-05	-5.83E-03	0	-5.78E-03	-.1619	.13121	-.99914	.02464
0	0	-.02712	0	-31.11617	-2.70358	1.15497	0
0	0	5.02E-03	0	2.58697	-.19554	-.47212	0
0	0	.11428	.08855	0	1	.06429	0

B-MATRIX

0	.02264	0
-.13471	-3E-05	0
-15.93334	0	0
0	0	0
0	.04532	0
0	8.41085	-18.59192
0	-4.55313	.34535
0	0	0

Table 2-8

BASIC A AND B MATRICES 3G

A-MATRIX

-.03219	-129.25338	0	-31.42671	29.99142	.22491	-1.20113	-5.51601
2.8E-04	-1.01903	.99822	6.34E-03	.01812	9.1E-04	5.4E-04	-.04662
2.1E-04	-1.95777001	-.70965	-2.3E-04	-2.1E-03	.0419	-.02013	5.4E-03
0	0	.00727	0	0	0	-.95159	-.14093
-7E-05	-.01812	0	8.9E-03	-.17485	.18419	-.98091	.01531
0	0	-.02848	0	-32.01253	-2.21356	1.38213	0
0	0	.01516	0	2.18127	-.16626	-.48117	0
0	0	.17722	.14595	0	1	.05741	0

B MATRIX

0	.02675	0
-.13471	-2E-05	0
-15.9-324	0	0
0	0	0
0	.04532	0
0	6.09363	-15..217
0	-4.67322	.17245
0	0	0

Up to this point the programs used are for any conventional aircraft, given a data package in stability axes, to generate A and B matrices in body axes for an aircraft in turning or straight and level flight. The limitation at this point is the flight control system is not included, and depending on the intended use of these matrices they may or may not be sufficient. Since the intent of this work is to compare analytical and flight test data, the flight control system must be modeled.

Incorporation of the A-7D Flight Control System

A description of the A-7D flight control system, including simplified block diagrams and detailed development of the differential equations describing the system are presented in Appendix C.

Elements with bandwidth greater than or equal to 20 rad/sec, which included the actuator dynamics, were ignored. Control system limiters

[illegible] matrices only being valid for small inputs.

The Augmented AMAT HMAT/Ver 2 program (Appendix D) uses these flight control state equations to supplement the original A and B matrices already generated. A summary of these equations are repeated here for convenience, and the definitions of the notation can be found in Appendix C or the "List of Symbols".

Pitch Axis:

All δ_e's in the original equations will be replaced by

$$\delta_e = K_T\delta_{em_2} + \delta_{e_2} + .25q \tag{2.30}$$

The mechanical pitch path equation is

$$\dot{\delta}_{em_2} = .5[\delta_{ep} + 9.6\dot{q} - .0855a_Z] - .5K_{f_s}\delta_{em_2} \tag{2.31}$$

and the control augmentation path is described by

$$\dot{\delta}_{e_2} = 1.8182[.0054\ \delta_{ep} - .00054a_Z + .003794\dot{q}] - 1.8182\ \delta_{e_2} \tag{2.32}$$

Roll Axis:

All δ_a's in the original equations will be replaced by

$$\delta_a = \delta_{am_3} + \delta_{a_3} + .1p \tag{2.33}$$

Two mechanical path equations result

$$\dot{\delta}_{am_2} = 2\delta_{ap} - 12.8\ \delta_{am_2} \tag{2.34}$$

$$\dot{\delta}_{am_3} = 1.238\ \delta_{am_2} - 12.5\ \delta_{am_3} \tag{2.35}$$

The two control augmentation model equations are

$$\dot{\delta}_{a_2} = .663\ \delta_{ap} - 3\ \delta_{a_2} \tag{2.36}$$

[illegible]

Yaw Axis:

All δ_r's in the original equations will be replaced by

$$\delta_r = .001\,\delta_{rp} + .2[\delta_{am_3} + \delta_{a_3} + .1p] + \delta_{r_3} + \delta_{r_6} + .003\,\delta_{r_6}$$

The yaw stabilization mode equations are

$$\dot{\delta}_{r_3} = .25\dot{r} - .001\dot{p} - \delta_{r_3} \tag{2.38}$$

$$\dot{\delta}_{r_6} = 2a_y + 14\dot{r} - 2\delta_{r_6} \tag{2.39}$$

$$\dot{\delta}_{r_8} = .0009\delta_{r_6} \tag{2.40}$$

Total Aircraft Equations

The Augmented AMAT B1AT program finally generates a 17 x 17 A matrix and a 17 x 3 B matrix with the following state and control vectors (the δ's have been omitted).

$$\bar{X} = \begin{bmatrix} V \\ \alpha \\ q \\ \theta \\ \beta \\ p \\ r \\ \Phi \\ \delta_{em_2} \\ \delta_{e_2} \\ \delta_{am_2} \\ \delta_{am_3} \\ \delta_{a_2} \\ \delta_{a_3} \\ \delta_{r_3} \\ \delta_{r_6} \\ \delta_{r_8} \end{bmatrix} \qquad \bar{u} = \begin{bmatrix} \delta_{ep} \\ \delta_{rp} \\ \delta_{ap} \end{bmatrix} \qquad (2.41)$$

(pilot inputs in pounds)

The following sets of A and B matrices are presented by load factor (1, 2, and 3G), with three different A and B matrices under each load factor (Tables 2-9 through 2-17). The first set under each load factor represents the A-7D with only the mechanical flight control path; the second set represents the A-7D with both the mechanical and control augmentation system (Yaw Stabilization and Control Augmentation - ON) which is the normal aircraft state; the third set is a special case for

rudder inputs (full augmentation except lateral acceleration feedback disconnected). Since the lateral acceleration feedback path is deactivated when the rudder pedal is deflected more than .02 radians, this case allowed rudder doublet inputs. The output of this rudder doublet was then used as initial conditions for the fully augmented model. Linear systems analysis techniques will be applied to these sets of matrices in the next chapter.

A-MATRIX

-.011	4.60561	0	-32.1725	0	0	0	0	0	0	0	0	0	0	0	0	0
-1.7E-04	-1.02849	.99622	0	0	0	0	0	-6.74E-02	-.13471	0	0	0	0	0	0	0
2E-04	-7.95875	-.70965	0	0	0	0	0	-.79667	-15.93334	0	0	0	0	0	0	0
0	0	1	0	0	0	0	0	0	0	0	0	0	0	0	0	0
0	0	0	0	-.1619	.07678	-.99485	.05054	0	0	0	0	0	0	04532	1.4E-04	.04532
0	0	0	0	-26.74231	-2.44543	.84871	0	0	0	0	-18.4286	0	-18.4286	7.8129e001	.02344	7.8129e001
0	0	0	0	3.61883	-.09883	-.46702	0	0	0	0	.45114	0	.45114	-4.65753	-.01397	-4.65753
0	0	0	0	0	1	.07624	0	0	0	0	0	0	0	0	0	0
5.5e-02	-.03333	-3.33417	0	0	0	0	0	-19.64178	-72.83557	0	0	0	0	0	0	0
0	0	0	0	0	0	0	0	0	-1.8182	0	0	0	0	0	0	0
0	0	0	0	0	0	0	0	0	0	-12.8	0	0	0	0	0	0
0	0	0	0	0	0	0	0	0	0	1.238	-12.5	0	0	0	0	0
0	0	0	0	0	0	0	0	0	0	0	0	-3	0	0	0	0
0	0	0	0	0	0	0	0	0	0	0	0	10	-10	0	0	0
0	0	0	0	0	0	0	0	0	0	0	0	0	0	-1	0	0
0	0	0	0	0	0	0	0	0	0	0	0	0	0	0	-2	0
0	0	0	0	0	0	0	0	0	0	0	0	0	0	0	9E-04	0

B MATRIX

0	0	0
0	0	0
0	0	0
0	0	0
0	5E-05	0
0	7.81E-02	0
0	-4.88E-03	0
0	0	0
.5	0	0
0	0	0
0	0	0
0	0	0
0	0	0
0	0	0
0	0	0
0	0	0

Table 2-9

1G MECHANICAL FLIGHT CONTROL A AND B MATRICES

A-MATRIX

[illegible]	[illegible]	0	[illegible]	0	0	0	0	0	0	0	0	0	0	0	0	0
[illegible]	[illegible]	[illegible]	0	0	0	0	0	-6.74E-02	-.13471	0	0	0	0	0	0	0
[illegible]	[illegible]	[illegible]	0	0	0	0	0	-.37867	-15.93324	0	0	0	0	0	0	0
0	0	0	0	0	0	0	0	0	0	0	0	0	0	0	0	0
0	0	0	0	-.1619	.07768	-.99485	.05054	0	0	0	9.06E-03	0	9.06E-03	.04532	1.4E-04	.04532
0	0	0	0	-26.74221	-4.13204	.84871	0	0	0	0	-16.86601	0	-16.86601	7.81296001	.02344	7.81296001
0	0	0	0	3.61885	-.14687	-.48721	0	0	0	0	-.48036	0	-.48036	-4.65753	-.01397	-4.65752
0	0	0	0	0	1	.07624	0	0	0	0	0	0	0	0	0	0
5.5E-02	-22.90229	-21.51336	0	0	0	0	0	-19.64178	-72.82557	0	0	0	0	0	0	0
1.1E-04	.57139	-9.1E-03	0	0	0	0	0	-1.31E-03	-1.84441	0	0	0	0	0	0	0
0	0	0	0	0	0	0	0	0	0	-12.8	0	0	0	0	0	0
0	0	0	0	0	0	0	0	0	0	1.238	-12.5	0	0	0	0	0
0	0	0	0	0	0	0	0	0	0	0	0	-5	0	0	0	0
0	0	0	0	0	0	0	0	0	0	0	0	10	-10	0	0	0
0	0	0	0	.19987	8.74E-03	-.12659	0	0	0	0	.06544	0	.06544	-2.25033	-3.75E-03	-1.25033
0	0	0	0	-154.85287	.05241	-3.6596	0	0	0	0	4.78177	0	4.78177	-7.67115	-2.02301	-7.67115
0	0	0	0	0	0	0	0	0	0	0	0	0	0	0	9E-04	0

B-MATRIX

0	0	0
0	0	0
0	0	0
0	0	0
0	5E-05	0
0	7.81E-03	0
0	-4.66E-03	0
0	0	0
.5	0	0
9.81E-01	0	0
0	0	0
0	0	0
0	0	.063
0	0	0
0	-1.25E-01	0
0	-5.67E-03	0
0	0	0

Table 2-10

1G FULLY AUGMENTED FLIGHT CONTROL A AND B MATRICES

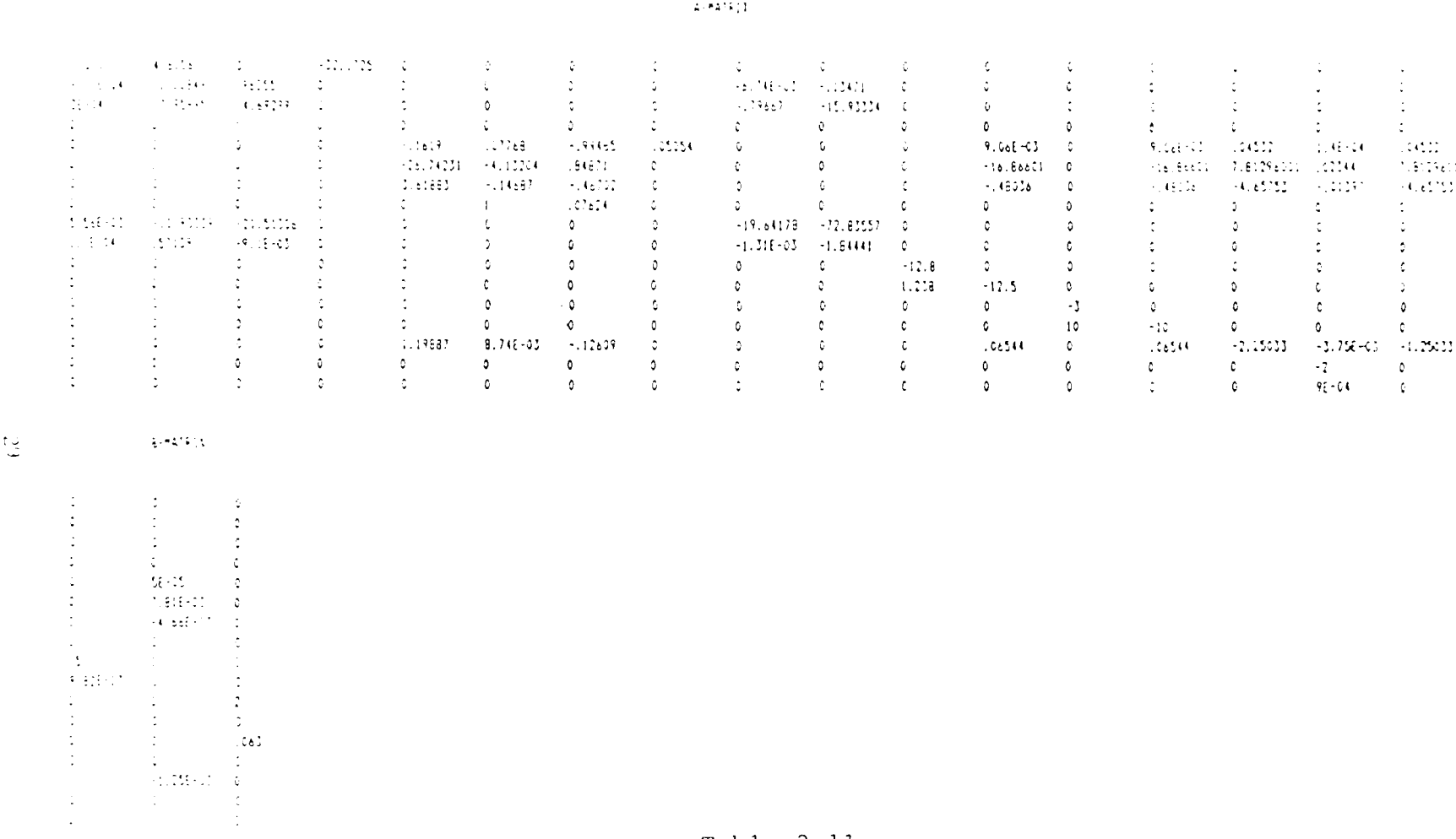

Table 2-11

1G PARTIALLY AUGMENTED FLIGHT CONTROL A AND B MATRICES

A-MATRIX

[illegible]	[illegible]		[illegible]	[illegible]	[illegible]	-1.00682	-3.60219	0	0	0	0	0	0	.02264	[illegible]E-05	.02264
[illegible]E-04	[illegible]	.99522	[illegible]E-02	5.66E-03	7.8E-04	3.1E-04	-.04344	[illegible]	[illegible]	0	0	0	0	-1E-05	0	[illegible]E-05
[illegible]	[illegible]	[illegible]	[illegible]E-04	-6.8E-04	.03987	-6.56E-03	5.03E-03	[illegible]	-15.93334	0	0	0	0	0	0	[illegible]
0	0	[illegible]	0	0	0	-.87155	-.06705	0	0	0	0	0	0	0	0	[illegible]
[illegible]	[illegible]	0	[illegible]	[illegible]	.13121	-.98914	.02464	0	0	0	0	0	0	.04502	[illegible]E-04	.04502
0	0	[illegible]	0	[illegible]	-2.70258	1.15497	0	0	0	0	-18.59192	0	-18.59192	8.41085	[illegible]	8.41085
0	0	[illegible]	0	[illegible]	-.19554	[illegible]	0	0	0	0	.34535	0	.34535	-4.55313	[illegible]	-4.55313
0	0	[illegible]	[illegible]	0	[illegible]	.06429	0	0	0	0	0	0	0	0	0	0
[illegible]E-02	[illegible]	[illegible]	[illegible]E-02	-3.26E-02	.19139	-.03151	.02415	-21.4642	-72.85601	0	0	0	0	1E-05	0	1E-05
0	0	0	0	0	0	0	0	0	-1.8182	0	0	0	0	0	0	0
0	0	0	0	0	0	0	0	0	0	-12.8	0	0	0	0	0	0
0	0	0	0	0	0	0	0	0	0	1.728	-12.5	0	0	0	0	0
0	0	0	0	0	0	0	0	0	0	0	0	-3	0	0	0	0
0	0	0	0	0	0	0	0	0	0	0	0	10	-10	0	0	0
0	0	0	0	0	0	0	0	0	0	0	0	0	0	-1	0	0
0	0	0	0	0	0	0	0	0	0	0	0	0	0	0	-2	0
0	0	0	0	0	0	0	0	0	0	0	0	0	0	0	9E-04	0

B-MATRIX

[illegible]	[illegible]	[illegible]
[illegible]	[illegible]	[illegible]
[illegible]	[illegible]	[illegible]
[illegible]	[illegible]	[illegible]
[illegible]	[illegible]	[illegible]
[illegible]	[illegible]	[illegible]
[illegible]	[illegible]	[illegible]
[illegible]	[illegible]	[illegible]
[illegible]	[illegible]	[illegible]
[illegible]	[illegible]	[illegible]
[illegible]	[illegible]	[illegible]
[illegible]	[illegible]	[illegible]
[illegible]	[illegible]	[illegible]
[illegible]	[illegible]	[illegible]
[illegible]	[illegible]	[illegible]
[illegible]	[illegible]	[illegible]
[illegible]	[illegible]	[illegible]

Table 2-12

?? MECHANICAL FLIGHT CONTROL A AND B MATRICES

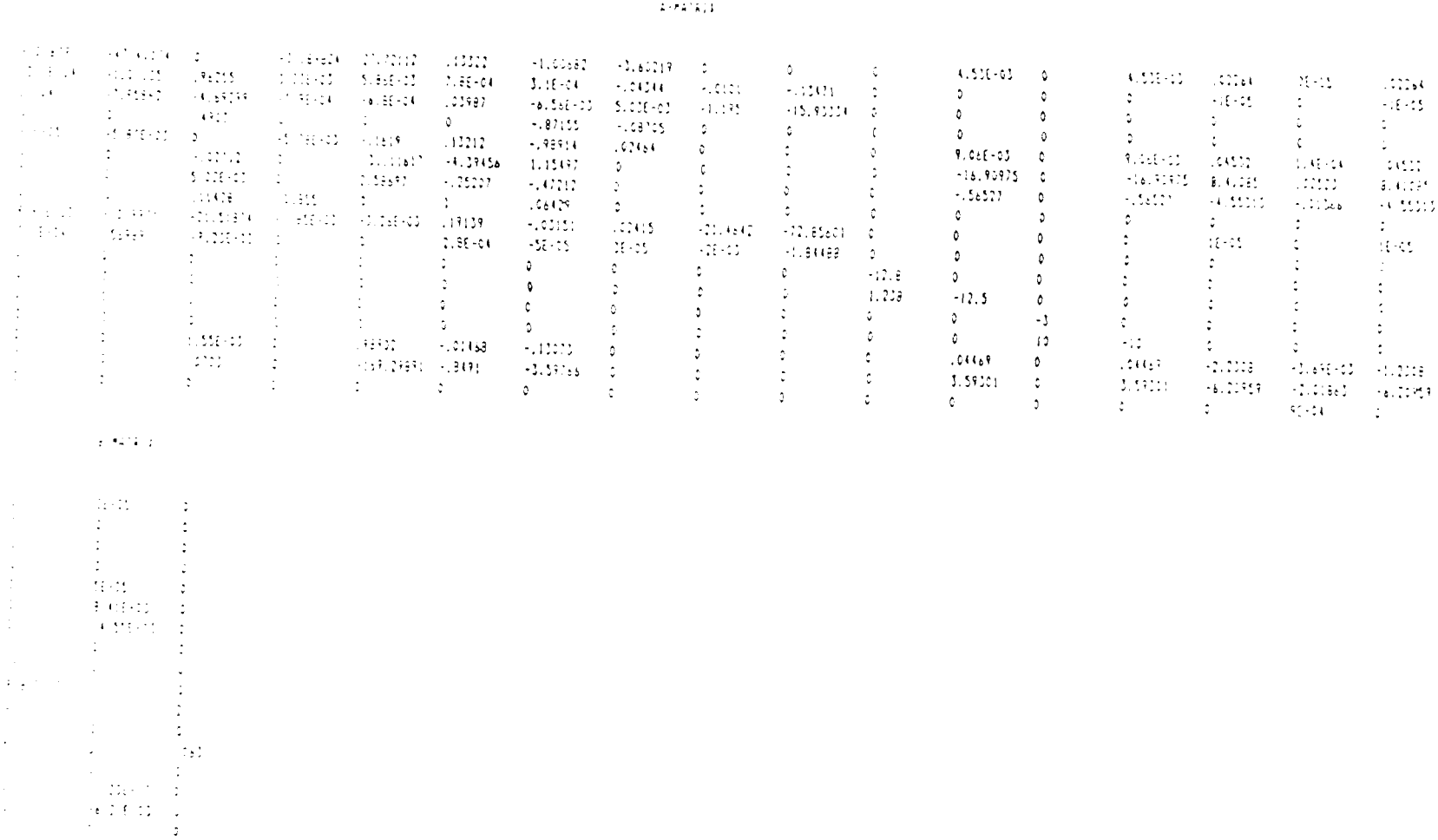

Table 2-13

2G FULLY AUGMENTED FLIGHT CONTROL A AND B MATRICES

A-MATRIX

[illegible]	-47.41174	0	-31.84824	27.72112	.13322	-1.00682	-3.60219	0	0	0	4.53E-03	0	4.53E-03	.02264	7E-05	.02264
[illegible]	-1.01125	.96255	3.37E-03	5.96E-03	7.8E-04	3.1E-04	-.04344	-.0101	-.13471	0	0	0	0	-1E-05	0	-1E-05
2E-04	-7.95662	4.69299	-3.9E-04	-6.9E-04	.03987	-6.56E-03	5.03E-03	-1.195	-15.93334	0	0	0	0	0	0	0
0	0	.4903	0	0	0	-.87155	-.08705	0	0	0	0	0	0	0	0	0
-7E-05	-5.83E-03	0	-5.73E-03	-.1619	.13212	-.98914	.02464	0	0	0	9.06E-03	0	9.06E-03	.04532	1.4E-04	.04532
0	0	-.02712	0	-31.11617	-4.39456	1.15497	0	0	0	0	-16.90975	0	-16.90975	8.41085	.02523	8.41085
0	0	5.02E-03	0	2.58697	-.25207	-.47212	0	0	0	0	-.56527	0	-.56527	-4.55313	-.01366	-4.55313
0	0	.11429	.08855	0	1	.06429	0	0	0	0	0	0	0	0	0	0
9.91E-03	-10.9971	-21.51874	-1.85E-03	-3.26E-03	.19139	-.03151	.02415	-21.4642	-72.85601	0	0	0	0	1E-05	0	1E-05
[illegible]	.56989	-9.23E-03	0	0	2.8E-04	-5E-05	3E-05	-2E-03	-1.84488	0	0	0	0	0	0	0
0	0	0	0	0	0	0	0	0	0	-12.8	0	0	0	0	0	0
0	0	0	0	0	0	0	0	0	0	1.238	-12.5	0	0	0	0	0
0	0	0	0	0	0	0	0	0	0	0	0	-3	0	0	0	0
0	0	0	0	0	0	0	0	0	0	0	0	10	-10	0	0	0
0	0	1.55E-03	0	.98902	-.01468	-.13073	0	0	0	0	.04469	0	.04469	-2.2306	-3.69E-03	-1.2308
0	0	0	0	0	0	0	0	0	0	0	0	0	0	0	-2	0
0	0	0	0	0	0	0	0	0	0	0	0	0	0	0	9E-04	0

B-MATRIX

0	2E-05	0
0	0	0
0	0	0
0	0	0
0	5E-05	0
0	8.41E-03	0
0	-4.55E-03	0
0	0	[illegible]
[illegible]	0	0
[illegible]	0	0
0	0	0
0	0	0
0	0	[illegible]
0	0	0
0	[illegible]	0
0	0	0
0	0	0

Table 2-14

2G PARTIALLY AUGMENTED FLIGHT CONTROL A AND B MATRICES

A-MATRIX

[illegible]	-109.35338	0	-31.42621	29.99342	.22491	-1.20113	-5.51601	0	0	0	0	0	0	.02675	8E-05	.02675
[illegible]	-1.01903	.99622	6.34E-03	.01812	9.1E-04	5.4E-04	-.04662	-.01347	-.13471	0	0	0	0	-2E-05	0	-2E-05
[illegible]	[illegible]	-.70965	-7.3E-04	-2.1E-01	.0418	-.02013	5.4E-03	-1.59333	-15.93334	0	0	0	0	0	0	0
0	0	.22727	0	0	0	-.95159	-.14093	0	0	0	0	0	0	0	0	0
[illegible]	-.01812	0	-8.4E-03	-.17485	.18419	-.98091	.01531	0	0	0	0	0	0	.04532	1.4E-04	.04532
0	0	-.03848	0	-32.01253	-2.31356	1.38213	0	0	0	0	-15.1317	0	-15.1317	6.08363	.01825	6.08363
0	0	.01516	0	3.18227	-.16626	-.48117	0	0	0	0	.17345	0	.17345	-4.67322	-.01402	-4.67322
0	0	.17772	.14585	0	1	.05741	0	0	0	0	0	0	0	0	0	0
[illegible]	[illegible]	-3.3556i	-3.53E-03	-.01507	.20062	-.09661	.02592	-23.29871	-72.88712	0	0	0	0	1E-05	0	1E-05
0	0	0	0	0	0	0	0	0	-1.8182	0	0	0	0	0	0	0
0	0	0	0	0	0	0	0	0	0	-12.8	0	0	0	0	0	0
0	0	0	0	0	0	0	0	0	0	1.238	-12.5	0	0	0	0	0
0	0	0	0	0	0	0	0	0	0	0	0	-3	0	0	0	0
0	0	0	0	0	0	0	0	0	0	0	0	10	-10	0	0	0
0	0	0	0	0	0	0	0	0	0	0	0	0	0	-1	0	0
0	0	0	0	0	0	0	0	0	0	0	0	0	0	0	-2	0
0	0	0	0	0	0	0	0	0	0	0	0	0	0	0	9E-04	0

B-MATRIX

0	3E-05	0
0	0	0
0	0	0
0	0	0
0	5E-05	0
0	9.5E-03	0
0	4.4E-03	0
0	.	0
0	.	0
0	.	0
0	.	0
0	.	0
0	.	0
0	.	0
0	.	0
0	.	0

Table 2-15

3G MECHANICAL FLIGHT CONTROL A AND B MATRICES

A-MATRIX

		0			.22545			0	0	0		0		.02675		.02675
		.96255								0	0	0	0		0	
										0	0	0	0	0	0	0
		.30737	0		0			0	0	0	0	0	0	0	0	0
	0	-.02848	0					0	0	0		0				
	0	.01516	0					0	0	0		0				
	0	.17772			1			0	0	0	0	0	0	0	0	0
										0	0	0	0		0	
										0	0	0	0	0	0	0
	0	0	0	0	0	0	0	0	0	-12.8	0	0	0	0	0	0
	0	0	0	0	0	0	0	0	0	1.228	-12.5	0	0	0	0	0
	0	0	0	0	0	0	0	0	0	0	0	-3	0	0	0	0
	0	0	0	0	0	0	0	0	0	0	0	10	-10	0	0	0
	0															
	0	.21217	0					0	0	0	0	.8501	0	.8501		
	0	0	0	0	0	0	0	0	0	0	0	0	0	0		0

B-MATRIX

		0
	0	0
	0	0
	0	0
		0
		0
		0
		0
	0	0
	0	0
	0	0
	0	.063
	0	0
		0
		0
		0

Table 2-16

3G FULLY AUGMENTED FLIGHT CONTROL A AND B MATRICES

A-MATRIX

[illegible]	[illegible]	0	[illegible]	[illegible]	.22545	-1.20113	-5.51601	0	0	0	5.25E-03	0	[illegible]	[illegible]	[illegible]
[illegible]	[illegible]	.96355	[illegible]	[illegible]	9.1E-04	5.4E-04	-.04662	-.01347	-.12471	0	0	0	0	-25-05	0	2E-05
[illegible]	[illegible]	-4.69299	[illegible]	[illegible]	.0418	-.02013	5.4E-03	-1.59333	-15.93334	0	0	0	0	.	0	.
0	0	.20737	0	0	0	-.95159	-.14093	0	0	0	0	0	0	0	0	0
[illegible]	-.01862	0	[illegible]	[illegible]	.1851	-.98091	.01531	0	0	0	9.06E-03	0	9.06E-03	.24522	1.4E-04	.24522
.	0	-.02848	0	-20.01253	-3.70505	1.38213	0	0	0	0	-13.91497	0	-13.91497	6.08262	.01825	6.08262
0	0	.01516	0	3.19027	-.24238	-.48117	0	0	0	0	-.7612	0	-.7612	-4.67322	-.01402	-4.67322
0	0	.17772	.14585	0	1	.05741	0	0	0	0	0	0	0	0	0	0
.01429	-10.67091	-21.52739	-3.52E-03	-.01907	.20062	-.09661	.02592	-23.28871	-72.89712	0	0	0	0	1E-05	0	1E-05
[illegible]	.57729	-9.43E-03	-1E-05	-1E-05	2.9E-04	-1.4E-04	4E-05	-2.74E-03	-1.84559	0	0	0	0	0	0	0
0	0	0	0	0	0	0	0	0	0	-12.8	0	0	0	0	0	0
0	0	0	0	0	0	0	0	0	0	1.238	-12.5	0	0	0	0	0
0	0	0	0	0	0	0	0	0	0	0	0	-3	0	0	0	0
0	0	0	0	0	0	0	0	0	0	0	0	10	-10	0	0	0
0	0	4.1E-03	0	1.14721	-.01984	-.1355	0	0	0	0	-.03723	0	-.03723	-2.23523	-3.71E-03	-1.23523
0	0	0	0	0	0	0	0	0	0	0	0	0	0	0	-2	0
0	0	0	0	0	0	0	0	0	0	0	0	0	0	0	9E-04	0

B-MATRIX

[illegible]	[illegible]	0
0	[illegible]	0
[illegible]	0	0
[illegible]	[illegible]	0
[illegible]	[illegible]	0
[illegible]	[illegible]	0
[illegible]	[illegible]	0
[illegible]	0	0
[illegible]	[illegible]	0
[illegible]	[illegible]	0
[illegible]	[illegible]	0
[illegible]	[illegible]	0
[illegible]	0	0
[illegible]	[illegible]	.063
[illegible]	[illegible]	0
[illegible]	[illegible]	[illegible]
[illegible]	[illegible]	[illegible]
[illegible]	[illegible]	[illegible]

Table 2-17

3G PARTIALLY AUGMENTED FLIGHT CONTROL A AND B MATRICES

III. Analytical Prediction of Load Factor Effects on Aircraft Handling Qualities

Introduction

The purpose of this chapter is to use linear systems analysis on the derived matrices to predict the effect of load factor on aircraft handling qualities. Information will be extracted from the eigenvalues, eigenvectors, Bode plots, and time histories to predict the load factor effects on aircraft handling qualities. These load factor effects are shown for three different cases: the basic aircraft with no flight control system included; the aircraft with just the mechanical flight control path operating; and the aircraft with the mechanical and control augmentation paths operating, which is referred to as the fully augmented case. This chapter ends with an overall analytical prediction of what the pilot should experience while flight testing at 1G, 2G and 3G's.

Eigenvalues

The five basic dynamic modes of aircraft motion are of course the phugoid, short period, dutch roll, spiral, and roll modes. The eigenvalues of the A matrix identify these modes and provide frequency and damping information for the oscillatory modes and time constant information for the aperiodic modes. The eigenvalues for the different A matrices in this paper were obtained using Control [Ref 6]. The three cases given are the basic system prior to including the flight control system, the system including only the mechanical flight control path,

and the fully augmented system which includes the mechanical and control augmentation paths. In these last two cases additional eigenvalues relating to the flight control dynamics have been omitted.

Several types of information can be extracted from the data provided in Table 3-1. The effect of load factor and flight control configuration on pole location is shown in Figure 3-1.

The phugoid mode becomes less stable as the flight control system is added, which is attributed to the pitch system bob weights sensing small changes in normal and pitching accelerations. As load factor increases for a given flight control configuration frequency increases and damping starts to increase approaching 2G's and then decreases as 3G's is approached. The destablizing effect of the flight control system is exaggerated with increasing load factor resulting in the poles migrating to the right half plane with full augmentation.

The short period mode very slightly experiences a decrease in frequency and damping with just the mechanical flight control path operating but with full augmentation the frequency returns to it basic value and damping doubles. Increasing load factor has different effects depending on the flight control configuration. Frequency remains fixed with the basic and fully augmented aircraft, but decreased with just the mechanical path operating. Damping increases slightly for the basic aircraft, but decreases with the mechanical and fully augmented cases.

The dutch roll mode is essentially the same for the basic and mechanical path cases. With the fully augmented case the frequency decreases and damping increases. As load factor increases the frequency and damping both increase causing a migration of the dutch roll poles toward the short period poles.

Table 3-1

MODAL CHARACTERISTICS

Modes	Parameters											
	Eigenvalues (λ)			Frequency (ω_n)			Damping (ζ)			Period (T_i)		
	1G	2G	3G	1G	2G	3G	1G	2G	3G	1G	2G	3G
Phugoid												
Basic	-.0053 ± i .0759	-.0121 ± i .1124	-.0088 ± i .1574	.0761	.1131	.1577	.0694	.1074	.0558	82.78	55.90	39.92
Mechanical	-.0050 ± i .0703	-.0111 ± i .1080	-.0052 ± i .1543	.0710	.1085	.1544	.0705	.1020	.0338	88.62	58.16	40.72
Full Aug	-.0047 ± i .0510	.0008 ± i .0955	.0032 ± i .1451	.0512	.0955	.1451	.0912	-.0084	-.0219	123.20	65.79	43.30
Short Period												
Basic	-.8593 ± i 2.811	-.8621 ± i 2.810	-.8667 ± i 2.806	2.939	2.939	2.937	.2923	.2933	.2951	2.235	2.236	2.239
Mechanical	-.8017 ± i 2.717	-.7835 ± i 2.681	-.7754 ± i 2.655	2.833	2.793	2.766	.2830	.2806	.2804	2.313	2.344	2.367
Full Aug	-1.733 ± i 2.386	-1.653 ± i 2.433	-1.586 ± i 2.477	2.949	2.941	2.942	.5876	.5619	.5393	2.633	2.532	2.537
Dutch Roll												
Basic	-.3338 ± i 2.357	-.4649 ± i 2.490	-.6147 ± i 2.884	2.381	2.533	2.949	.1402	.1835	.2085	2.665	2.524	2.179
Mechanical	-.3338 ± i 2.356	-.4647 ± i 2.490	-.6134 ± i 2.884	2.381	2.533	2.948	.1402	.1835	.2080	2.665	2.523	2.179
Full Aug	-.6321 ± i 1.941	-.8412 ± i 2.060	-1.085 ± i 2.550	2.090	2.230	2.771	.3024	.3781	.3913	3.160	3.050	2.464
Spiral												
Basic	-.0321	-.0031	-.0130									
Mechanical	-.0321	-.0012	-.0035									
Full Aug	-.0769	-.0632	-.0047									
Roll												
Basic	-2.375	-2.394	-1.737									
Mechanical	-2.375	-2.394	-1.736									
Full Aug	-3.964	-3.911	-3.165									

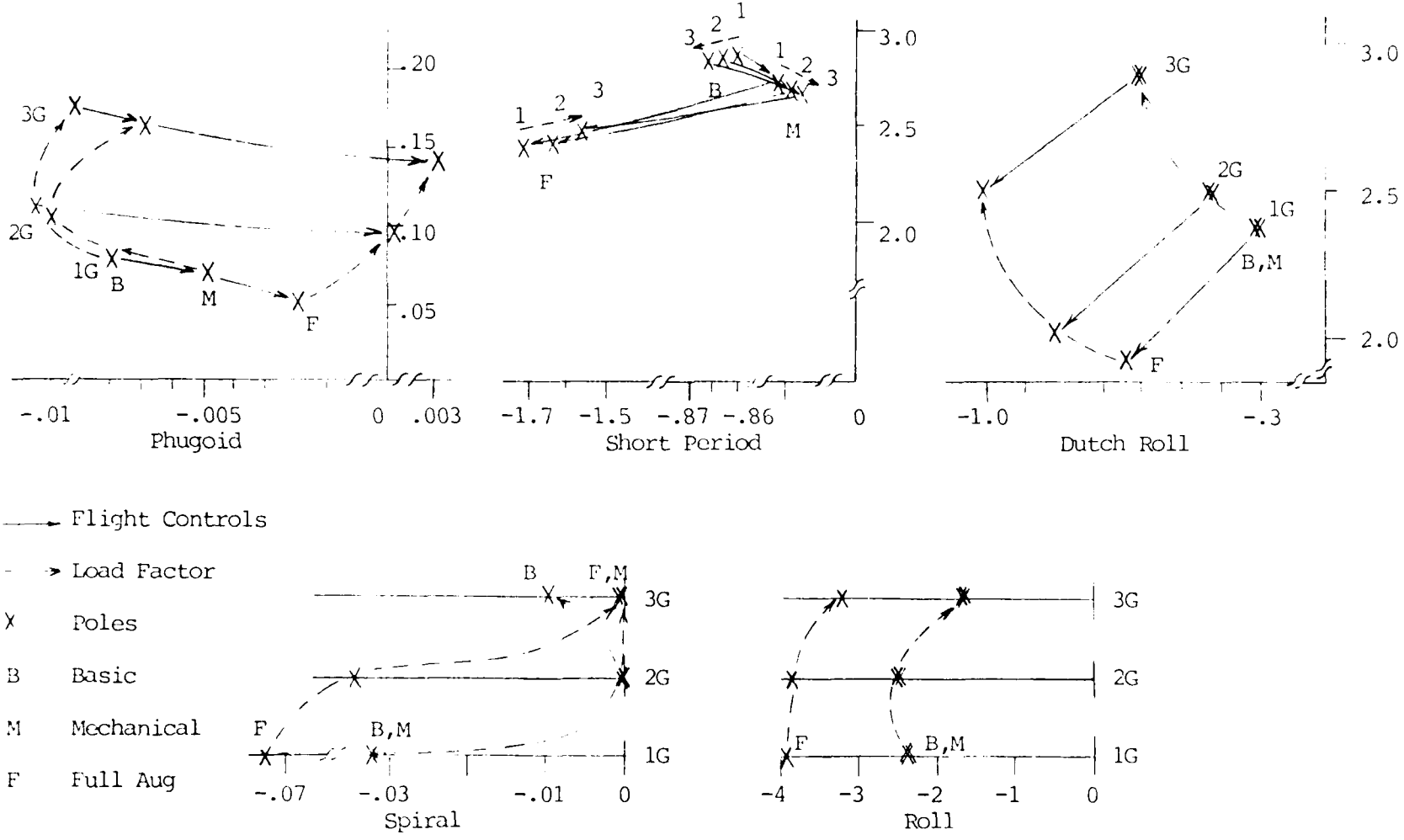

Figure 3-1. Effect of Load Factor and Flight Control Configuration on Pole Location

The spiral mode is affected differently by the flight control system depending on load factor. At 1 and 2G's the basic and mechanical path cases are nearly the same with increased stability (poles moving further left) with full augmentation. At 3G's the basic aircraft pole for the spiral starts near the 2G fully augmented location and moves to the right as the flight control system is included, resulting in a less stable spiral mode.

The roll mode is the same for the basic and mechanical path cases at a given load factor, and the roll mode time constant decreases as expected with full augmentation. As load factor is increased the roll mode time constant slightly decreases approaching 2G's and increases rapidly approaching 3G's. This rapid increase is attributed to the increase in sideslip while rolling at higher angles of attack causing a resistance to roll from C_{ℓ_β} becoming more negative.

The eigenvalue analysis has provided good insight into how the various dynamic modes change with different flight control configurations and as load factor is increased. These results can be compared with MIL-F-8785C criteria to forecast the flying qualities. Another aid available is to use the eigenvectors for predicting which variable will be dominate in each mode of the aircraft response.

Eigenvectors

The Eigenvectors corresponding to the five dynamic modes of the aircraft contain information about how much each state variable participates in the aircraft response.

An effective way to display the information contained in a complex eigenvector is the Argand diagram. Since the magnitudes of the eigenvectors are arbitrary, the Argand diagram shows the relative

lengths of each of the components making up the eigenvector. For a meaningful representation the state variables must be in nondimensional form to eliminate any scaling errors due to units. The following expressions are used to nondimensionalize V, q, p and r.

$$\hat{V} = V/V_e \tag{3.1}$$

$$\hat{q} = \bar{q}\bar{c}/2V_e \tag{3.2}$$

$$\hat{p} = pb/2V_e \tag{3.3}$$

$$\hat{r} = rb/2V_e \tag{3.4}$$

With the nondimensional variables available the magnitudes are normalized by the pitch angle, angle of attack and bank angle component magnitudes for the phugoid, short period, and dutch roll respectively, to obtain the relative length of each component. The phase angles are measured in a counter clockwise direction starting with zero degrees at the positive real axis, since the eigenvectors presented correspond to the eigenvalues with the positive imaginary part ($\omega>0$). The eigenvectors and the magnitude and phase angles are presented in Tables 3-2 through 3-6 for the various modes.

Argand diagrams are only plotted for the oscillatory modes, with primary emphasis on the short period and dutch roll modes. The diagrams are arranged by mode with 1G, 2G, and 3G cases displayed for each of the basic, mechanical, and fully augmented flight control configurations. The effect of the flight control configuration can be observed by looking vertically down the page at any given load factor, and the effect of load factor for any given flight control configuration is obtained by looking horizontally across the page.

Table 3-2

PHUGOID EIGENVECTORS

Dimensional State Variables	Eigenvectors			Non Dimensional State Variables	Magnitude/Phase		
	1G	2G	3G		1G	2G	3G
Levels							
V	118.1 + i 505.7	-170.8 + i 378.6	-395.9 + i 226.6	V	.67 / 077	.46 / 114	.32 / 150
α	.0019 + i .0043	-2.505 + i .0052	-.0060 + i .0042	α	.0038 / 067	.0041 / 116	.0033 / 145
q	.0217 + i .0964	-.0108 + i .0462	-.0364 + i .0174	q	.001 / 077	0 / 103	0 / 155
θ	1.072 - i .3674	1.280 + i .6318	1.125 + i 1.938	θ	1 / 343	1 / 026	1 / 060
β	0	.0032 - i .0048	.0053 - i .0033	β	0	.0041 / 304	.0028 / 328
p	0	-.0278 + i .0362	-.0487 + i .0235	p	0	.0010 / 128	.0010 / 154
r	0	.0186 - i .0463	.0373 - i .8112	r	0	.0011 / 292	.0010 / 311
ϕ	0	.7482 - i .8417	1.902 - i .8112	ϕ	0	.79 / 312	.92 / 337
Maximum							
V	-412.9 - i 126.3	-293.0 + i 8.121	-96.28 + i 169.6	V	.7013 / 197	.4720 / 178	.3253 / 120
α	.0063 + i .0025	.0097 - i .0006	.0049 - i .0090	α	.0070 / 022	.0010 / 356	.0109 / 299
q	-.0673 - i .0194	-.0196 + i .0087	-.0004 + i .0046	q	.0006 / 196	.0002 / 156	0 / 095
θ	-.2044 + i .9481	-.0209 + i .9785	.8022 + i .4974	θ	1 / 102	1 / 091	1 / 032
β	0	.0040 + i .0006	.0012 - i .0023	β	0	.0041 / 008	.0028 / 298
p	0	-.0314 - i .0066	-.0129 + i .0187	p	0	.0010 / 192	.0007 / 125
r	0	.0351 - i .0021	.0051 - i .0236	r	0	.0011 / 357	.0008 / 282
ϕ	0	.7638 + i .2242	.5525 - i .6936	ϕ	0	.8132 / 016	.9396 / 309
Pull Up							
V	214.4 - i 344.7	336.0 - i 102.6	-56.71 + i 224.4	V	.9777 / 302	.5232 / 343	.3414 / 104
α	-.0110 + i .0334	-.0466 + i .0163	.0072 - i .0434	α	.0600 / 121	.0466 / 161	.0412 / 279
q	.0164 - i .0289	-.0062 + i .0005	.0086 - i .0207	q	.0004 / 300	.0001 / 175	.0002 / 292
θ	-.5909 - i .2669	-.3385 - i .0030	1.009 + i .3482	θ	1 / 204	1 / 251	1 / 341
β	0	-.0032 - i .0023	.0023 - i .0019	β	0	.0036 / 217	.0028 / 321
p	0	.0152 + i .0147	-.0180 + i .0080	p	0	.0006 / 044	.0006 / 156
r	0	-.0390 + i .0200	-.0033 - i .0367	r	0	.0012 / 152	.0009 / 264
ϕ	0	-.7583 + i .1823	.3821 - i .8887	ϕ	0	.7372 / 167	.9057 / 293

Table 3-3

SHORT PERIOD EIGENVECTORS

Dimensional State Variable	Eigenvectors 1G	2G	3G	Non Dimensional State Variable	Magnitude/Phase 1G	2G	3G
Basic							
V	-21037 + i 35337	-53346 + i 47379	-56272 + i 37374	V	.0144 / 121	.0334 / 138	.0748 / 214
α	1544 + i 4220	1202 + i 3139	- 1099 + i 903.1	α	1 / 070	1 / 069	1 / 141
q	-11669 + i 5240	- 8671 + i 4059	- 2820 + i 2915	q	.0243 / 155	.0243 / 155	.0243 / 226
θ	2805 + i 3328	1046 + i 1237	-236.1 + i 418.4	θ	.9600 / 050	.4800 / 050	.3378 / 119
β	0	-23.84 + i 51.10	-70.61 + i 118.3	β	0	.0168 / 115	.0968 / 121
p	0	-235.1 - i 541.2	-626.7 - i 1258	p	0	.0054 / 247	.0302 / 244
r	0	92.66 + i 9.892	195.9 + i 34.68	r	0	0 / 006	.0043 / 010
ϕ	0	116.9 + i 365.5	-451.4 + i 538.1	ϕ	0	.1142 / 072	.4938 / 130
Mechanical							
V	2.888 + i 1.626	-.0197 - i 6.675	-9.721 - i 21.24	V	.0016 / 331	.0346 / 270	.0775 / 245
α	.3121 - i .1115	-.2832 - i .1096	-.4711 + i .0579	α	1 / 340	1 / 201	1 / 173
q	.3752 + i .8419	.2403 - i .7954	-.2633 - i 1.273	q	.0238 / 066	.0234 / 287	.0234 / 258
θ	.2506 - i .2157	-.1464 - i .0030	-.1326 + i .0775	θ	.9976 / 319	.4825 / 181	.3236 / 150
β	0	-.0032 - i .0049	-.0235 + i .0276	β	0	.0194 / 237	.0764 / 130
p	0	.0606 + i .0102	-.1035 - i .3624	p	0	.0062 / 009	.0204 / 254
r	0	-.0060 + i .0077	.0494 + i .0167	r	0	.0010 / 128	.0034 / 019
ϕ	0	-.0347 - i .0172	-.1779 + i .1147	ϕ	0	.1277 / 206	.4458 / 147
Full Aero							
V	-1.462 - i 1.024	5.967 - i 14.91	-8.362 - i 7.564	V	.0126 / 215	.0325 / 292	.0737 / 222
α	-.2257 - i .0115	-.3670 - i .6874	-.2367 + i .0464	α	1 / 183	1 / 242	1 / 169
q	.1974 - i .5403	1.950 - i .3793	.0601 - i .6162	q	.0217 / 290	.0218 / 349	.0219 / 276
θ	-.1870 + i .0535	-.2427 - i .2296	-.0588 + i .0343	θ	.8628 / 164	.4288 / 223	.2823 / 150
β	0	.0009 - i .0075	-.0074 + i .0025	β	0	.0097 / 277	.0326 / 161
p	0	.0191 + i .0675	.0406 - i .0679	p	0	.0028 / 074	.0100 / 301
r	0	-.0121 - i .0003	.0065 + i .0093	r	0	.0005 / 181	.0015 / 055
ϕ	0	-.0427 - i .0609	-.0553 + i .0223	ϕ	0	.0955 / 237	.2472 / 156

Table 3-4

DUTCH ROLL EIGENVECTORS

Dimensional State Variables	Eigenvectors 1G	2G	3G	Non Dimensional State Variables	Magnitude/Phase 1G	2G	3G
Basic							
V	0	415.5 - i 1049	2394 - i 1409	V	0	.0006 / 292	.0012 / 271
α	0	-18.37 - i 13.99	-27.99 - i 2.547	α	0	.0083 / 217	.0153 / 185
q	0	63.37 + i 57.75	-63.35 - i 34.86	q	0	.0003 / 042	.0003 / 269
θ	0	350.0 + i 84.94	-47.70 + i 219.7	θ	0	.1293 / 014	.1227 / 102
β	697.8 + i 314.7	603.0 + i 437.2	-261.1 + i 490.4	β	.2828 / 024	.2689 / 036	.3033 / 118
p	- 6093 + i 2233	- 7022 + i 1106	- 2566 - i 4805	p	.0734 / 159	.0779 / 171	.0907 / 242
r	460.5 - i 1301	373.1 - i 1183	822.8 + i 102.1	r	.0156 / 289	.0136 / 236	.0138 / 007
ϕ	1269 + i 2890	910.9 + i 2631	- 1400 + i 1181	ϕ	1 / 062	1 / 071	1 / 140
Mathematical							
V	0	-.0999 - i .0264	-.1139 - i .0419	V	0	.0008 / 195	.0013 / 200
α	0	-.0019 + i .0019	-.0011 + i .0018	α	0	.0132 / 135	.0137 / 122
q	0	-.0002 - i .0104	.0006 - i .0013	q	0	.0004 / 269	0 / 298
θ	0	-.0086 - i .0252	.0167 - i .0083	θ	0	.1287 / 251	.1183 / 334
β	-.0262 + i .0472	.0049 - i .0554	.0472 - i .0085	β	.2829 / 119	.2694 / 275	.3039 / 350
p	-.1257 - i .4415	.3367 + i .4067	-.1886 + i .4303	p	.0734 / 336	.0780 / 050	.0909 / 114
r	.0787 + i .0599	-.0897 + i .0210	-.0370 - i .0612	r	.0156 / 024	.0136 / 167	.0138 / 348
ϕ	-.1753 + i .6293	.1335 - i .1576	.1544 + i .0324	ϕ	1 / 157	1 / 310	1 / 012
Full Aero							
V	0	-.1953 - i .2571	-.3846 + i .0821	V	0	.0015 / 233	.0028 / 168
α	0	-.0086 + i .0004	-.0018 + i .0071	α	0	.0248 / 177	.0326 / 104
q	0	.0114 - i .0120	-.0089 - i .0070	q	0	.0004 / 314	.0005 / 216
θ	0	.0403 - i .0420	.0130 - i .0295	θ	0	.1678 / 314	.1447 / 294
β	.[illegible]	.0980 - i .0432	.0501 - i .0514	β	.3400 / 088	.3085 / 336	.3211 / 314
p	-.1661 - i [illegible]	-.5377 + i .5688	-.0781 + i .6224	p	.0644 / 246	.0688 / 133	.0857 / 047
r	.1010 + i [illegible]	-.0861 - i .1556	-.0991 - i .0622	r	.0180 / 028	.0156 / 241	.0161 / 212
ϕ	-.1429 + i .1.[illegible]	.3219 + i .1299	.2154 - i .0589	ϕ	1 / 139	1 / 022	1 / 345

Table 3-5

SPIRAL MODE EIGENVECTORS

Dimensional State Variables	Eigenvectors			Non Dimensional State Variables'	Magnitude/Phase		
	1G	2G	3G		1G	2G	3G
[illegible]							
V	0	-954.4	- 1731	V	0	.8646 / 180	1.717 / 180
α	0	.0006	.0023	α	0	.0004 / 0	.0015 / 0
q	0	-.2793	-.5674	q	0	.0014 / 180	.0031 / 180
θ	0	.6098	1.333	θ	0	.3515 / 0	.8384 / 0
β	-.0146	.0025	.0091	β	.0047 / 180	.0014 / 0	.0057 / 0
p	.1134	-.0179	-.0768	p	.0011 / 0	.0004 / 180	.0015 / 180
r	-.1466	.0181	.0707	r	.0015 / 180	.0004 / 0	.0014 / 0
ϕ	-3.689	-1.735	-1.592	ϕ	1 / 180	1 / 180	1 / 180
Mach Hold							
V	0	17.68	-250.4	V	0	.9971 / 0	1.930 / 180
α	0	-.0008	.0170	α	0	.0280 / 180	.0832 / 0
q	0	.0042	-.0650	q	0	.0014 / 0	.0029 / 180
θ	0	-.0103	.1615	θ	0	.3696 / 180	.7901 / 0
β	-.0046	-.0001	.0013	β	.0048 / 180	.0020 / 180	.0064 / 0
p	.0345	.0004	-.0110	p	.0011 / 0	.0004 / 0	.0017 / 180
r	-.0458	-.0004	.0161	r	.0015 / 180	.0004 / 180	.0024 / 0
ϕ	-.9665	.0280	-.2044	ϕ	1 / 180	1 / 0	1 / 180
[illegible]							
V	0	1273	1674	V	0	.6280 / 0	2.624 / 0
α	0	-.2469	-.4100	α	0	.0773 / 180	.4080 / 180
q	0	.1838	.1298	q	0	.0005 / 0	.0011 / 0
θ	0	1.923	.1488	θ	0	.6021 / 0	.1481 / 0
β	.0656	.0695	.0036	β	.0171 / 0	.0218 / 0	.0036 / 0
p	-.2616	-.3885	-.0452	p	.0025 / 180	.0037 / 180	.0014 / 180
r	.1419	-.0760	-.1060	r	.0013 / 0	.0007 / 180	.0032 / 180
ϕ	3.258	3.194	1.006	ϕ	1 / 0	1 / 0	1 / 0

Table 3-6

ROLL MODE EIGENVECTORS

Dimensional State Variables	Eigenvectors			Non Dimensional State Variables	Magnitude/Phase		
	1G	2G	3G		1G	2G	3G
Basic							
V	0	- 3170	- 2644	V	0	.0007 / 180	.0022 / 180
α	0	8.110	2.352	α	0	.0011 / 0	.0012 / 0
q	0	-335.3	-94.75	q	0	.0004 / 180	.0004 / 180
θ	0	486.2	151.6	θ	0	.0677 / 0	.0789 / 0
β	-17.47	-97.45	-36.46	β	.0022 / 180	.0136 / 180	.0189 / 180
p	18561	17096	3301	p	.0722 / 0	.0727 / 0	.0524 / 0
r	994.4	1868	530.7	r	.0039 / 0	.0079 / 0	.0084 / 0
ϕ	- 7842	- 7178	- 1921	ϕ	1 / 180	1 / 180	1 / 180
Mechanical							
V	0	-.1733	-.5704	V	0	.0008 / 180	.0024 / 180
α	0	-.0005	-.0004	α	0	.0014 / 180	.0011 / 180
q	0	-.0148	-.0175	q	0	.0004 / 180	.0005 / 180
θ	0	.0231	.0289	θ	0	.0669 / 0	.0785 / 0
β	-.0009	-.0047	-.0070	β	.0022 / 180	.0136 / 180	.0190 / 180
p	.9023	.8217	.6324	p	.0722 / 0	.0727 / 0	.0524 / 0
r	.0484	.0897	.1017	r	.0039 / 0	.0079 / 0	.0084 / 0
ϕ	-.3815	-.3456	-.3681	ϕ	1 / 180	1 / 180	1 / 180
Full Aug							
V	0	.0395	-1.658	V	0	.0003 / 0	.0114 / 180
α	0	.0051	-.0402	α	0	.0217 / 0	.1750 / 180
q	0	-.0264	.1026	q	0	.0010 / 180	.0038 / 0
θ	0	.0197	-.0433	θ	0	.0837 / 0	.1883 / 180
β	-.0046	-.0053	-.0031	β	.0187 / 180	.0226 / 180	.0136 / 180
p	.9655	.9132	-.7325	p	.1205 / 0	.1187 / 0	.0972 / 180
r	.0455	.0968	-.1451	r	.0057 / 0	.0126 / 0	.0193 / 180
ϕ	-.2444	-.2348	.2300	ϕ	1 / 180	1 / 180	1 / 180

[illegible] pitch angle variations (Figure 3-2). The eigenvector shows that as the aircraft picks up speed the aircraft rolls out of the bank and as the speed decreases the bank increases.

The short period mode at 1G is characterized primarily by changes in angle of attack and pitch angle. As load factor increases bank angle begins to participate which in turn cause some sideslip activity. This suggests that a pure longitudinal input results in some lateral-directional oscillations. This is attributed to kinematic coupling between angle of attack and sideslip (Figure 3-3).

The dutch roll mode is affected in a similar manner to the short period. As load factor increases pitch angle starts to emerge with a very small, but noticeable angle of attack presence. Roll rate also becomes slightly more active (Figure 3-4). These pitch angle and angle of attack changes are due to a pure directional input which again suggest some kinematic coupling.

The spiral mode is of little concern at other than 1G, but the roll mode can be analyzed by looking at the tabular magnitude data (Table 3-6). As load factor increases velocity and pitch angle become active as well as a small angle of attack change.

The eigenvectors have given a means to determine which state variables characterized the modes of interest as load factor changed. The Bode plot will now be used to show the effect of load factor on aircraft response vs. frequency.

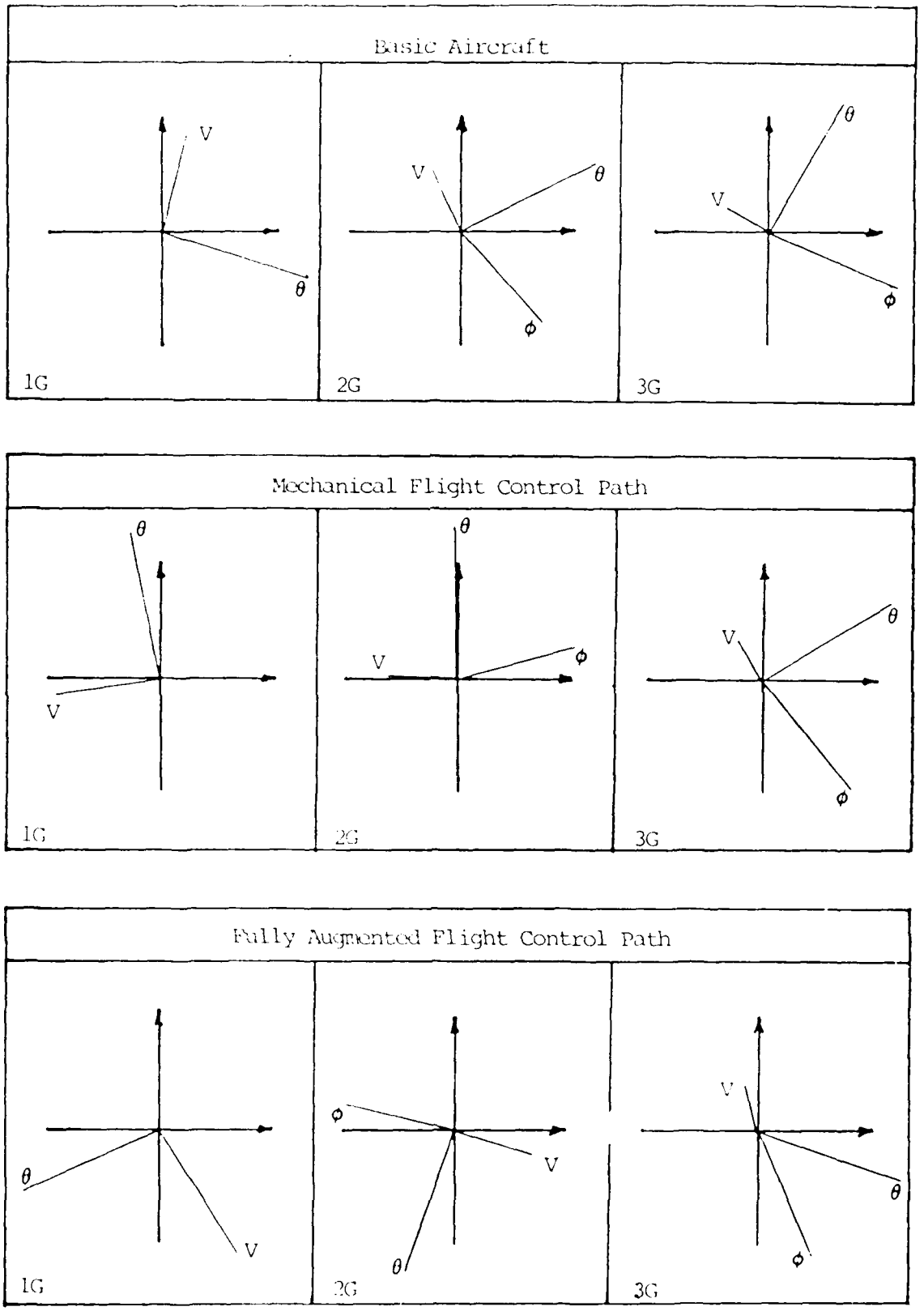

Figure 3-2. Phugoid Argand Diagrams

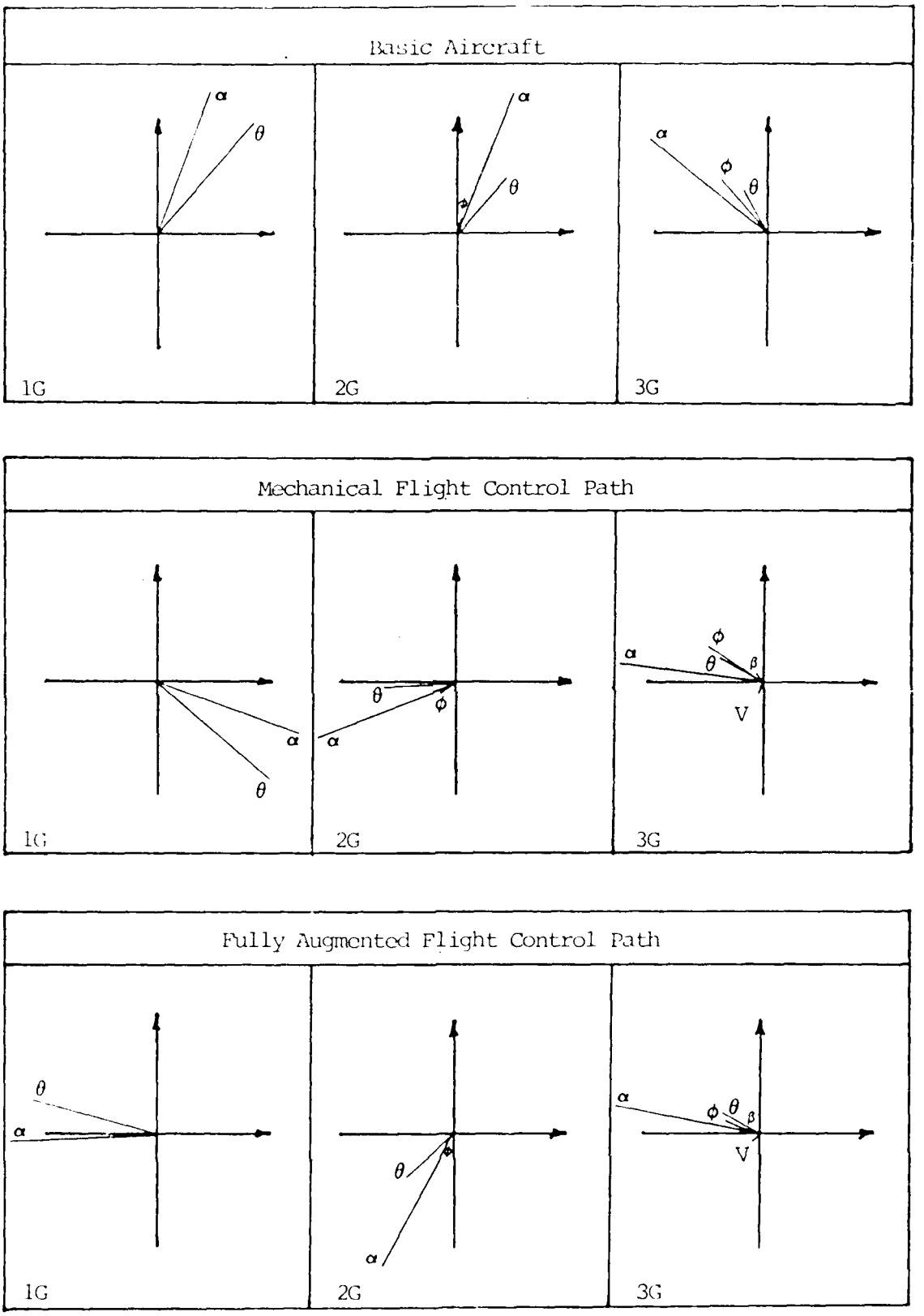

Figure 3-3. Short Period Argand Diagrams

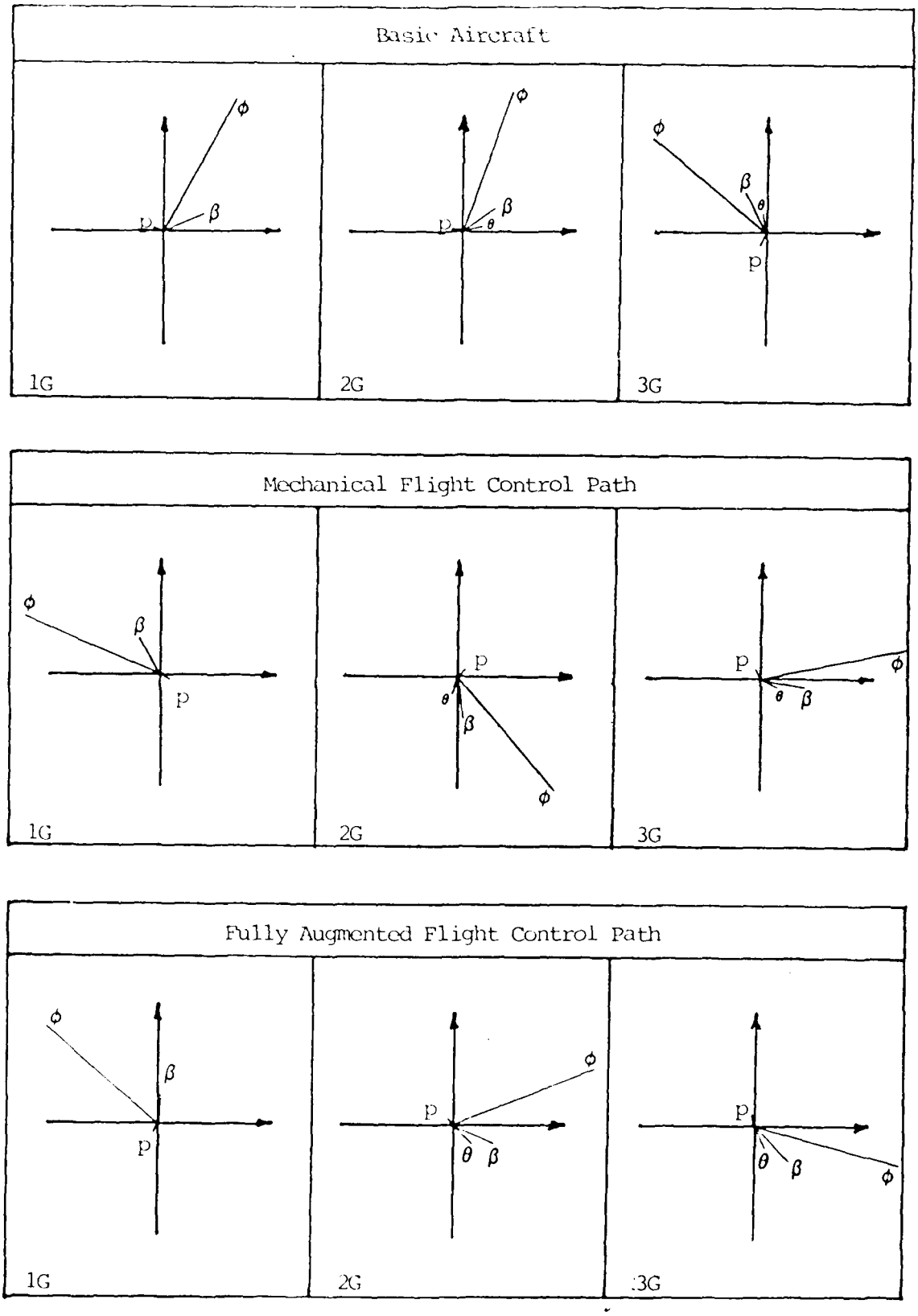

Figure 3-4. Dutch Roll Argand Diagrams

Frequency Analysis

The eigenvalue/eigenvector analysis compared the basic aircraft, to the mechanical and fully augmented flight control cases of 1G, 2G and 3G's. The frequency analysis will compare the mechanical and fully augmented cases for selected transfer functions, and will show the cross coupling for just the 3G mechanical and fully augmented cases. The three modes that will be addressed are the short period, the dutch roll and the roll mode. The bode plots presented are for transfer functions between the output and the pilot's control stick inputs in pounds. To convert the magnitude scale from output per lb of stick force to output per radian of surface deflection the following approximate numbers can be used.

		Mechanical		Fully Augmented		
$\frac{\text{output}}{\delta_{ep}}$	+	1G 56.1 dB 2G 52.6 dB 3G 50.1 dB	or	45.4 dB 44.2 dB 43.2 dB	=	$\frac{\text{output}}{\delta_{e}}$
$\frac{\text{output}}{\delta_{rp}}$	+	60.0 dB	or	60.0 dB	=	$\frac{\text{output}}{\delta_{r}}$
$\frac{\text{output}}{\delta_{ap}}$	+	36.2 dB	or	34.9 dB	=	$\frac{\text{output}}{\delta_{a}}$

These numbers were derived by combining the elements of the flight control system and evaluating the resulting transfer functions written in bode form as S→0. The transfer functions with negative gain must have 180 degrees of phase added to use the conventional 180 degree point for determining stability.

The transfer function between angle of attack and the pilot's elevator input in pounds of stick force will be used to analyze the short period mode (Figures F1 through F6). When comparing the mechanical

and fully augmented cases at all three load factors two effects are noticed. First the obvious effect is the increased damping at the short period frequency in the fully augmented cases. Secondly is the low frequency effect that results from feeding back normal acceleration which gets amplified with augmentation. As load factor increases there is very little change around the short period frequency; however, the low frequency effect is attenuated as the low frequency zeroes move closer to the phugoid poles.

Two transfer functions are used to look at the dutch roll mode, bank angle and sideslip due to pilot's rudder pedal force input in pounds (Figures F7 through F18). The fully augmented cases at all three load factors increase the damping at the dutch roll frequency as expected. As load factor increases the increased damping at the dutch roll frequency can be seen for both the mechanical and fully augmented cases. In addition a low frequency disturbance is seen similar to the short period. This is again attributed to the movement of the numerator zeroes as load factor

increases. By taking the ratio of the magnitudes of the ϕ/δ_{rp} and the β/δ_{rp} transfer functions at the dutch roll frequency an estimate of the ϕ/β ratio is obtained. For example, analysis of the 1G fully augmented bode plots shows

$$|\phi/\delta_{rp}| = -46 \text{ db} \tag{3.5}$$

$$|\beta/\delta_{rp}| = -56 \text{ db} \tag{3.6}$$

$$|\phi/\beta| = 10 \text{ db} = 3.16 \tag{3.7}$$

This agrees with the corresponding value obtained by analyzing the dutch roll mode eigenvector given in Table 3-4. For the 1G fully

augmented case, the ratio of $|\phi/\beta|$ is 1/0.34 which equales 2.94. Two transfer functions are also used to look at the roll mode, roll rate and sideslip due to pilot's aileron force input in pounds (Figure F19 through F30). The effectiveness of the augmentation can be seen by comparing Figure F19 and F20. With the addition of ARI and a_y feedback the steady state roll response becomes more uniform, as indicated by the flatter magnitude curve. The increased damping of the dutch roll mode, when augmentation is added can be seen at all three load factors. The addition of flight control augmentation at 2 and 3G's amplifies the low frequency changes. For the mechanical flight control configuration, the combination of light damping and high ϕ/β ratio cause pronounced roll rate oscillations which will also be shown in the time histories. The effect becomes much more pronounced at 3G's which can be seen by comparing Figures F19 and F27. As load factor increase, the relative pole/zero movement is shown by the phugoid cross coupling effect at low frequency and the more oscillatory dutch roll mode. The effectiveness of the ailerons to produce roll rate with no augmentation is seen to decrease as the input is held (low frequency) as load factor increases (Figure F19 and F27). The sideslip due to aileron is just the opposite and increases with load factor (Figures F21 and F29). The eigenvalue analysis showed the effect of augmentation and load factor on the characteristic roots for the different modes. With the transfer functions available the effect of augmentation and load factor on the numerator zeros can be observed. At 1G a longitudinal transfer function such as α/δ_{ep} has exact pole/zero cancellation of the lateral directional modes which results in no cross coupling. As augmentation is added new zeros appear and their effect on the frequency response

will depend on their location with respect to the new poles. As load factor is increased, the relative movement of the poles and zeros is what changes the frequency response. Poles and zeros which cancelled at 1G start to move apart which allows the cross coupling between the longitudinal and lateral-directional modes. This cross coupling is shown in Figures F31 through F46.

Simulation

Introduction. The final step in the analytical approach to this problem was to simulate the A7-D on an Apple II Plus computer. The simulation provided a means of seeing graphically the effects that were predicted using the other analytical methods. In addition these time histories were compared with the flight test strip chart time histories to validate the analysis.

The phugoid mode was not evaluated. The spiral mode was evaluated at 1G for the mechanical flight control case and the fully augmented case. All other modes were evaluated at 1G, 2G and 3G's for the mechanical, and fully augmented flight control cases. The flight control configurations and load factors evaluated were at a flight condition of 15,000 feet (Hc), 0.6 IMN. The aircraft weight was fixed at 25,338 lbs with a center of gravity at 28.71% MAC. The cruise configuration was considered with no external stores.

Method. The computer programs used for this simulation are presented in Appendix D. The A and B matrices previously derived were used to form a discrete-time model which uses the state transition matrix to propagate the states from one time increment to the next. The inputs used to obtain the various time histories are as follows:

Table 3-7

EXCITATION INPUTS

Modes	Inputs
Short Period	Pitch Doublet
Dutch Roll	Rudder Doublet
Spiral	Initial condition on bank angle of 20 degrees
Roll	Step aileron input

These inputs are the same type as used during the flight test portion of the evaluation.

Results. Time histories were generated for the above mentioned inputs using a time increment between calculations of .1 seconds. The actual duration of the time histories varied from 5 seconds to 20 seconds depending on the type of information desired. These plots are contained in Appendix G and will be discussed in Chapter V.

Analytical Predictions

From the preceding analysis the pilot can be briefed on the expected handling qualities of the aircraft as load factor increases. This information can also be used to identify areas where the pilot should look for specific occurrences that are not normally seen.

For the phugoid mode as load factor increases to 3G's the pilot should expect a divergent oscillation with a period of approximately 43 seconds, which is 75% quicker than the 1G case. Bank angle oscillations should take place along with pitch and airspeed variations. The only significance of this mode at the higher load factors is that the aircraft will be harder to trim for the equilibrium conditions.

The pilot should not see any appreciable change in the short period frequency and damping, but with the augmentation on, there should be an increased load factor sensitivity to angle of attack changes. Also, the kinematic cross coupling between angle of attack and sideslip should start to become evident at 3G's, with some bank and sideslip oscillations.

The dutch roll dynamics should be improved as load factor increases. Again, the cross coupling should cause some pitch oscillation due to lateral inputs.

The aircraft should roll a little slower at 3G's due to the increase in sideslip which resists the roll.

Overall, these cross coupling effects should increase as the size of the inputs increase.

IV. Flight Test

Introduction

This chapter presents the results of a limited flying qualities test to evaluate the effect of load factor on aircraft response/handling qualities.

The two test aircraft USAF serial numbers 67-14582 and 67-14584 were considered production representative for the purpose of this test. Both aircraft were modified with a Yaw, Angle of Attack, Pitot-Statics System (YAPS) head mounted on a flight test nose boom, a Base-10 Airborne Telemetry System, and sensitive flight instruments. The test was conducted in the cruise configuration with 6 MAU-12B/A pylon racks. The most forward and aft cg during testing were 28.2 and 28.9% MAC. The heaviest and lightest gross weight tested were 24,550 and 26,550 pounds.

The tests were flown at 15,000 ft (H_{ic}) and 0.6 IMN at 1, 2, and 3G's inaccordance with limitations specified in the TPS A-7D Flying Qualities Test Plan, the A-7D Flight Manual, and AFFTC Regulation 55-2 [Ref 7, 8, and 9].

Four test sorties (6.0 hours) were flown from 2 April 1984 to 25 May 1984 at the Air Force Flight Test Center (AFFTC), Edwards AFB, California.

Test Objectives

The test objectives are as follows:

1. Determine aircraft response at 1, 2, and 3G's for elevator and rudder doublets, and aileron impulse and step inputs.

[illegible]

[illegible]

The A-7D is a single engine, single place, transonic tactical surface attack aircraft manufactured by the Vought Aeronautics Company. It is powered by the Allison TF41-A-1 non-afterburning turbofan engine. Detailed information pertaining to the physical dimensions, areas, airfoil types, etc. are contained in Appendix D.

Test Instrumentation/Data Reduction

The test aircraft were production representative A-7D's modified with a nose-mounted Yaw, Angle of Attack, and Pitot-static (YAPS) flight test boom, a Base-10 Telemetry System (TM), and sensitive airspeed indicator, machometer, and g meter [Ref 10]. The data were recorded by on-board magnetic tape, cockpit voice recorder, and ground based strip charts via TM. Data were reduced by hand from the strip charts using the log decrement and time ratio techniques [Ref 11].

Test Methods and Condition

The aircraft response to elevator and rudder doublets, and aileron impulse and step inputs were determined by trimming the aircraft at the following conditions and applying the desired inputs.

Table 4-1

Test Matrix

CONDITIONS	Altitude (± 1000 ft) 15,000 Mach (± .02 Mach) 0.6 Weight (± 1200 lb) 25,338 Center of Gravity (-.5, +.2% MAC) 28.71					
	Load Factor	1G		2G		3G	
	Flight Control Configuration						
	Mechanical	X		X		X	
	Fully Augmented		X		X		X
INPUTS	Elevator Doublet	X	X	X	X	X	X
	Rudder Doublet	X	X	X	X	X	X
	Aileron Impulse	X	X	X	X	X	X
	Aileron Step (1/4)	X	X	X	X	X	X
	Aileron Step (1/2)	X	X	X	X	X	X
	Aileron Step (Full)	X	X	X	X	X	X

Trimming the aircraft at the 1G points was performed, using the front side method [Ref 12] where throttle controlled airspeed and elevator controlled altitude. However, at the 2 and 3G points it was necessary to modify the front side method to stabilize at the desired equilibrum conditions. Throttle was still used to control airspeed, but elevator was the primary control for load factor, while Bank angle was the primary control for altitude. Since there is only one combination of thrust, airspeed, and bank angle to stabilize at a given load factor, these trim shots required several iterations to stabilize on conditions. With just the mechanical flight control path operating there is no rudder trim available. Therefore these trim shots were performed by

AD-A152 118 THE EFFECT OF LOAD FACTOR ON AIRCRAFT HANDLING QUALITIES(U) AIR FORCE INST OF TECH WRIGHT-PATTERSON AFB OH SCHOOL OF ENGINEERING J R RIEMER 10 AUG 84 2/4

UNCLASSIFIED AFIT/GAE/AA/84J-2 F/G 20/4 NL

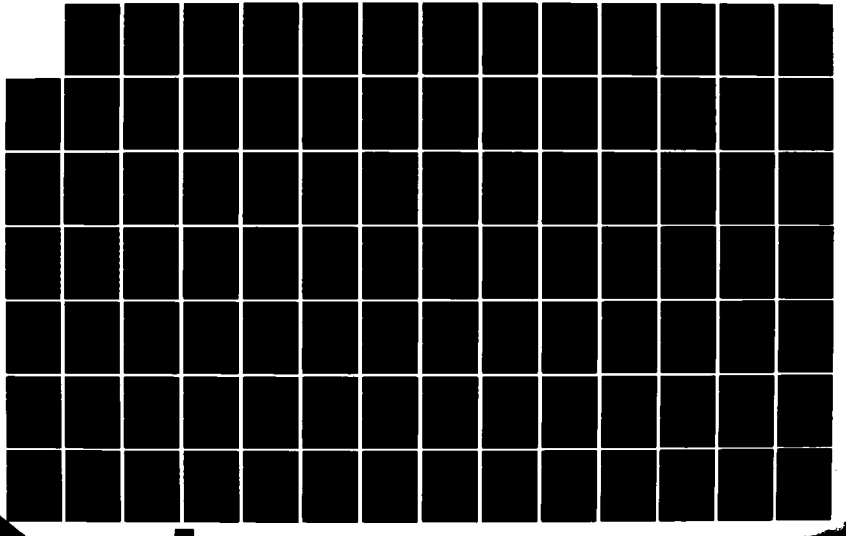

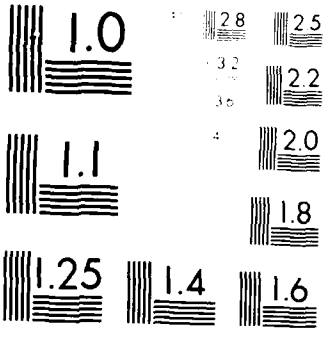

Table 4-1

Test Matrix

CONDITIONS	Altitude (± 1000 ft) 15,000 Mach (± .02 Mach) 0.6 Weight (± 1200 lb) 25,338 Center of Gravity (-.5, +.2% MAC) 28.71					
	Load Factor	1G		2G		3G	
	Flight Control Configuration						
	Mechanical	X		X		X	
	Fully Augmented		X		X		X
INPUTS	Elevator Doublet	X	X	X	X	X	X
	Rudder Doublet	X	X	X	X	X	X
	Aileron Impulse	X	X	X	X	X	X
	Aileron Step (1/4)	X	X	X	X	X	X
	Aileron Step (1/2)	X	X	X	X	X	X
	Aileron Step (Full)	X	X	X	X	X	X

Trimming the aircraft at the 1G points was performed, using the front side method [Ref 12] where throttle controlled airspeed and elevator controlled altitude. However, at the 2 and 3G points it was necessary to modify the front side method to stabiize at the desired equilibrum conditions. Throttle was still used to control airspeed, but elevator was the primary control for load factor, while Bank angle was the primary control for altitude. Since there is only one combination of thrust, airspeed, and bank angle to stabilize at a given load factor, these trim shots required several iterations to stabilize on conditions. With just the mechanical flight control path operating there is no rudder trim available. Therefore these trim shots were performed by

trimming to zero rolling moment, rather than coordinated flight. A trim shot was performed prior to each sequence of inputs. Depending on outside air temperature the thrust available at the 3G points was a limiting factor occasionally requiring a slight descent into the data band to maintain 3G's.

The parameters monitored during the test are listed in Table H2. The test was conducted in the cruise configuration with 6 MAU-12B/A pylons.

Test Results and Analysis

All test points in the Test Matrix (Table 4-1) were flown. Actual quantitative data in the form of time histories as well as qualitative comments where significant, are presented.

The equilibrum conditions obtained at 1, 2, and 3G's by trimming the aircraft in a steady level turn are as follows:

TABLE 4-2

EQUILIBRIUM CONDITIONS
15,000 ft 0.6 IMN

Load Factor (G)	Weight (lbs)	AoA (deg)	Roll Rate (deg/sec)	Pitch Rate (deg/sec)	Yaw Rate (deg/sec)	Elevator Deflection (deg)
1	26,500	4.0	0	0	0	0
2	25,370	6.7	-0.8	4.0	1.8	5.6
3	24,550	9.9	-1.5	7.4	2.4	6.6

Note: These values are generally within 10% of the prediced values.

The phugoid mode was not evaluated during this test. The modal characteristics for the short period and dutch roll are summarized

below. The frequency and damping were determined using the log decrement and time ratio methods where possible.

Table 4-3

MODAL CHARACTERISTICS (FLIGHT TEST)

Mode	Load Factor (G)	Frequency (ω_n)	Damping (ζ)	Damped Period (T_d)	n/α (g/rad)	Φ/β
Short Period	1GM	2.83	.27	2.3		-
	1GFA	-	.6*	-	22.9	-
	2GM	-	-	-	-	-
	2GFA	-	.6*	-	-	-
	3GM	-	-	-	22.5	-
	3GFA	-	.5*	-	34.9	-
Dutch Roll	1GM	2.13	.187	3.0	-	4.3
	1GFA	2.11	.303	3.2	-	3.1
	2GM	2.53	.136	2.5	-	2.3
	2GFA	-	-	-	-	-
	3GM	2.79	.206	2.3	-	3.6
	3GFA	-	-	-	-	-

*estimate by the pilot

Note: These values are generally within 10% of the predicted values.

At a load factor of one the short period response to an elevator pitch doublet for the mechanical and fully augmented flight control configurations can be seen in Figures G2 and G4. The effect of adding flight control augmentation can be seen in the UHT position trace, along with the resulting increased damping as shown by the pitch rate, pitch attitude and load factor traces. By comparing the 1, 2, and 3G fully augmented cases (Figures G4, G7, and G10) the effect of load factor on the short period dynamics can be seen to be negligible. However, the cross coupling effect can start to be seen in the 3G case (Figure G10)

by the very small sideslip oscillation. For small inputs, as those used in fine tracking, this cross coupling presented no problem from a flying qualities standpoint. However, as the inputs became larger the beta oscillations were more noticeable to the pilot which could affect the gross acquisition task. Recommend further testing to analyze this open loop cross coupling on the closed loop flying qualities (R2).

The dutch roll mode exhibited similar behavior to short period as augmentation was added (Figures G12 and G13). The effect of load factor on the dutch roll can be seen by comparing the 1 and 3G traces for the mechanical flight control configuration (Figure G12 and G21). The beta traces reveal an increase in damping. The cross coupling effect is also more pronounced as seen by the load factor, angle of attack and pitch rate variations due to the pure rudder doublet input (Figure G22).

This kinematic cross coupling although more pronounced than for the longitudinal input case still is not a problem from a flying qualities point of view for small inputs. For larger inputs these longitudinal oscillations became more apparent to the pilot for the mechanical flight control configuration, which may be equated to an aircraft with lower damping of the short period and dutch roll modes. With the augmentation engaged these longitudinal oscillations due to larger rudder doublets were more subdued resulting in less attention by the pilot.

Impulse aileron inputs were applied to observe the effect of load factor on bank angle oscillations. As load factor increased a hesitation in bank angle was noticeable by the pilot and can be seen by comparing the mechanical flight control configuration at 1 and 3G's (Figures G26 and G32). This hesitation is attributed to the beta increase from the adverse yaw which resists the roll due to C_{ℓ_β} for the

mechanical flight control configuration.

The step roll input was the most interesting of the inputs tested. This input caused the largest excursions in the monitored parameters. The technique used to terminate the maneuver also had an effect on the aircraft's motion. If the input was removed slowly the aircraft oscillations were mild compared to the oscillations resulting from abruptly stopping the roll. The resulting oscillations from abrupt roll terminations increased with an increase in load factor, which again is attributed to the increased adverse yaw at higher angles of attack. This increased adverse yaw creates a larger sideslip which in turn provides for more kinematic cross coupling between sideslip and angle of attack. Comparing the mechanical and fully augmented flight control configuration shows how the augmented system helps to minimize the aircraft oscillations (Figures G35 and G39). The effect of load factor is better shown by comparing the mechanical flight control configuration at 1 and 3Gs (Figures G35 and G49).

Performing this flight test has shown that load factor does have an effect on aircraft response to doublet, impulse, and step inputs. The cross coupling was more pronounced when the dutch roll mode was excited which was attributed to the kinematic exchange between sideslip and angle of attack. The aircraft oscillations at higher load factors resulting from abrupt roll terminations is primarily due to adverse yaw. The following chapter will compare the analytical predictions to the flight test results to determine the validity of linear systems analysis in describing the aircraft response as a function of load factor. In addition MIL-F-8785C will be used to discuss the effect of load factor on aircraft handling qualities.

V. Comparison of Results

Introduction

This chapter will compare the analytical and flight test results, and evaluate these results with respect to MIL F-8785C to determine the effect of load factor on the flying qualities.

Comparison Pitfalls

Most analytical solutions to real world problems are based on assumptions. The validity of these assumptions can determine how well the analytical model predicts the real world. The nice feature of flight testing is that the aircraft doesn't make assumption, and the aircraft response to a given input should be the standard from which to judge the analytical prediction. However, there are several difficulties which arise when comparing the flight test data to the analytical predictions.

The best way to illustrate where differences between flight and analytical data arise is to make an assumption. The assumption is that the analytical methods exactly model the real world. This is of course not the case, but it will illustrate where some of the difference between flight test and analytical results come from. If the answer could be (No) to one of the following questions a difference can occur.

1. Was the test flown at the same flight condition modelled? (i.e. was the weight, cg, altitude, mach number, moments of inertia and equilibilum parameters the same.)

2. Was the input made by the pilot the same as the one modelled? (i.e., magnitude, symmetry, period, and shape.)

3. Is the range of the transducers sufficient to measure the required information?

4. Is the sampling rate of the instrumentation sufficient to document the actual response? (i.e. Is the data giving a distorted view of the real world occurrence?)

5. Is the sampling rate used by the data system consistent with that used to model the system?

6. Is the scale used to display the data appropriate for the data reduction scheme used to extract the required parameters? (i.e. can you read the output to the desired accuracy?)

7. Is the technique used to reduce the data 100% accurate or is it an approximate method?

If the answer to all these questions are (yes) then the flight test and analytical results should match, based on the assumption that the real world and the model were the same. The importance of requiring a (yes) answer is primarily a function of what type of data you need, trend data or specific numbers. Other factors such as cost, availability and overall purpose must also be considered.

For this project the answers to most of the above questions were (no), which automatically builds in a difference in results. The other differences of course come from the fact that the model doesn't exactly match the real world, the assumptions may not be valid, and the assumptions if valid may have been violated. Therefore, comparing similar trends rather than exact numerical correlation of the analytical and flight test results are performed, and areas where the assumptions necessary to model the real world caused a difference in the results will be identified.

Simulation vs Flight Test

A number of differences were noted between the simulation and the flight test with the exception of the time to achieve steady-state oscillations which appeared significant in the magnitude of the simulated plots, did not show up in the flight test traces for the same size input. This was a factor of the TM system resolution. For example, the Base-10 TM system is a 10 bit system with a resolution expressed by

$$\text{Resolution} = \frac{\text{Transducer Range}}{2^{10}} \tag{5.1}$$

Using roll rate as an example gives the following

Roll Rate Transducer Range = $\pm$ 250 deg/sec

$$\text{Resolution} = \frac{500 \text{ deg/sec}}{1024} = .48 \text{ deg/sec} = 8 \times 10^{-3} \text{ rad/sec} \tag{5.2}$$

This is the best resolution the system can provide for this parameter. The scale used on the strip chart for roll rate was $\pm$ 20 deg/sec, and with 50 divisions each division equates to .8 deg/sec. Therefore, the limiting factor for this parameter is the TM system not the display (strip chart), since the strip chart can be read to half divisions. Roll angle on the other hand is limited by the resolution of the strip chart. The resolution of the remaining parameters is summarized in Table E2, Appendix E. The cross coupling at 2G's for a doublet elevator input of 5 lbs is shown by the presence of roll rate and bank angle oscillations during simulation (Figure G6). Since the roll rate due to cross coupling only reached a maximum value of 1.7 x 10^{-3} rad/sec in the simulation, the strip chart from flight test would indicate no response. To provide input from flight test to show the effect of cross coupling a larger than doublet input was required.

[illegible] flying qualities. The 1 and 3 pitch doublet traces correlate well in terms of the response shapes (Figures G1 through G7).

The rudder doublet traces show good agreement (Figures G11 through G23). The bank and pitch angles traces from simulation (Figures G19 and G20) show the presence of these two variables in the phugoid mode which is not reflected by the strip charts since the maneuver was terminated after approximately 10 seconds. This is of little concern from a flying qualities standpoint, since the pilot does not fly hands off at 3G's.

The impulse roll inputs were simulated by using the real parts of the dutch roll eigenvector (Figures G24, G25, G27, G28, G30, G31). At 1G the flight test trace shows little response (Figure G29). At 3G's the flight test trace shows good correlation with the increase in dutch roll frequency at 3G's indicated by the roll rate trace (Figure G32).

Up to this point the linear simulation has worked relatively well in predicting the actual aircraft response at load factor increases if actual inputs are large than [illegible]. The basic limitation is the requirement for small inputs as dictated by the assumptions used in modeling the flight control system and linearizing the equations of motion. This limitation if used in flight test basically results in aircraft responses which does not reflect the cross coupling predicted, because the pilot stick inputs are so small they cannot be detected by the pilot or the data system's sensors. This implies that the cross coupling [illegible] small inputs is not applicable with

regard to flying qualities. The only flying qualities concern is the change in the modal responses in terms of frequency, damping ratio, n/α, etc. As the inputs grow in magnitude the cross coupling becomes a concern. However, a non-linear model would better facilitiate this type of analysis.

The linear models validity for step roll inputs, resulting in large changes in bank angle, breaks down because the small angle assumption is violated. However, initial response still provides some useful information using this type of analysis. In addition the cross coupling predicted by simulation is seen as the actual inputs grow in magnitude. The 1G step roll response for the mechanical flight control configuration shows the initial adverse yaw and a reduction in roll rate as sideslip increases (Figures G33 and G34). Turning on the augmentation shows the elimination of the adverse yaw and the reduction in roll rate oscillation making the roll response more nearly first order. The simulation and flight test responses agree well (Figures G36 through G39). With a full aileron input, the flight test data for the mechanical and fully augmented cases show the improved roll response predicted by the model (Figures G35 and G39). At 2G's the lateral directional variables still look reasonable and agree with the flight test data but the model breaks down with the longitudinal variables (Figures G40 through G44). The 3G roll response shows the situation at 2G's is aggravated with greater oscillations in roll and a smaller roll rate with more adverse yaw (Figures G45 through G49). All these characteristics were noted in flight test with one maneuver being terminated due to a buildup in sideslip which approached the test limit of ±2°; however, the validity of the linear model at this condition is

questionable. Although not shown, another limitation of the model was discovered simulating this condition for the fully augmented case. The model did not include the limiters for the control augmentation system, and during the rolls sideslip would start to build creating lateral acceleration. The lateral acceleration feedback would sense this buildup and would command rudder as necessary to zero the lateral acceleration. The rudder command was well in excess of that available on the aircraft.

MIL-F-8785C Compliance

The results were evaluated for compliance with MIL-F-8785C requirements for a class IV aircraft in Flight Phase Categories A and B. The level 1, 2, or 3 flying qualities necessary for an aircraft to comply with, are normally a function of abnormalities that may occur as a result of either flight outside the Operational Flight Envelope, failure of aircraft components, or both. The A-7D only has to meet level 3 flying qualities when operating in the mechanical flight control configuration and level 1 flying qualities for the fully augmented aircraft, at the condition tested. Therefore, this discussion will be referenced to these criteria with regard to pass or fail.

The phugoid mode although not important from a flying qualities point of view at other than 1G is affected by load factor and fails level 1 at 2G's due to damping and 3G's due to damping and period.

Load factor had very little affect on the short period damping and frequency, however a change in the n/α parameter used to determine acceptable flying qualities is affected. Mathematically the n/α parameter is approximated by

$$n/\alpha = \frac{V}{g} (1/T_{\theta 2}). \qquad (5.3)$$

Since load factor causes movement of the numerator zeros for the A-7D, this parameter increases with load factor. The movement of this root was small as load factor increased for the mechanical flight control configuration, but with the fully augmented configuration at 3G's it resulted in a noticeable increase in n/α. This increase can be seen from flight test n/α sweeps in Figures G52 and G53. The mathematical approximation gives a much larger increase than actually experienced for this case. This increased n/α to 34.9 at 3G's resulting in a degradation from level 1 to level 2 [Ref 1:14].

Dutch roll dynamics were improved as load factor increased with both frequency and damping increasing, which moves the parameters further from the flying qualities boundaries.

The spiral mode passed at 1G but was not evaluated at higher load factors during flight test.

The roll mode was predicted to pass using the initial response to step roll inputs with very little change in roll mode time constant. The flight test data also passed; however, the roll mode time constant tended to increase from .4 to 1G to .7 at 3G with the mechanical flight control configuration. Recommend the Test Pilot School incorporate loaded flying qualities testing into the curriculum to comply with the intent of paragraph 3.3.4, and 3.3.4.2.1 of MIL-F-8785C for determining flying qualities at other than 1G. (R3)

The simulation validity for lateral dynamic response is questionable for reasons mentioned earlier, therefore, compliance to the mil spec for lateral inputs were not evaluated. The flight test data does indicate an effect on roll rate as load factor increases even though for both flight control configurations the time to roll was within paragraph

3.3.4.1 limits for time to change bank angle 90 degrees. Recommend the use of a non-linear model to analyze lateral inputs, and more flight testing to determine the effect of load factor on the lateral flying qualities of the A-7D. (R1)

VI. Conclusions and Recommendations

The question to be answered was -- what effect may load factor have on aircraft handling qualities, and can the effect, if any, be predicted analytically? Load factor does effect the handling qualities; however, linear systems analysis is limited in predicting the effects.

The characteristics of the short period mode were not significantly affected by increasing load factor; however, the parameter n/α increased with load factor causing a degradation from level 1 to level 2 flying qualities. Analytical predictions correlated well with flight test data.

The dutch roll characteristics improved with an increase in load factor. These improvements in dutch roll damping and frequency were predicted with good results.

Flight test indicated a reduced roll effectiveness as load factor increased. Time to roll through 90 degrees of bank increased, but was still within MIL-F-8785C tolerances. Roll oscillations during small roll inputs were more noticeable as load factor increased. The linear systems analysis was determined to be invalid for analyzing lateral response to step roll inputs, since the small perturbation assumption used in linearizing the equations was violated as bank angle increased.

(R1) NON-LINEAR ANALYSIS TECHNIQUES SHOULD BE USED TO ANALYZE ROLLING MANEUVERS. (Page 71)

Cross-couping of the longitudinal and lateral directional modes resulted in small oscillation for small inputs which did not present a flying qualities problem; however, as inputs increased in magnitude the oscillations reached magnitudes which could affect gross acquisition tasks.

(R2) RECOMMEND FURTHER TESTING TO ANALYZE THIS OPEN LOOP CROSS COUPLING ON THE CLOSED LOOP FLYING QUALITIES. (Page 62)

The most noticeable cross coupling that took place during testing occurred when rolls due to step inputs were terminated. The faster the roll was stopped the more noticeable the cross coupling. This was attributed to the larger adverse yaw as load factor increased which aggravated the cross coupling.

(R3) RECOMMEND THE TEST PILOT SCHOOL INCORPORATE LOADED FLYING QUALITIES INTO THE CURRICULUM TO COMPLY WITH THE INTENT OF PARAGRAPH 3.3.4, AND 3.3.4.2.1 OF MIL-F-8785C FOR DETERMINING FLYING QUALITIES AT OTHER THAN 1G. (Page 70)

Bibliography

1. MIL-F-8785C, Military Specification for Flying Qualities of Piloted Airplanes, Wright-Patterson AFB, Ohio: ASD/ENESS, 5 November 1980.

2. Moorehouse, D.J., Woodcock, R.J., Background Information and Users Guide for MIL-F-5785C, Military Specification - Flying Qualities of Piloted Airplanes, Wright-Patterson AFB, Ohio: Flight Dynamics Laboratory, July 1982.

3. Etkin, Bernard, Dynamics of Atmospheric Flight, New York: John Wiley and Sons, Inc., 1972.

4. 2-53310/5R-1981, A-7 Aerodynamic Data Report, Dallas, Texas: LTV Vought Aeronautics Division, 21 May 1965 (Revised 18 March 1968.

5. 2-53320/8R-8089, A-7D Estimated Flying Qualities, Dallas Texas: LTV Vought Aeronautics Division, 15 January 1968.

6. Edwards, J.W., A Fortran Program for the Analysis of Linear Continuons and Sampled-Data Systems, Edwards AFB, California: NASA Dryden Flight Research Center, January 1976.

7. Brooks, W.J., Captain, A-7D Limited Flying Qualities Test Plan, Edwards AFB, California: USAF Test Pilot School, August 1981.

8. T.O. 1A-7D-1, Flight Manual, Tinker AFB, Oklahoma: ALC/MMED, 15 February 1979; Change 11, 1 August 1983.

9. AFFTCR 55-2 Vol I, Aircrew Operations, Edwards AFB, California: HQ Air Force Flight Test Center, 15 October 1983.

10. Partial Flight Manual, A-7D Serial Numbers 67-14582 and 67-14584, Edwards AFB, California: USAF Test Pilot School, 15 March 1979.

11. Flying Qualities Theory and Flight Test Techniques, Chapter 7, Dynamics, Edwards AFB, California, USAF Test Pilot School, July 1981.

12. Performance Theory and Flight Test Techniques, Chapter 1, Performance Introduction, Edwards AFB, California: USAF Test Pilot School, July 1983.

13. IMSL Library Edition 8, Routine EIGFR, Houston, TX: IMSL, Inc., 1980

Appendix A

Reference Frames

APPENDIX A

Reference Frames

When solving flight dynamics problems it is necessary to use several frames of reference to represent the various quantitites of interest, such as, velocity, accelerations, forces, moments, and products of inertia to name a few. It is also useful to represent quantities in one frame in terms of the other frames. This appendix gives definitions of each reference frame used, and presents the steps necessary to obtain the transformations between reference frames.

INERTIAL REFERENCE FRAME, F_I - This frame is fixed in space by definition, allowing the use of Newton's second law, F = ma. For this problem the earth is assumed to be fixed in space, and the origin of the inertial frame is located at the earth's center (Figure A1).

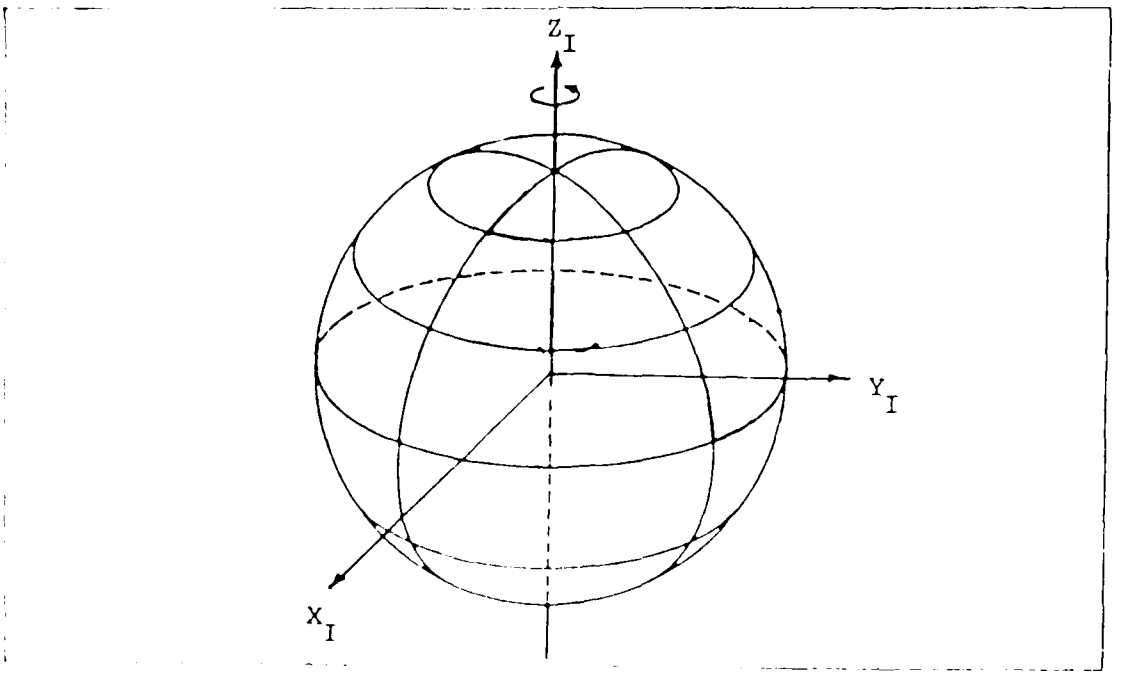

Figure A1. Inertial Frame

EARTH CENTERED FRAME, F_{EC} - This frame will also have its origin located at the earth's center, but it will be fixed in the earth and

rotate with the earth. The X_{EC} axis will go through the prime meridian at the equator, and the Z_{EC} and Z_I axes are aligned. This reference frame is normally used in flight dynamics problems where the rotation of the earth is considered; however, this problem will assume a nonrotating earth and the only reason for including it is to show a logical build-up of the reference frames. The rotation of this frame wrt the inertial frame, written in the earth centered frame will be designated as

$$\bar{\omega}_{EC/I\ EC} = \begin{bmatrix} 0 \\ 0 \\ \omega \end{bmatrix}_{EC} \tag{A1}$$

and is equal to the earth's rotational velocity. The angle measured from the X_I axis to the X_{EC} axis is designated μ (Figure A2).

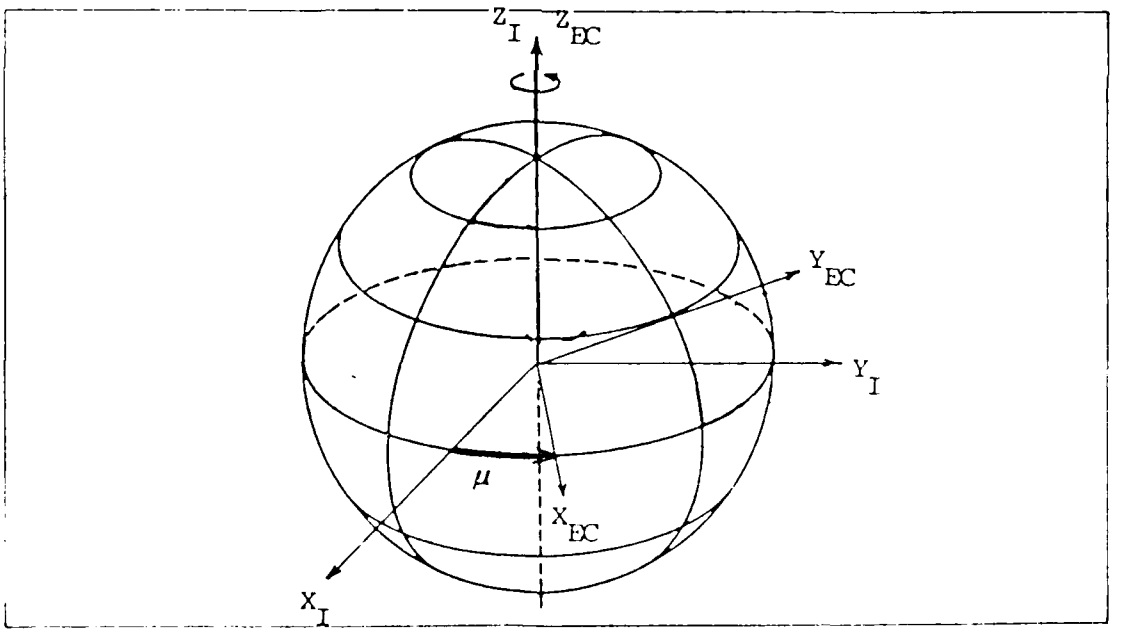

Figure A2. Earth Centered Frame

EARTH FIXED FRAME F_E - This frame is useful to locate on the earth's surface near the aircraft's location. It is also fixed to rotate with the earth making the following true

$$\bar{\omega}_{E/I} = \bar{\omega}_{EC/I} \tag{A2}$$

Its orientation is such that Z_E axis is directed into the earth, X_E points north, and Y_E points east. The plane formed by the X_E and Y_E axis represents the local horizontal. To arrive at this frame an intermediate frame F_X will be used with rotations about the X_3 and then the X_2 axes. The notation $[L_{XEC}]$ designates the transformation matrix from the earth centered frame to the intermediate frame F_X. Rotation about X_3, through μ_E yields

$$[L_{XEC}] = \begin{bmatrix} \cos\mu_E & \sin\mu_E & 0 \\ -\sin\mu_E & \cos\mu_E & 0 \\ 0 & 0 & 1 \end{bmatrix} \tag{A3}$$

Rotation about X_2, through $(90 + \lambda_E)$ places F_E in the desired orientation. The reason for the additional 90 degrees is due to the fact that the Z_E axis needs to point down.

Using the relations

$$\cos(90 + \lambda_E) = -\sin\lambda_E \tag{A4}$$

$$\sin(90 + \lambda_E) = \cos\lambda_E \tag{A5}$$

This rotation yields

$$[L_{EX}] = \begin{bmatrix} -\sin\lambda_E & 0 & \cos\lambda_E \\ 0 & 1 & 0 \\ -\cos\lambda_E & 0 & -\sin\lambda_E \end{bmatrix} \tag{A6}$$

The composite rotation from F_{EC} to F_E is

$$[L_{EEC}] = [L_{EX}][L_{XEC}] = \begin{bmatrix} -\sin\lambda_E\cos\mu_E & -\sin\lambda_E\sin\mu_E & \cos\lambda_E \\ -\sin\mu_E & \cos\mu_E & 0 \\ -\cos\lambda_E\cos\mu_E & -\cos\lambda_E\sin\mu_E & -\sin\lambda_E \end{bmatrix} \tag{A7}$$

The angles μ_E and λ_E can be thought of as latitude and longitude respectively (Figure A3).

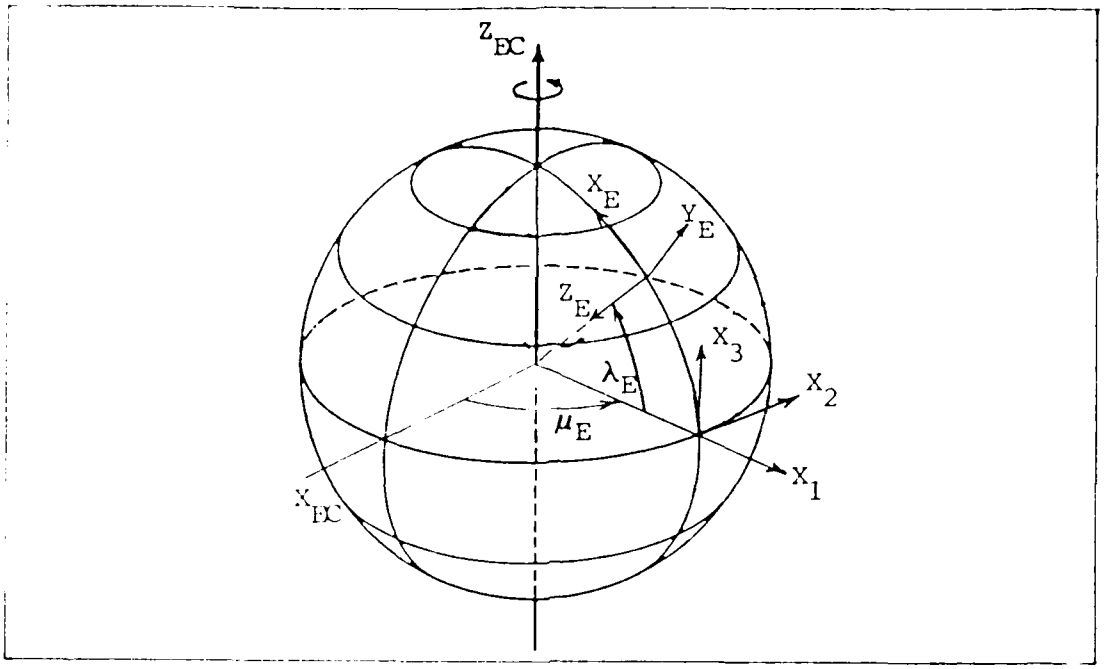

Figure A3. Earth Fixed Frame

VEHICLE CARRIED FRAME F_V - This frame will have its origin located at the aircraft's center of mass, with the X_V axis arbitrarily pointing north, and the Y_V axis pointing east. This aligns the F_E and F_V reference frames if the earth's curvature is neglected, which is valid for the case when the two frames are close to one another. Assuming this is the case, then

$$[L_{VEC}] = [L_{EEC}] \tag{A8}$$

with $\mu = \mu_E$, and $\lambda = \lambda_E$.

The rotation of the vehicle carried frame wrt the earth fixed frame $\bar{\omega}_{V/E}$, can be written in the following components

$$\bar{\omega}_{V/E} = \dot{\mu} Z_{EC} - \dot{\lambda} Y_V \tag{A9}$$

writing this in terms of the vehicle frame gives

$$\bar{\omega}_{V/E\ V} = \bar{\omega}_{V/EC} + \bar{\omega}_{EC/E} = [L_{VEC}]\begin{bmatrix} 0 \\ 0 \\ \dot{\mu} \end{bmatrix}_{EC} + \begin{bmatrix} 0 \\ -\dot{\lambda} \\ 0 \end{bmatrix}_V + \begin{bmatrix} \dot{\mu}\cos\lambda \\ -\dot{\lambda} \\ -\dot{\mu}\sin\lambda \end{bmatrix}_V \tag{A10}$$

Since it's needed in a later relationship the rotation of the vehicle carried frame wrt to the inertial frame will be obtained as follows

$$\bar{\omega}_{V/I} = \bar{\omega}_{V/EC} + \bar{\omega}_{EC/I} \tag{A11}$$

and to write this rotation in terms of the vehicle carried frame gives

$$\begin{aligned} \bar{\omega}_{V/I\ V} &= \bar{\omega}_{V/EC\ V} + [L_{VEC}]\bar{\omega}_{EC/I\ EC} \\ &= \begin{bmatrix} \dot{\mu}\cos\lambda \\ -\dot{\lambda} \\ -\dot{\mu}\sin\lambda \end{bmatrix}_V + [L_{VEC}]\begin{bmatrix} 0 \\ 0 \\ \omega \end{bmatrix}_{EC} \\ &= \begin{bmatrix} (\dot{\mu} + \omega)\cos\lambda \\ -\dot{\lambda} \\ -(\dot{\mu} + \omega)\sin\lambda \end{bmatrix}_V \end{aligned} \tag{A12}$$

WIND FRAME F_W - This frame's origin is located at the aircraft's center of mass with the X_W axis directed along the velocity vector of the aircraft, and the Z_W axis lying in the plane of symmetry. To establish this frame, two intermediate frames will be used. These intermediate frames will be designated F_g and F_h respectively (Figure A4).

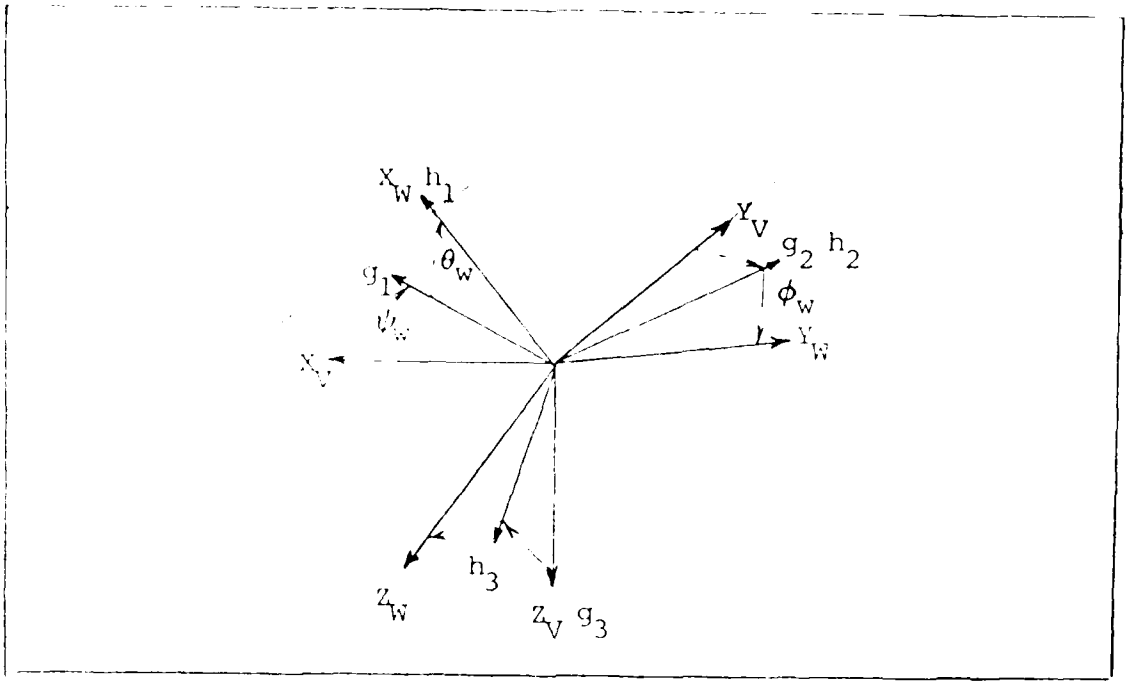

Figure A4. Rotations for F_V to F_W

The first rotation is about the Z_V axis through an angle Ψ_W, which yields the transformation matrix

$$[L_{gv}] = \begin{bmatrix} \cos\Psi_W & \sin\Psi_W & 0 \\ -\sin\Psi_W & \cos\Psi_W & 0 \\ 0 & 0 & 1 \end{bmatrix} \qquad \text{(A13)}$$

The second rotation is about g_2 through an angle θ_W, resulting in

$$[L_{hg}] = \begin{bmatrix} \cos\theta_W & 0 & -\sin\theta_W \\ 0 & 1 & 0 \\ \sin\theta_W & 0 & \cos\theta_W \end{bmatrix} \qquad \text{(A14)}$$

The third rotation is about X_W through an angle Φ_W, which gives

$$[L_{wh}] = \begin{bmatrix} 1 & 0 & 0 \\ 0 & \cos\Phi_W & \sin\Phi_W \\ 0 & -\sin\Phi_W & \cos\Phi_W \end{bmatrix} \qquad \text{(A15)}$$

The composite rotation from F_V to F_W is obtained by

$$[L_{WV}] = [L_{Wh}][L_{hg}][L_{gv}] \qquad \text{(A16)}$$

with the final transformation matrix being

$$[L_{WV}] = \begin{bmatrix} \cos\theta_W\cos\psi_W & \cos\theta_W\sin\psi_W & -\sin\theta_W \\ -\cos\phi_W\sin\psi_W & \cos\phi_W\cos\psi_W & \sin\phi_W\cos\theta_W \\ +\sin\phi_W\sin\theta_W\cos\psi_W & +\sin\phi_W\sin\theta_W\sin\psi_W & \\ \sin\phi_W\sin\psi_W & -\sin\phi_W\cos\psi_W & \cos\phi_W\cos\theta_W \\ +\cos\phi_W\sin\theta_W\cos\psi_W & +\cos\phi_W\sin\theta_W\sin\psi_W & \end{bmatrix} \quad (A17)$$

The rotation of the wind frame wrt the inertial frame $\bar{\omega}_{W/I}$ can be written as

$$\bar{\omega}_{W/I} = \bar{\omega}_{W/V} + \bar{\omega}_{V/I} \quad (A18)$$

where $\bar{\omega}_{W/V}$ can be formulated by recalling the angles in Figure A4 that the axes were rotated through, and denoting $\dot{\psi}_W$, $\dot{\theta}_W$, and $\dot{\phi}_W$ as the rates of rotation about the respective axes. The second term in (A18) is given by (A12). Substituting into (A18) yields the following expression

$$\begin{bmatrix} \\ \omega_{W/I} \\ \\ \end{bmatrix}_W = [L_{WV}]\begin{bmatrix} 0 \\ 0 \\ \dot{\psi}_W \end{bmatrix}_V + [L_{Wh}][L_{hg}]\begin{bmatrix} 0 \\ \dot{\theta}_W \\ 0 \end{bmatrix}_g + \begin{bmatrix} \dot{\phi} \\ 0 \\ 0 \end{bmatrix}_W + [L_{WV}]\begin{bmatrix} (\dot{\mu}+\dot{\omega})\cos\lambda \\ -\dot{\lambda} \\ -(\dot{\mu}+\dot{\omega})\sin\lambda \end{bmatrix}_V \quad (A19)$$

The following definition is also helpful in discussing rotations

$$\begin{bmatrix} \\ \omega_{W/I} \\ \\ \end{bmatrix}_W = p_W X_W + q_W Y_W + r_W Z_W \quad (A20)$$

where p_W, q_W, and r_W are the components of the rotation in the respective wind axes directions. Now enacting the assumption of the non-rotating earth, which is certainly valid for subsonic aircraft velocities, and considering the vehicle carried frame to be inertial wrt rotation, which is valid if we assume the earth to be flat, the last term in (A19) can be neglected. This yields the following expression.

for the components of (A20).

$$\begin{bmatrix} p_W \\ q_W \\ r_W \end{bmatrix} = \begin{bmatrix} \dot{\Phi}_W \\ 0 \\ 0 \end{bmatrix}_W + [L_{Wh}][L_{hg}] \begin{bmatrix} 0 \\ \dot{\theta}_W \\ 0 \end{bmatrix}_W + [L_{WV}] \begin{bmatrix} 0 \\ 0 \\ \dot{\Psi}_W \end{bmatrix}_V \tag{A21}$$

Substituting (A14), (A15), and (A17) into (A21) yields the following expression for the rotations about the wind axes.

$$\begin{bmatrix} p_W \\ q_W \\ r_W \end{bmatrix} = \begin{bmatrix} \dot{\Phi}_W - \dot{\Psi}_W \sin\theta_W \\ \dot{\theta}_W \cos\Phi_W + \dot{\Psi}_W \sin\Phi_W \cos\theta_W \\ -\dot{\theta}_W \sin\Phi_W + \dot{\Psi}_W \cos\Phi_W \cos\theta_W \end{bmatrix} \tag{A22}$$

BODY FRAME F_B - This frame's origin is also located at the aircraft's center of mass and remains fixed in the body with X_B directed out the nose of the aircraft, Y_B directed out the right wing and Z_B lying in the plane of symmetry. To establish this frame an intermediate frame F_f will be used, with rotations about Z_W and f_2 through the respective angles $-\beta$ and α (see Figure A5).

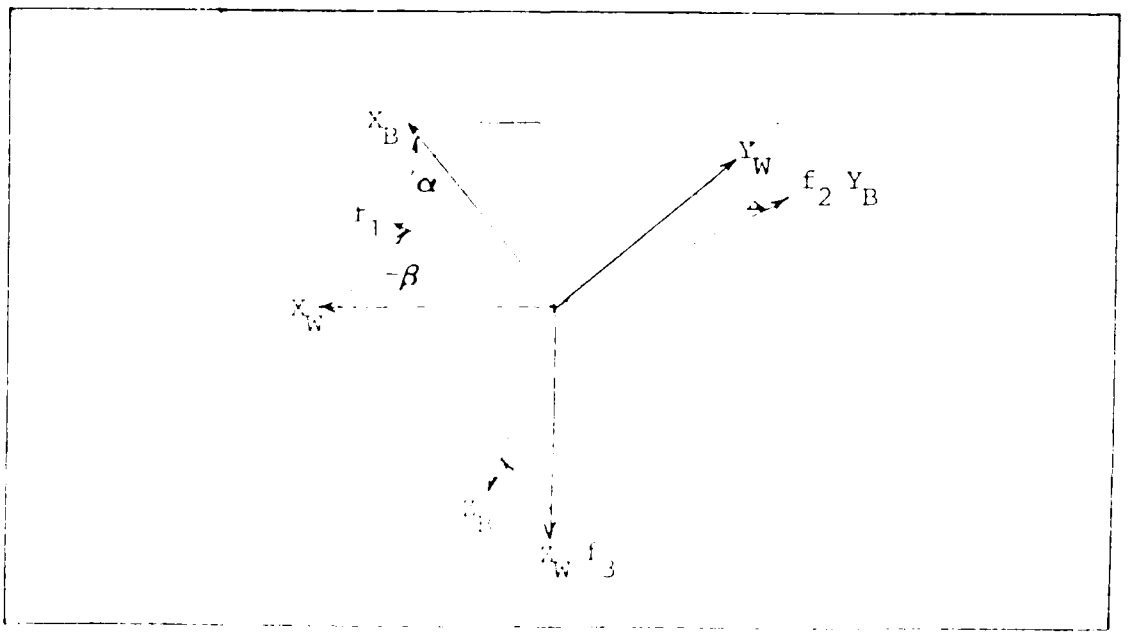

Figure A5. Rotations for F_W to F_B

The first rotation is about the Z_W axis through an angle $-\beta$. The reason for the $-\beta$ is the result of convention which defines positive β as the relative wind from the right. Using the relationships

$$\cos(-\beta) = \cos\beta \tag{A23}$$

$$\sin(-\beta) = -\sin\beta \tag{A24}$$

the following transformation results

$$[L_{fW}] = \begin{bmatrix} \cos\beta & -\sin\beta & 0 \\ \sin\beta & \cos\beta & 0 \\ 0 & 0 & 1 \end{bmatrix} \tag{A25}$$

The second rotation is about f_2 through an angle α, resulting in

$$[L_{Bf}] = \begin{bmatrix} \cos\alpha & 0 & -\sin\alpha \\ 0 & 1 & 0 \\ \sin\alpha & 0 & \cos\alpha \end{bmatrix} \tag{A26}$$

The composite rotation from F_W to F_B is obtained by

$$[L_{BW}] = [L_{Bf}][L_{fW}] \tag{A27}$$

with the final transformation matrix being

$$[L_{BW}] = \begin{bmatrix} \cos\alpha\cos\beta & -\cos\alpha\sin\beta & -\sin\alpha \\ \sin\beta & \cos\beta & 0 \\ \sin\alpha\cos\beta & -\sin\alpha\sin\beta & \cos\alpha \end{bmatrix} \tag{A28}$$

By removing the W subscript from (A17), (A20), and (A22) the following is true regarding rotation about the body axes

$$[L_{BV}] = [L_{WV}] \quad \text{(W subscript removed)} \tag{A29}$$

$$\bar{\omega}_{B/I} = pX_B + qY_B + rZ_B \tag{A30}$$

$$\begin{bmatrix} p \\ q \\ r \end{bmatrix}_B = \begin{bmatrix} \dot{\phi} & - & \dot{\psi}\sin\theta \\ \dot{\theta}\cos\phi & + & \dot{\psi}\sin\phi\cos\theta \\ -\dot{\theta}\sin\phi & + & \dot{\psi}\cos\phi\cos\theta \end{bmatrix} \tag{A31}$$

Velocity in this frame is defined as

$$\overline{V} = \begin{bmatrix} u \\ v \\ w \end{bmatrix}_B \tag{A32}$$

STABILITY FRAME F_S - This frames is a special set of body axes. For symmetric flight (velocity vector in the plane of symmetry) F_S coincides with F_W initially, but remains fixed in the body and moves with the body during disturbances. In non-symmetric flight, i.e. with sideslip the X_S axis is aligned with the projection of the velocity vector into the plane of symmetry, with Z_S remaining in the plane of symmetry.

Appendix B

Development of Equations of Motion

APPENDIX B

Development of Equations of Motion

Introduction

A detailed development of the differential equations describing the aircraft's motion is presented for an aircraft in straight and level unaccelerated flight, and for level turning flight. The assumptions made in the development are outlined where appropriate. The equations are presented in body axes to allow direct comparison with flight test data.

Newtons Second Law

The sum of the external forces are equal to the time rate of change of the linear momentum

$$\Sigma \bar{F} = m\bar{a}_{cm/I} \tag{B1}$$

and the sum of the applied moments is equal to the time rate of change of the angular momentum.

$$\Sigma \bar{M} = \frac{d\bar{H}}{dt} \tag{B2}$$

For these relationships to be valid the earth is assumed to be fixed in space i.e. inertial frame, and the aircraft is assumed to be a rigid body allowing the motion to be described by a translating center of mass and rotation about the center of mass. It is also assumed that the mass of the aircraft remains constant.

The acceleration of the center of mass written in body axes is expressed by

$$\bar{a}_{cm/I}\Big]_B = \frac{{}^B d\bar{V}_{cm/I}}{dt}\Big]_B + \bar{\omega}_{B/I} \times \bar{V}_{cm/I}\Big]_B \tag{B3}$$

the cross product in (B3) can be written in matrix form as

$$\bar{\omega}_{B/I} \times \bar{V}_{cm/I} = \tilde{\omega}_{B/I}\bar{V}_{cm/I} \tag{B4}$$

where

$$\tilde{\omega}_{B/I} = \begin{bmatrix} 0 & -r & q \\ r & 0 & -p \\ -q & p & 0 \end{bmatrix} \tag{B5}$$

using (B4) and substituting (A32) for the velocity (B3) is written as:

$$\bar{a}_{cm/I}\Big]_B = \begin{bmatrix} \dot{u} \\ \dot{v} \\ \dot{w} \end{bmatrix}_B + \begin{bmatrix} 0 & -r & q \\ r & 0 & -p \\ -q & p & 0 \end{bmatrix} \begin{bmatrix} u \\ v \\ w \end{bmatrix}_B \tag{B6}$$

which yields

$$\bar{a}_{cm/I}\Big|_B = \begin{bmatrix} \dot{u} + qw - rv \\ \dot{v} + ru - pw \\ \dot{w} + pv - qu \end{bmatrix}_B \tag{B7}$$

Forces - The sumation of forces will comprise propulsive, ($\bar{F}_T$), aerodynamic ($\bar{F}_A$), and gravitational ($\bar{F}_G$) contributions in each of the coordinate directions.

$$\Sigma\bar{F} = \bar{F}_T + \bar{F}_A + \bar{F}_G \tag{B8}$$

where

$$\Sigma X = F_{TX} + F_{AX} + F_{GX} \tag{B9}$$

$$\Sigma Y = F_{TY} + F_{AY} + F_{GY} \tag{B10}$$

$$\Sigma Z = F_{TZ} + F_{AZ} + F_{GZ} \tag{B11}$$

The propulsive force vector in this development lies in the plane of symmetry and has an inclination with respect to the X-body reference axis designated by α_T which is fixed by aircraft geometry. The components in the respective coordinate directions are as follows:

$$\bar{T} = \begin{bmatrix} T_X \\ T_Y \\ T_Z \end{bmatrix}_B = \begin{bmatrix} T\cos\alpha_T \\ 0 \\ -T\sin\alpha_T \end{bmatrix}_B \tag{B12}$$

where $\bar{T}$ is thrust in lbs.

The aerodynamic forces are normally thought of as lift, drag and side force, which are measured in the wind axes, and designated by

$$\bar{F}_A = \begin{bmatrix} -D \\ -C \\ -L \end{bmatrix}_W \tag{B13}$$

This can be written in body axes by using the transformation defined by (A28); however, at this point the body axes aerodynamic forces will be designated by

$$\bar{F}_A \Big]_B = \begin{bmatrix} F_{AX} \\ F_{AY} \\ F_{AZ} \end{bmatrix}_B \tag{B14}$$

The gravitational force is simply the weight of the aircraft. Written in the vehicle carried frame F_v, gives

$$\bar{W}_v = \begin{bmatrix} 0 \\ 0 \\ mg \end{bmatrix}_v \tag{B15}$$

or in body axes

$$\bar{W}_B = \left[L_{BV} \right] \begin{bmatrix} 0 \\ 0 \\ mg \end{bmatrix}_V = \begin{bmatrix} -mg \sin\theta \\ mg \sin\phi \cos\theta \\ mg \cos\phi \cos\theta \end{bmatrix}_B \tag{B16}$$

where $\left[L_{BV} \right]$ is defined by (A17) without the wind axes subscript.

Using (B9) through (B16) the three force equations can be written as

$$X: T\cos\alpha_T + F_{AX_B} - mg\sin\theta = m(\dot{u} + qw - rv) \tag{B17}$$

$$Y: F_{AY_B} + mg \sin\phi \cos\theta = m(\dot{v} + ru - pw) \tag{B18}$$

$$Z: -T\sin\alpha_T + F_{AZ_B} + mg \cos\phi \cos\theta = m(\dot{w} + pv - qu) \tag{B19}$$

Moments - The sumation of the moments as stated earlier is equal to

$$\Sigma\bar{M} = \frac{d\bar{H}}{dt}$$

where H is the angular momentum.

The angular momentum can be determined by looking at an elemental mass at some point away from the center of mass (Figure B1).

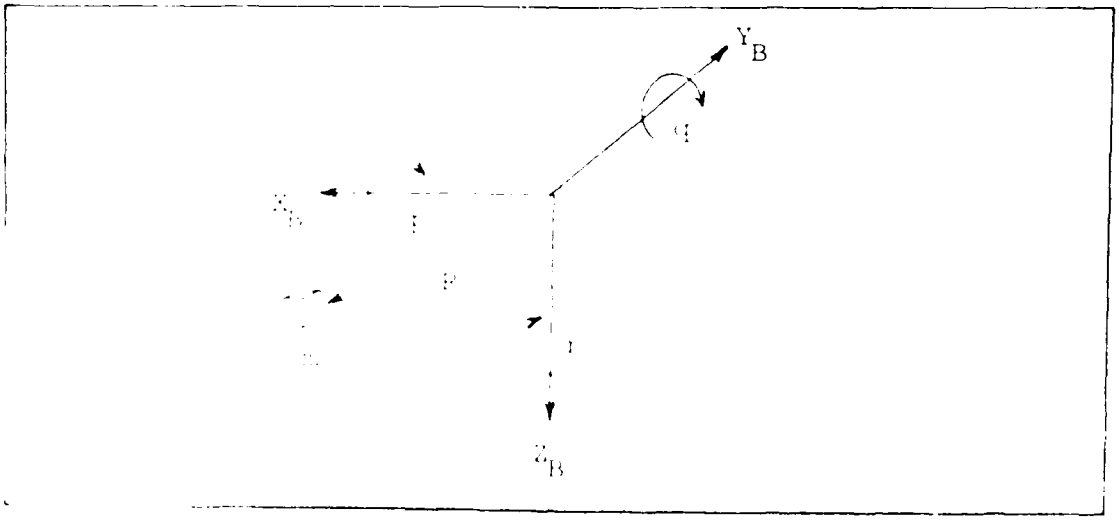

Figure B1. Rotating Elemental Mass

To calculate the relative velocity of this elemental mass, the position

$$\bar{I} = \quad + y\,\bar{J} \quad + z\,\bar{K} \tag{B20}$$

$$\dot{\bar{R}} = \frac{d\bar{R}}{dt} = \frac{{}^{B}d\bar{R}}{dt} + \bar{\omega}_{B/I} \times \bar{R} \tag{B21}$$

Since the aircraft is assumed to be a rigid body, $\bar{R}$ is constant in body axes resulting in

$$\bar{V} = \bar{\omega}_{B/I} \times \bar{R} = \tilde{\omega}\bar{R} = \begin{bmatrix} 0 & -r & q \\ r & 0 & -p \\ -q & p & 0 \end{bmatrix} \begin{bmatrix} x \\ y \\ z \end{bmatrix}_B$$

which yields

$$\bar{V} = \begin{bmatrix} qz - ry \\ rx - pz \\ py - qx \end{bmatrix}_B \tag{B22}$$

Associated with each of these linear velocities is a linear momentum (P)

$$d\bar{P} = \bar{V}dm \tag{B23}$$

Multiplying by the appropriate moment arms produces the components of angular momentum

$$d\bar{H} = \bar{R} \times d\bar{P} = \tilde{R}\, d\bar{P} \tag{B24}$$

which yields

$$d\bar{H} = \begin{bmatrix} 0 & -z & y \\ z & 0 & -x \\ -y & x & 0 \end{bmatrix} \begin{bmatrix} qz - ry \\ rx - pz \\ py - qx \end{bmatrix} dm$$

expanding and combining terms yields

$$d\bar{H} = \begin{bmatrix} p(y^2 + z^2) & - qxy & - rxz \\ -pyx & + q(x^2 + z^2) & - ryz \\ -pzx & - qzy & + r(x^2 + y^2) \end{bmatrix} dm \tag{B25}$$

$$I_{xy} = I_{yx}$$

etc., yields the following expression for angular momentum.

$$\bar{H} = \begin{bmatrix} I_{xx} & -I_{xy} & -I_{xz} \\ -I_{yx} & I_{yy} & -I_{yz} \\ -I_{zx} & -I_{zy} & I_{zz} \end{bmatrix} \begin{bmatrix} p \\ q \\ r \end{bmatrix}_B \tag{B26}$$

Now taking the derivative of the angular momentum to obtain the moments

$$\frac{I d\bar{H}}{dt} = \frac{B d\bar{H}}{dt} + \bar{\omega}_{B/I} \times \bar{H} \tag{B27}$$

Since in the body axes system the moments of inertia matrix is constant, the following is obtained

$$\Sigma\bar{M} = \frac{d\bar{H}}{dt} = \dot{I}\,\bar{\omega}_{B/I} + I\,\dot{\bar{\omega}}_{B/I} + \bar{\omega}_{B/I} \times \bar{H}$$

Assuming the xz plane is a plane of symmetry, the following is done

$$I_{xy} = I_{yx} = I_{yz} = I_{zy} = 0$$

If the moments about each axis are labeled L, M, N respectively, then

$$\Sigma M = \Sigma \begin{bmatrix} L \\ M \\ N \end{bmatrix} = \begin{bmatrix} I_{xx} & 0 & -I_{xz} \\ 0 & I_{yy} & 0 \\ -I_{zx} & 0 & I_{zz} \end{bmatrix} \begin{bmatrix} \dot{p} \\ \dot{q} \\ \dot{r} \end{bmatrix}_B$$

$$+ \begin{bmatrix} 0 & -r & q \\ r & 0 & -p \\ -q & p & 0 \end{bmatrix} \begin{bmatrix} I_{xx} & 0 & -I_{xz} \\ 0 & I_{yy} & 0 \\ -I_{zx} & 0 & I_{zz} \end{bmatrix} \begin{bmatrix} p \\ q \\ r \end{bmatrix}_B$$

expanding and grouping terms yields the three moment equations

$$\Sigma L = \dot{p} I_{xx} - \dot{r} I_{xz} + qr(I_{zz} - I_{yy}) - pq I_{xz} \quad \text{(B28)}$$

$$\Sigma M = \dot{q} I_{yy} + pr(I_{xx} - I_{zz}) + I_{xz}(p^2 - r^2) \quad \text{(B29)}$$

$$\Sigma N = \dot{r} I_{zz} - \dot{p} I_{zx} + pq(I_{yy} - I_{xx}) + qr I_{xz} \quad \text{(B30)}$$

Kinematics - The equations relating the angular rate of the aircraft to the rates of change of the Euler angles can be determined from (A31)

$$\begin{bmatrix} p \\ q \\ r \end{bmatrix}_B = \begin{bmatrix} \dot{\phi} - \dot{\psi} \sin\theta \\ \dot{\theta} \cos\phi + \dot{\psi} \sin\phi \cos\theta \\ -\dot{\theta} \sin\phi + \dot{\psi} \cos\phi \cos\theta \end{bmatrix}_B$$

solving for $\dot{\phi}$, $\dot{\theta}$, $\dot{\psi}$ yields three first order differential equations relating the angular orientation of the aircraft.

$$\dot{\phi} = p + q \sin\phi \tan\theta + r \cos\phi \tan\theta \quad \text{(B31)}$$

$$\dot{\theta} = q \cos\phi - r \sin\phi \quad \text{(B32)}$$

$$\dot{\psi} = [\, q \sin\phi + r \cos\phi \,] \sec\theta \quad \text{(B33)}$$

Equations of Motion

Grouping the three force, moment, and kinematic equations just developed into a set, allows the motion of the aircraft to be described.

Summary of the Body Axis Equations of Motion

Forces

$$X: \quad T\cos\alpha_T + F_{AX_B} - mg \sin\theta = m(\dot{u} + qw - rv)$$

$$Y: \quad F_{AY_B} + mg \sin\phi \cos\theta = m(\dot{v} + ru - pw)$$

$$Z: \quad -T \sin\alpha_T + F_{AZ_B} + mg \cos\phi \cos\theta = m(\dot{w} + pv - qu)$$

Moments

$$L = \dot{p} I_{xx} - \dot{r} I_{xz} + qr(I_{zz} - I_{yy}) - pq I_{xz}$$

$$M = \dot{q} I_{yy} + pr(I_{xx} - I_{zz}) + I_{xz}(p^2 - r^2)$$

$$N = \dot{r} I_{zz} - \dot{p} I_{zx} + pq(I_{yy} - I_{xx}) + qr I_{xz}$$

Kinematics

$$\dot{\Phi} = p + q \sin \Phi \tan \theta + r \cos \Phi \tan \theta$$

$$\dot{\theta} = q \cos \Phi - r \sin \Phi$$

$$\dot{\Psi} = [\, q \sin \Phi + r \cos \Phi \,] \sec \theta$$

Note: Since none of the equations depend on Ψ, the $\dot{\Psi}$ equation can be omitted.

At this point it is necessary to write these equations in terms of the variables used in the data package, and those measured from flight test. The velocities u, v, w can be written in terms of angle of attack α, sideslip β, and free stream velocity V, from

$$\begin{bmatrix} u \\ v \\ w \end{bmatrix}_B = \left[L_{I\&W} \right] \begin{bmatrix} V \\ 0 \\ 0 \end{bmatrix}_W = \begin{bmatrix} V \cos \alpha \cos \beta \\ V \sin \beta \\ V \sin \alpha \cos \beta \end{bmatrix}_B \tag{B34}$$

where $\left[L_{I\&W} \right]$ is defined in Appendix A.

The derivatives of u, v, and w in terms of these variables are

$$\begin{bmatrix} \dot{u} \\ \dot{v} \\ \dot{w} \end{bmatrix}_B = \begin{bmatrix} \dot{V} \cos \alpha \cos \beta - V \dot{\alpha} \sin \alpha \cos \beta - V \dot{\beta} \cos \alpha \sin \beta \\ \dot{V} \sin \beta + V \dot{\beta} \cos \beta \\ \dot{V} \sin \alpha \cos \beta + V \dot{\alpha} \cos \alpha \cos \beta - V \dot{\beta} \sin \alpha \sin \beta \end{bmatrix}_B \tag{B35}$$

The aerodynamic forces can be expressed in terms of the lift L, drag D, and [illegible]

$$\begin{bmatrix} F_{AX} \\ F_{AY} \\ F_{AZ} \end{bmatrix}_B = \begin{bmatrix} L_{BW} \end{bmatrix} \begin{bmatrix} -D \\ -C \\ -L \end{bmatrix}_W \tag{B36}$$

However, all the available data in [Ref 4] is presented in stability axes which is equivalent to wind axes at zero degree sideslip, $\beta = 0$. Therefore, $Y = -C$, and the body axes forces in terms of the lift; drag and sideforce Y, will be represented as

$$\begin{bmatrix} F_{AX} \\ F_{AY} \\ F_{AZ} \end{bmatrix}_B = \begin{bmatrix} L_{BS} \end{bmatrix} \begin{bmatrix} -D \\ Y \\ -L \end{bmatrix}_S = \begin{bmatrix} \cos\alpha & 0 & -\sin\alpha \\ 0 & 1 & 0 \\ \sin\alpha & 0 & \cos\alpha \end{bmatrix} \begin{bmatrix} -D \\ Y \\ -L \end{bmatrix}_S \tag{B37}$$

$$= \begin{bmatrix} -D\cos\alpha + L\sin\alpha \\ Y \\ -D\sin\alpha - L\cos\alpha \end{bmatrix}_B$$

where $\begin{bmatrix} L_{BS} \end{bmatrix}$ is the transformation from stability to body axes. Both the gravitational and inertial forces are proportional to the mass of the aircraft, this makes it convenient to combine these terms into components of the accelerations. The remaining aerodynamic and propulsive forces can be represented in the following set of body axes force equations written in terms of V, α, β, L, D, Y, p, q, r, ϕ, θ.

X Force Equation:

$$-D\cos\alpha + T\cos\alpha_T = m\left[\dot{V}\cos\alpha\cos\beta - V\dot{\alpha}\sin\alpha\cos\beta - V\dot{\beta}\cos\alpha\sin\beta + q(V\sin\alpha\cos\beta) - r(V\sin\beta) + g\sin\theta\right] \tag{B38}$$

Y Force Equation:

$$Y = m\left[\dot{V}\sin\beta + V\dot{\beta}\cos\beta + r(V\cos\alpha\cos\beta) - p(V\sin\alpha\cos\beta) - g\sin\phi\cos\theta\right] \tag{B39}$$

Z Force Equation:

$$-D\sin\alpha - L\cos\alpha - T\sin\alpha_T = m\left[\dot{V}\sin\alpha\cos\beta + V\dot{\alpha}\cos\alpha\cos\beta - V\dot{\beta}\sin\alpha\sin\beta + p(V\sin\beta) - q(V\cos\alpha\cos\beta) - g\cos\phi\cos\theta\right] \quad (B40)$$

Linearization

Now the equations of motion are expressed in terms of variables that can be measured, calculated or obtained from the references. There are several approaches that can be taken at this point to solve this system of equations. Numerical integration techniques can be employed to solve the non-linear differential equations, or the equations can be linearized for small deviations, about an equilibrium condition of interest. This latter technique has been used with great success in the past to give excellent engineering results. The limitations of this approach require that the variations in the variables of interest remain relatively small, i.e., small enough so that the sines and cosines of the disturbance angles are approximated by the angles themselves, and one respectively. Also the products and squares of the disturbance variables are negligible when compared to the actual values. Thus

$$\sin\Delta x = \Delta x$$

$$\cos\Delta x = 1$$

In order to use the linearization technique, the differential equations must first be evaluated at an equilibrium (trim) condition. Equilibrium can be found by setting the rates of change of the state variables equal to zero producing the following set of trim equations.

$$-D_e\cos\alpha_e + L_e\sin\alpha_e + T_e\cos\alpha_T = m\left[q_e(V_e\sin\alpha_e\cos\beta_e) - r_e(V_e\sin\beta_e) + g\sin\theta_e\right] \quad (B41)$$

$$Y_e = m\left[r_e(V_e\cos\alpha_e\cos\beta_e) - p_e(V_e\sin\alpha_e\cos\beta_e) - q\sin\phi_e\cos\theta_e \right] \quad (B42)$$

$$-D_e\sin\alpha_e - L_e\cos\alpha_e - T_e\sin\alpha_T = m\left[p_e(V_e\sin\beta_e - q_e(V_e\cos\alpha_e\cos\beta_e) \right.$$

$$\left. - q\cos\phi_e\cos\theta_e \right] \quad (B43)$$

$$L_e = q_e r_e(I_{zz} - I_{yy}) - p_e q_e I_{xz} \quad (B44)$$

$$M_e = p_e r_e(I_{xx} - I_{zz}) + I_{xz}(p_e^2 - r_e^2) \quad (B45)$$

$$N_e = p_e q_e(I_{yy} - I_{xx}) + q_e r_e I_{xz} \quad (B46)$$

$$p_e + q_e\sin\phi_e\tan\theta_e + r_e\cos\phi_e\tan\theta_e = 0 \quad (B47)$$

$$q_e\cos\phi_e - r_e\sin\phi_e = 0 \quad (B48)$$

$$\left[q_e\sin\phi_e + r_e\cos\phi_e \right]\sec\theta_e = 0 \quad (B49)$$

The perturbed motions are defined by subtracting the trimmed motion from the total motion. So the variables of interest can be written as

$$V = V_e + \Delta V \quad (B50)$$

$$\alpha = \alpha_e + \Delta\alpha \quad (B51)$$

etc.

By substituting appropriate expressions in the form of (B50) and (B51) for all the variables, into equations (B38), (B39), (B40), (B28), (B29), (B30), (B31), (B32), (B33) and making the small deviation assumptions will produce a linearized set of equations.

The X-Force equation becomes

$$D_e\sin\alpha_e\Delta\alpha - \Delta D\cos\alpha_e + L_e\cos\alpha_e\Delta\alpha + \Delta L\sin\alpha_e + \Delta T\cos\alpha_T =$$

$$m\left[\dot{\Delta V}\cos\alpha_e\cos\beta_e - V_e\dot{\Delta\alpha}\sin\alpha_e\cos\beta_e - V_e\dot{\Delta\beta}\cos\alpha_e\sin\beta_e \right.$$

$$\left. - V_e q_e\sin\alpha_e\sin\alpha_e\Delta\alpha + V_e p_e\cos\alpha_e\cos\beta_e\Delta\alpha + q_e\sin\alpha_e\cos\beta_e\Delta V \right.$$

$$+ V_{e}\sin\alpha_{e}\cos\phi_{e}\Delta q - V_{e}\cos\alpha_{e}\cos\phi_{e}\Delta\alpha - r_{e}\sin\phi_{e}\Delta V - V_{e}\sin\phi_{e}\Delta r$$

$$+ g\cos\theta_{e}\Delta\phi \Big] \tag{B74}$$

In the above expression the ΔD, ΔL, and ΔT terms account for the change in the given variable due to changes in all variables that affect it, i.e., the idea of a total differential. By knowing the variables that affect drag for instance one can write $D(V, \alpha, \delta_e)$ therefore

$$\Delta D = \frac{\partial D}{\partial V}\Big|_{V_e}\Delta V + \frac{\partial D}{\partial \alpha}\Big|_{\alpha_e}\Delta\alpha + \frac{\partial D}{\partial \delta_e}\Delta\delta_e \tag{B75}$$

for the ΔL & ΔT terms the following applies

$$\Delta L = \frac{\partial L}{\partial V}\Delta V + \frac{\partial L}{\partial \alpha}\Delta\alpha + \frac{\partial L}{\partial \dot{\alpha}}\Delta\dot{\alpha} + \frac{\partial L}{\partial q}\Delta q + \frac{\partial L}{\partial \delta_e}\Delta\delta_e$$

$$\Delta T = \frac{\partial T}{\partial V}\Delta V + \frac{\partial T}{\partial \delta_e}\Delta\delta_e \tag{B76}$$

where $\Delta\delta_e$ represents the control surface deflections, and is made up of δ_e, δ_a, δ_r, and δ_T for elevator, aileron, rudder and throttle movements. The partial derivative terms are commonly referred to as dimensional stability and control derivatives and will be written as follows

$$\frac{\partial D}{\partial V}\Big|_{V_e} = D_V, \quad \frac{\partial D}{\partial \alpha}\Big|_{\alpha_e} = D_\alpha \quad \text{etc.} \tag{B77}$$

these derivatives will be discussed later.

Using the above notation, grouping like terms, and placing the ΔV, $\Delta\alpha$, and $\Delta\theta$ terms on the left side of the equations results in a linearized X-force equation for a level turn in body axes. The equation for straight and level flight can be obtained from this equation by setting the appropriate equilibrium variables equal to zero. The general equation is

X-Force Equation:

$$\left[m\cos\alpha_e\cos\beta_e\right]\Delta\dot{V} + \left[-mV_e\sin\alpha_e\cos\beta_e - L_{\dot{\alpha}}\sin\alpha_e\right]\Delta\dot{\alpha} + \left[mV_e\cos\alpha_e\sin\beta_e\right]\Delta\dot{\beta}$$

$$= \left[(D_V\cos\alpha_e + L_V\sin\alpha_e + T_V\cos\alpha_T) - mq_e\sin\alpha_e\cos\beta_e + mr_e\sin\beta_e\right]\Delta V$$

$$+ \left[(D_e\sin\alpha_e - D_\alpha\cos\alpha_e + L_e\cos\alpha_e + L_\alpha\sin\alpha_e) - mq_eV_e\cos\alpha_e\cos\beta_e\right]\Delta\alpha$$

$$+ \left[L_q\sin\alpha_e - mV_e\sin\alpha_e\cos\beta_e\right]\Delta q + \left[-mg\cos\theta_e\right]\Delta\theta$$

$$+ \left[mq_eV_e\sin\alpha_e\sin\beta_e + mr_eV_e\cos\beta_e\right]\Delta\beta + \left[mV_e\sin\beta_e\right]\Delta r$$

$$+ \left[L_{\delta_e}\sin\alpha_e - D_{\delta_e}\cos\alpha_e\right]\delta_e + \left[T_{\delta_T}\cos\alpha_T\right]\delta_T \qquad \text{(B78)}$$

The above process for linearizing the remaining equations was carried out in a similar manner using the following functional relationships $M(v, \alpha, \dot{\alpha}, q, \delta)$, $L(\beta, p, r, \delta)$, and $N(\beta, p, r, \delta)$

so

$$\Delta M = M_V\Delta V + M_\alpha\Delta\alpha + M_{\dot{\alpha}}\Delta\dot{\alpha} + M_q\Delta q + M_{\delta_e}\delta_e + M_{\delta_T}\delta_T \qquad \text{(B79)}$$

$$\Delta L = L_\beta\Delta\beta + L_p\Delta p + L_r\Delta r + L_{\delta_r}\delta_r + L_{\delta_a}\delta_a \qquad \text{(B80)}$$

$$\Delta N = N_\beta\Delta\beta + N_p\Delta p + N_r\Delta r + N_{\delta_r}\delta_r + N_{\delta_a}\delta_a \qquad \text{(B81)}$$

the following equations result

Y Force Equation:

$$\left[m\sin\beta_e\right]\Delta\dot{V} + \left[mV_e\cos\beta_e\right]\Delta\dot{\beta} = \left[-mr_e\cos\alpha_e\cos\beta_e + mp_e\sin\alpha_e\cos\beta_e\right]\Delta V$$

$$+ \left[mr_eV_e\sin\alpha_e\cos\beta_e + mp_eV_e\cos\alpha_e\cos\beta_e\right]\Delta\alpha + \left[-mg\sin\phi_e\sin\theta_e\right]\Delta\theta$$

$$+ \left[Y_\beta + mr_eV_e\cos\alpha_e\sin\beta_e - mp_eV_e\sin\alpha_e\sin\beta_e\right]\Delta\beta + \left[Y_p + mV_e\sin\alpha_e\cos\beta_e\right]\Delta p$$

$$+ \left[Y_r - mV_e\cos\alpha_e\cos\beta_e\right] \Delta r + \left[mg\cos\Phi_e\cos\theta_e\right] \Delta\Phi + \left[Y_{\delta_r}\right] \delta_r + \left[Y_{\delta_a}\right] \delta_a \tag{B82}$$

Z Force Equation:

$$\left[m\sin\alpha_e\cos\beta_e\right] \Delta\dot{V} + \left[mV_e\cos\alpha_e\cos\beta_e + L_{\dot{\alpha}}\cos\alpha_e\right] \Delta\dot{\alpha} + \left[-mV_e\sin\alpha_e\sin\beta_e\right] \Delta\dot{\beta}$$

$$= \left[(-D_V\sin\alpha_e - L_V\cos\alpha_e - T_V\sin\alpha_T) - mp_e\sin\beta_e + mq_e\cos\alpha_e\cos\beta_e\right] \Delta V$$

$$+ \left[(-D_e\cos\alpha_e + L_e\sin\alpha_e - L_{\dot{\alpha}}\cos\alpha_e - D_{\dot{\alpha}}\sin\alpha_e) - mq_eV_e\sin\alpha_e\cos\beta_e\right] \Delta\alpha$$

$$+ \left[-L_q\cos\alpha_e + mV_e\cos\alpha_e\cos\beta_e\right] \Delta q + \left[-mg\cos\Phi_e\sin\theta_e\right] \Delta\theta$$

$$+ \left[-mp_eV_e\cos\beta_e - mq_eV_e\cos\alpha_e\sin\beta_e\right]\Delta\beta + \left[-mV_e\sin\beta_e\right]\Delta p + \left[-mg\sin\Phi_e\cos\theta_e\right] \Delta\Phi$$

$$+ \left[-L_{\delta_e}\cos\alpha_e - D_{\delta_e}\sin\alpha_e\right] \delta_e - T_{\delta_T}\sin\alpha_T\delta_T \tag{B83}$$

The three moment equations are

L Moment Equation: (Rolling Moment)

$$I_x\Delta\dot{p} - I_{xz}\Delta\dot{r} = \left[r_e(I_y - I_z) + p_eI_{xz}\right] \Delta q + \left[L_\beta\right] \Delta\beta + \left[L_{\dot{\beta}} + q_eI_{xz}\right] \Delta p$$

$$+ \left[L_r + q_e(I_y - I_z)\right] \Delta r + L_{\delta_r}\delta_r + L_{\delta_a}\delta_a \tag{B84}$$

M Moment Equation: (Pitching Moment)

$$I_y\Delta\dot{q} - M_{\dot{\alpha}}\Delta\dot{\alpha} = M_V\Delta V + M_\alpha\Delta\alpha + M_q\Delta q + \left[r_e(I_z - I_x) - 2p_eI_{xz}\right] \Delta p$$

$$+ \left[p_e(I_z - I_x) + 2r_eI_{xz}\right] \Delta r + M_{\delta_e}\delta_e + M_{\delta_t}\delta_t \tag{B85}$$

N Moment Equation: (Yawing Moment)

$$I_z\Delta\dot{r} - I_{zx}\Delta\dot{p} = \left[p_e(I_x - I_y) - r_eI_{xz}\right] \Delta q + N_\beta\Delta\beta + \left[q_e(I_x - I_y) + N_p\right] \Delta p$$

$$+ \left[-q_e I_{xz} + N_r\right] \Delta r + N_{\delta_r} \delta_r + N_{\delta_a} \delta_a \qquad \text{(B86)}$$

The two kinematic equations

$\dot{\Phi}$ Equation:

$$\Delta\dot{\Phi} = \left[r_e \cos\Phi_e \sec^2\theta_e + q_e \sin\Phi_e \sec^2\theta_e\right] \Delta\theta + \left[\sin\Phi_e \tan\theta_e\right] \Delta q$$

$$+ \Delta p + \left[\cos\Phi_e \tan\theta_e\right] \Delta r + \left[q_e \cos\Phi_e \tan\theta_e - r_e \sin\Phi_e \tan\theta_e\right] \Delta\Phi \qquad \text{(B87)}$$

$\dot{\theta}$ Equation:

$$\Delta\dot{\theta} = \left[\cos\Phi_e\right] \Delta q + \left[-\sin\Phi_e\right] \Delta r + \left[-q_e \sin\Phi_e - r_e \cos\Phi_e\right] \Delta\Phi \qquad \text{(B88)}$$

This set of equations (B78) thru (B88) represent the linearized coupled equations of motion generalized for a steady level turn in body axes. This set of equations also describes the aircraft motion for a straight and level 1G equilibrium condition by setting the appropriate equilibrium values to zero. Recall the assumptions under which these equations are valid

1. Earth is fixed in space, i.e. inertial frame.
2. Aircraft is a rigid body.
3. Aircraft mass remains constant.
4. Thrust vector lies in the plane of symmetry.
5. Perturbations from the equilibrium condition remain relatively small.
6. The products and squares of the perturbation variables are negligible.
7. The earth is considered flat and non rotating.
8. The XZ plane is a plane of symmetry.

9. The flow about the aircraft is quasi-steady.

10. Atmospheric properties are constant such as density for a given equilibrium and associated perturbations.

First Order Format

To use linear control analysis techniques the system of equations will be expressed in first order state variable form

$$\dot{\bar{x}} = A\bar{x} + B\bar{u} \tag{B89}$$

where $\bar{x}$ is the state vector and and $\bar{u}$ is the input vector. The A is the system matrix and the B is the control matrix. The two vectors $\bar{x}$ and $\bar{u}$ are defined as follows:

$$\bar{x} = \begin{bmatrix} \Delta V \\ \Delta\alpha \\ \Delta q \\ \Delta\theta \\ \Delta\beta \\ \Delta p \\ \Delta r \\ \Delta\phi \end{bmatrix} \qquad \bar{u} = \begin{bmatrix} \delta_e \\ \delta_r \\ \delta_a \\ \delta_t \end{bmatrix} \tag{B90}$$

To manipulate the force equations (B78), (B82) and (B83) into first order form the coefficients of all the variables will be designated by a capital letter and a subscript. The capital letter will be associated with a given variable and the subscript denotes the force equation the coefficient is associated with. Primed coefficients are the result of coefficient groupings occurring from mathematical manipulation of the equations. The definition of these coefficients are presented in the List of Symbols section.

X-Force Equation

$$A_x\dot{\Delta v} + B_x\dot{\Delta\alpha} + C_x\dot{\Delta\beta} = D_x\Delta v + E_x\Delta\alpha + F_x\Delta q + G_x\Delta\theta + H_x\Delta\beta + K_x\Delta r + W_x\delta_e + T_x\delta_t \quad \text{(B91)}$$

Y-Force Equation

$$A_y\dot{\Delta v} + C_y\dot{\Delta\beta} = D_y\Delta v + E_y\Delta\alpha + G_y\Delta\theta + H_y\Delta\beta + J_y\Delta p + K_y\Delta r + Q_y\Delta\Phi + R_y\delta r + S_y\delta a \quad \text{(B92)}$$

Z-Force Equation

$$A_z\dot{\Delta v} + B_z\dot{\Delta\alpha} + C_z\dot{\Delta\beta} = D_z\Delta v + E_z\Delta\alpha + F_z\Delta q + G_z\Delta\theta + H_z\Delta\beta + I_z\Delta p + Q_z\Delta\Phi + W_z\delta_e + T_z\delta_t \quad \text{(B93)}$$

Now solving for the different derivatives of the state variables $\dot{\Delta v}$, $\dot{\Delta\alpha}$ and $\dot{\Delta\beta}$ in terms of each other starting with the Y-Force equation:

Solving for $\dot{\Delta\beta}$ in terms of $\dot{\Delta v}$

$$\dot{\Delta\beta} = \frac{1}{C_y}\left[D_y\Delta v + E_y\Delta\alpha + G_y\Delta\theta + H_y\Delta\beta + J_y\Delta p + K_y\Delta r + Q_y\Delta\Phi + R_y\delta r + S_y\delta - A_y\dot{\Delta v}\right] \quad \text{(B94)}$$

substituting (B94) into the x-equation (B91) and grouping like terms

$$\left[A_x - \frac{C_x}{C_y}A_y\right]\dot{\Delta v} + B_x\dot{\Delta\alpha} = \left[D_x - \frac{C_x}{C_y}D_y\right]\Delta v + \left[E_x - \frac{C_x}{C_y}E_y\right]\Delta\alpha + F_x\Delta q + \left[G_x - \frac{C_x}{C_y}G_y\right]\Delta\theta + \left[H_x - \frac{C_x}{C_y}H_y\right]\Delta\beta + \left[-\frac{C_x}{C_y}J_y\right]\Delta p + \left[K_x - \frac{C_x}{C_y}K_y\right]\Delta r + \left[-\frac{C_x}{C_y}Q_y\right]\Delta\Phi + W_x\delta_e + T_x\delta_t + \left[-\frac{C_x}{C_y}R_y\right]\delta_r$$

$$+ \left[- \frac{C_x}{C_Y} S_y \right] \delta_a \tag{B95}$$

Now substituting (B94) into (B93) and grouping yields

$$\left[A_z - \frac{C_z}{C_y} A_y \right] \dot{\Delta v} + B_z \dot{\Delta \alpha} = \left[D_z - \frac{C_z}{C_y} D_y \right] \Delta v + \left[E_z - \frac{C_z}{C_y} E_y \right] \Delta \alpha$$

$$+ F_z \Delta q + \left[G_z - \frac{C_z}{C_y} G_y \right] \Delta \theta + \left[H_z - \frac{C_z}{C_y} H_y \right] \Delta \beta + \left[J_z - \frac{C_z}{C_y} J_y \right] \Delta p$$

$$+ \left[- \frac{C_z}{C_y} K_y \right] \Delta r + \left[Q_z - \frac{C_z}{C_y} Q_y \right] \Delta \Phi + W_z \delta_e + T_z \delta_t + \left[- \frac{C_z}{C_y} R_y \right] \delta_r$$

$$+ \left[- \frac{C_z}{C_y} S_y \right] \delta_a \tag{B96}$$

Further simplifying the notation, let the coefficients on equations (B95) and (B96) be designated as follows

$$A_{x'} = \left[A_x - \frac{C_x}{C_y} A_y \right]$$

$$A_{z'} = \left[A_z - \frac{C_z}{C_y} A_y \right]$$

and so on, to yield

$$A_{x'} \dot{\Delta v} + B_x \dot{\Delta \alpha} = D_{x'} \Delta v + E_{x'} \Delta \alpha + F_x \Delta q + G_{x'} \Delta \theta + H_{x'} \Delta \beta + J_{x'} \Delta p + K_{x'} \Delta r$$

$$+ Q_{x'} \Delta \Phi + W_x \delta_e + T_x \delta_t + R_{x'} \delta_r + S_{x'} \delta_a \tag{B97}$$

and

$$A_{z'} \dot{\Delta v} + B_z \dot{\Delta \alpha} = D_{z'} \Delta v + E_{z'} \Delta \alpha + F_z \Delta q + G_{z'} \Delta \theta + H_{z'} \Delta \beta + J_{z'} \Delta p + K_{z'} \Delta r$$

$$+ Q_{z'} \Delta \Phi + W_z \delta_e + T_z \delta_t + R_{z'} \delta_r + S_{z'} \delta_a \tag{B98}$$

Solving (B98) for $\Delta\dot{\alpha}$ in terms of $\Delta\dot{v}$ yields

$$\Delta\dot{\alpha} = \frac{1}{B_z}\left[-A_z,\Delta\dot{v} + D_z,\Delta v + E_z,\Delta\alpha + F_z\Delta q + G_z,\Delta\theta + H_z,\Delta\beta + J_z,\Delta p\right.$$

$$\left. + K_z,\Delta r + Q_z,\Delta\phi + W_z\delta_e + T_z\delta_t + R_z,\delta_r + S_z,\delta_a\right] \qquad \text{(B99)}$$

Now substituting equation (B99) into (B97) $\Delta\dot{v}$ can be solved for explicity, resulting in the following expression

$$\Delta\dot{v} = \frac{B_z}{A_x,B_z - A_z,B_x}\left[\left[D_x, - \frac{B_x}{B_z} D_z,\right]\Delta v + \left[E_x, - \frac{B_x}{B_z} E_z,\right]\Delta\alpha\right.$$

$$+ \left[F_x - \frac{B_x}{B_z} F_z\right]\Delta q + \left[G_x, - \frac{B_x}{B_z} G_z,\right]\Delta\theta + \left[H_x, - \frac{B_x}{B_z} H_z,\right]\Delta\beta$$

$$+ \left[J_x, - \frac{B_x}{B_z} J_z,\right]\Delta p + \left[K_x, - \frac{B_x}{B_z} K_z,\right]\Delta r + \left[Q_x, - \frac{B_x}{B_z} Q_z,\right]\Delta\theta$$

$$+ \left[W_x - \frac{B_x}{B_z} W_z\right]\delta_e + \left[T_x - \frac{B_x}{B_z} T_z\right]\delta_t + \left[R_x, - \frac{B_x}{B_z} R_z,\right]\delta_r$$

$$\left. + \left[S_x, - \frac{B_x}{B_z} S_z,\right]\delta_a\right] \qquad \text{(B100)}$$

Going back to equations (B97) and (B98), and solving (B97) for $\Delta\dot{v}$ in terms of $\Delta\dot{\alpha}$ results in

$$\Delta\dot{v} = \frac{1}{A_x,}\left[-B_x\Delta\dot{\alpha} + D_x,\Delta v + E_x,\Delta\alpha + F_x\Delta q + G_x,\Delta\theta + H_x,\Delta\beta + J_x,\Delta p\right.$$

$$\left. + K_x,\Delta r + Q_x,\Delta\phi + W_x\delta_e + T_x\delta_t + R_x,\delta_r + S_x,\delta_a\right] \qquad \text{(B101)}$$

Substituting equation (B101) into (B98) yields the following expression for $\Delta\dot{\alpha}$ in terms desired variables

$$\Delta\dot{\alpha} = \frac{A_{x'}}{B_z A_{x'} - B_x A_{z'}} \left[\left[D_{z'} - \frac{A_{z'}}{A_{x'}} D_{x'} \right] \Delta v + \left[E_{z'} - \frac{A_{z'}}{A_{x'}} E_{x'} \right] \Delta\alpha \right.$$

$$+ \left[F_z - \frac{A_{z'}}{A_{x'}} F_x \right] \Delta q + \left[G_{z'} - \frac{A_{z'}}{A_{x'}} G_{x'} \right] \Delta\theta + \left[H_{z'} - \frac{A_{z'}}{A_{x'}} H_{x'} \right] \Delta\beta$$

$$+ \left[J_{z'} - \frac{A_{z'}}{A_{x'}} J_{x'} \right] \Delta p + \left[K_{z'} - \frac{A_{z'}}{A_{x'}} K_{x'} \right] \Delta r + \left[Q_{z'} - \frac{A_{z'}}{A_{x'}} Q_{x'} \right] \Delta\phi$$

$$+ \left[W_z - \frac{A_{z'}}{A_{x'}} W_x \right] \delta_e + \left[T_z - \frac{A_{z'}}{A_{x'}} T_x \right] \delta_t + \left[R_{z'} - \frac{A_{z'}}{A_{x'}} R_{x'} \right] \delta_r$$

$$\left. + \left[S_{z'} - \frac{A_{z'}}{A_{x'}} S_{x'} \right] \delta_a \right] \qquad \text{(B102)}$$

Again, simplifying notation, let the coefficients in equations (B100) and (B102) be designated as follows

$$D_x'' = \frac{B_z}{A_x' B_z - A_z' B_x} \left[D_x' - \frac{B_x}{B_z} D_z' \right] \qquad \text{(B103)}$$

$$D_z'' = \frac{A_x'}{B_z A_x' - B_x A_z'} \left[D_z' - \frac{A_z'}{A_x'} D_x' \right] \qquad \text{(B104)}$$

Note: Terms in (B100) and (B102) that do not include primed terms such as the coefficient on Δq will be designated as

$$F_x' = \frac{B_z}{A_x' B_z - A_z' B_x} \left[F_x - \frac{B_x}{B_z} F_z \right] \qquad \text{(B105)}$$

This notation results in equations (B100) and (B102) being written as follows

$$\dot{\Delta\alpha} = D_x''\Delta v + E_x''\Delta\alpha + F_x'\Delta q + G_x''\Delta\theta + H_x''\Delta\beta + J_x''\Delta p + K_x''\Delta r$$
$$+ Q_x''\Delta\phi + W_x'\delta_e + T_x'\delta_T + R_x''\delta_r + S_x''\delta_a \qquad \text{(B106)}$$

and

$$\dot{\Delta\alpha} = D_z''\Delta v + E_z''\Delta\alpha + F_z'\Delta q + G_z''\Delta\theta + H_z''\Delta\beta + J_z''\Delta p + K_z''\Delta r$$
$$+ Q_z''\Delta\phi + W_z'\delta_e + T_z'\delta_T + R_z''\Delta r + S_z''\delta a \qquad \text{(B107)}$$

With this less cumbersome notation equation (B106) can be substituted into equation (B94) to obtain the desired expression for $\dot{\Delta\beta}$.

$$\dot{\Delta\beta} = \frac{1}{Cy}\Big[\left[D_y - A_yD_x''\right]\Delta V + \left[E_y - A_yE_x''\right]\Delta\alpha + \left[-A_yF_x'\right]\Delta q$$
$$+ \left[G_y - A_yG_x''\right]\Delta\theta + \left[H_y - A_yH_x''\right]\Delta\beta + \left[J_y - A_yJ_x''\right]\Delta p$$
$$+ \left[K_y - A_yK_x''\right]\Delta r + \left[Q_y - A_yQ_x''\right]\Delta\phi + \left[-A_yW_x'\right]\delta_e$$
$$+ \left[-A_yT_x'\right]\delta_T + \left[R_y - A_yR_x''\right]\delta_r + \left[S_y - A_yS_x''\right]\delta_a\Big] \qquad \text{(B108)}$$

The preceding manipulations enabled equations (B80), (B82), and (B83), the force equations, to be written in first order form. Using similar techniques the moment equations will be written in this same form. Starting with the pitching moment equations (B85), the $\dot{\Delta\alpha}$ equation (B107) is substituted in for $\dot{\Delta\alpha}$ and (B85) is then solved for $\dot{\Delta q}$. Grouping like terms results in the following expression.

$$\dot{\Delta q} = \frac{1}{I_y}\Big[\left[M_v + M_{\dot\alpha}D_z''\right]\Delta V + \left[M_\alpha + M_{\dot\alpha}E_z''\right]\Delta\alpha + \left[M_q + M_{\dot\alpha}F_z'\right]\Delta q$$
$$+ \left[M_{\dot\alpha}G_z''\right]\Delta\theta + \left[M_{\dot\alpha}H_z''\right]\Delta\beta + \left[r_e(I_z - I_x) - 2p_eI_{XZ} + M_{\dot\alpha}J_z''\right]\Delta p$$
$$+ \left[p_e(I_z - I_x) + 2r_eI_{xz} + M_{\dot\alpha}K_z''\right]\Delta r + \left[M_{\dot\alpha}Q_z''\right]\Delta\phi$$
$$+ \left[M_{\delta e} + M_{\dot\alpha}W_z'\right]\delta_e + \left[M_{\delta_T} + M_{\dot\alpha}T_z'\right]\delta_T + \left[M_{\dot\alpha}R_z''\right]\delta_r$$
$$+ \left[M_{\dot\alpha}S_z''\right]\delta_a\Big] \qquad \text{(B109)}$$

The rolling moment equation (B84) includes $\Delta\dot{p}$ and $\Delta\dot{r}$ terms, as does the yawing moment equation (B86). Using (B86) to express $\Delta\dot{r}$ in terms of $\Delta\dot{p}$ yields

$$\Delta\dot{r} = \frac{1}{I_y}\left[I_{zx}\Delta\dot{p} + \left[p_e(I_x - I_y) - r_e I_{xz}\right]\Delta q + N_\beta \Delta\beta + \left[q_e(I_x - I_y) + N_p\right]\Delta p + \left[-q_e I_{xz} + N_r\right]\Delta r + N_{\delta_r}\delta_r + N_{\delta_a}\delta_a\right] \quad \text{(B110)}$$

substituting (B110) into (B84) and grouping like terms produces the following expression for $\Delta\dot{p}$

$$\Delta\dot{p} = \left[r_e\left[\frac{I_z(I_y - I_z) - I_{xz}^2}{I_x I_z - I_{zx}^2}\right] + p_e\left[\frac{I_{xz}I_z + I_{zx}(I_x - I_y)}{I_x I_z - I_{zx}^2}\right] \right]\Delta q + \left[\frac{L_\beta I_z + N_\beta I_{xz}}{I_x I_z - I_{zx}^2}\right]\Delta\beta + \left[\left[\frac{L_p I_z + N_p I_{zx}}{I_x I_z - I_{xz}^2}\right] + q_e\left[\frac{I_z I_{xz} + I_{zx}(I_x - I_y)}{I_x I_z - I_{xz}^2}\right] \right]\Delta p + \left[\left[\frac{L_r I_z + N_r I_{zx}}{I_x I_z - I_{xz}^2}\right] + q_e\left[\frac{I_z(I_y - I_z) - I_{zx}^2}{I_x I_z - I_{zx}^2}\right] \right]\Delta r + \left[\frac{L_{\delta r} I_z + N_{\delta r} I_{zx}}{I_x I_z - I_{zx}^2}\right]\delta_r + \left[\frac{L_{\delta a} I_z + N_{\delta a} I_{zx}}{I_x I_z - I_{zx}^2}\right]\delta_a \quad \text{(B111)}$$

The yawing moment equation (B86) can be solved for $\Delta\dot{r}$ by writing $\Delta\dot{p}$ in terms of $\Delta\dot{r}$ from the rolling moment equation (B84) which is

$$\Delta\dot{p} = \frac{1}{I_x}\left[\Delta\dot{r} I_{xz} + \left[r_e(I_y - I_z) + p_e I_{xz}\right]\Delta q + L_\beta \Delta\beta + \left[L_p + q_e I_{xz}\right]\Delta p + \left[L_r + q_e(I_y - I_z)\right]\Delta r + L_{\delta_r}\delta_r + L_{\delta_a}\delta_a\right] \quad \text{(B112)}$$

and substituting (B112) into (B86) which yields the following expression for $\Delta\dot{r}$

$$\dot{\Delta r} = \left[p_e\left[\frac{I_x(I_x - I_y) + I_{xz}^2}{I_xI_z - I_{zx}^2}\right] + r_e\left[\frac{I_{zx}(I_y - I_z) - I_{xz}I_x}{I_xI_z - I_{zx}^2}\right] \right] \Delta q$$

$$+ \left[\frac{N_\beta I_x + L_\beta I_{zx}}{I_xI_z - I_{zx}^2}\right] \Delta\beta + \left[\left[\frac{N_p I_x + L_p I_{zx}}{I_xI_z - I_{zx}^2}\right] + q_e\left[\frac{I_x(I_x - I_y) + I_{zx}^2}{I_xI_z - I_{zx}^2}\right] \right] \Delta p$$

$$+ \left[\left[\frac{N_r I_x + L_r I_{zx}}{I_xI_z - I_{zx}^2}\right] + q_e\left[\frac{I_{zx}(I_y - I_z) - I_{zx}I_x}{I_xI_z - I_{zx}^2}\right] \right] \Delta r$$

$$+ \left[\frac{N_{\delta_r} I_x + L_{\delta_r} I_{zx}}{I_xI_z - I_{zx}^2}\right] \delta_r + \left[\frac{N_{\delta_a} I_x + L_{\delta_a} I_{zx}}{I_xI_z - I_{zx}^2}\right] \delta_a \qquad \text{(B113)}$$

Equations (B110) and (B112) can be simplified notation wise by using the following expressions

$$I1 = I_xI_z - I_{zx}^2$$

$$I2 = \frac{I_z(I_y - I_z) - I_{zx}^2}{I1}$$

$$I3 = \frac{I_{zx}I_z + I_{zx}(I_x - I_y)}{I1} \qquad \text{(B114)}$$

$$I4 = \frac{I_x(I_x - I_y) + I_{zx}^2}{I1}$$

$$I5 = \frac{I_{zx}(I_y - I_z) - I_{zx}I_x}{I1}$$

$$L_\beta' = \frac{L_\beta I_z + N_\beta I_{xz}}{I1} \qquad N_\beta' = \frac{N_\beta I_x + L_\beta I_{zx}}{I1}$$

$$L_p' = \frac{L_p I_z + N_p I_{zx}}{I1} \qquad N_p' = \frac{N_p I_x + L_p I_{zx}}{I1}$$

$$L_r' = \frac{L_r I_z + N_r I_{zx}}{I1} \qquad N_r' = \frac{N_r I_x + L_r I_{zx}}{I1} \qquad \text{(B115)}$$

$$L_{\delta_r}' = \frac{L_{\delta r} I_z + N_{\delta r} I_{zx}}{I1} \qquad N_{\delta_r}' = \frac{N_{\delta r} I_x + L_{\delta r} I_{zx}}{I1}$$

$$L_{\delta_a}' = \frac{L_{\delta_a} I_z + N_{\delta_a} I_{zx}}{\Pi} \qquad N_{\delta_a}' = \frac{N_{\delta_a} I_x + L_{\delta_a} I_{zx}}{\Pi}$$

Substituting (B114) and (B115) into (B111) and (B113) results in the following equations for $\Delta\dot{p}$ and $\Delta\dot{r}$

$$\Delta\dot{p} = \left[r_e(I2) + p_e(I3)\right] \Delta q + L_\beta'\Delta\beta + \left[L_p' + q_e(I3)\right] \Delta p + \left[L_r' + q_e(I2)\right] \Delta r + L_{\delta_r}'\delta_r + L_{\delta_a}'\delta_a \tag{B116}$$

and

$$\Delta\dot{r} = \left[p_e(I4) + r_e(I5)\right] \Delta q + N_\beta'\Delta\beta + \left[N_p' + q_e(I4)\right] \Delta p + \left[N_r' + q_e(I5)\right] \Delta r + N_{\delta_r}'\delta_r + N_{\delta_a}'\delta_a \tag{B117}$$

The $\Delta\dot{\Phi}$ and $\Delta\dot{\theta}$ equations (B87) and (B88), respectively, are already in the desired first order form. For convenience, the eight first order linearized differential equations of motion generalized for a steady level turn equilibrium condition are listed below

$$\Delta\dot{V} = D_x''\Delta V + E_x''\Delta\alpha + F_x'\Delta q + G_x''\Delta\theta + H_x''\Delta\beta + J_x''\Delta p + K_x''\Delta r + Q_x''\Delta\Phi + W_x'\delta_e + T_x'\delta_T + R_x''\delta_r + S_x''\delta_a \tag{B118}$$

$$\Delta\dot{\alpha} = D_z''\Delta V + E_z''\Delta\alpha + F_z'\Delta q + G_z''\Delta\theta + H_z''\Delta\beta + J_z''\Delta p + K_z''\Delta r + Q_z''\Delta\Phi + W_z'\delta_e + T_z'\delta_T + R_z''\delta_r + S_z''\delta_a \tag{B119}$$

$$\Delta\dot{q} = \frac{I}{I_y}\Big[\left[M_V + M_\alpha' D_z''\right] \Delta v + \left[M_\alpha + M_\alpha' E_z''\right] \Delta\alpha + \left[M_q + M_\alpha' F_z'\right] \Delta q + \left[M_\alpha' G_z''\right] \Delta\theta + \left[M_\alpha' H_z''\right] \Delta\beta + \left[r_e(I_z - I_x) - 2p_e I_{xz} + M_\alpha' J_z''\right]\Delta p + \left[p_e(I_z - I_x) + 2r_e I_{xz} + M_\alpha K_z''\right] \Delta r + \left[M_\alpha Q_z''\right] \Delta\Phi + \left[M_{\delta_e} + M_\alpha' W_z'\right] \delta_e + \left[M_{\delta_T} + M_\alpha' T_z'\right] \delta_T + \left[M_\alpha' R_z''\right] \delta_r + \left[M_\alpha' S_z''\right] \delta_a \Big] \tag{B120}$$

$$\Delta\dot{\theta} = \left[\cos\Phi_e\right] \Delta q + \left[-\sin\Phi_e\right] \Delta r + \left[-r_e\sin\Phi_e - r_e\cos\Phi_e\right] \Delta\Phi \tag{B121}$$

$$\Delta\dot{v} = \frac{1}{C_{y_\beta}}\Big[\left[F_y - A_y J_x''\right]\Delta v + \left[F_y - A_y E_x''\right]\Delta r + \left[-A_y F_x'\right]\Delta q + \left[G_y - A_y G_x''\right]\Delta\theta + \left[H_y - A_y H_x''\right]\Delta\beta + \left[J_y - A_y J_x''\right]\Delta p + \left[K_y - A_y K_x''\right]\Delta r + \left[L_y - A_y L_x''\right]\Delta\phi + \left[-A_y W_x'\right]\delta_e + \left[-A_y T_x'\right]\delta_T + \left[R_y - A_y R_x''\right]\delta_r + \left[S_y - A_y S_x''\right]\delta_a\Big] \quad \text{(B122)}$$

$$\Delta\dot{p} = \left[r_e(I2) + p_e(I3)\right]\Delta q + L_\beta'\,\Delta\beta + \left[L_p' + q_e(I3)\right]\Delta p + \left[L_r' + q_e(I2)\right]\Delta r + L_{\delta_r}'\delta_r + L_{\delta_a}'\delta_a \quad \text{(B123)}$$

$$\Delta\dot{r} = \left[p_e(I4) + r_e(I5)\right]\Delta q + N_\beta'\Delta\beta + \left[N_p' + q_e(I4)\right]\Delta p + \left[N_r' + q_e(I5)\right]\Delta r + N_{\delta_r}'\delta_r + N_{\delta_a}'\delta_a \quad \text{(B124)}$$

$$\Delta\dot{\phi} = \left[r_e\cos\phi_e\sec^2\theta_e + q_e\sin\phi_e\sec^2\theta\right]\Delta\theta + \left[\sin\phi_e\tan\theta_e\right]\Delta q + \Delta p + \left[\cos\phi_e\tan\theta_e\right]\Delta r + \left[q_e\cos\phi_e\tan\theta_e - r_e\sin\phi_e\tan\theta_e\right]\Delta\phi \quad \text{(B125)}$$

Appendix C

A-7D Flight Control System

Appendix C

A-7D Flight Control System

A-7D Flight Control Description

The A-7D flight control system is a hydraulically powered irreversible system. Longitudinal control is provided by a Unit Horizontal Tail (UHT). The longitudinal feel system consists of a dual gradient feel spring whose force varies with stick displacement, two bobweights to provide static and dynamic force gradients, and two viscous dampers to provide damping and stick forces proportional to stick velocity.

The lateral control is provided by a combination aileron and spoiler/deflector system. Both sets of surfaces are active at all times except near neutral stick where a small dead spot in spoiler motion occurs to allow small aileron inputs. Although full lateral stick travel remains the same, available surface deflections of aileron and spoilers increase from +/- 16 degrees and 36 degrees to +/- 25 degrees and 60 degrees, respectively, when control augmentation mode is engaged.

The directional control system is a conventional rudder system. In the cruise configuration +/- 6 degrees rudder deflection is available along with an aileron rudder interconnect (ARI) system which provides additional deflection when the yaw stabilization mode is engaged.

The aircraft has an automatic maneuvering flap system (AMF) which was not used during this test. In addition, general autopilot modes were not evaluated.

The three modes of the flight control system of concern here are the mechanical mode, the yaw stabilization mode, and the control augmentation mode. The mechanical path is paralleled by the other two. With just the mechanical path the pilot flies an unaugmented aircraft by

means of cables and pulleys. The first improvement occurs by selecting the yaw stabilization (YAW STAB) mode which gives rudder trim, lateral acceleration feedback and aileron rudder interconnect (ARI). The normal mode used is called the control augmentation (CONT AUG) mode and requires YAW STAB to be engaged. In this full up mode the pitch and roll mechanical paths are paralleled by electrical paths to provide improved aircraft dynamics. In this mode, pitch rate gyros and normal accelerometers improve pitch damping, while roll rate feedback improves roll damping.

For this analysis, the flight control system was simplified by eliminating the high frequency elements which included the actuators, making the non-linear elements linear, and omitting the limiters in the YAW STAB and CONT AUG modes. Each axes will be addressed separately.

Pitch Axis

The simplified pitch axis block diagram (Figure C1) is used as a guide for writing the differential equations describing the longitudinal flight control system.

Starting with the mechanical path the following variables are defined.

$\dot{q}$ = pitch acceleration available from existing state equation

a_z = acceleration in Z direction, computed from lift equation

K_{f_s} = spring constant for dual gradient feel spring

δ_{ep} = new input variable representing pilot elevator input in pounds

δ_{em_1} = new variable for mechanical path

δ_{em_2} = new state variable for mechanical path

$\delta_{em_2}^{1} = K_T \delta_{em_2}$; K_T is trim constant which varies with UHT trim position.

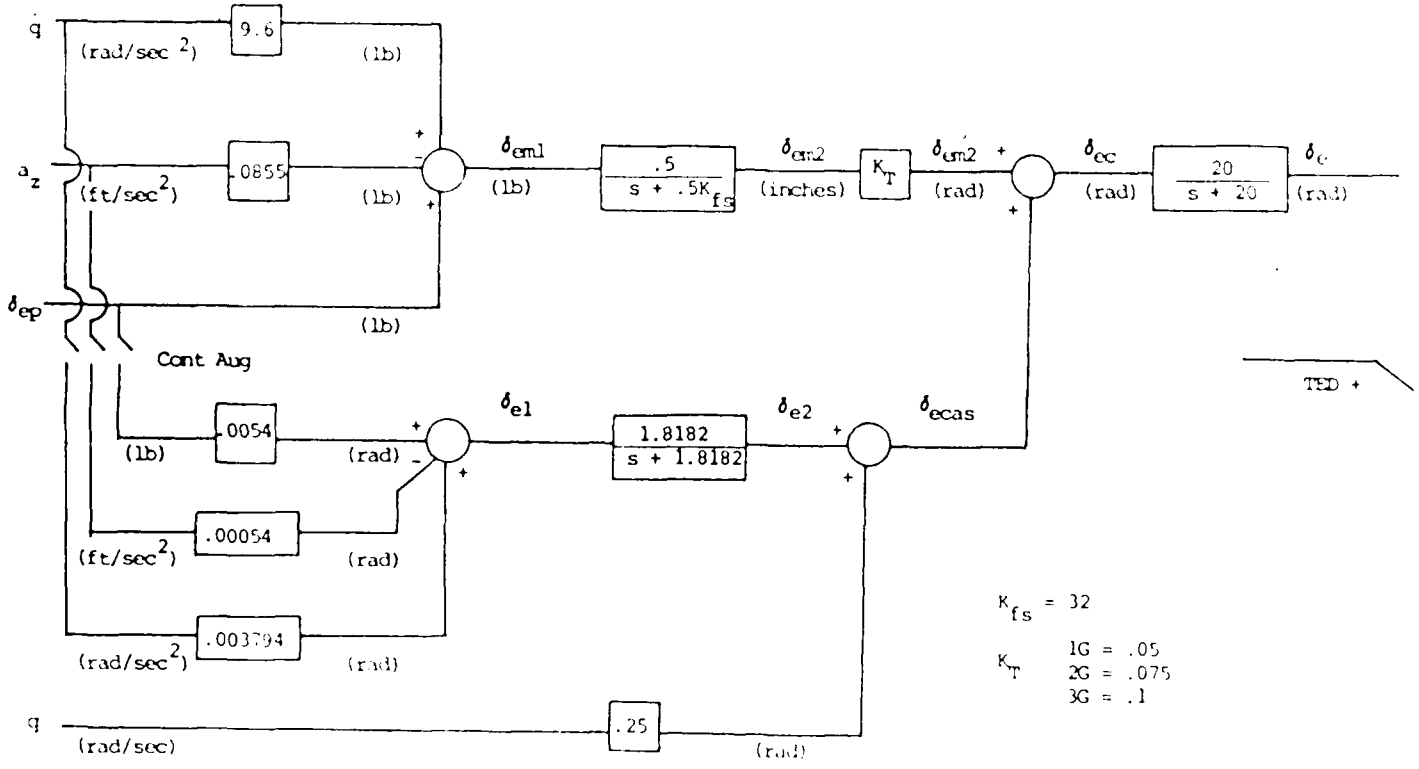

Figure C1. Pitch Axis (Mechanical + CAS)

Using block diagram algebra

$$\delta_{em_1} = \delta_{ep} + 9.6\dot{q} - .0855a_z \tag{C1}$$

$$\frac{\delta_{em_2}}{\delta_{em_1}} = \frac{.5}{s + .5K_{f_s}} \tag{C2}$$

The two constants 9.6 and .0855 are related to the dual bob weights in the aircraft. One bob weight is located forward of the control stick and one is located in the tail of the aircraft. Normally the ratio of these two numbers will give the location of the bob weight in relation to the center of rotation; however, in this case the ratio yields

$$\frac{9.6}{.0855}\left[\frac{\text{ft slug}}{\text{slug}}\right] = 112.3 \text{ ft}$$

This distance is an effective length due to the fore/aft bob weight configuration. This configuration results in the bob weight pair being most effective during pitch accelerations, and has a minor effect on stick forces during steady maneuvers.

The K_{f_s} is a spring constant for the dual gradient feel spring with the following schedule

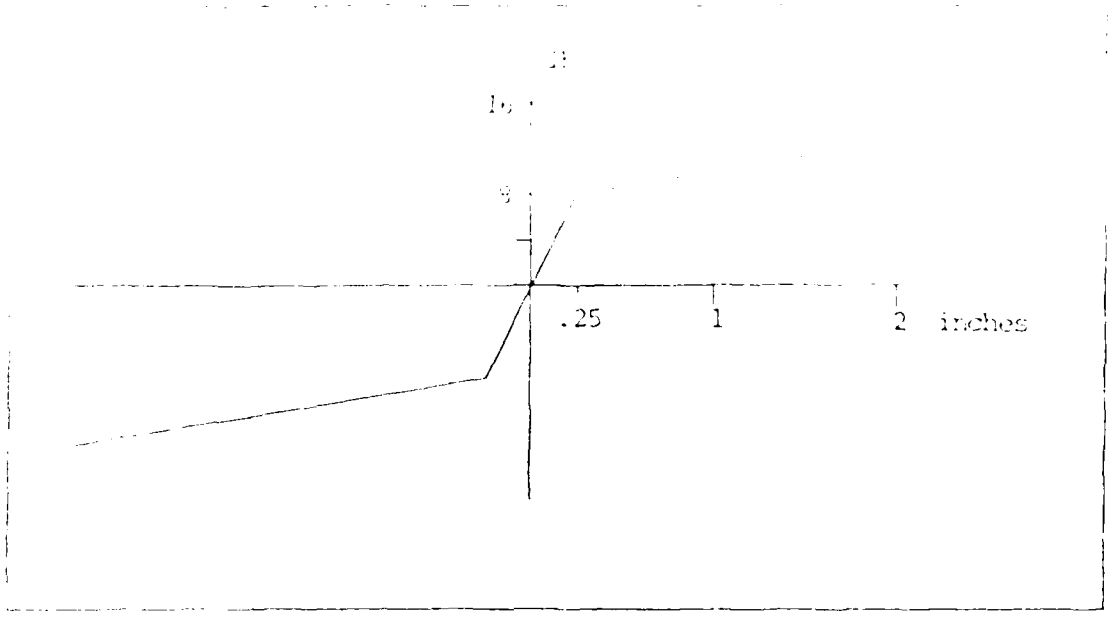

Figure C2. Dual Gradient Feel Spring

The initial value of K_{f_s} for the first 0.25 inches of control cable movement is 32 lb/in changing to 2.909 lb/in for larger deflection.

Continuing with the block diagram algebra gives

$$\delta_{em_2}\ (s + .5k_{f_s}) = .5\delta_{em_1}$$

or

$$\dot{\delta}_{em_2} = .5\delta_{em_1} - .5K_{f_s}\delta_{em_2} \tag{C3}$$

Substituting for δ_{em_1} yields

$$\dot{\delta}_{em_2} = .5\left[\delta_{ep} + 9.6\dot{q} - .0855a_z\right] - .5K_{f_s}\delta_{em_2} \tag{C4}$$

The control augmentation system (CAS) portion is reduced in a similar manner using the following variables:

δ_{c_1} = new variable

δ_{c_2} = new state variable

[illegible]

[illegible]

The .0054 constant [illegible]

$K_q = .00054$ with K_q being

$$.00054 \left[\frac{g\ sec^2\ rad}{ft\ deg}\right] = \frac{1}{(32.2(ft/sec^2)/g)(57.3deg/rad)}$$

The K_{sa} term is

$$10 \left[\frac{deg\ ft}{lb\ sec^2 g}\right] = \frac{.31\ deg}{lb} \quad \frac{32.2\ ft}{sec^2 g}$$

The .00054 coefficient on a_z is

$$.00054 \left[\frac{sec^2 rad}{ft}\right] = \frac{1\ deg}{g} K_q = \frac{1\ deg}{g} \left(\frac{.00054 g sec^2 rad}{ft\ deg}\right)$$

The coefficient on $\dot{q}$ is made up of the following

$$.0003794 \left[\frac{sec^2}{ft}\right] = 7ft \frac{1\ deg}{g} K$$

where the 7ft is the distance forward of the c.g. of the accelerometer.

Further reduction

$$\frac{\delta_{e_2}}{\delta_{e_1}} = \frac{1.8182}{s + 1.8182} \tag{C6}$$

which gives

$$\delta_{e_2} (s + 1.8182) = 1.8182\delta_{e_1}$$

or

$$\dot{\delta}_{e_2} = 1.8182\delta_{e_1} - 1.8182\delta_{e_2} \tag{C7}$$

substituting for δ_{e_1} yields

$$\dot{\delta}_{e_2} = 1.8182 \left[.0054 \delta_{e_1} - .00054 a_z + .0003794 \dot{q}\right] - 1.8182\delta_{e_2} \tag{C8}$$

Adding the pitch rate

$$\delta_{e_{CAS}} = \delta_{e_2} + .25q \tag{C9}$$

The pitch CAS limiter which limits CAS authority to $\pm$ .084 radians has been omitted to keep the equations linear. The total elevator commanded by the mechanical and CAS paths is represented by δ_{e_c}, which equals

$$\delta_{ec} = \delta_{em_2}' + \delta_{e_{CAS}} \tag{C10}$$

and from before

$$\delta_{em_2}' = k_T \delta_{em_2}$$

The trim constant K_T is a function of the trimmed position of the UHT which varies from .05 with UHT at 4° TEU and .1 with UHT at 8° TEU. (For this analysis .05 was used for 1g, .075 for 2G, and .1 for 3G.)

Actuator dynamics were considered negligible resulting in the

$$\frac{20}{s + 20} \approx 1$$

so

$$\delta_{ec} = \delta_e$$

Everywhere a δ_e appears in the original state equations, the expression

$$\delta_e = \delta_{em_2}' + \delta_{e_{CAS}} = k_T \delta_{em_2} + \delta_{e_2} + .25q \text{ (fully augmented)} \tag{C11}$$

$$\delta_e = \delta_{em_2}' \text{ (mechanical only)} \tag{C12}$$

will be substituted.

Summarizing the pitch axis equations yields

$$\delta_e = K_T \delta_{em_2} + \delta_{e_2} + .25q$$

$$\dot{\delta}_{em_2} = .5\left[\delta_{ep} + 9.6\dot{q} - .0855a_z\right] - .5K_{f_s}\delta_{em_2}$$

$$\dot{\delta}_{e_2} = 1.8182\left[.0054\delta_{ep} - .00054a_z + .003794\dot{q}\right] - 1.8182\delta_{e_2}$$

The a_z term is calculated using the lift equation

$$F_{AZ_B} = ma_z$$

where F_{AZ_B} is the z body axis aerodynamic force component, which gives

$$a_z = \frac{1}{m}\left[Z_V\Delta v + Z_\alpha\Delta\alpha + Z_q\Delta q + Z_{\delta_e}\delta_e\right] \qquad (C13)$$

Roll Axis

The simplified roll axis block diagram (Figure C3) is used to aid in writing the lateral flight control equations.

The variables used in the mechanical path

δ_{ap} = input variable representing pilot aileron input in pounds

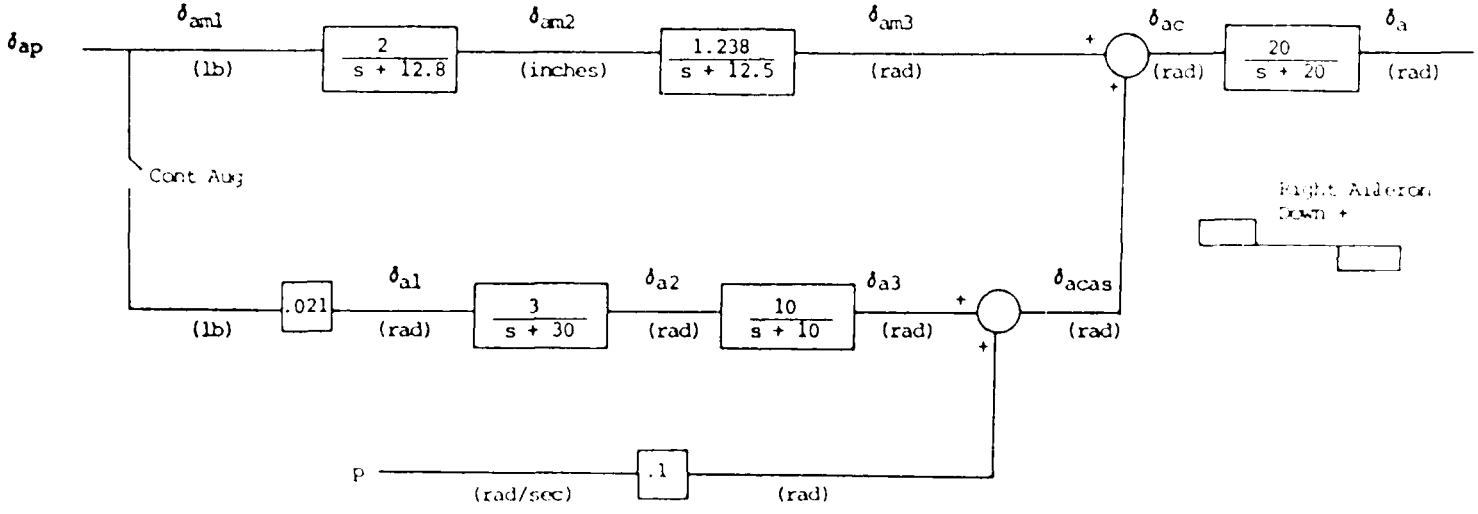

Figure C3. Roll Axis (Mechanical + CAS)

[illegible]

[illegible]

[illegible]

Using block diagram algebra

$$\delta_{am_1} = \delta_{ap} \tag{C14}$$

$$\frac{\delta_{am_2}}{\delta_{am_1}} = \frac{2}{s + 12.8} \quad \text{(feel spring)} \tag{C15}$$

which gives

$$\delta_{am_2}(s + 12.8) = 2\,\delta_{am_1}$$

or

$$\dot{\delta}_{am_2} = 2\,\delta_{am_1} - 12.8\,\delta_{am_2} = 2\,\delta_{ap} - 12.8\,\delta_{am_2} \tag{C16}$$

going through the feel isolation servo

$$\frac{\delta_{am_3}}{\delta_{am_2}} = \frac{1.238}{s + 12.5} \tag{C17}$$

which gives

$$\delta_{am_3}(s + 12.5) = 1.238\delta_{am_2}$$

or

$$\dot{\delta}_{am_3} = 1.238\,\delta_{am_2} - 12.5\,\delta_{am_3} \tag{C18}$$

The CAS path uses the following variables

δ_{a_1} = new variable

δ_{a_2} = new state variable

δ_{a_3} = new state variable

[illegible]

$$.021 \left[\frac{\text{rad}}{\text{lb}}\right] = \frac{1.2 \text{ deg}}{1\text{b}} \frac{\text{rad}}{57.3 \text{ deg}}$$

Now

$$\frac{\delta_{a_2}}{\delta_{a_1}} = \frac{3}{s + 3} \tag{C20}$$

which gives

$$\delta_{a_2} (s + 3) = 3\delta_{a_1}$$

or

$$\dot{\delta}_{a_2} = 3\delta_{a_1} - 3\,\delta_{a_2} \tag{C21}$$

Substituting for δ_{a_1} yields

$$\dot{\delta}_{a_2} = .063\,\delta_{ap} - 3\,\delta_{a_2} \tag{C22}$$

Now

$$\frac{\delta_{a_3}}{\delta_{a_2}} = \frac{10}{s + 10} \tag{C23}$$

which gives

$$\delta_{a_3} (s + 10) = 10\,\delta_{a_2}$$

or

$$\dot{\delta}_{a_3} = 10\,\delta_{a_2} - 10\,\delta_{a_3} \tag{C24}$$

Adding in roll rate

$$\delta_{a_{2S}} = \delta_{a_3} + .1p$$

[illegible]

therefore

$$\delta_a = \delta_{am_3} + \delta_{a_{CAS}} \tag{C25}$$

substituting for $\delta_{a_{CAS}}$

$$\delta_a = \delta_{am_3} + \delta_{a_3} + .1p \tag{C26}$$

This equation will be substituted for δ_a in the original state equations. Summarizing the new roll equations yields

$$\delta_a = \delta_{am_3} + \delta_{a_3} + .1p$$

$$\dot{\delta}_{am_2} = 2\,\delta_{ap} - 12.8\,\delta_{am_2}$$

$$\dot{\delta}_{am_3} = 1.238\,\delta_{am_2} - 12.5\,\delta_{am_3}$$

$$\dot{\delta}_{a_2} = .063\,\delta_{ap} - 3\,\delta_{a_2}$$

$$\dot{\delta}_{a_3} = [illegible]\,\delta_{a_2} - [illegible]\,\delta_{a_3}$$

Yaw Axis

The simplified yaw axis block diagram (Figure C4) is used to aid in writing the directional flight control equations.

The variables used in the yaw axis are listed below

δ_{rm} = mechanical path variable

δ_{r1-11} = new state or intermediate variables

which yields

$$\delta_{r_3}(s + 1) = \delta_{r_2} s$$

or

$$\dot{\delta}_{r_3} = \dot{\delta}_{r_2} - \delta_{r_3} \tag{C31}$$

Taking the derivative of δ_{r_2} yields

$$\dot{\delta}_{r_2} = .25\dot{r} - .011\dot{p} \tag{C32}$$

Substituting into the $\dot{\delta}_{r_3}$ equation gives

$$\dot{\delta}_{r_3} = .25\dot{r} - .011\dot{p} - \delta_{r_3} \tag{C33}$$

Summing δ_{r_1} and δ_{r_3} produces

$$\delta_{r_4} = \delta_{r_1} + \delta_{r_3} = .2\,\delta_a + \delta_{r_3} \tag{C34}$$

The lateral acceleration feedback path is ON/OFF depending on rudder pedal displacement. If the rudder pedal is deflected more than .03 radians, the loop is deactivated. To simulate this, it was necessary to produce two sets of state equations. The first represented the lateral acceleration feedback and was used for generating time responses due to rudder doublets. The output of this set was then used as initial conditions to a model that had the lateral acceleration loop deactivated. The signal for this lateral acceleration feedback was obtained from an accelerometer located 7 feet forward of the center of gravity. Therefore,

$$\frac{\delta r_6}{\delta r_5} = \frac{2}{s+2} \tag{C36}$$

which yields

$$\delta r_6 (s + 2) = 2\, \delta r_5$$

or

$$\dot{\delta} r_6 = 2\, \delta r_5 - 2\, \delta r_6 \tag{C37}$$

Substituting for δr_5

$$\dot{\delta} r_6 = 2(a_y + 7\dot{r}) - 2\, \delta r_6 = 2a_y + 14\dot{r} - 2\, \delta r_6 \tag{C38}$$

Continuing

$$\delta r_7 = .25\, \delta r_6 \tag{C39}$$

and

$$\frac{\delta r_8}{\delta r_7} = \frac{.0036}{s} \tag{C40}$$

Performing and substituting for δr_7

$$\dot{\delta} r_8 = .0036\, \delta r_7 = .0009\, \delta r_6 \tag{C41}$$

The .0036 constant is a combination of the roll wing constants

[illegible]

The .0009 constant in the parallel path consists of the roll wing

[illegible]

and

$$\delta_{r_{10}} = \delta_{r_8} + \delta_{r_9} \tag{C43}$$

also

$$\delta_{r_{11}} = \delta_{r_4} + \delta_{r_{10}} \tag{C44}$$

Again assuming actuator dynamics to be negligible

$$\delta_{r_c} = \delta_r$$

The total rudder equation becomes

$$\begin{aligned}\delta_r &= \delta_{rm} + \delta_{r_{11}} \\ &= .001\,\delta_{rp} + \delta_{r_4} + \delta_{r_{10}} \\ &= .001\,\delta_{rp} + .2\,\delta_a + \delta_{r_3} + \delta_{r_8} + \delta_{r_9} \\ &= .001\,\delta_{rp} + .2\,\delta_a + \delta_{r_3} + \delta_{r_8} + .003\,\delta_{r_6}\end{aligned} \tag{C45}$$

substituting for δ_a yields the following δ_r equation. In addition, the yaw axis state equations are summarized

$$\delta_r = .001\,\delta_{rp} + .2\,[\delta_{am_3} + \delta_{a_3} + .1p] + \delta_{r_3} + \delta_{r_8} + .003\,\delta_{r_6}$$

$$\dot{\delta}_{r_3} = .25\,\dot{r} - .011\dot{p} - \delta_{r_3}$$

$$\dot{\delta}_{r_6} = 2\,a_y + 14\dot{r} - 2\,\delta_{r_6}$$

$$\dot{\delta}_{r_8} = .0609\,\delta_{r_6}$$

The only term remaining to be calculated is the lateral acceleration which is obtained from the Y force equation

$$F_{AY_b} = m\,a_y$$

which gives

$$a_y = \frac{1}{m}\left[Y_\beta \Delta\beta + Y_p \Delta p + Y_r \Delta r + Y_{\delta_r} \delta_r + Y_{\delta_a} \delta_a\right] \qquad \text{(C46)}$$

Appendix D

Computer Programs

Appendix D

Computer Program Explanations and Code

I wrote several computer programs to aid my analysis. The programs are written in Applesoft Basic and were run on an Apple II Plus home computer in the following configuration:

Apple II Plus 48K 2 Disk Drives	Slot 6
Andromeda 16K RAM Expansion Card	Slot 0
Videx 80 Column Card	Slot 3
Hayes Micro Modem II	Slot 2
Epson MX-100 Printer with Parallel Interface	Slot 1
EPS Keyboard	

A brief description of each program and its code is provided for reference.

Data Creator

This program creates a random access data file on floppy disk for use with the other programs. Three options are used to input data.

1. New Data Entered: This option clears the disk of all prior data and allows entry of specific data for 1G flight conditions.

2. Change Current Data: This option allows incorrect entries to be changed without erasing data already on the disk.

3. Add Data: This option allows entry of data for other than 1G without erasing data already on the disk.

DATA CREATOR

```
10    REM  THESIS AID: CREATES RANDOM ACCESS DATA FILES
20    REM
30    REM  BY JEFFREY R. RIEMER
40    REM  14 APRIL 1983
50    REM
60    TEXT
    : HOME
    : PRINT CHR$ (12)
    : PRINT
70    D$ = CHR$ (4)
    : REM  CTRL-D
80    DIM K(100)
90    PRINT "1 - ENTER NEW DATA SET"
100   PRINT
    : PRINT
110   PRINT "2 - CHANGE CURRENT DATA"
120   PRINT
    : PRINT
125   PRINT "3 - ADD TO DATA"
    : PRINT
    : PRINT
130   PRINT "ENTER OPTION -->";
140   GET A
    : PRINT A
150   ON A GOTO 160,1000,1200
160   PRINT D$;"OPEN A7-D,D2"
170   PRINT D$;"DELETE A7-D,D2"
180   PRINT D$;"OPEN A7-D,L20,D2"
185   PRINT
    : PRINT
190   PRINT "ENTER THE FOLLOWING DATA"
195   PRINT
200   INPUT "ALTITUDE                    H= ";K(0)
210   INPUT "INDICATED MACH NUMBER     IMN= ";K(1)
```

```
220   INPUT "DENSITY                        RO= ";K(2)
230   INPUT "VELOCITY (FT/SEC)               V= ";K(3)
240   INPUT "WING AREA                       S= ";K(4)
250   INPUT "MEAN GEOMETRIC CHORD            C= ";K(5)
260   INPUT "WING SPAN                       B= ";K(6)
270   INPUT "ACCELERATION OF GRAVITY         G= ";K(7)
280   INPUT "CENTER OF GRAVITY              CG= ";K(8)
290   INPUT "GROSS WEIGHT                   WT= ";K(9)
300   PRINT
    : PRINT
310   INPUT "CM ALPHA                      CMA= ";K(10)
320   INPUT "CM DELTA ELEVATOR            CMDE= ";K(11)
330   INPUT "CL ALPHA                      CLA= ";K(12)
340   INPUT "CL DELTA ELEVATOR            CLDE= ";K(13)
350   INPUT "                              CMQ= ";K(14)
360   INPUT "                              CLQ= ";K(15)
370   INPUT "ALPHA ST & LEVEL FLT           AO= ";K(16)
380   INPUT "SIDE FORCE DUE TO BETA        CYB= ";K(17)
390   INPUT "CY DELTA RUDDER              CYDR= ";K(18)
400   INPUT "CY DELTA AILERON             CYDA= ";K(19)
410   INPUT "                              CYP= ";K(20)
420   INPUT "                              CYR= ";K(21)
430   INPUT "ROLLING DUE TO BETA           CLB= ";K(22)
440   INPUT "CL DELTA RUDDER              CLDR= ";K(23)
450   INPUT "CL DELTA AILERON             CLDA= ";K(24)
460   INPUT "                              CLP= ";K(25)
470   INPUT "                              CLR= ";K(26)
480   INPUT "YAW DUE TO BETA               CNB= ";K(27)
490   INPUT "CN DELTA RUDDER              CNDR= ";K(28)
500   INPUT "CN DELTA AILERON             CNDA= ";K(29)
```

```
510   INPUT "                              CNP= ";K(30)
-----------------------
520   INPUT "                              CNR= ";K(31)
-----------------------
530   INPUT "LIFT COEFFICIENT               CL= ";K(32)
-----------------------
540   INPUT "                              CLV= ";K(33)
-----------------------
550   INPUT "CL ALPHA DOT                 CLAD= ";K(34)
-----------------------
560   INPUT "DRAG COEFFICIENT               CD= ";K(35)
-----------------------
570   INPUT "                              CDV= ";K(36)
-----------------------
580   INPUT "CD ALPHA                      CDA= ";K(37)
-----------------------
590   INPUT "CD DELTA ELEVATOR            CDDE= ";K(38)
-----------------------
600   INPUT "                              CMV= ";K(39)
-----------------------
610   INPUT "CM DELTA THROTTLE            CMDT= ";K(40)
-----------------------
620   INPUT "CM ALPHA DOT                 CMAD= ";K(41)
-----------------------
625   IF A = 3 THEN GOTO 1230
-----------------------
630   INPUT "MOMENT OF INERTIA (SA)         IX= ";K(42)
-----------------------
640   INPUT "                               IY= ";K(43)
-----------------------
650   INPUT "                               IZ= ";K(44)
-----------------------
660   INPUT "PRODUCT OF INERTIA             ZX= ";K(45)
-----------------------
670   FOR I = 0 TO 45
-----------------------
680     PRINT D$;"WRITE A7-D,R";I
-----------------------
690     PRINT K(I)
-----------------------
700   NEXT
-----------------------
701   PRINT D$;"CLOSE A7-D"
-----------------------
702   PRINT D$;"OPEN A7-D,L20,D2"
-----------------------
703   PRINT
    : INPUT "DELTA ELEVATOR ST & LVL FLT ";IT
-----------------------
704   PRINT D$
    : PRINT D$;"WRITE A7-D,R";58
    : PRINT IT
-----------------------
710   PRINT D$;"CLOSE A7-D"
-----------------------
720   END
-----------------------
1000  PRINT "ENTER THE RECORD NUMBER TO BE CHANGED"
    : PRINT
-----------------------
```

```
1010  INPUT "RECORD NUMBER & STARTING BLOCK ";I,S
1020  INPUT "ENTER VALUE ";K(I - S)
1030  PRINT D$;"OPEN A7-D,L20,D2"
1040  PRINT D$;"WRITE A7-D,R";I
1050  PRINT K(I - S)
1060  PRINT D$;"CLOSE A7-D"
1070  PRINT "WOULD YOU LIKE TO CHANGE ANOTHER RECORD? ";
1080  INPUT A$
1090  IF A$ = "Y" THEN 1000
1100  END
1200  REM  ADDS DATA TO EXISTING DATA DISK
1210  PRINT D$;"OPEN A7-D,L20,D2"
1220  GOTO 310
1230  INPUT "ENTER STARTING RECORD NUMBER FOR STORAGE ";S
1240  I = 10
1250  FOR R = S TO (S + 31)
1260     PRINT D$;"WRITE A7-D,R";R
1270     PRINT K(I)
1280     I = I + 1
    : NEXT
1290  PRINT D$;"CLOSE A7-D"
1300  PRINT "DO YOU NEED TO MAKE ANY CHANGES?"
1310  INPUT A$
1320  IF A$ = "N" THEN END
1330  GOTO 1000
```

Delta Alpha Solver

This program uses 1G data from the data disk created by "Data Creator" to calculate the change in angle of attack (α) and the change in horizontal tail deflection (δe) for a range of load factors. From the specified load factors, bank angles are calculated. These load factors and bank angles in stability axes are converted to body axes, and equilibrium values of roll rate (p_e), pitch rate (q_e), and yaw rate (r_e) are calculated. All the results of this program are stored on the same data disk containing the "Data Creator" files. A printout of $\Delta\alpha$, $\Delta\delta_e$, Φ_s, n_s, Φ_b, and n_b is also available.

Once these $\Delta\alpha$'s are available for the various load factors, the stability derivatives for the new equilibrium angle of attacks are manually extracted from the aerodynamic data package and entered onto the data disk using "Data Creator" option 3.

The equations used in this program are developed by considering an aircraft in a steady turn [Ref 3].

Steady Turn

The axis system used to describe turning flight can greatly affect the expressions that define the parameters of interest. The development in [Ref 3] starts with body axes expressions for the angular rates p, q, and r; however, the assumptions made subtlely result in stability axes expressions when solving for the changes in angle of attack and elevator deflection.

Since the aerodynamic data package used in this work contains stability axes data, the assumptions necessary to go from body axes expressions to stability axes expressions will be described. Once the change in α and δe are calculated using stability axes the expressions

necessary to relate bank angle and load factor between the stability and body axes systems will be developed to calculate the required equilibrium values for p, q, and r in body axes.

The body axes angular rates are given by

$$\begin{bmatrix} p \\ q \\ r \end{bmatrix}_B = \begin{bmatrix} \dot{\phi} - \dot{\psi}\sin\theta \\ \dot{\theta}\cos\phi + \dot{\psi}\sin\phi\cos\theta \\ -\dot{\theta}\sin\phi + \dot{\psi}\cos\phi\cos\theta \end{bmatrix}_B \tag{D1}$$

For the steady turn $\dot{\phi} = \dot{\theta} = 0$ at equilibrium, therefore

$$\begin{bmatrix} p_e \\ q_e \\ r_e \end{bmatrix}_B = \begin{bmatrix} -\dot{\psi}\sin\theta_e \\ \dot{\psi}\sin\phi_e\cos\theta_e \\ \dot{\psi}\cos\phi_e\cos\theta_e \end{bmatrix}_B \tag{D2}$$

In addition, the ball in the turn and slip indicator will be centered resulting in zero side force, Y = 0. Looking at the body axes Y force equation

$$F_{AY_B} + mg\cos\theta_e\sin\phi_e = m(\dot{v} + r_e u - p_e w) \tag{D3}$$

where

$$F_{AY_B} = Y = 0 \tag{D5}$$

$$\dot{v} = 0 \text{ (equilibrium)}$$

which gives

$$mg\cos\theta_e\sin\phi_e = mr_e u - mp_e w \tag{D6}$$

The Z force equation is

$$-T\sin\alpha_T + F_{AZ} + mg\cos\phi_e\cos\theta_e = m(\dot{w} + p_e v - q_e u) \tag{D7}$$

where

$$T\sin\alpha_T \approx 0 \tag{D8}$$

$$F_{AZ_B} = -D_e\sin\alpha - L_e\cos\alpha$$

$$\dot{w} = 0 \text{ (equilibrium)}$$

which gives

$$-D_e \sin\alpha - L_e \cos\alpha + mg\cos\phi_e \cos\theta_e = mp_e v - mq_e u \tag{D9}$$

Etkin [Ref 3] assumes mpw and mpv to be much smaller than mru and mqu respectively and thereby neglecting them is the subtle assumption that makes his resulting expresisons equivalent to stability axes expressions. For stability axes the following is true

$$\alpha_e = \theta_e = \beta_e = p_e = v = w = 0$$

therefore, the Y and Z force equations at equilibrium become

Y Force (stability axes)

$$mg\sin\phi_e = mr_e u \tag{D10}$$

Z Force (stability axes)

$$L_e = mg\cos\phi_e + mqu \tag{D11}$$

where

$$u = V\cos\alpha_e \cos\beta_e = V \tag{D12}$$

substituting for r_e and q_e using

$$\begin{bmatrix} p_e \\ q_e \\ r_e \end{bmatrix}_S = \begin{bmatrix} 0 \\ \dot{\psi}\sin\phi_e \\ \dot{\psi}\cos\phi_e \end{bmatrix}_S \tag{D13}$$

yields

$$Y: \quad mg\sin\phi_e = m\dot{\psi}\cos\phi_e V \tag{D14}$$

$$Z: \quad L_e = mg\cos\phi_e + m\dot{\psi}\sin\phi_e V \tag{D15}$$

Using the Y equation to solve for $\dot{\psi}$ gives

$$\dot{\psi} = \frac{g\tan\phi_e}{V}_S \tag{D16}$$

The subscript "s" denoting stability axes will be omitted in the following steps. Substituting into the Z equation gives

$$L_e = mg\cos\phi_e + mg\tan\phi_e\sin\phi_e \tag{D17}$$

rearranging

$$\frac{L_e}{mg} = \frac{\cos^2\phi_e + \sin^2\phi_e}{\cos\phi_e} = \frac{1}{\cos\phi_e} \tag{D18}$$

This expression defines load factor n.

$$\frac{L}{W} = n = \frac{1}{\cos\phi_e} \tag{D19}$$

Determining a change in α relates to a change in lift. Taking the difference between 1G and nG's of lift yields.

$$\Delta \text{ lift} = \delta L = L-W = nW - W \tag{D20}$$

so

$$\delta L = (n-1)W \tag{D21}$$

Also recall that in equilibrium

$$\Sigma \text{ Moments } (L = M = N) = 0$$
$$Y = 0 \tag{D22}$$

Using the functional relationships given in Appendix B, and neglecting the L_v, M_v and $M_{\dot{\alpha}}$ terms which are very small compared to the other terms give the following set of equations.

$$\begin{aligned}
&M_\alpha\alpha + M_q q + M_{\delta_e}\delta_e = 0 \\
&L_\alpha\alpha + L_q q + L_{\delta_e}\delta_e = (n-1)W \\
&Y_\beta\beta + Y_p p + Y_r r + Y_{\delta_r}\delta_r + Y_{\delta_a}\delta_a = 0 \\
&N_\beta\beta + N_p p + N_r r + N_{\delta_r}\delta_r + N_{\delta_a}\delta_a = 0 \\
&L_\beta\beta + L_p p + L_r r + L_{\delta_r}\delta_r + L_{\delta_a}\delta_a = 0
\end{aligned} \tag{D23}$$

To solve for the change in α and δe as load factor increases the pitching moment and lift equations above are written in matrix form and solved

$$\begin{bmatrix} M_\alpha & M_{\delta e} \\ L_\alpha & L_{\delta e} \end{bmatrix} \begin{bmatrix} \Delta\alpha \\ \Delta\delta e \end{bmatrix} = -\begin{bmatrix} M_q \\ L_q \end{bmatrix} q_e + \begin{bmatrix} 0 \\ (n-1)w \end{bmatrix} \tag{D24}$$

The pitch rate q can be expressed in terms of load factor and velocity

$$q_e = \dot{\psi}\sin\phi e$$

substituting for $\dot{\psi}$ D(16) and letting $\frac{1}{\cos\phi e} = n$

$$q_e = \frac{g\tan\phi e\sin\phi e}{V} = \frac{ng\sin^2\phi e}{V} \tag{D25}$$

Using the trigometric identity $\cos^2\phi e + \sin^2\phi e = 1$ gives

$$q_e = \frac{ng(1 - \cos^2\phi e)}{V} \tag{D26}$$

letting

$$\cos^2\phi e = \frac{1}{n^2} \tag{D27}$$

and simplifying

$$q_e = \frac{g(n^2-1)}{Vn} \tag{D28}$$

This expression can also be written in the following form which allows for convenient grouping of terms

$$q_e = \frac{g(n+1)(n-1)}{Vn} = \frac{ng(n+1)(n-1)}{nVn} \tag{D29}$$

Using this expression for q_e and applying Cramer's rule to solve the matrix equation for $\Delta\alpha_e$ and $\Delta\delta_e$ yields

$$\Delta\alpha_e = \frac{(n-1)W\left[-M_{\delta e} + \frac{n+1}{Vn}(M_{\delta_e} L_q - M_q L_{\delta_e})\right]}{M_\alpha L_{\delta_e} - L_\alpha M_{\delta_e}} \tag{D30}$$

$$\Delta\delta e = \frac{(n-1)W\left[M_{\alpha} + \frac{n+1}{V_{TR}} (M_{\quad} - M_{\quad}) \right]}{M_{\alpha} L_{\delta_e} - L_{\alpha} M_{\delta_e}} \tag{D31}$$

The coefficient form of these equations given below were actually programmed since the dimensional derivatives are not available at this point on the data disk.

$$\Delta\alpha_e = \frac{(n-1)\ C_w\left[-C_{m\delta_e} + \frac{(n+1)(pS\bar{c})}{4mn} (C_{m\delta_e} C_{L_q} - C_{m_q} C_{L_{\delta_e}})\right]}{C_{m\alpha} C_{L_{\delta_e}} - C_{L_\alpha} C_{m_{\delta_e}}} \tag{D32}$$

$$\Delta\delta e = \frac{(n-1)\ C_w\left[C_{m_\alpha} + \frac{(n+1)(pS\bar{c})}{4mn} (C_{m_q} C_{L_\alpha} - C_{m_\alpha} C_{L_q})\right]}{C_{m_\alpha} C_{L_{\delta_e}} - C_{L_\alpha} C_{m_{\delta_e}}} \tag{D33}$$

With $\Delta\alpha e$ available, it can be added to α_o for 1G level flight to obtain the new equilibrium α for the steady turn. The aerodynamic data package can be reentered to determine new values for stability derivatives affected by angle of attack.

To obtain equilibrium angular rates p_e, q_e and r_e in body axes, it is necessary to relate stability axes and body axes bank angles. In addition, the load factors will also be related between these axes. Returning to the body axes expressions for the angular rates and the Y force equation we have

$$\begin{bmatrix} p_e \\ q_e \\ r_e \end{bmatrix}_B = \begin{bmatrix} -\dot{\psi}\sin\theta_e \\ \dot{\psi}\sin\phi_e\cos\theta_e \\ \dot{\psi}\cos\phi_e\cos\theta_e \end{bmatrix}_B \tag{D34}$$

$$Y = mu\cos\theta_e\sin\phi_e = mr_e u - mp_e w \tag{D35}$$

Using the Y equation and substituting with the following

$$r_e = \dot{\psi}\cos\Phi_e\cos\theta_e$$

$$p_e = -\dot{\psi}\sin\theta_e$$

$$u = V\cos\alpha_e\cos\beta_e \qquad (I$$

$$w = V\sin\alpha_e\cos\beta_e$$

gives

$$mg\cos\theta_e\sin\Phi_e = m\dot{\psi}\cos\Phi_e\cos\theta_e V\cos\alpha_e\cos\beta_e + m\dot{\psi}\sin\theta_e V\sin\alpha_e\cos\beta_e$$

rearranging and assumbing $\beta \approx 0$ gives

$$\frac{\dot{\psi}V}{g} = \left[\frac{\cos\theta_e\sin\Phi_e}{\cos\Phi_e\cos\theta_e\cos\alpha_e + \sin\theta_e\sin\alpha_e}\right]_B \qquad (I$$

Recall in stability axes

$$\frac{\dot{\psi}V}{g} = \left[\tan\Phi_e\right]_S$$

therefore

$$\left[\tan\Phi_e\right]_S = \left[\frac{\cos\theta_e\sin\Phi_e}{\cos\Phi_e\cos\theta_e\cos\alpha_e + \sin\theta_e\sin\alpha_e}\right]_B \qquad (I$$

Since in body axes $\alpha_e = \theta_e$, α_e can be substituted for θ_e which gives

$$\left[\tan\Phi_e\right]_S = \left[\frac{\cos\alpha_e\sin\Phi_e}{\cos^2\alpha_e\cos\Phi_e + \sin^2\alpha_e}\right]_B \qquad (I$$

The value for α_e is known and $\left[\Phi_e\right]_S$ can be determined from

$$\left[\Phi_e\right]_S = \cos^{-1}\left(\frac{1}{n}\right) \qquad (I$$

To solve for $\left[\Phi_e\right]_B$ the above equation can be written in the following form

$$C_1 = \frac{C_2\sin\Phi_e}{C_3\cos\Phi_e + C_4} \qquad (I$$

where

$$C_1 = \tan\phi_{e_S}$$

$$C_2 = \cos\alpha_e$$

$$C_3 = \cos^2\alpha_e \qquad \text{(D42)}$$

$$C_4 = \sin^2\alpha_e$$

rearranging gives

$$C_1C_4 = C_2\sin\phi_e - C_1C_3\cos\phi_e \qquad \text{(D43)}$$

by letting

$$C_5 = -C_1C_3$$

this expression becomes

$$C_1C_4 = C_2\sin\phi_e + C_5\cos\phi_e \qquad \text{(D44)}$$

Using the trigometric identity

$$\sin(\phi_e + \eta) = \sin\phi_e\cos\eta + \cos\phi_e\sin\eta$$

where η is an arbritrary angle, and multiplying by an arbritrary constant C, gives

$$C\sin(\phi_e + \eta) = C\sin\phi_e\cos\eta + C\cos\phi_e\sin\eta$$

which can be written as

$$C\sin(\phi_e + \eta) = C_2\sin\phi_e + C_5\cos\phi_e \qquad \text{(D45)}$$

by letting

$$C_2 = C\cos\eta$$

$$C_5 = C\sin\eta$$

Solving for C and η gives

$$C = \sqrt{C_2^2 + C_5^2} \qquad \text{(D46)}$$

$$\eta = \tan^{-1}\frac{C_5}{C_2}$$

Equating (D44) and (D45) yields

$$C_1 C_4 = C\sin(\phi_e + \eta) \tag{D46}$$

or

$$\phi_{e_B} = \sin^{-1}\left(\frac{C_1 C_4}{C}\right) - \eta \tag{D47}$$

This expression gives the body axes bank angle in terms of α_e and ϕ_{e_S}. With ϕ_{e_B} computed and realizing $\alpha_e = \theta_e$ for body axes the equilibrium values for p_e, q_e and r_e can be calculated using (D34). The expression for $\dot{\psi}$ is obtained from (D16). The body axes load factor can also be calculated as follows.

Repeating the body axes Z force equation

$$-T\sin\alpha_T - D_e\sin\alpha - L_e\cos\alpha + mg\cos\phi_e\cos\theta_e = mp_e v - mq_e u \tag{D48}$$

and noting that the lifting force is in the -Z direction gives

$$T\sin\alpha_T + D_e\sin\alpha + L_e\cos\alpha = mg\cos\phi_e\cos\theta_e - mp_e V + mq_e u \tag{D49}$$

substituting the following

$$\begin{aligned} p_e &= -\dot{\psi}\sin\theta_e \\ q_e &= \dot{\psi}\sin\phi_e\cos\theta_e \\ u &= V\cos\alpha_e\cos\beta_e \\ V &= V\sin\beta_e \end{aligned} \tag{D50}$$

gives

$$T\sin\alpha_T + D_e\sin\alpha_e + L_e\cos\alpha_e = mg\cos\phi_e\cos\theta_e + m\dot{\psi}\sin\theta_e V\sin\beta_e + m\dot{\psi}\sin\phi_e\cos\theta_e V\cos\alpha_e\cos\beta_e \tag{D51}$$

Assuming $\beta \approx 0$ and substituting for $\dot{\psi}V$ using (D16) gives

$$T\sin\alpha_T + D_e\sin\alpha_e + L_e\cos\alpha_e = mg\cos\phi_e\cos\theta_e$$

$$+ mg\left[\frac{\cos\theta_e\sin\phi_e}{\cos\phi_e\cos\theta_e\cos\alpha_e + \sin\alpha_e\sin\theta_e}\right]\sin\phi_e\cos\theta_e\cos\alpha_e \qquad (D52)$$

Again noting that $\alpha_e = \theta_e$ in body axes, and rearranging the expression the body axes load factor becomes

$$n_B = \frac{T\sin\alpha_T + D_e\sin\alpha_e + L_e\cos\alpha_e}{mg} = \frac{\cos\alpha_e(\cos^2\alpha_e(1-\cos\phi_e) + \cos\phi_e)}{1 + \cos^2\alpha_e(\cos\phi_e - 1)} \qquad (D53)$$

The equilibrium values for sideslip, rudder and aileron deflection are calculated in the AMAT and BMAT program using data from this program and solving the side force, yawing and rolling moment equations given by (D23). These equations written in matrix form are given below

$$\begin{bmatrix} Y_\beta & Y_{\delta r} & 0 \\ L_\beta & L_{\delta r} & L_{\delta a} \\ N_\beta & N_{\delta r} & N_{\delta a} \end{bmatrix}\begin{bmatrix} \beta_e \\ \delta_r \\ \delta_a \end{bmatrix} = \begin{bmatrix} Y_p & Y_r \\ L_p & L_r \\ N_p & N_r \end{bmatrix}\begin{bmatrix} -p_e \\ -r_e \end{bmatrix} \qquad (D54)$$

Again, the coefficient form was used in the program. The p_e and r_e are changed to $\hat{p}_e$ and $\hat{r}_e$ by multiplying by $(b/2V_e)$. In the program the matrix pre-multiplying $[\beta e\ \delta r\ \delta a]^T$ is inverted using the cofactor method.

This gives

$$\begin{bmatrix} \beta_e \\ \delta_r \\ \delta_a \end{bmatrix} = \begin{bmatrix} C_{Y_\beta} & C_{Y_{\delta r}} & 0 \\ C_{\ell_\beta} & C_{\ell_{\delta r}} & C_{\ell_{\delta a}} \\ C_{n_\beta} & C_{n_{\delta r}} & C_{n_{\delta a}} \end{bmatrix}^{-1}\begin{bmatrix} C_{Y_p} & C_{Y_r} \\ C_{\ell_p} & C_{\ell_r} \\ C_{n_p} & C_{n_r} \end{bmatrix}\begin{bmatrix} -p_e(b/2V_e) \\ -r_e(b/2V_e) \end{bmatrix} \qquad (D55)$$

DELTA ALPHA SOLVER

```
----------
2000  REM  DELTA ALPHA AND DELTA STABILATOR SOLVER
----------
2010  REM
----------
2020  REM  PRINTS OUT LOAD FACTOR AND BANK ANGLE FOR BOTH
         STABILITY AND BODY AXIS
----------
2030  REM
----------
2040  REM  BY JEFFREY R. RIEMER
----------
2050  REM  14 APRIL 1983
----------
2060  REM
----------
2070  TEXT
    : HOME
    : PRINT CHR$ (12)
    : PRINT
----------
2080  D$ = CHR$ (4)
----------
2082  DR = 57.29577951
----------
2090  DEF FN SE(X) = ATN ( SQR (X * X - 1)) + ( SGN (X) -
         1) * 1.5707963
----------
2095  DEF FN R(X) = INT (X * 1000000 + .5) / 1000000
----------
2100  DIM C(200),AN(100),FE(100),NB(100),F(100),DS(100),DA
         (100)
----------
2105  DIM AE(100),CI(100),PE(100),QE(100),RE(100),Q(2,100)
----------
2110  PRINT "THIS PROGRAM FINDS DELTA ALPHA AND DELTA STAB
         ILATOR USING STABILITY AXIS DATA"
----------
2120  PRINT
----------
2130  PRINT "ENTER FLIGHT CONDITION"
    : PRINT
----------
2140  PRINT "1 - 15000 FT, MACH .6"
----------
2150  PRINT "2 - 15000 FT, MACH .8"
----------
2160  PRINT "3 - OTHER"
----------
2170  PRINT
    : INPUT "ENTER CHOICE ";FC
----------
2180  PRINT
    : PRINT "INSERT A7-D DATA DISK FOR FLIGHT CONDITION "
         ;FC;" IN DRIVE 2"
----------
2190  PRINT
    : PRINT "PRESS ANY KEY TO CONTINUE"
```

```
2200  GET C$
2205  PRINT D$
2210  PRINT D$;"OPEN A7-D,L20,D2"
2220  FOR I = 0 TO 15
2230     PRINT D$;"READ A7-D,R";I
2240     INPUT C(I)
2250  NEXT
2260  PRINT D$;"CLOSE A7-D"
2270  MU = (2 * C(9) / C(7)) / (C(2) * C(4) * C(5))
2280  CW = 2 * C(9) / (C(2) * C(3) ^ 2 * C(4))
2290  PRINT
    : PRINT "ENTER DESIRED LOAD FACTOR RANGE AND INTERVAL
      "
2300  PRINT
    : PRINT "   STARTING LOAD FACTOR= ";
2310  INPUT N1
2320  PRINT "      ENDING LOAD FACTOR= ";
2330  INPUT N2
2340  PRINT "                INTERVAL= ";
2350  INPUT S
2360  I = 1
2370  FOR X = N1 TO N2 STEP S
2375     AN(I) = X
2380     DS(I) = (AN(I) - 1) * CW * (C(10) + ((AN(I) + 1) /
            (2 * MU * AN(I))) * (C(12) * C(14) - C(15) * C
            (10))) / (C(13) * C(10) - C(12) * C(11))
2390     DA(I) = (AN(I) - 1) * CW * ( - C(11) + ((AN(I) + 1
            ) / (2 * MU * AN(I))) * (C(11) * C(15) - C(14)
            * C(13))) / (C(13) * C(10) - C(12) * C(11))
2400     FE(I) = FN SE(AN(I))
2410     GOSUB 3000
2415     GOSUB 4000
2420     I = I + 1
```

```
2430  NEXT
--------------------
2440  R = 1001
--------------------
2450  PRINT D$;"OPEN A7-D,L20,D2"
--------------------
2460  FOR J = 1 TO (I - 1)
    :   PRINT D$;"WRITE A7-D,R";R
    :   PRINT AN(J)
    :   R = R + 1
    : NEXT
--------------------
2470  FOR J = 1 TO (I - 1)
    :   PRINT D$;"WRITE A7-D,R";R
    :   PRINT FE(J)
    :   R = R + 1
    : NEXT
--------------------
2480  FOR J = 1 TO (I - 1)
    :   PRINT D$;"WRITE A7-D,R";R
    :   PRINT DA(J)
    :   R = R + 1
    : NEXT
--------------------
2490  FOR J = 1 TO (I - 1)
    :   PRINT D$;"WRITE A7-D,R";R
    :   PRINT DS(J)
    :   R = R + 1
    : NEXT
--------------------
2500  FOR J = 1 TO (I - 1)
    :   PRINT D$;"WRITE A7-D,R";R
    :   PRINT F(J)
    :   R = R + 1
    : NEXT
--------------------
2510  FOR J = 1 TO (I - 1)
    :   PRINT D$;"WRITE A7-D,R";R
    :   PRINT NB(J)
    :   R = R + 1
    : NEXT
--------------------
2511  FOR J = 1 TO (I - 1)
    :   PRINT D$;"WRITE A7-D,R";R
    :   PRINT CI(J)
    :   R = R + 1
    : NEXT
--------------------
2512  FOR J = 1 TO (I - 1)
    :   PRINT D$;"WRITE A7-D,R";R
    :   PRINT PE(J)
    :   R = R + 1
    : NEXT
--------------------
2513  FOR J = 1 TO (I - 1)
    :   PRINT D$;"WRITE A7-D,R";R
    :   PRINT QE(J)
    :   R = R + 1
    : NEXT
--------------------
```

```
2514  FOR J = 1 TO (I - 1)
    :   PRINT D$;"WRITE A7-D,R";R
    :   PRINT RE(J)
    :   R = R + 1
    : NEXT
--------------------
2515  FOR J = 1 TO (I - 1)
    :   PRINT D$;"WRITE A7-D,R";R
    :   PRINT AE(J)
    :   R = R + 1
    : NEXT
--------------------
2516  FOR J = 1 TO (I - 1)
    :   PRINT D$;"WRITE A7-D,R";R
    :   PRINT Q(1,J)
    :   R = R + 1
    : NEXT
--------------------
2517  FOR J = 1 TO (I - 1)
    :   PRINT D$;"WRITE A7-D,R";R
    :   PRINT Q(2,J)
    :   R = R + 1
    : NEXT
--------------------
2518  N3 = 13 * ((N2 - N1) / S + 1)
    : PRINT D$;"WRITE A7-D,R";1000
    : PRINT N3
--------------------
2519  PRINT D$;"WRITE A7-D,R";998
    : PRINT N2
    : PRINT D$;"WRITE A7-D,R";999
    : PRINT S
--------------------
2520  PRINT D$;"CLOSE A7-D"
--------------------
2530  PRINT
--------------------
2540  PRINT "WOULD YOU LIKE A PRINT OUT (Y/N)? "
    : INPUT A$
--------------------
2550  IF A$ = "N" THEN END
--------------------
2560  PRINT
    : PRINT "SET PRINTER PAPER"
--------------------
2570  PRINT D$
--------------------
2580  PRINT D$;"PR#1"
--------------------
2590  PRINT CHR$ (15)
--------------------
2600  FOR J = 1 TO (I - 1)
--------------------
2610    AN(J) = FN R(AN(J))
--------------------
2620    NB(J) = FN R(NB(J))
--------------------
2630    DS(J) = DR * DS(J)
--------------------
2635    DS(J) = FN R(DS(J))
```

```
2640    DA(J) = DR * DA(J)
2645    DA(J) = FN R(DA(J))
2650    FE(J) = DR * FE(J)
2655    FE(J) = FN R(FE(J))
2660    F(J) = DR * F(J)
2665    F(J) = FN R(F(J))
2670    AE(J) = DR * AE(J)
2675    AE(J) = FN R(AE(J))
2680  NEXT
2690  PRINT
    : PRINT
    : PRINT
    : PRINT
2700  POKE 36,23
    : PRINT "FLIGHT CONDITION: ";FC
    : PRINT
    : PRINT
2710  POKE 36,69
    : PRINT "STABILITY AXIS";
    : POKE 36,105
    : PRINT "BODY AXIS"
2720  POKE 36,23
    : PRINT "DELTA ALPHA";
    : POKE 36,43
    : PRINT "DELTA STABILATOR";
    : POKE 36,63
    : PRINT "LOAD FACTOR";
    : POKE 36,80
    : PRINT "BANK ANGLE";
    : POKE 36,95
    : PRINT "LOAD FACTOR";
    : POKE 36,112
    : PRINT "BANK ANGLE"
2730  POKE 36,26
    : PRINT "(DEG)";
    : POKE 36,48
    : PRINT "(DEG)";
    : POKE 36,67
    : PRINT "(G)";
    : POKE 36,82
    : PRINT "(DEG)";
    : POKE 36,99
    : PRINT "(G)";
    : POKE 36,114
    : PRINT "(DEG)"
    : PRINT
```

```
2740  FOR J = 1 TO (I - 1)
2750     POKE 36,24
     :   PRINT DA(J);
     :   POKE 36,46
     :   PRINT DS(J);
     :   POKE 36,67
     :   PRINT AN(J);
     :   POKE 36,81
     :   PRINT FE(J);
     :   POKE 36,99
     :   PRINT NB(J);
     :   POKE 36,113
     :   PRINT F(J)
2760  NEXT
2770  PRINT CHR$ (18)
2780  PRINT D$
    : PRINT D$;"PR#0"
    : PRINT D$;"IN#0"
2790  END
3000  REM  SUBROUTINE TO CALCULATE BODY AXIS BANK AND LOAD
          FACTOR
3010  DEF FN ASN(X) = ATN (X / SQR ( - X * X + 1))
3020  PRINT D$;"OPEN A7-D,L20,D2"
3030  PRINT D$;"READ A7-D,R";16
3040  INPUT A0
3050  PRINT D$;"CLOSE A7-D"
3060  AE(I) = A0 + DA(I)
3065  AE = AE(I)
3070  AA = COS (AE)
3080  BB = AA ^ 2
3090  CC = ( SIN (AE)) ^ 2
3100  DD = TAN (FE(I))
3110  TH = ATN ( - BB * DD / AA)
3120  MG = SQR (BB + ( - DD * BB) ^ 2)
3130  F(I) = FN ASN(DD * CC / MG) - TH
3140  NB(I) = AA * (BB * (1 - COS (F(I))) + COS (F(I))) /
          (1 + BB * ( COS (F(I)) - 1))
```

```
3150  RETURN
---------------------
4000  REM  SUBROUTINE TO CALCULATE P,Q,& R EQUILIBRIUM
---------------------
4010  CI(I) = (C(7) * COS (AE(I)) * SIN (F(I))) / (C(3) *
         ( COS (F(I)) * ( COS (AE(I))) ^ 2 + ( SIN (AE(I)
         )) ^ 2))
---------------------
4020  PE(I) = - CI(I) * SIN (AE(I))
---------------------
4030  QE(I) = CI(I) * SIN (F(I)) * COS (AE(I))
---------------------
4040  RE(I) = CI(I) * COS (F(I)) * COS (AE(I))
---------------------
4050  Q(1,I) = SIN (AE(I)) * CI(I) * C(6) / (2 * C(3))
---------------------
4060  Q(2,I) = - COS (F(I)) * COS (AE(I)) * CI(I) * C(6) /
         (2 * C(3))
---------------------
4070  RETURN
```

Augmented AMAT and BMAT/Ver 2

This program calculates the individual elements of the A and B matrices. To accomplish this, several intermediate steps are performed. First, the desired load factor is entered into the program, and the equilibrium values for body axes bank angle Φ_e, roll rate p_e, pitch rate q_e, yaw rate r_e, and angle of attack α_e are loaded from the data disk. By answering questions as to the location of various sets of stability derivatives on the data disk, which is determined from Table D1, the stability axes non-dimensional derivatives and moments of inertia are converted to body axes. These stability derivatives are dimensionalized and the X and Z body axes derivatives are calculated and stored to the data disk. During this process the equilibrium sideslip βe, rudder δr, and aileron δa were also calculated and stored to the disk. With all the equilibrium conditions calculated and all the stability derivatives converted to body axes, the A and B matrices are computed by evaluating the individual elements. These matrices are stored to disk for later use. Up until this point the program is very general, and given the stability derivatives and flight condition the A and B matrices are calculated by evaluating the linearized equations of motion for a steady level turn or straight and level flight depending on the input load factor.

The next option asks if you want to calculate an augmented set of A and B matrices. This option specifically contains the A-7D mechanical and augmented control paths resulting in a 17 x 17 A matrix and a 17 x 3 B matrix. Various levels of augmentation can be selected

1 - Control Augmentation with lateral acceleration feedback

2 - Control Augmentation without lateral acceleration feedback

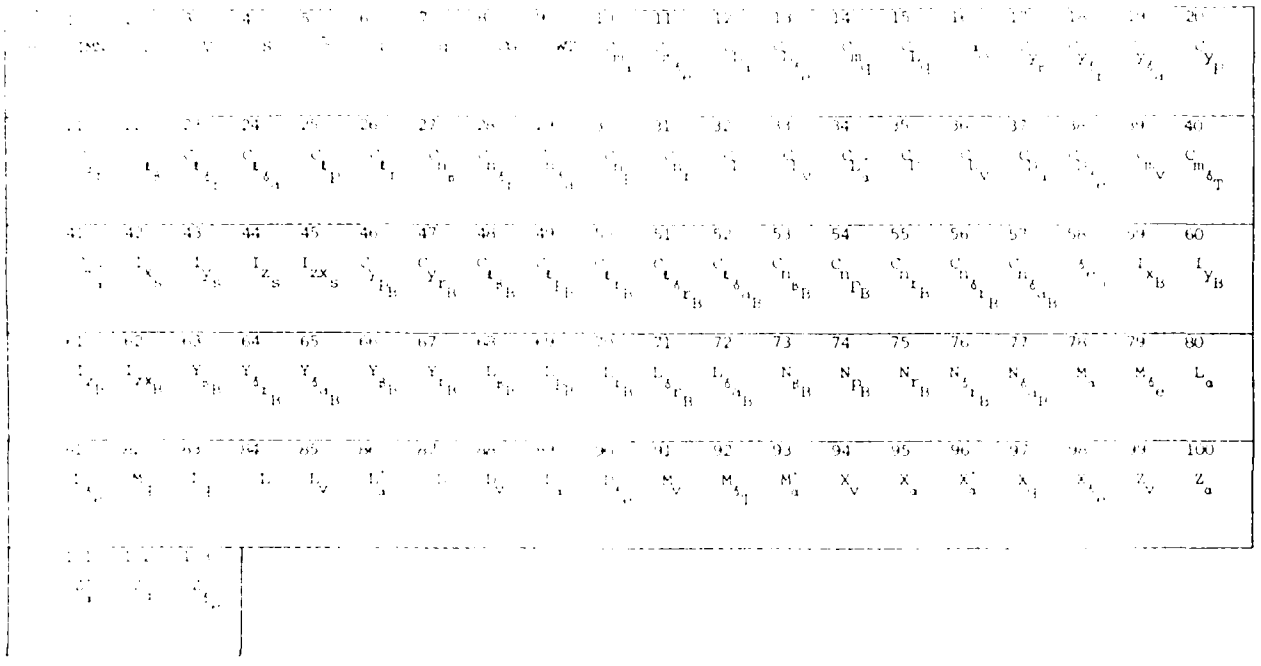

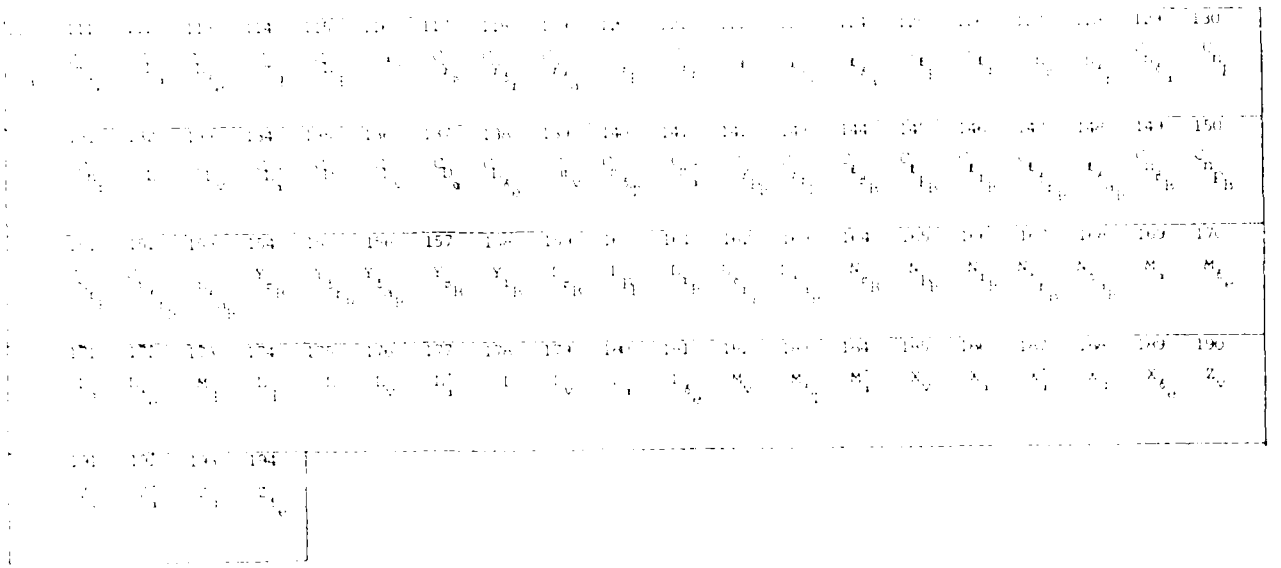

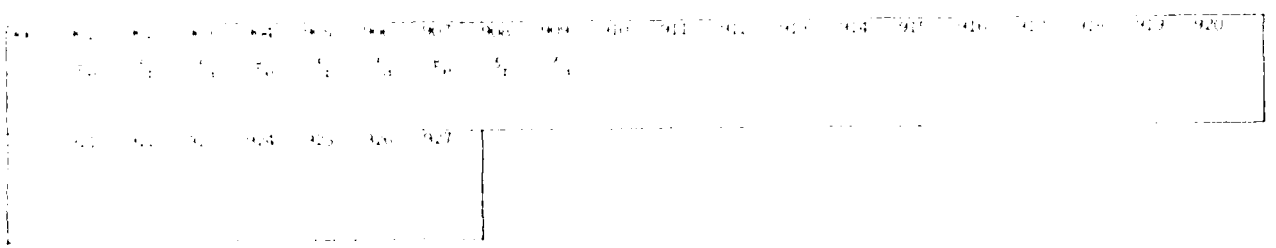

AD-A152 118 THE EFFECT OF LOAD FACTOR ON AIRCRAFT HANDLING QUALITIES(U) AIR FORCE INST OF TECH WRIGHT-PATTERSON AFB OH SCHOOL OF ENGINEERING J R RIEMER 10 AUG 84 3/4

UNCLASSIFIED AFIT/GAE/AA/84J-2 F/G 20/4 NL

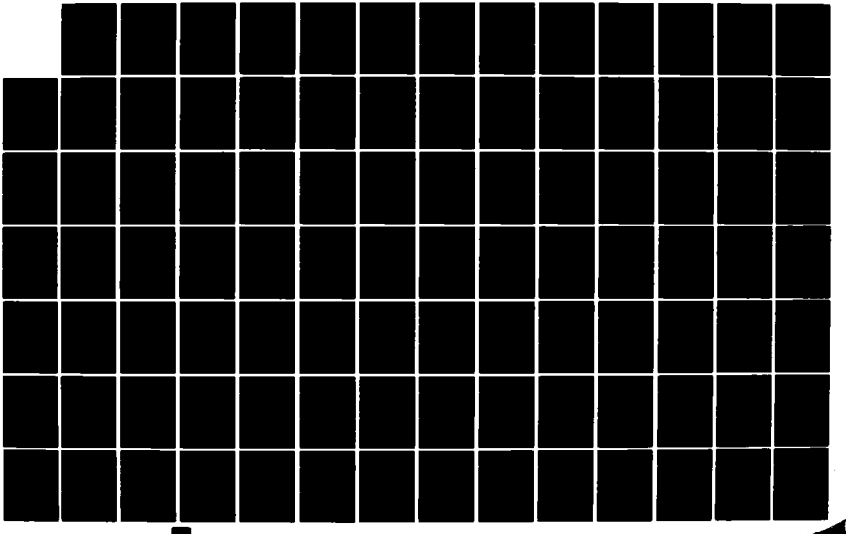

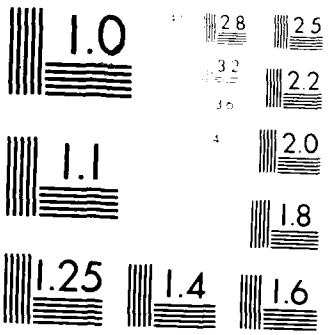
1.0
2.8
2.5
3.2
2.2
3.6
4
2.0
1.1
1.8
1.25
1.4
1.6

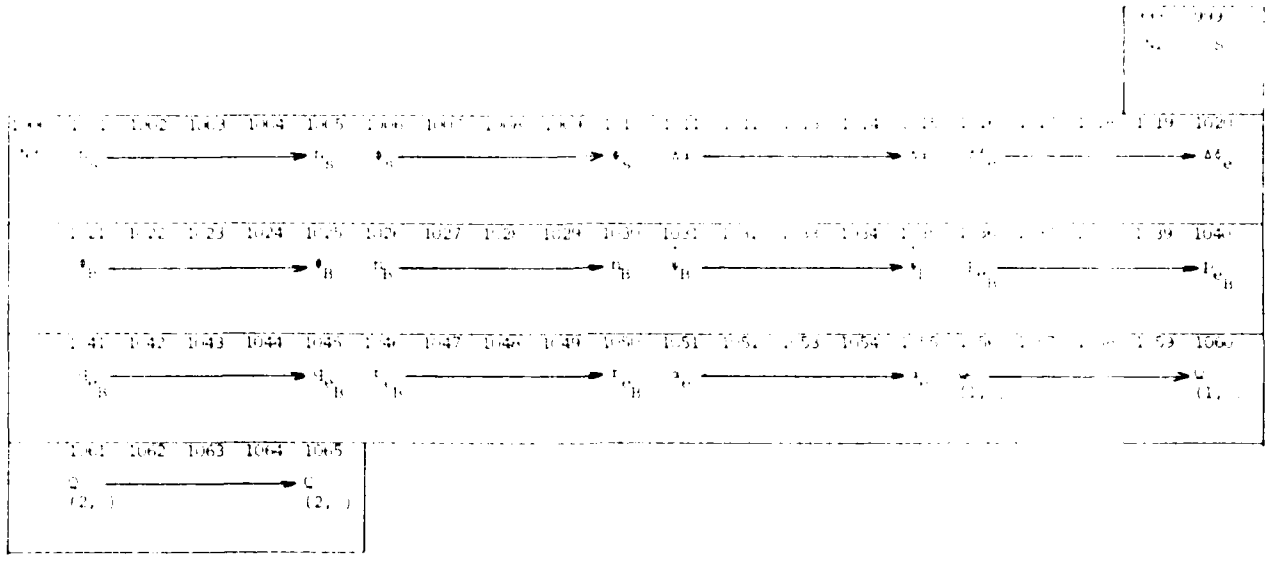

Notes:

N2 = Determines # load factor ranges (usually 15)

S = Load factor interval (.5 in this example)

N1 = Number of records required for this set of data (60 in this example)

I = Initial number of records taken up by each variable (depends on N1, N2, and S)

$C(1,) = -p_0(b/2V_0)$

$C(2,) = -r_0(1/2V_0)$

If the interval results in 0 additional load factors then records 1001 + 1111 will be filled.

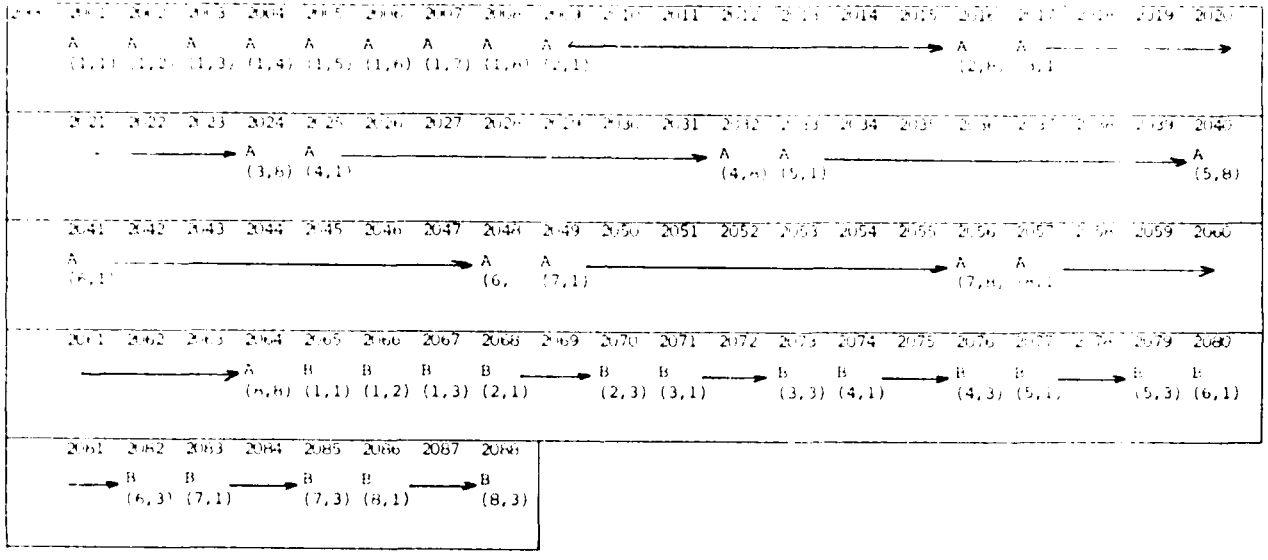

Notes:

This format is used for A and B matrices at each load factor. Records 2001 • 2088, 2101 • 2188, 2201 • 2288 .... 2801 • 2888 are available.

A similar format is used for the augmented matrices starting at record 4001 • 4340, 4501 • 4840, 5001 • 5340, et .

The F and G matrices are convenient to store on a separate disk and require 289 records each. A recommended format is 1 • 578, 1001 • 1578, 2001 • 2578, ... 8001 • 8578.

3 - Yaw Stabilization with lateral acceleration feedback

4 - Yaw Stabilization without lateral acceleration feedback

5 - Mechanical Path Only

Control system limiters in the augmented control path have not been modeled. Also the dual gradient feel spring in the mechanical pitch axis is only modeled for pitch inputs up to and including 8 lbs. These limitations result in the A and B matrices only being valid for small inputs.

To run the next two programs for large order A matrices (greater than 10 x 10) it is necessary to run a machine language commercially obtained program "Diversi-DOS Mover" which relocates the disk operating system (DOS) in the language card.

AUGMENTED AMAT BMAT/VER 2

```
---------------------
10    REM  CONVERTS LATERAL DERIVATIVES FROM STABILITY AXI
        S TO BODY AXIS
---------------------
20    REM
---------------------
30    REM  BY JEFFREY R. RIEMER
---------------------
40    REM  20 APRIL 1983
---------------------
50    D$ = CHR$ (4)
    : REM  CTRL-D
---------------------
60    DIM C(110),CB(20),MI(5),DB(20),DL(20),X(6),ZD(6),PR(
        3,2),CFT(3,3),PP(3,1),Q(2,1),Z(3,3),ZE(3,1),A(20
        ,20),B(20,3)
---------------------
70    DIM AE(20),PE(20),QE(20),RE(20),AN(20),F(20)
---------------------
80    DIM K(100),AZ(20)
---------------------
90    TEXT
    : HOME
    : PRINT CHR$ (12)
    : PRINT
---------------------
100   DEF FN R(X) = INT (X * 1000000 + .5) / 1000000
---------------------
110   INPUT "      LOAD FACTOR= ";AN
---------------------
120   GOSUB 1940
---------------------
130   GOSUB 2500
---------------------
140   AE = AE(B)
---------------------
150   PE = PE(B)
---------------------
160   QE = QE(B)
---------------------
170   RE = RE(B)
---------------------
180   F = F(B)
---------------------
190   PRINT "ENTER RECORD NUMBERS FOR LATERAL        DERIV
        ATIVES"
    : PRINT
---------------------
200   INPUT "   STARTING RECORD  CYB ";R
---------------------
210   INPUT "     ENDING RECORD  CNR ";E
---------------------
220   PRINT
---------------------
230   PRINT D$
    : PRINT D$;"OPEN A7-D,L20,D2"
---------------------
240   FOR I = R TO E
```

```
250      PRINT D$;"READ A7-D,R"I
260      INPUT C(I - R)
270   NEXT
280   PRINT D$;"CLOSE A7-D"
290   CA = COS (AE)
300   SA = SIN (AE)
310   CS = CA ^ 2
    : SS = SA ^ 2
320   S = 0
330   CB(1) = C(S)
340   CB(2) = C(S + 1)
350   CB(3) = C(S + 2)
360   CB(4) = C(S + 3) * CA - C(S + 4) * SA
370   CB(5) = C(S + 3) * SA + C(S + 4) * CA
380   CB(6) = C(S + 5) * CA - C(S + 10) * SA
390   CB(7) = C(S + 8) * CS - (C(S + 9) + C(S + 13)) * SA
        * CA + C(S + 14) * SS
400   CB(8) = C(S + 9) * CS - (C(S + 14) - C(S + 8)) * SA
        * CA - C(S + 13) * SS
410   CB(9) = C(S + 6) * CA - C(S + 11) * SA
420   CB(10) = C(S + 7) * CA - C(S + 12) * SA
430   CB(11) = C(S + 10) * CA + C(S + 5) * SA
440   CB(12) = C(S + 13) * CS - (C(S + 14) - C(S + 8)) * S
        A * CA - C(S + 9) * SS
450   CB(13) = C(S + 14) * CS + (C(S + 9) + C(S + 13)) * S
        A * CA + C(S + 8) * SS
460   CB(14) = C(S + 11) * CA + C(S + 6) * SA
470   CB(15) = C(S + 12) * CA + C(S + 7) * SA
480   PRINT
    : PRINT "LATERAL BODY AXIS DERIVATIVES"
    : PRINT
490   INPUT "ENTER STARTING RECORD ";N
500   PRINT D$
    : PRINT D$;"OPEN A7-D,L20,D2"
```

```
510   FOR I = 4 TO 15
520      PRINT D$;"WRITE A7-D,R";N
530      PRINT CB(I)
540      N = N + 1
    : NEXT
550   PRINT D$;"CLOSE A7-D"
560   GOSUB 2100
570   GOSUB 1150
580   GOSUB 1440
590   PRINT
    : INPUT "CALCULATE INERTIAS (Y/N)? ";A$
600   IF A$ = "Y" THEN 650
610   PRINT D$
    : PRINT D$;"OPEN A7-D,L20,D2"
620   R = 59
    : FOR I = 1 TO 4
    :   PRINT D$;"READ A7-D,R";R
    :   INPUT MI(I)
    :   R = R + 1
    : NEXT
630   PRINT D$;"CLOSE A7-D"
640   GOTO 660
650   GOSUB 1010
660   GOSUB 1770
670   GOSUB 2610
680   PRINT
    : INPUT "CALCULATE AUGMENTED A & B MATRICES (Y/N)?";A
        $
690   IF A$ = "Y" THEN GOSUB 4370
700   PRINT
    : INPUT "ANOTNER EQUILIBRIUM (Y/N)? ";A$
710   IF A$ = "Y" THEN GOTO 110
720   PRINT
730   PRINT "WOULD YOU LIKE A PRINT OUT (Y/N)? "
    : INPUT A$
740   IF A$ = "N" THEN END
```

```
750   PRINT D$
    : PRINT D$;"PR#1"
760   PRINT CHR$ (15)
770   FOR I = 1 TO 15
    :   CB(I) = FN R(C(I))
    : NEXT
780   FOR I = R TO E
    :   C(I - R) = FN R(C(I - R))
    : NEXT
790   PRINT
    : PRINT
800   PRINT "LATERAL DERIVATIVES"
    : PRINT
810   PRINT "LOAD FACTOR ";AN
820   PRINT
    : PRINT
830   POKE 36,23
    : PRINT "DERIVATIVES";
    : POKE 36,40
    : PRINT "STABILITY AXIS";
    : POKE 36,60
    : PRINT "BODY AXIS"
    : PRINT
    : PRINT
840   POKE 36,30
    : PRINT "CYB";
    : POKE 36,43
    : PRINT C(S);
    : POKE 36,62
    : PRINT CB(1)
850   POKE 36,30
    : PRINT "CYP";
    : POKE 36,43
    : PRINT C(S + 3);
    : POKE 36,62
    : PRINT CB(4)
860   POKE 36,30
    : PRINT "CYR";
    : POKE 36,43
    : PRINT C(S + 4);
    : POKE 36,62
    : PRINT CB(5)
870   POKE 36,30
    : PRINT "CYDR";
    : POKE 36,43
    : PRINT C(S + 1);
    : POKE 36,62
```

```
     : PRINT CB(2)
-----------------------
880    POKE 36,30
     : PRINT "CYDA";
     : POKE 36,43
     : PRINT C(S + 2);
     : POKE 36,62
     : PRINT CB(3)
-----------------------
890    POKE 36,30
     : PRINT "CLB";
     : POKE 36,43
     : PRINT C(S + 5);
     : POKE 36,62
     : PRINT CB(6)
-----------------------
900    POKE 36,30
     : PRINT "CLP";
     : POKE 36,43
     : PRINT C(S + 8);
     : POKE 36,62
     : PRINT CB(7)
-----------------------
910    POKE 36,30
     : PRINT "CLR";
     : POKE 36,43
     : PRINT C(S + 9);
     : POKE 36,62
     : PRINT CB(8)
-----------------------
920    POKE 36,30
     : PRINT "CLDR";
     : POKE 36,43
     : PRINT C(S + 6);
     : POKE 36,62
     : PRINT CB(9)
-----------------------
930    POKE 36,30
     : PRINT "CLDA";
     : POKE 36,43
     : PRINT C(S + 7);
     : POKE 36,62
     : PRINT CB(10)
-----------------------
940    POKE 36,30
     : PRINT "CNB";
     : POKE 36,43
     : PRINT C(S + 10);
     : POKE 36,62
     : PRINT CB(11)
-----------------------
950    POKE 36,30
     : PRINT "CNP";
     : POKE 36,43
     : PRINT C(S + 13);
     : POKE 36,62
     : PRINT CB(12)
-----------------------
960    POKE 36,30
     : PRINT "CNR";
```

```
     : POKE 36,43
     : PRINT C(S + 14);
     : POKE 36,62
     : PRINT CB(13)
--------------------
970   POKE 36,30
     : PRINT "CNDR";
     : POKE 36,43
     : PRINT C(S + 11);
     : POKE 36,62
     : PRINT CB(14)
--------------------
980   POKE 36,30
     : PRINT "CNDA";
     : POKE 36,43
     : PRINT C(S + 12);
     : POKE 36,62
     : PRINT CB(15)
--------------------
990   PRINT CHR$ (18)
--------------------
1000  PRINT D$
     : PRINT D$;"PR#0"
     : PRINT D$;"IN#0"
     : END
--------------------
1010  REM  CONVERTS STABILITY AXIS INERTIAS TO BODY AXIS
--------------------
1020  TEXT
     : HOME
     : PRINT CHR$ (12)
     : PRINT
--------------------
1030  PRINT D$;"OPEN A7-D,L20,D2"
--------------------
1040  R = 1
--------------------
1050  FOR I = 42 TO 45
     :   PRINT D$;"READ A7-D,R";I
     :   INPUT MI(R)
     :   R = R + 1
     : NEXT
--------------------
1060  MI(1) = MI(1) * CS + 2 * MI(4) * SA * CA + MI(3) * S
        S
--------------------
1070  MI(3) = MI(3) * CS - 2 * MI(4) * SA * CA + MI(1) * S
        S
--------------------
1080  MI(4) = (MI(3) - MI(1)) * SA * CA + MI(4) * (CS - SS
        )
--------------------
1090  R = 1
--------------------
1100  FOR I = 59 TO 62
     :   PRINT D$;"WRITE A7-D,R";I
     :   PRINT MI(R)
     :   R = R + 1
     : NEXT
--------------------
```

```
1110  PRINT D$;"CLOSE A7-D"
---------------------
1120  PRINT MI(1),MI(2)
---------------------
1130  PRINT MI(3),MI(4)
---------------------
1140  RETURN
---------------------
1150  REM  DIMENSIONALIZES LATERAL DERIVATIVES
---------------------
1160  PRINT D$
    : PRINT D$;"OPEN A7-D,L20,D2"
---------------------
1170  FOR I = 2 TO 9
    :   PRINT D$;"READ A7-D,R";I
    :   INPUT C(I)
    : NEXT
---------------------
1180  PRINT D$;"CLOSE A7-D"
---------------------
1190  Q1 = .5 * C(2) * (C(3) ^ 2) * C(4)
---------------------
1200  Q2 = Q1 * C(6)
---------------------
1210  Q3 = Q2 / (2 * C(3))
---------------------
1220  Q4 = Q3 * C(6)
---------------------
1230  DB(1) = Q1 * CB(1)
---------------------
1240  DB(2) = Q1 * CB(2)
---------------------
1250  DB(3) = Q1 * CB(3)
---------------------
1260  DB(4) = Q3 * CB(4)
---------------------
1270  DB(5) = Q3 * CB(5)
---------------------
1280  DB(6) = Q2 * CB(6)
---------------------
1290  DB(7) = Q4 * CB(7)
---------------------
1300  DB(8) = Q4 * CB(8)
---------------------
1310  DB(9) = Q2 * CB(9)
---------------------
1320  DB(10) = Q2 * CB(10)
---------------------
1330  DB(11) = Q2 * CB(11)
---------------------
1340  DB(12) = Q4 * CB(12)
---------------------
1350  DB(13) = Q4 * CB(13)
---------------------
1360  DB(14) = Q2 * CB(14)
---------------------
1370  DB(15) = Q2 * CB(15)
---------------------
1380  PRINT
---------------------
```

```
1390  INPUT "STARTING RECORD DIMENSIONAL ";N
1400  PRINT D$
    : PRINT D$;"OPEN A7-D,L20,D2"
1410  FOR I = 1 TO 15
    :   PRINT D$;"WRITE A7-D,R";N
    :   PRINT DB(I)
    :   N = N + 1
    : NEXT
1420  PRINT D$;"CLOSE A7-D"
1430  RETURN
1440  REM  DIMENSIONALIZES LONGITUDINAL DERIVATIVES
1450  INPUT "ENTER RECORD NUMBER FOR CM ALPHA ";N
1460  PRINT D$
    : PRINT D$;"OPEN A7-D,L20,D2"
1470  FOR I = 1 TO 6
    :   PRINT D$
    :   PRINT D$;"READ A7-D,R";N
    :   INPUT K(I)
    :   N = N + 1
    : NEXT
1480  N = N + 16
1490  FOR I = 7 TO 16
    :   PRINT D$;"READ A7-D,R";N
    :   INPUT K(I)
    :   N = N + 1
    : NEXT
1500  PRINT D$;"CLOSE A7-D"
1510  Q5 = Q1 * C(5)
1520  Q6 = Q5 * C(5) / (2 * C(3))
1530  Q7 = Q6 / C(5)
1540  Q8 = Q1 / C(3)
1550  DL(1) = Q5 * K(1)
1560  DL(2) = Q5 * K(2)
1570  DL(3) = Q1 * K(3)
1580  DL(4) = Q1 * K(4)
1590  DL(5) = Q6 * K(5)
1600  DL(6) = Q7 * K(6)
1610  DL(7) = Q1 * K(7)
```

```
1620  DL(8) = Q4 * (2 * K(7) + K(8))
---------------------
1630  DL(9) = Q7 * K(9)
---------------------
1640  DL(10) = Q1 * K(10)
---------------------
1650  DL(11) = Q8 * (2 * K(10) + K(11))
---------------------
1660  DL(12) = Q1 * K(12)
---------------------
1670  DL(13) = Q1 * K(13)
---------------------
1680  DL(14) = (Q5 / C(3)) * K(14)
---------------------
1690  DL(15) = Q5 * K(15)
---------------------
1700  DL(16) = Q6 * K(16)
---------------------
1710  PRINT
---------------------
1720  INPUT "STARTING RECORD LONG DIMENSIONAL ";N
---------------------
1730  PRINT D$
    : PRINT D$;"OPEN A7-D,L20,D2"
---------------------
1740  FOR I = 1 TO 16
    :   PRINT D$
    :   PRINT D$;"WRITE A7-D,R";N
    :   PRINT DL(I)
    :   N = N + 1
    : NEXT
---------------------
1750  PRINT D$;"CLOSE A7-D"
---------------------
1760  RETURN
---------------------
1770  REM  SUBROUTINE TO CALCULATE X & Z DERIVATIVES
---------------------
1780  X(1) = - DL(11) * CA + DL(8) * SA
---------------------
1790  X(2) = DL(10) * SA - DL(12) * CA + DL(7) * CA + DL(3
        ) * SA
---------------------
1800  X(3) = - DL(9) * SA
---------------------
1810  X(4) = DL(6) * SA
---------------------
1820  X(5) = - DL(4) * SA - DL(12) * CA
---------------------
1830  ZD(1) = - DL(11) * SA - DL(8) * CA
---------------------
1840  ZD(2) = - DL(10) * CA + DL(7) * SA - DL(3) * CA - DL
        (12) * SA
---------------------
1850  ZD(3) = DL(9) * CA
---------------------
1860  ZD(4) = - DL(6) * CA
---------------------
1870  ZD(5) = - DL(4) * CA - DL(13) * SA
```

```
1880  PRINT
    : INPUT "RECORD NUMBER FOR X & Z DERIVATIVES ";N
1890  PRINT D$
    : PRINT D$;"OPEN A7-D,L20,D2"
1900  FOR I = 1 TO 5
    :   PRINT D$
    :   PRINT D$;"WRITE A7-D,R";N
    :   PRINT X(I)
    :   N = N + 1
    : NEXT
1910  FOR I = 1 TO 5
    :   PRINT D$;"WRITE A7-D,R";N
    :   PRINT ZD(I)
    :   N = N + 1
    : NEXT
1920  PRINT D$;"CLOSE A7-D"
1930  RETURN
1940  REM  SOLVES FOR BETA,DELTA RUDDER, & DELTA AILERON
1950  PRINT D$;"OPEN A7-D,L20,D2"
1960  PRINT D$;"READ A7-D,R";998
    : INPUT N2
1970  PRINT D$;"READ A7-D,R";999
    : INPUT S
1980  PRINT D$;"READ A7-D,R";1000
    : INPUT N3
1990  R = 0
    : FOR I = 1 TO N2 STEP S
    :   R = R + 1
2000    IF AN = I THEN B = R
2010  NEXT
2020  N4 = N3 / 13
2030  N5 = 1000 + N3 - N4 * 2
2040  N6 = N5 + B
2050  N7 = N6 + N4
2060  PRINT D$;"READ A7-D,R";N6
    : INPUT Q(1,1)
2070  PRINT D$;"READ A7-D,R";N7
    : INPUT Q(2,1)
2080  PRINT D$;"CLOSE A7-D"
```

```
2090  RETURN
2100  REM
2110  PR(1,1) = CB(4)
2120  PR(1,2) = CB(5)
2130  PR(2,1) = CB(7)
2140  PR(2,2) = CB(8)
2150  PR(3,1) = CB(12)
2160  PR(3,2) = CB(13)
2170  CFT(1,1) = CB(9) * CB(15) - CB(14) * CB(10)
2180  CFT(1,2) = - (CB(2) * CB(15) - CB(14) * CB(3))
2190  CFT(1,3) = CB(2) * CB(10) - CB(9) * CB(3)
2200  CFT(2,1) = - (CB(6) * CB(15) - CB(11) * CB(10))
2210  CFT(2,2) = CB(1) * CB(15) - CB(11) * CB(3)
2220  CFT(2,3) = - (CB(1) * CB(10) - CB(6) * CB(3))
2230  CFT(3,1) = CB(6) * CB(14) - CB(11) * CB(9)
2240  CFT(3,2) = - (CB(1) * CB(14) - CB(11) * CB(2))
2250  CFT(3,3) = CB(1) * CB(9) - CB(6) * CB(2)
2260  DET = CB(1) * CFT(1,1) - CB(2) * CFT(2,1) + CB(3) *
          CFT(3,1)
2270  FOR I = 1 TO 3
2280     FOR J = 1 TO 3
2290        Z(I,J) = CFT(I,J) / DET
2300     NEXT
     : NEXT
2310  FOR I = 1 TO 3
2320     PP(I,1) = 0
2330     FOR L = 1 TO 2
2340        PP(I,1) = PP(I,1) + PR(I,L) * Q(L,1)
2350     NEXT
     : NEXT
2360  FOR I = 1 TO 3
```

```
2370    ZE(I,1) = 0
--------------------
2380    FOR L = 1 TO 3
--------------------
2390      ZE(I,1) = ZE(I,1) + Z(I,L) * PP(L,1)
--------------------
2400    NEXT
    : NEXT
--------------------
2410  PRINT
    : INPUT "ENTER DESIRED STORAGE RECORD 900--> ";R
--------------------
2420  PRINT D$
    : PRINT D$;"OPEN A7-D,L20,D2"
--------------------
2430  J = 1
--------------------
2440  FOR I = R TO R + 2
--------------------
2450    PRINT D$;"WRITE A7-D,R";I
--------------------
2460    PRINT ZE(J,1)
--------------------
2470    J = J + 1
    : NEXT
--------------------
2480  PRINT D$;"CLOSE A7-D"
--------------------
2490  RETURN
--------------------
2500  REM
--------------------
2510  PRINT D$;"OPEN A7-D,L20,D2"
--------------------
2520  R = 1001
    : FOR J = 1 TO N4
    :   PRINT D$;"READ A7-D,R";R
    :   INPUT AN(J)
    :   R = R + 1
    : NEXT
--------------------
2530  R = R + 3 * N4
--------------------
2540  FOR J = 1 TO N4
    :   PRINT D$;"READ A7-D,R";R
    :   INPUT F(J)
    :   R = R + 1
    : NEXT
--------------------
2550  R = R + 2 * N4
    : FOR J = 1 TO N4
    :   PRINT D$;"READ A7-D,R";R
    :   INPUT PE(J)
    :   R = R + 1
    : NEXT
--------------------
2560  FOR J = 1 TO N4
    :   PRINT D$;"READ A7-D,R";R
    :   INPUT QE(J)
    :   R = R + 1
```

```
    : NEXT
--------------------
2570  FOR J = 1 TO N4
    :   PRINT D$;"READ A7-D,R";R
    :   INPUT RE(J)
    :   R = R + 1
    : NEXT
--------------------
2580  FOR J = 1 TO N4
    :   PRINT D$;"READ A7-D,R";R
    :   INPUT AE(J)
    :   R = R + 1
    : NEXT
--------------------
2590  PRINT D$;"CLOSE A7-D"
--------------------
2600  RETURN
--------------------
2610  REM  COMPONENTS OF AMAT & BMAT
--------------------
2620  REM
--------------------
2630  M = C(9) / C(7)
--------------------
2640  BE = ZE(1,1)
--------------------
2650  CB = COS (BE)
--------------------
2660  SB = SIN (BE)
--------------------
2670  CF = COS (F)
--------------------
2680  SF = SIN (F)
--------------------
2690  VE = C(3)
--------------------
2700  AX = M * CA * CB
--------------------
2710  BX = X(3) - M * VE * SA * CB
--------------------
2720  CX = M * VE * CA * SB
--------------------
2730  DX = X(1) - M * QE * SA * CB + M * RE * SB
--------------------
2740  EX = X(2) - M * QE * VE * CA * CB
--------------------
2750  FX = X(4) - M * VE * SA * CB
--------------------
2760  GX = - C(9) * CA
--------------------
2770  HX = M * VE * (QE * SA * SB + RE * CB)
--------------------
2780  KX = M * VE * SB
--------------------
2790  WX = X(5)
--------------------
2800  AY = M * SB
--------------------
2810  CY = M * VE * CB
--------------------
```

```
2820  DY = M * CB * (PE * SA - RE * CA)
2830  EY = M * VE * CB * (RE * SA + PE * CA)
2840  GY = - C(9) * SF * SA
2850  HY = DB(1) + M * VE * SB * (RE * CA - PE * SA)
2860  JY = DB(4) + M * VE * SA * CB
2870  KY = DB(5) - M * VE * CA * CB
2880  QY = C(9) * CF * CA
2890  RY = DB(2)
2900  SY = DB(3)
2910  AZ = M * SA * CB
2920  BZ = ZD(3) + M * VE * CA * CB
2930  CZ = - M * VE * SA * SB
2940  DZ = ZD(1) - M * PE * SB + M * QE * CA * CB
2950  EZ = ZD(2) - M * QE * VE * SA * CB
2960  FZ = ZD(4) + M * VE * CA * CB
2970  GZ = - C(9) * CF * SA
2980  HZ = - M * VE * (PE * CB + QE * CA * SB)
2990  JZ = - M * VE * SB
3000  QZ = - C(9) * SF * CA
3010  WZ = ZD(5)
3020  C1 = CX / CY
3030  A1 = AX - C1 * AY
3040  D1 = DX - C1 * DY
3050  E1 = EX - C1 * EY
3060  G1 = GX - C1 * GY
3070  H1 = HX - C1 * HY
3080  J1 = - C1 * JY
3090  K1 = KX - C1 * KY
3100  Q1 = - C1 * QY
3110  R1 = - C1 * RY
```

```
3120  S1 = - C1 * SY
3130  C2 = CZ / CY
3140  A2 = AZ - C2 * AY
3150  D2 = DZ - C2 * DY
3160  E2 = EZ - C2 * EY
3170  G2 = GZ - C2 * GY
3180  H2 = HZ - C2 * HY
3190  J2 = JZ - C2 * JY
3200  K2 = - C2 * KY
3210  Q2 = QZ - C2 * QY
3220  R2 = - C2 * RY
3230  S2 = - C2 * SY
3240  C3 = BZ / (A1 * BZ - A2 * BX)
3250  B1 = BX / BZ
3260  A(1,1) = C3 * (D1 - B1 * D2)
3270  A(1,2) = C3 * (E1 - B1 * E2)
3280  A(1,3) = C3 * (FX - B1 * FZ)
3290  A(1,4) = C3 * (G1 - B1 * G2)
3300  A(1,5) = C3 * (H1 - B1 * H2)
3310  A(1,6) = C3 * (J1 - B1 * J2)
3320  A(1,7) = C3 * (K1 - B1 * K2)
3330  A(1,8) = C3 * (Q1 - B1 * Q2)
3340  B(1,1) = C3 * (WX - B1 * WZ)
3350  B(1,2) = C3 * (R1 - B1 * R2)
3360  B(1,3) = C3 * (S1 - B1 * S2)
3370  A3 = A2 / A1
3380  C4 = A1 / (BZ * A1 - BX * A2)
3390  A(2,1) = C4 * (D2 - A3 * D1)
3400  A(2,2) = C4 * (E2 - A3 * E1)
3410  A(2,3) = C4 * (FZ - A3 * FX)
```

```
3420  A(2,4) = C4 * (G2 - A3 * G1)
---------------------
3430  A(2,5) = C4 * (H2 - A3 * H1)
---------------------
3440  A(2,6) = C4 * (J2 - A3 * J1)
---------------------
3450  A(2,7) = C4 * (K2 - A3 * K1)
---------------------
3460  A(2,8) = C4 * (Q2 - A3 * Q1)
---------------------
3470  B(2,1) = C4 * (WZ - A3 * WX)
---------------------
3480  B(2,2) = C4 * (R2 - A3 * R1)
---------------------
3490  B(2,3) = C4 * (S2 - A3 * S1)
---------------------
3500  C5 = 1 / MI(2)
---------------------
3510  A(3,1) = C5 * (DL(14) + DL(16) * A(2,1))
---------------------
3520  A(3,2) = C5 * (DL(1) + DL(16) * A(2,2))
---------------------
3530  A(3,3) = C5 * (DL(5) + DL(16) * A(2,3))
---------------------
3540  A(3,4) = C5 * DL(16) * A(2,4)
---------------------
3550  A(3,5) = C5 * DL(16) * A(2,5)
---------------------
3560  A(3,6) = C5 * (RE * (MI(3) - MI(1)) - 2 * PE * MI(4)
        + DL(16) * A(2,6))
---------------------
3570  A(3,7) = C5 * (PE * (MI(3) - MI(1)) + 2 * RE * MI(4)
        + DL(16) * A(2,7))
---------------------
3580  A(3,8) = C5 * DL(16) * A(2,8)
---------------------
3590  B(3,1) = C5 * (DL(2) + DL(16) * B(2,1))
---------------------
3600  B(3,2) = C5 * DL(16) * B(2,2)
---------------------
3610  B(3,3) = C5 * DL(16) * B(2,3)
---------------------
3620  A(4,1) = 0
---------------------
3630  A(4,2) = 0
---------------------
3640  A(4,3) = CF
---------------------
3650  A(4,4) = 0
---------------------
3660  A(4,5) = 0
---------------------
3670  A(4,6) = 0
---------------------
3680  A(4,7) = - SF
---------------------
3690  A(4,8) = - (QE * SF + RE * CF)
---------------------
3700  B(4,1) = 0
---------------------
```

```
3710  B(4,1) = 0
3720  B(4,3) = 0
3730  C6 = 1 / CY
3740  A(5,1) = C6 * (DY - AY * A(1,1))
3750  A(5,2) = C6 * (EY - AY * A(1,2))
3760  A(5,3) = - C6 * AY * A(1,3)
3770  A(5,4) = C6 * (GY - AY * A(1,4))
3780  A(5,5) = C6 * (HY - AY * A(1,5))
3790  A(5,6) = C6 * (JY - AY * A(1,6))
3800  A(5,7) = C6 * (KY - AY * A(1,7))
3810  A(5,8) = C6 * (QY - AY * A(1,8))
3820  B(5,1) = - C6 * B(1,1)
3830  B(5,2) = C6 * (RY - B(1,2))
3840  B(5,3) = C6 * (SY - B(1,3))
3850  IX = MI(1)
3860  IY = MI(2)
3870  IZ = MI(3)
3880  ZX = MI(4)
3890  I1 = IX * IZ - ZX ^ 2
3900  I2 = (IZ * (IY - IZ) - ZX ^ 2) / I1
3910  I3 = (ZX * IZ + ZX * (IX - IY)) / I1
3920  I4 = (IX * (IX - IY) + ZX ^ 2) / I1
3930  I5 = (ZX * (IY - IZ) - ZX * IX) / I1
3940  A(6,1) = 0
3950  A(6,2) = 0
3960  A(6,3) = RE * I2 + PE * I3
3970  A(6,4) = 0
3980  A(6,5) = (DB(6) * IZ + DB(11) * ZX) / I1
3990  A(6,6) = (DB(7) * IZ + DB(12) * ZX) / I1 + QE * I3
4000  A(6,7) = (DB(8) * IZ + DB(13) * ZX) / I1 + QE * I2
```

```
4010  A(6,8) = 0
---------------------
4020  B(6,1) = 0
---------------------
4030  B(6,2) = (DB(9) * IZ + DB(14) * ZX) / I1
---------------------
4040  B(6,3) = (DB(10) * IZ + DB(15) * ZX) / I1
---------------------
4050  A(7,1) = 0
---------------------
4060  A(7,2) = 0
---------------------
4070  A(7,3) = PE * I4 + RE * I5
---------------------
4080  A(7,4) = 0
---------------------
4090  A(7,5) = (DB(11) * IX + DB(6) * ZX) / I1
---------------------
4100  A(7,6) = (DB(12) * IX + DB(7) * ZX) / I1 + QE * I4
---------------------
4110  A(7,7) = (DB(13) * IX + DB(8) * ZX) / I1 + QE * I5
---------------------
4120  A(7,8) = 0
---------------------
4130  B(7,1) = 0
---------------------
4140  B(7,2) = (DB(14) * IX + DB(9) * ZX) / I1
---------------------
4150  B(7,3) = (DB(15) * IX + DB(8) * ZX) / I1
---------------------
4160  A(8,1) = 0
---------------------
4170  A(8,2) = 0
---------------------
4180  A(8,3) = SF * TAN (AE)
---------------------
4190  A(8,4) = (RE * CF + QE * SF) / (CA ^ 2)
---------------------
4200  A(8,5) = 0
---------------------
4210  A(8,6) = 1
---------------------
4220  A(8,7) = CF * TAN (AE)
---------------------
4230  A(8,8) = (QE * CF - RE * SF) * TAN (AE)
---------------------
4240  B(8,1) = 0
---------------------
4250  B(8,2) = 0
---------------------
4260  B(8,3) = 0
---------------------
4270  PRINT
    : INPUT "AMAT STORAGE LOCATION 2001 -->";R
---------------------
4280  PRINT D$;"OPEN A7-D,L20,D2"
---------------------
4290  FOR I = 1 TO 8
---------------------
4300    FOR J = 1 TO 8
```

```
4310        PRINT D$;"WRITE A7-D,R";R
    :       PRINT A(I,J)
    :       R = R + 1
    :     NEXT
    : NEXT
4320  FOR I = 1 TO 8
4330      FOR J = 1 TO 3
4340        PRINT D$;"WRITE A7-D,R";R
    :       PRINT B(I,J)
    :       R = R + 1
    :     NEXT
    : NEXT
4350  PRINT D$;"CLOSE A7-D"
4360  RETURN
4370  REM  CALCULATES AUGMENTED AMAT & BMAT
4380  INPUT "ENTER THE ELEVATOR INPUT IN POUNDS -->  ";E
4390  PRINT
    : INPUT "ENTER THE TRIM CONSTANT --> ";KT
4400  PRINT
    : PRINT "SELECT FLIGHT CONTROL AUGMENTATION"
    : PRINT
    : PRINT
4410  PRINT "     1  CONTROL AUG - ON; WITH AY FEEDBACK"
    : PRINT
4420  PRINT "     2  CONTROL AUG - ON; WITHOUT AY FEEDBACK"
    : PRINT
4430  PRINT "     3  YAW STAB - ON; CONTROL AUG - OFF; WITH
          AY FEEDBACK"
    : PRINT
4440  PRINT "     4  YAW STAB - ON; CONTROL AUG - OFF; WITH
          OUT AY FEEDBACK"
    : PRINT
4450  PRINT "     5  MECHANICAL PATH ONLY"
    : PRINT
    : PRINT
4460  INPUT "ENTER SELECTION -->  ";S
4470  ON S GOTO 4480,4490,4500,4510,4520
4480  QQ = 1
    : PP = 1
    : RI = 1
    : NY = 1
    : GOTO 4530
```

```
4490  QQ = 1
    : PP = 1
    : RI = 1
    : NY = 0
    : GOTO 4530
----------
4500  QQ = 0
    : PP = 0
    : RI = 1
    : NY = 1
    : GOTO 4530
----------
4510  QQ = 0
    : PP = 0
    : RI = 1
    : NY = 0
    : GOTO 4530
----------
4520  QQ = 0
    : PP = 0
    : RI = 0
    : NY = 0
----------
4530  REM  CHANGES EXISTING ELEMENTS OF AMAT & BMAT FOR CO
       NT AUG - ON & OFF
----------
4540  FOR I = 1 TO 8
----------
4550    A(I,3) = A(I,3) + .25 * QQ * B(I,1)
----------
4560    A(I,6) = A(I,6) + .02 * PP * B(I,2) + .1 * PP * B(
          I,3)
----------
4570    A(I,9) = KT * B(I,1)
----------
4580    A(I,10) = B(I,1)
----------
4590    A(I,11) = 0
----------
4600    A(I,12) = .2 * RI * B(I,2) + B(I,3)
----------
4610    A(I,13) = 0
----------
4620    A(I,14) = .2 * RI * B(I,2) + B(I,3)
----------
4630    A(I,15) = B(I,2)
----------
4640    A(I,16) = .003 * B(I,2)
----------
4650    A(I,17) = B(I,2)
----------
4660    B(I,1) = 0
----------
4670    B(I,2) = .001 * B(I,2)
----------
4680    B(I,3) = 0
----------
4690  NEXT
----------
```

```
4700  REM  ACCEPT NEW  MATE EQUATIONS FOR E...
      N
4710  L1 = 1
      : REM  ELEVATOR STIC FORCE COEFFICIENT
4720  L2 = 9.6
      : REM  ROB WEIGHT COEFFICIENT FOR QDOT
4730  L3 = .0855
      : REM  BOB WEIGHT COEFFICIENT FOR A2
4740  L4 = .5 * L2
4750  M = C(9) / C(7)
4760  L5 = .5 * L3 / M
4770  A(9,1) = L4 * A(3,1) - L5 * ZD(1)
4780  A(9,2) = L4 * A(3,2) - L5 * ZD(2)
4790  A(9,3) = L4 * A(3,3) - L5 * (ZD(4) + .25 * QQ * ZD(5
      ))
4800  A(9,4) = L4 * A(3,4)
4810  A(9,5) = L4 * A(3,5)
4820  A(9,6) = L4 * A(3,6)
4830  A(9,7) = L4 * A(3,7)
4840  A(9,8) = L4 * A(3,8)
4850  A(9,9) = L4 * A(3,9) - L5 * KT * ZD(5) - 16
4860  A(9,10) = L4 * A(3,10) - L5 * ZD(5)
4870  A(9,11) = L4 * A(3,11)
4880  A(9,12) = L4 * A(3,12)
4890  A(9,13) = L4 * A(3,13)
4900  A(9,14) = L4 * A(3,14)
4910  A(9,15) = L4 * A(3,15)
4920  A(9,16) = L4 * A(3,16)
4930  A(9,17) = L4 * A(3,17)
4940  B(9,1) = L4 * B(3,1) + .5 * L1
4950  B(9,2) = L4 * B(3,2)
4960  B(9,3) = L4 * B(3,3)
4970  L4 = .0852 * PP
```

```
    : REM  ELEVATOR CONTROL STICK FORCE COEFFICIENT
----------
4980  L7 = .00054 * PP
    : REM  A2 COEFFICIENT
----------
4990  L8 = 1.8182 * (L7 / M) * PP
----------
5000  NQ = .006898 * PP
----------
5010  A(10,1) = NQ * A(3,1) - L8 * ZD(1)
----------
5020  A(10,2) = NQ * A(3,2) - L8 * ZD(2)
----------
5030  A(10,3) = NQ * A(3,3) - L8 * (ZD(4) + .25 * QQ * ZD(
      5))
----------
5040  A(10,4) = NQ * A(3,4)
----------
5050  A(10,5) = NQ * A(3,5)
----------
5060  A(10,6) = NQ * A(3,6)
----------
5070  A(10,7) = NQ * A(3,7)
----------
5080  A(10,8) = NQ * A(3,8)
----------
5090  A(10,9) = NQ * A(3,9) - L8 * ZD(5) * KT
----------
5100  A(10,10) = NQ * A(3,10) - L8 * ZD(5) - 1.8182
----------
5110  FOR I = 11 TO 17
    :   A(10,I) = NQ * A(3,I)
    : NEXT
----------
5120  B(10,1) = NQ * B(3,1) + 1.8182 * L6
----------
5130  B(10,2) = NQ * B(3,2)
    : B(10,3) = NQ * B(3,3)
----------
5140  L9 = 1
    : REM  AILERON COEFFIECIENT
----------
5150  FOR I = 1 TO 10
    :   A(11,I) = 0
    : NEXT
----------
5160  A(11,11) = - 12.8
----------
5170  FOR I = 12 TO 17
    :   A(11,I) = 0
    : NEXT
----------
5180  B(11,1) = 0
    : B(11,2) = 0
----------
5190  B(11,3) = 2 * L9
----------
5200  FOR I = 1 TO 10
    :   A(12,I) = 0
    : NEXT
```

```
5210  A(12,11) = 1.4
5220  A(12,12) = - 12.5
5230  FOR I = 13 TO 17
    :   A(12,I) = 0
    : NEXT
5240  FOR I = 1 TO 3
    :   B(12,I) = 0
    : NEXT
5250  FOR I = 1 TO 12
    :   A(13,I) = 0
    : NEXT
5260  A(13,13) = - 3
5270  FOR I = 14 TO 17
    :   A(13,I) = 0
    : NEXT
5280  B(13,1) = 0
    : B(13,2) = 0
5290  B(13,3) = .063 * PP
5300  FOR I = 1 TO 12
    :   A(14,I) = 0
    : NEXT
5310  A(14,13) = 10
5320  A(14,14) = - 10
5330  FOR I = 15 TO 17
    :   A(14,I) = 0
    : NEXT
5340  FOR I = 1 TO 3
    :   B(14,I) = 0
    : NEXT
5350  YR = .25 * RI
    : YP = .011 * RI
5360  FOR I = 1 TO 12
    :   A(15,I) = YR * A(7,I) - YP * A(6,I)
    : NEXT
5370  A(15,15) = YR * A(7,15) - YP * A(6,15) - 1
5380  FOR I = 1 TO 3
    :   B(15,I) = YR * B(7,I) - YP * B(6,I)
    : NEXT
5390  N1 = 2 * NR / M
5400  N2 = 14 * NR
```

```
5410  FOR I = 1 TO 4
    :   A(16,I) = N2 * A(7,I)
    : NEXT
5420  A(16,5) = N2 * A(7,5) + N1 * DB(1)
5430  A(16,6) = N2 * A(7,6) + N1 * DB(4) + .02 * N1 * DB(2
        ) + .1 * N1 * DB(3)
5440  A(16,7) = N2 * A(7,7) + N1 * DB(5)
5450  FOR I = 8 TO 13
    :   A(16,I) = N2 * A(7,I)
    : NEXT
5460  A(16,12) = N2 * A(7,12) + .2 * N1 * DB(2) + N1 * DB(
        3)
5470  A(16,14) = N2 * A(7,14) + .2 * N1 * DB(2) + N1 * DB(
        3)
5480  A(16,15) = N2 * A(7,15) + N1 * DB(2)
5500  A(16,16) = N2 * A(7,16) + .003 * N1 * DB(2) - 2
5510  A(16,17) = N2 * A(7,17) + N1 * DB(2)
5520  B(16,1) = N2 * B(7,1)
    : B(16,3) = N2 * B(7,3)
5530  B(16,2) = N2 * B(7,2) + .001 * N1 * DB(2)
5540  FOR I = 1 TO 15
    :   A(17,I) = 0
    : NEXT
5550  A(17,16) = .0009
5560  A(17,17) = 0
5570  FOR I = 1 TO 3
    :   B(17,I) = 0
    : NEXT
5580  GOSUB 5710
5590  PRINT
    : PRINT "NEW AMAT OPTIONS"
    : PRINT
    : PRINT
5600  PRINT "     1  SAME AUGMENTATION, DIFFERENT ELEVATOR
        INPUT"
    : PRINT
5610  PRINT "     2  DIFFERENT AUGMENTATION"
    : PRINT
5620  PRINT "     3  EXIT AUGMENTATION"
```

```
    : PRINT
    : PRINT
-- --------------------
5630  INPUT "ENTER SELECTION --->  ";S
---------------------
5640  ON S GOTO 5650,4370,5700
---------------------
5650  REM  CHANGES AMAT A(9,9) FOR DIFFERENT ELEVATOR INPU
        T
---------------------
5660  PRINT
    : INPUT "ENTER NEW ELEVATOR INPUT IN POUNDS  ";E
---------------------
5670  A(9,9) = L4 * A(3,9) - L5 * ZD(5) - 16
---------------------
5680  GOSUB 5710
---------------------
5690  GOTO 5590
---------------------
5700  RETURN
---------------------
5710  REM  SUBROUTINE FOR STORING AMAT & BMAT TO DISK
---------------------
5720  PRINT
    : INPUT "STORAGE LOCATION DESIRED FOR AUGMENTED AMAT
        & BMAT --) ";R
---------------------
5730  PRINT
    : INPUT "ORDER OF AMAT  ";OA
---------------------
5740  PRINT D$
    : PRINT D$;"OPEN A7-D,L20,D2"
---------------------
5750  FOR I = 1 TO OA
---------------------
5760    FOR J = 1 TO OA
---------------------
5770      PRINT D$;"WRITE A7-D,R";R
    :     PRINT A(I,J)
    :     R = R + 1
    :   NEXT
    : NEXT
---------------------
5780  FOR I = 1 TO OA
---------------------
5790    FOR J = 1 TO 3
---------------------
5800      PRINT D$;"WRITE A7-D,R";R
    :     PRINT B(I,J)
    :     R = R + 1
    :   NEXT
    : NEXT
---------------------
5810  PRINT D$;"CLOSE A7-D"
    : PRINT
---------------------
5820  RETURN
```

State Transition Matrix

This program calculates e^{AT} where A is a matrix and T is the step size desired to propagate the state variables forward in time. The program asks for the size of the A matrix and the desired number of terms in the exponential series expansion. It calculates the state transition matrix (F-matrix) and the matrix used to propagate the input which is labeled G-matrix. These matrices are stored to disk and a printout is available. The algorithm used in this program is presented in the digital solution section of this appendix.

STATE TRANSITION MATRIX

```
----------------------
10     D$ = CHR$ (4)
     : REM  CTRL-D
----------------------
20     M = 1
     : P = 10
     : Q = 11
----------------------
30     DEF FN R(X) = INT (X * 1000000 + .5) / 1000000
----------------------
40     HOME
     : TEXT
     : PRINT CHR$ (12)
     : PRINT
----------------------
50     INPUT "KEY IN ORDER OF MATRIX A ";N
----------------------
60     INPUT "HOW MANY TERMS IN 'FMAT' DO YOU WANT EVALUATE
          D? ";RR
----------------------
70     DIM A(N,N),F(N,N,RR + 1),G(N,N,RR + 1),IM(N,N),AM(N,
          N),FM(N,N),GM(N,N),FP(N,N),GP(N,N)
----------------------
80     FOR I = 1 TO N
----------------------
90       IM(I,I) = 1
----------------------
100    NEXT I
----------------------
110    PRINT "INPUT ELEMENTS OF MATRIX A"
----------------------
120    PRINT
     : PRINT
----------------------
130    PRINT "1 - ENTER AMAT FROM DISK"
     : PRINT
----------------------
140    PRINT "2 - ENTER AMAT FROM KEYBOARD"
     : PRINT
----------------------
150    PRINT "ENTER OPTION -->";
----------------------
160    GET A
     : PRINT A
----------------------
170    ON A GOTO 240,180
----------------------
180    FOR I = 1 TO N
----------------------
190      FOR J = 1 TO N
----------------------
200        PRINT "     A(";I;",";J;") =";
----------------------
210        INPUT A(I,J)
----------------------
220      NEXT J
     :   PRINT
     : NEXT I
```

```
230   GOTO 300
240   INPUT "STORAGE LOCATION FOR AMAT ";R
250   PRINT D$
    : PRINT D$;"OPEN A7-D,L20,D2"
260   FOR I = 1 TO N
270     FOR J = 1 TO N
280       PRINT D$;"READ A7-D,R";R
    :     INPUT A(I,J)
    :     R = R + 1
    :   NEXT
    : NEXT
290   PRINT D$;"CLOSE A7-D"
300   INPUT "ENTER TAU AND T-STAR ";TAU,T1
310   T = TAU / T1
320   PRINT
    : POKE 36,12
    : INVERSE
    : PRINT "PLEASE STANDBY"
    : PRINT
    : PRINT "CALCULATING THE STATE TRANSITION MATRIX"
    : NORMAL
    : PRINT
330   FOR I = 1 TO N
340     FOR J = 1 TO N
350       K = 1
360       F(I,J,K) = IM(I,J)
370       G(I,J,K) = IM(I,J) * T
380     NEXT J
    : NEXT I
390   REM
400   FOR I = 1 TO N
410     FOR J = 1 TO N
420       F(I,J,K + 1) = 0
430       FOR L = 1 TO N
440         F(I,J,K + 1) = F(I,J,K + 1) + A(I,L) * G(L,J,K
                  )
450       NEXT L
```

```
    :   NEXT J
    : NEXT I
--------------------
460   FOR I = 1 TO N
--------------------
470     FOR J = 1 TO N
--------------------
480       G(I,J,K + 1) = F(I,J,K + 1) * (T / (K + 1))
--------------------
490     NEXT J
    : NEXT I
--------------------
500   IF K = RR THEN 520
--------------------
510   K = K + 1
    : GOTO 390
--------------------
520   REM
--------------------
530   FOR I = 1 TO N
--------------------
540     FOR J = 1 TO N
--------------------
550       FP(I,J) = 0
--------------------
560       GP(I,J) = 0
--------------------
570       FOR K = 1 TO RR + 1
--------------------
580         FP(I,J) = FP(I,J) + F(I,J,K)
--------------------
590         GP(I,J) = GP(I,J) + G(I,J,K)
--------------------
600       NEXT K
    :   NEXT J
    : NEXT I
--------------------
610   PRINT
--------------------
620   PRINT "DO YOU WANT A PRINTOUT OF THE MATRICES? "
--------------------
630   INPUT A$
    : IF A$ = "N" THEN 940
--------------------
640   PRINT D$
    : PRINT D$;"PR#1"
    : PRINT CHR$ (15)
--------------------
650   POKE 36,6 * N
    : PRINT "A-MATRIX"
    : PRINT
    : PRINT
--------------------
660   I = 1
--------------------
670   FOR J = 1 TO N
--------------------
680     AM(I,J) = FN R(A(I,J))
--------------------
690     POKE 36,12 * J
```

```
    :   PRINT AM(I,J);
    : NEXT
--------------------
700   PRINT
--------------------
710   IF I = N THEN 730
--------------------
720   I = I + 1
    : GOTO 670
--------------------
730   PRINT
    : PRINT
--------------------
740   POKE 36,6 * N
    : PRINT "F-MATRIX"
    : PRINT
    : PRINT
--------------------
750   I = 1
--------------------
760   FOR J = 1 TO N
--------------------
770     FM(I,J) = FN R(FP(I,J))
--------------------
780     POKE 36,12 * J
    :   PRINT FM(I,J);
    : NEXT
--------------------
790   PRINT
--------------------
800   IF I = N THEN 820
--------------------
810   I = I + 1
    : GOTO 760
--------------------
820   PRINT
--------------------
830   POKE 36,6 * N
    : PRINT "G-MATRIX"
    : PRINT
    : PRINT
--------------------
840   I = 1
--------------------
850   FOR J = 1 TO N
--------------------
860     GM(I,J) = FN R(GP(I,J))
--------------------
870     POKE 36,12 * J
    :   PRINT GM(I,J);
    : NEXT
--------------------
880   PRINT
--------------------
890   IF I = N THEN 910
--------------------
900   I = I + 1
    : GOTO 850
--------------------
910   PRINT
```

```
    : S = FRE (0)
--------------------
920   PRINT D$
    : PRINT D$;"PR#0"
    : PRINT D$;"IN#0"
--------------------
930   HOME
    : PRINT CHR$ (12)
    : PRINT
--------------------
940   PRINT
    : INPUT "FMAT & GMAT STORAGE LOCATION 4000+ -->";R
--------------------
950   PRINT D$
    : PRINT D$;"OPEN A7-D,L20,D2"
--------------------
960   FOR I = 1 TO N
--------------------
970     FOR J = 1 TO N
--------------------
980       PRINT D$;"WRITE A7-D,R";R
    :     PRINT FP(I,J)
    :     R = R + 1
    :   NEXT
    : NEXT
--------------------
990   FOR I = 1 TO N
--------------------
1000    FOR J = 1 TO N
--------------------
1010      PRINT D$;"WRITE A7-D,R";R
    :     PRINT GP(I,J)
    :     R = R + 1
    :   NEXT
    : NEXT
--------------------
1020  PRINT D$;"CLOSE A7-D"
```

Discrete Time Response

This program solves the discrete state differential equations to produce a discrete time response to step, pulse, and doublet inputs. The program asks for the desired number of seconds for the time solution. The response to this question must result in some multiple of 50 when the time is divided by the time increment. The order of the system matrix is input and the A matrix can be loaded from disk or from the keyboard. The state transition matrix is loaded from disk along with the G matrix which premultiplies $B\bar{u}$. The appropriate column of the B matrix is input from the keyboard, as are the initial conditions for the state variables. The magnitude of the input is entered in pounds, and the choice of a step pulse or doublet is made. If the input is a pulse or doublet, the approximate period of the primary mode being excited is needed, i.e., rudder input implies dutch roll. The program calculates the state variables at each time increment and stores these values on a disk for future use. A tabular listing of the response is available and the stored data is used for plotting time responses for each state variable, using the program called Augmented Plotter.

This program solves

$$\dot{\bar{x}}(t) = A\,\bar{x}(t) + B\,\bar{u}(t) \tag{D56}$$

which has a solution form of

$$\bar{x}(t) = e^{At}x(o) + \int_o^t e^{A(T-\tau)}Bu(\tau)d\tau \tag{D57}$$

letting $t = kT$

$$x(kT) = e^{AkT}x(o) + \int_o^{kT} e^{A(T-\tau)}Bu(\tau)d\tau$$

$$x(kT) = e^{AkT}x(o) + e^{AkT}\int_{o}^{kT} e^{-A\tau}Bu(\tau)d\tau$$

$$= e^{kAT}x(o) + e^{kAT}\int_{o}^{T} e^{-A\tau}Bu(o)d\tau + e^{kAT}\int_{T}^{2T} e^{-A\tau}Bu(\tau)d\tau$$

$$+ e^{kAT}\int_{(k-1)T}^{kT} e^{-A\tau}Bu[(k-1)T]d\tau$$

so

$$x(kT) = e^{kAT}x(o) + \sum_{k=0}^{k}\int_{(k-1)T}^{kT} e^{A(kT-\tau)}Bu[(k-1)T]d\tau \qquad (D58)$$

looking at k=1,2,3

k=1

$$x(T) = e^{AT}x(o) + \int_{o}^{T} e^{A(T-\tau)}Bu(o)d\tau \qquad (D59)$$

k=2

$$x(2T) = e^{A2T}x(o) + \int_{o}^{2T} e^{A(2T-\tau)}Bu(\tau)d\tau$$

$$= e^{A2T}x(o) + \int_{o}^{T} e^{A(2T-\tau)}Bu(o)d\tau + \int_{T}^{2T} e^{A(2T-\tau)}u(T)d\tau \qquad (D60)$$

k=3

$$x(3T) = e^{A3T}x(o) + \int_{o}^{3T} e^{A(3T-\tau)}Bu(\tau)d\tau$$

$$= e^{A3T}x(o) + \int_{o}^{T} e^{A(3T-\tau)}Bu(o)d\tau + \int_{T}^{2T} e^{A(3T-\tau)}Bu(T)d\tau$$

$$+ \int_{2T}^{3T} e^{A(3T-\tau)}Bu(2T)d\tau \qquad (D61)$$

Using x(2T) from above

$$x(2T) = e^{2AT}x(o) + \int_0^T e^{A(2T-\tau)}Bu(o)d\tau + \int_T^{2T} e^{A(2T-\tau)}Bu(T)d\tau$$

$$= e^{AT}[e^{AT}x(o) + \int_o^T e^{A(T-\tau)}Bu(o)d\tau] + \int_T^{2T} e^{A(2T-\tau)}Bu(T)d\tau$$

$$= e^{AT}[x(T)] + \int_T^{2T} e^{A(2T-\tau)}B(T)d\tau \qquad (D62)$$

so $e^{AkT}x(o) = e^{AT}$ x [(k-1)T] and from above

Now changing variable of integration for k=2 and k=3 to show this integral has the same form

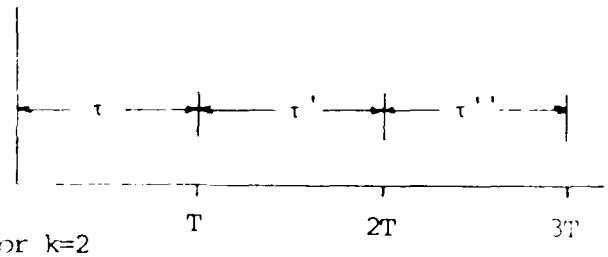

let $\tau = \tau$

$\tau = T + \tau'$ $\quad d\tau = d\tau'$

$\tau = 2T + \tau''$ $\quad d\tau = d\tau''$

for k=2

$$\int_T^{2T} e^{A(2T-(\tau'+T))}Bu(T)d\tau' = \int_o^T e^{A(T-\tau')}Bu(T)d\tau' \qquad (D64)$$

$$\int_{2T}^{3T} e^{A(3T-(\tau''+2T))}Bu(2T)d\tau'' = \int_o^T e^{A(T-\tau'')}Bu(2T)d\tau'' \qquad (D65)$$

since τ' and τ'' are just dummy variables integrals are equal so

$$x(k+1)T) = e^{AT}x(kT) + e^{AT}\int_o^T e^{-A\tau}Bd\tau u(kT) \qquad (D66)$$

solving

$$e^{AT}\int_o^T e^{-A\tau}Bd\tau u(kT)$$

$$e^{AT}[-A^{-1}e^{-A\tau}B\,|_o^T]u(kT)$$

$$e^{AT}[-A^{-1}e^{-AT} + A^{-1}]Bu(kT)$$

$$[e^{AT}(-A^{-1})e^{-AT} + e^{AT}A^{-1}]Bu(kT)$$

$$[-A^{-1} + e^{AT}A^{-1}]Bu(kT)$$

$$A^{-1}[e^{AT} - I]Bu(kT)$$

$$\int_0^T e^{A\tau}d\tau = A^{-1}e^{A\tau}\Big|_0^T = A^{-1}e^{AT}-A^{-1} = A^{-1}(e^{AT} - I) \qquad (D67)$$

$$x[(k+1)T] = e^{AT}x(kT) + A^{-1}(e^{AT}-I)Bu(kT) \qquad (D68)$$

I used a series expansion of e^{AT}

$$e^{AT} = [I + AT + \frac{A^2T^2}{2!} + \frac{A^3T^3}{3!} + \ldots] \qquad (D69)$$

and

$$A^{-1}e^{AT}-A^{-1} = [A^{-1} + A^{-1}AT + \frac{A^{-1}AAT^2}{2!} + \frac{A^{-1}AA^2T^3}{3!} + \ldots]-A$$

$$= IT + \frac{AT^2}{2!} + \frac{A^2T^3}{3!} + \frac{A^3T^4}{4!} \qquad (D70)$$

therefore,

$$x[(k+1)T] = [\sum_{k=0}^{\infty} \frac{A^kT^k}{k!}]x(kT) + [\sum_{k=0} \frac{A^kT^{k+1}}{(k+1)!}]u(kT) \qquad (D71)$$

This was implemented in the following program written in Applesoft Basic.

```
AUGMENTED RESPONSE/VER. 1

----------
10    D$ = CHR$ (4)
    : REM  CTRL-D
----------
20    M = 1
    : P = 10
    : Q = 15
----------
30    DEF FN R(X) = INT (X * 1000000 + .5) / 1000000
----------
40    HOME
    : TEXT
    : PRINT CHR$ (12)
    : PRINT
----------
50    INPUT "ENTER SECONDS OF TRACE DESIRED";HX
----------
60    INPUT "KEY IN ORDER OF MATRIX A ";N
----------
70    DIM A(N,N),FX(N,1,50),GB(N,1),B(N,1),GP(N,N),FP(N,N)
        ,TIME(50),LY(N),HY(N),YS(N),XM(N,50)
----------
80    DIM GU(N,1,50),X(N,1,50)
----------
85    Q = N + 3
----------
90    TIME(0) = 0
----------
100   PRINT "INPUT ELEMENTS OF MATRIX A"
----------
110   PRINT
    : PRINT
----------
120   PRINT "1 - ENTER AMAT FROM DISK"
    : PRINT
----------
130   PRINT "2 - ENTER AMAT FROM KEYBOARD"
    : PRINT
----------
140   PRINT "ENTER OPTION --->";
----------
150   GET A
    : PRINT A
----------
160   ON A GOTO 230,170
----------
170   FOR I = 1 TO N
----------
180     FOR J = 1 TO N
----------
190       PRINT "     A(";I;",";J;") =";
----------
200       INPUT A(I,J)
----------
210     NEXT J
    :   PRINT
    : NEXT I
----------
```

```
220    GOTO 290
230    INPUT "STORAGE LOCATION FOR AMAT ";R
240    PRINT D$
     : PRINT D$;"OPEN A7-D,L20,D2"
250    FOR I = 1 TO N
260      FOR J = 1 TO N
270        PRINT D$;"READ A7-D,R";R
     :     INPUT A(I,J)
     :     R = R + 1
     :   NEXT
     : NEXT
280    PRINT D$;"CLOSE A7-D"
290    INPUT "ENTER TAU AND T-STAR ";TAU,T1
300    T = TAU / T1
310    INPUT "STORAGE LOCATION FOR FMAT ";R
320    PRINT D$
     : PRINT D$;"OPEN A7-D,L20,D2"
330    FOR I = 1 TO N
340      FOR J = 1 TO N
350        PRINT D$;"READ A7-D,R";R
     :     INPUT FP(I,J)
     :     R = R + 1
     :   NEXT
     : NEXT
360    FOR I = 1 TO N
370      FOR J = 1 TO N
380        PRINT D$;"READ A7-D,R";R
     :     INPUT GP(I,J)
     :     R = R + 1
     :   NEXT
     : NEXT
390    PRINT D$;"CLOSE A7-D"
400    PRINT "INPUT DESIRED COLUMN OF 'B' MATRIX"
410    PRINT
420    FOR I = 1 TO N
430      PRINT "     B(";I;",1) =";
440      INPUT B(I,1)
```

```
450   NEXT I
-----------------------
460   PRINT
    : INPUT "ARE ALL ENTRIES CORRECT (Y/N)? ";A$
    : IF A$ = "N" THEN 400
-----------------------
470   PRINT
    : PRINT "INPUT INITIAL CONDITION MATRIX"
-----------------------
480   PRINT
-----------------------
490   FOR I = 1 TO N
-----------------------
500     PRINT "     X(";I;",1,0) =";
-----------------------
510     INPUT X(I,1,0)
-----------------------
520   NEXT I
-----------------------
530   PRINT
    : INPUT "ARE ALL ENTRIES CORRECT (Y/N)? ";A$
    : IF A$ = "N" THEN 470
-----------------------
540   PRINT
    : PRINT "BE SURE DATA-TR DISK IS IN DRIVE 2"
    : PRINT
-----------------------
550   PRINT
    : PRINT "ENTER MAGNITUDE OF INPUT FUNCTION"
-----------------------
560   PRINT
-----------------------
561   PRINT "1 - MAGNITUDE IN POUNDS"
    : PRINT
-----------------------
562   PRINT "2 - MAGNITUDE IN DEGREES"
    : PRINT
-----------------------
563   PRINT "ENTER OPTION -->";
-----------------------
564   GET A
    : PRINT A
-----------------------
565   ON A GOTO 573,570
-----------------------
570   INPUT "MAGNITUDE IN DEGREES";IP
--------- -----------
571   IP = IP / 57.29578
-----------------------
572   GOTO 580
-----------------------
573   INPUT "MAGNITUDE IN POUNDS";IP
-----------------------
580   HOME
    : PRINT CHR$ (12)
    : PRINT
-----------------------
590   PRINT
    : PRINT "TYPE OF INPUT DESIRED"
    : PRINT
```

```
    : PRINT
---------------------
600   PRINT "1 - STEP"
    : PRINT
---------------------
610   PRINT "2 - PULSE"
    : PRINT
---------------------
620   PRINT "3 - DOUBLET"
    : PRINT
    : PRINT
---------------------
630   PRINT "ENTER OPTION --> ";
---------------------
640   GET A
    : PRINT A
---------------------
650   IF A = 1 THEN 680
---------------------
660   PRINT
    : INPUT "ENTER PERIOD --> ";T
---------------------
670   N1 = INT (T / (2 * TAU))
---------------------
680   PRINT D$;"OPEN DATA-TR,D2"
---------------------
690   PRINT D$;"DELETE DATA-TR"
---------------------
700   PRINT D$;"OPEN DATA-TR,L20,D2"
---------------------
710   PRINT D$;"WRITE DATA-TR, R";0
---------------------
720   PRINT HX
---------------------
730   PRINT D$;"WRITE DATA-TR,R";N + 2
---------------------
740   PRINT TAU
---------------------
750   XS = 260 / HX
    : PRINT D$;"WRITE DATA-TR,R";N + 1
---------------------
760   PRINT XS
---------------------
770   PRINT D$;"CLOSE DATA-TR"
---------------------
780   FOR I = 1 TO N
---------------------
790     GB(I,1) = 0
---------------------
800     FOR L = 1 TO N
---------------------
810       GB(I,1) = GB(I,1) + GP(I,L) * B(L,1)
---------------------
820     NEXT L
    : NEXT I
---------------------
830   FOR I = 1 TO N
    :   LY(I) = 1E38
    :   HY(I) = - 1E38
    : NEXT I
```

```
840   K = 1
850   FOR I = 1 TO N
860     FX(I,1,K) = 0
870     FOR L = 1 TO N
880       FX(I,1,K) = FX(I,1,K) + FP(I,L) * X(L,1,K - 1)
890     NEXT L
    : NEXT I
900   ON A GOTO 950,910,930
910   IF K = N1 AND M = 1 THEN IP = 0
920   GOTO 950
930   IF K = N1 AND M = 1 THEN IP = - IP
940   IF K = 2 * N1 AND M = 1 THEN IP = 0
950   FOR I = 1 TO N
960     GU(I,1,K) = 0
970     GU(I,1,K) = GU(I,1,K) + GB(I,1) * IP
980   NEXT I
990   TIME(K) = TIME(K - 1) + TAU
1000  PRINT D$;"OPEN DATA-TR,L20,D2"
1010  PRINT D$;"WRITE DATA-TR, R";Q
1020  PRINT TIME(K)
1030  FOR I = 1 TO N
1040    X(I,1,K) = FX(I,1,K) + GU(I,1,K)
1050    IF X(I,1,K) < LY(I) THEN LY(I) = X(I,1,K)
1060    IF X(I,1,K) > HY(I) THEN HY(I) = X(I,1,K)
1070    PRINT D$;"WRITE DATA-TR, R";Q + I
1080    PRINT X(I,1,K)
1090  NEXT I
1100  Q = Q + N + 1
1110  IF K = 50 THEN 1130
1120  K = K + 1
    : GOTO 850
```

```
1130  FOR I = 1 TO N
1140     IF HY(I) = 0 AND LY(I) = 0 THEN YS(I) = 0
  * :    GOTO 1170
1150     IF ABS (HY(I)) > ABS (LY(I)) THEN YS(I) = INT (80
            / ABS (HY(I)))
  * :    GOTO 1170
1160     YS(I) = INT (80 / ABS (LY(I)))
1170     PRINT D$;"WRITE DATA-TR,R";I
     :    PRINT YS(I)
1180  NEXT I
1190  PRINT D$;"CLOSE DATA-TR"
1200  PRINT
     : INPUT "DO YOU WANT A TABULAR PRINTOUT OF DATA (Y/N)
          ? ";A$
     : IF A$ = "N" THEN 1320
1210  PRINT D$
     : PRINT D$;"PR#1"
     : PRINT CHR$ (15)
1220  PRINT "TIME";
1230  FOR I = 1 TO N
     :    POKE 36,12 * I
     :    PRINT "VARIABLE #";I;
     : NEXT
1240  POKE 36,0
1250  PRINT
     : PRINT
1260  FOR K = 1 TO 50
1270     PRINT TIME(K);
1280     FOR I = 1 TO N
     :       XM(I,K) = FN R(X(I,1,K))
1290        POKE 36,12 * I
     :       PRINT XM(I,K);
     :    NEXT
1300     PRINT
1310  NEXT
1320  IF M = MX / (50 * TAU) THEN 1400
1330  FOR I = 1 TO N
     :    X(I,1,0) = X(I,1,50)
     : NEXT I
```

```
1340  TIME(0) = TIME(50)
1350  M = M + 1
    : K = 1
1360  PRINT D$
    : PRINT D$;"PR#0"
    : PRINT D$;"IN#0"
1370  PRINT D$;"OPEN DATA-TR,L20,D2"
1380  GOTO 850
1390  END
1400  PRINT "RUN AUGMENTED PLOTTER"
```

Augmented Plotter

This program plots the data generated by Augmented Response/Ver 1 onto the high resolution screen. It also allows the generated plots to be saved to diskette.

```
REM COMPUTED FLUTTER
5     INPUT "ENTER DIMENSION OF AMAT --> ";N
10    K = 1
    : P = N + 3
15    S = P
20    D$ = CHR$ (4)
30    INPUT "WHICH VARIABLE DO YOU WANT?";I
40    PRINT D$;"OPEN DATA-TR,L20,D2"
50    PRINT D$;"READ DATA-TR, R";0
60    INPUT HX
70    PRINT D$;"READ DATA-TR, R";I
80    INPUT YS
90    PRINT D$;"READ DATA-TR,R";N + 2
100   INPUT TAU
110   PRINT D$;"READ DATA-TR,R";N + 1
120   INPUT XS
130   PRINT D$;"CLOSE DATA-TR"
150   HGR
160   HPLOT 19,0 TO 19,160
    : HPLOT 19,80 TO 279,80
170   PRINT D$;"OPEN DATA-TR,L20,D2"
180   PRINT D$;"READ DATA-TR, R";P
190   INPUT X
200   T = 19 + X * XS
210   PRINT D$;"READ DATA-TR,R";I + S
220   INPUT Z
230   Y = 80 - Z * YS
240   HPLOT T,Y
250   I = I + N + 1
260   P = P + N + 1
265   S% = HX / TAU
```

```
270   IF K = S% THEN 290
280   K = K + 1
    : GOTO 180
290   PRINT D$;"CLOSE DATA-TR"
300   INPUT "WOULD YOU LIKE TO SAVE THIS? ";A$
310   IF A$ = "N" THEN 330
320   INPUT "FILE NAME --> ";B$
325   PRINT D$;"BSAVE";B$;",A$2000,L$2000,D2"
330   END
```

Augmented Print Data/Ver 1

This program provides the means of printing the stability derivatives, equilibrium conditions, and A and B matrices. For systems larger than 8 x 8, a wide paper printer is required.

AUGMENTED PRINT DATA/DEV 1

```
10    REM  PROGRAM FOR PRINTING OUT DATA FROM DISK
20    REM
30    REM  BY JEFFREY R. RIEMER
40    REM  5 MAY 1983
50    REM
60    DIM C(110),BE(20),DR(20),DA(20),DS(20),AN(20),F(20),
         NB(20),PE(20),RE(20),QE(20),AE(20)
70    DIM A(20,20),B(20,20),AM(20,20),BM(20,20)
80    DEF FN R(X) = INT (X * Z1 + .5) / Z1
90    TEXT
    : HOME
    : PRINT CHR$ (12)
    : PRINT
100   D$ = CHR$ (4)
    : REM  CTRL-D
110   REM  MENU
120   PRINT
    : PRINT SPC( 15);
    : INVERSE
    : PRINT "MAIN MENU"
    : NORMAL
    : PRINT
    : PRINT
130   PRINT "1 - PRINT DERIVATIVES"
    : PRINT
140   PRINT "2 - PRINT EQUILIBRIUM FLIGHT CONDITION"
    : PRINT
150   PRINT "3 - PRINT AMAT AND BMAT"
    : PRINT
160   PRINT "4 - END"
    : PRINT
    : PRINT
170   PRINT "ENTER OPTION --> ";
180   GET A
    : PRINT A
190   ON A GOTO 200,1040,1740,2130
200   REM  DERIVATIVES
```

```
210   PRINT D$;"OPEN A7-D,L20,D2"
220   FOR I = 0 TO 9
230      PRINT D$;"READ A7-D,R";I
     :   INPUT C(I)
     : NEXT
240   PRINT D$;"CLOSE A7-D"
250   INPUT "ENTER LOAD FACTOR -->";AN
     : PRINT
260   IF A = 3 THEN 1780
270   PRINT D$
     : PRINT D$;"PR#1"
     : PRINT CHR$ (15)
280   IF AN > 1 THEN 350
290   PRINT D$;"OPEN A7-D,L20,D2"
300   R = 10
310   FOR I = 10 TO 103
320      PRINT D$;"READ A7-D,R";R
     :   INPUT C(I)
     :   R = R + 1
     : NEXT
330   PRINT D$;"CLOSE A7-D"
340   GOTO 440
350   INPUT "STORAGE RECORD YOU WANT TO START AT";R
360   PRINT D$;"OPEN A7-D,L20,D2"
370   FOR I = 10 TO 41
380      PRINT D$;"READ A7-D,R";R
     :   INPUT C(I)
     :   R = R + 1
     : NEXT
390   FOR I = 46 TO 57
400      PRINT D$;"READ A7-D,R";R
     :   INPUT C(I)
     :   R = R + 1
     : NEXT
410   FOR I = 63 TO 103
420      PRINT D$;"READ A7-D,R";R
     :   INPUT C(I)
     :   R = R + 1
     : NEXT
```

```
430   PRINT D$;"CLOSE A7:D"
------------------------------
440   GOSUB 930
------------------------------
450   POKE 36,23
    : PRINT "DERIVATIVE";
    : POKE 36,45
    : PRINT "STABILITY AXIS";
    : POKE 36,64
    : PRINT "BODY AXIS";
    : POKE 36,86
    : PRINT "DERIVATIVES";
    : POKE 36,108
    : PRINT "STABILITY AXIS";
    : POKE 36,127
    : PRINT "BODY AXIS"
    : PRINT
    : PRINT
------------------------------
460   POKE 36,15
    : PRINT "CL";
    : POKE 36,45
    : PRINT C(32);
    : POKE 36,78
    : PRINT "CYB";
    : POKE 36,108
    : PRINT C(17);
    : POKE 36,127
    : PRINT C(17)
------------------------------
470   POKE 36,15
    : PRINT "CLV";
    : POKE 36,45
    : PRINT C(33);
    : POKE 36,78
    : PRINT "CYP";
    : POKE 36,108
    : PRINT C(20);
    : POKE 36,127
    : PRINT C(46)
------------------------------
480   POKE 36,15
    : PRINT "CLA (CL ALPHA)";
    : POKE 36,45
    : PRINT C(12);
    : POKE 36,78
    : PRINT "CYR";
    : POKE 36,108
    : PRINT C(21);
    : POKE 36,127
    : PRINT C(47)
------------------------------
490   POKE 36,15
    : PRINT "CLAD (CL ALPHA DOT)";
    : POKE 36,45
    : PRINT C(34);
    : POKE 36,78
    : PRINT "CYDR (CY DELTA RUDDER)";
    : POKE 36,108
```

```
      : PRINT "CDA (CD ALPHA)";
      : POKE 36,45
      : PRINT C(37);
      : POKE 36,78
      : PRINT "CLDR (CL DELTA RUDDER)";
      : POKE 36,108
      : PRINT C(23);
      : POKE 36,127
      : PRINT C(51)
------------------------
550   POKE 36,15
```

```
    : PRINT "CLDDL (CL DELTA ELEVATOR)";
    : POKE 36,45
    : PRINT C(28);
    : POKE 36,78
    : PRINT "CLDA (CL DELTA AILERON)";
    : POKE 36,108
    : PRINT C(24);
    : POKE 36,127
    : PRINT C(52)
--------------------
540   POKE 36,15
    : PRINT "CMV";
    : POKE 36,45
    : PRINT C(39);
    : POKE 36,64
    : PRINT C(39);
    : POKE 36,78
    : PRINT "CNB";
    : POKE 36,108
    : PRINT C(27);
    : POKE 36,127
    : PRINT C(53)
---------------------
570   POKE 36,15
    : PRINT "CMA (CM ALPHA)";
    : POKE 36,45
    : PRINT C(10);
    : POKE 36,64
    : PRINT C(10);
    : POKE 36,78
    : PRINT "CNP";
    : POKE 36,108
    : PRINT C(30);
    : POKE 36,127
    : PRINT C(54)
---------------------
580   POKE 36,15
    : PRINT "CMAD (CM ALPHA DOT)";
    : POKE 36,45
    : PRINT C(41);
    : POKE 36,64
    : PRINT C(41);
    : POKE 36,78
    : PRINT "CNR";
    : POKE 36,108
    : PRINT C(31);
    : POKE 36,127
    : PRINT C(55)
--------------------
590   POKE 36,15
    : PRINT "CMQ";
    : POKE 36,45
    : PRINT C(14);
    : POKE 36,64
    : PRINT C(14);
    : POKE 36,78
    : PRINT "CNDR (CN DELTA RUDDER)";
    : POKE 36,108
    : PRINT C(29);
    : POKE 36,127
```

```
    : PRINT C(56)
--------------------
600   POKE 36,15
    : PRINT "CMDE (CM DELTA ELEVATOR)";
    : POKE 36,45
    : PRINT C(11);
    : POKE 36,64
    : PRINT C(11);
    : POKE 36,78
    : PRINT "CNDA (CN DELTA AILERON)";
    : POKE 36,108
    : PRINT C(29);
    : POKE 36,127
    : PRINT C(57)
--------------------
610   POKE 36,15
    : PRINT "CMDT (CM DELTA THROTTLE)";
    : POKE 36,45
    : PRINT 0;
    : POKE 36,64
    : PRINT 0
--------------------
620   PRINT CHR$ (12)
    : Z = 2
    : GOSUB 930
--------------------
630   POKE 36,23
    : PRINT "DERIVATIVES";
    : POKE 36,45
    : PRINT "BODY AXIS";
    : POKE 36,86
    : PRINT "DERIVATIVES";
    : POKE 36,115
    : PRINT "BODY AXIS"
    : PRINT
    : PRINT
--------------------
640   POKE 36,15
    : PRINT "XV";
    : POKE 36,45
    : PRINT C(94);
    : POKE 36,78
    : PRINT "YB (SIDE FORCE DUE TO BETA)";
    : POKE 36,115
    : PRINT C(63)
--------------------
650   POKE 36,15
    : PRINT "XA (X ALPHA)";
    : POKE 36,45
    : PRINT C(95);
    : POKE 36,78
    : PRINT "YP";
    : POKE 36,115
    : PRINT C(66)
--------------------
660   POKE 36,15
    : PRINT "XAD (X ALPHA DOT)";
    : POKE 36,45
    : PRINT C(96);
    : POKE 36,78
```

```
     : PRINT "LR";
     : POKE 36,115
     : PRINT C(67)
--------------------
670    POKE 36,15
     : PRINT "XQ";
     : POKE 36,45
     : PRINT C(97);
     : POKE 36,78
     : PRINT "YDR (Y DELTA RUDDER)";
     : POKE 36,115
     : PRINT C(64)
--------------------
680    POKE 36,15
     : PRINT "XDE (X DELTA ELEVATOR)";
     : POKE 36,45
     : PRINT C(98);
     : POKE 36,78
     : PRINT "YDA (Y DELTA AILERON)";
     : POKE 36,115
     : PRINT C(65)
--------------------
690    POKE 36,15
     : PRINT "XDT (X DELTA THROTTLE)";
     : POKE 36,45
     : PRINT 0;
     : POKE 36,78
     : PRINT "LB";
     : POKE 36,115
     : PRINT C(68)
--------------------
700    POKE 36,15
     : PRINT "ZV";
     : POKE 36,45
     : PRINT C(99);
     : POKE 36,78
     : PRINT "LP";
     : POKE 36,115
     : PRINT C(69)
--------------------
710    POKE 36,15
     : PRINT "ZA (Z ALPHA)";
     : POKE 36,45
     : PRINT C(100);
     : POKE 36,78
     : PRINT "LR";
     : POKE 36,115
     : PRINT C(70)
--------------------
720    POKE 36,15
     : PRINT "ZAD (Z ALPHA DOT)";
     : POKE 36,45
     : PRINT C(101);
     : POKE 36,78
     : PRINT "LDR (L DELTA RUDDER)";
     : POKE 36,115
     : PRINT C(71)
--------------------
730    POKE 36,15
     : PRINT "ZQ";
```

```
     : POKE 36,45
     : PRINT C(102);
     : POKE 36,78
     : PRINT "LDA (L DELTA AILERON)";
     : POKE 36,115
     : PRINT C(72)
----------------------
740    POKE 36,15
     : PRINT "ZDE (Z DELTA ELEVATOR)";
     : POKE 36,45
     : PRINT C(103);
     : POKE 36,78
     : PRINT "NB";
     : POKE 36,115
     : PRINT C(73)
----------------------
750    POKE 36,15
     : PRINT "ZDT (Z DELTA THROTTLE)";
     : POKE 36,45
     : PRINT 0;
     : POKE 36,78
     : PRINT "NP";
     : POKE 36,115
     : PRINT C(74)
----------------------
760    POKE 36,15
     : PRINT "L";
     : POKE 36,45
     : PRINT C(84);
     : POKE 36,78
     : PRINT "NR";
     : POKE 36,115
     : PRINT C(75)
----------------------
770    POKE 36,15
     : PRINT "LV";
     : POKE 36,45
     : PRINT C(85);
     : POKE 36,78
     : PRINT "NDR (N DELTA RUDDER)";
     : POKE 36,115
     : PRINT C(76)
----------------------
780    POKE 36,15
     : PRINT "LA (L ALPHA)";
     : POKE 36,45
     : PRINT C(80);
     : POKE 36,78
     : PRINT "NDA (N DELTA AILERON)";
     : POKE 36,115
     : PRINT C(17)
----------------------
790    POKE 36,15
     : PRINT "LAD (L ALPHA DOT)";
     : POKE 36,45
     : PRINT C(86)
----------------------
800    POKE 36,15
     : PRINT "LQ";
     : POKE 36,45
```

```
    : PRINT C(83)
---------------------
810   POKE 36,15
    : PRINT "LDE (L DELTA ELEVATOR)";
    : POKE 36,45
    : PRINT C(81)
---------------------
820   POKE 36,15
    : PRINT "MV";
    : POKE 36,45
    : PRINT C(91)
---------------------
830   POKE 36,15
    : PRINT "MA (M ALPHA)";
    : POKE 36,45
    : PRINT C(78)
---------------------
840   POKE 36,15
    : PRINT "MAD (M ALPHA DOT)";
    : POKE 36,45
    : PRINT C(93)
---------------------
850   POKE 36,15
    : PRINT "MQ";
    : POKE 36,45
    : PRINT C(82)
---------------------
860   POKE 36,15
    : PRINT "MDE (M DELTA ELEVATOR)";
    : POKE 36,45
    : PRINT C(79)
---------------------
870   POKE 36,15
    : PRINT "MDT (M DELTA THROTTLE)";
    : POKE 36,45
    : PRINT C(92)
---------------------
880   PRINT CHR$ (12)
---------------------
890   PRINT D$
    : PRINT D$;"PR#0"
    : PRINT D$;"IN#0"
---------------------
900   INPUT "ANOTHER CONDITION (Y/N)? ";A$
---------------------
910   IF A$ = "Y" THEN 250
---------------------
920   GOTO 90
---------------------
930   PRINT
    : PRINT
    : PRINT
    : PRINT
    : PRINT
---------------------
940   IF Z = 2 THEN POKE 36,50
  * : PRINT "DIMENSIONAL STABILITY AND CONTROL DERIVATIVE
      S"
  * : PRINT
  * : PRINT
```

```
950   IF Z = 2 THEN 970
960   POKE 36,50
    : PRINT "NON DIMENSIONAL STABILITY AND CONTROL DERIVA
        TIVES"
    : PRINT
    : PRINT
970   POKE 36,15
    : PRINT "   ALTITUDE : ";C(0)
980   POKE 36,15
    : PRINT "       MACH : ";C(1)
990   POKE 36,15
    : PRINT "     WEIGHT : ";C(9)
1000  POKE 36,15
    : PRINT "         CG : ";C(8)
1010  POKE 36,15
    : PRINT "LOAD FACTOR : ";AN
    : PRINT
    : PRINT
1020  POKE 36,40
    : PRINT "LONGITUDINAL";
    : POKE 36,100
    : PRINT "LATERAL-DIRECTIONAL"
1030  RETURN
1040  INPUT "ENTER LOAD FACTOR -->";AN
1050  PRINT D$
    : PRINT D$;"OPEN A7-D,L20,D2"
1060  PRINT D$;"READ A7-D,R";998
    : INPUT N2
1070  PRINT D$;"READ A7-D,R";999
    : INPUT S
1080  PRINT D$;"READ A7-D,R";1000
    : INPUT N3
1090  PRINT D$;"CLOSE A7-D"
1100  R = 0
    : FOR I = 1 TO N2 STEP S
    :   R = R + 1
1110    IF AN = I THEN B = R
1120  NEXT
1130  N4 = N3 / 13
1140  N5 = 1000 + N3 - N4 * 2
```

```
--------------------
1150  PRINT
    : PRINT
--------------------
1160  PRINT D$
    : PRINT D$;"PR#1"
    : PRINT CHR$ (15)
--------------------
1170  PRINT D$;"OPEN A7-D,L20,D2"
--------------------
1180  R = 901
    : FOR J = 1 TO N4
    :   PRINT D$;"READ A7-D,R";R
    :   INPUT BE(J)
    :   R = R + 3
    : NEXT
--------------------
1190  R = 902
    : FOR J = 1 TO N4
    :   PRINT D$;"READ A7-D,R";R
    :   INPUT DR(J)
    :   R = R + 3
    : NEXT
--------------------
1200  R = 903
    : FOR J = 1 TO N4
    :   PRINT D$;"READ A7-D,R";R
    :   INPUT DA(J)
    :   R = R + 3
    : NEXT
--------------------
1210  R = 1001
    : FOR J = 1 TO N4
    :   PRINT D$;"READ A7-D,R";R
    :   INPUT AN(J)
    :   R = R + 1
    : NEXT
--------------------
1220  R = R + 2 * N4
    : FOR J = 1 TO N4
    :   PRINT D$;"READ A7-D,R";R
    :   INPUT DS(J)
    :   R = R + 1
    : NEXT
--------------------
1230  FOR J = 1 TO N4
    :   PRINT D$;"READ A7-D,R";R
    :   INPUT F(J)
    :   R = R + 1
    : NEXT
--------------------
1240  FOR J = 1 TO N4
    :   PRINT D$;"READ A7-D,R";R
    :   INPUT NB(J)
    :   R = R + 1
    : NEXT
--------------------
1250  R = R + N4
    : FOR J = 1 TO N4
    :   PRINT D$;"READ A7-D,R";R
```

```
    :   INPUT PE(J)
    :   R = R + 1
    : NEXT
--------------------
1260  FOR J = 1 TO N4
    :   PRINT D$;"READ A7-D,R";R
    :   INPUT QE(J)
    :   R = R + 1
    : NEXT
--------------------
1270  FOR J = 1 TO N4
    :   PRINT D$;"READ A7-D,R";R
    :   INPUT RE(J)
    :   R = R + 1
    : NEXT
--------------------
1280  FOR J = 1 TO N4
    :   PRINT D$;"READ A7-D,R";R
    :   INPUT AE(J)
    :   R = R + 1
    : NEXT
--------------------
1290  PRINT D$;"READ A7-D,R";0
    : INPUT H
--------------------
1300  PRINT D$;"READ A7-D,R";1
    : INPUT IMN
--------------------
1310  PRINT D$;"READ A7-D,R";58
    : INPUT IT
    : PRINT D$;"CLOSE A7-D"
--------------------
1320  DR = 57.29577951
--------------------
1330  Z1 = 1000
--------------------
1340  FOR J = 1 TO N4
--------------------
1350    BE(J) = BE(J) * DR
--------------------
1360    BE(J) = FN R(BE(J))
--------------------
1370    DR(J) = DR(J) * DR
--------------------
1380    DR(J) = FN R(DR(J))
--------------------
1390    DA(J) = DA(J) * DR
--------------------
1400    DA(J) = FN R(DA(J))
--------------------
1410    F(J) = F(J) * DR
--------------------
1420    F(J) = FN R(F(J))
--------------------
1430    NB(J) = FN R(NB(J))
--------------------
1440    PE(J) = PE(J) * DR
--------------------
1450    PE(J) = FN R(PE(J))
--------------------
```

```
1460    QE(J) = QE(J) * DR
--------------------
1470    QE(J) = FN R(QE(J))
--------------------
1480    RE(J) = RE(J) * DR
--------------------
1490    RE(J) = FN R(RE(J))
--------------------
1500    AE(J) = AE(J) * DR
--------------------
1510    AE(J) = FN R(AE(J))
--------------------
1520    DS(J) = (DS(J) + IT) * DR
--------------------
1530    DS(J) = FN R(DS(J))
--------------------
1540  NEXT
--------------------
1550  POKE 36,23
    : PRINT "ALTITUDE: ";H
--------------------
1560  POKE 36,23
    : PRINT "    MACH: ";IMN
--------------------
1570  PRINT
    : PRINT
    : POKE 36,23
    : PRINT "BODY AXIS EQUILIBRIUM VALUES"
    : PRINT
    : PRINT
--------------------
1580  POKE 36,24
    : PRINT "LOAD";
    : POKE 36,34
    : PRINT "ANGLE OF";
    : POKE 36,46
    : PRINT "SIDESLIP";
    : POKE 36,58
    : PRINT "BANK";
    : POKE 36,69
    : PRINT "ROLL";
    : POKE 36,79
    : PRINT "PITCH";
    : POKE 36,91
    : PRINT "YAW";
    : POKE 36,101
    : PRINT "ELEVATOR";
    : POKE 36,115
    : PRINT "RUDDER";
--------------------
1590  POKE 36,128
    : PRINT "AILERON"
--------------------
1600  POKE 36,23
    : PRINT "FACTOR";
    : POKE 36,35
    : PRINT "ATTACK";
    : POKE 36,47
    : PRINT "ANGLE";
    : POKE 36,58
```

```
     : PRINT "ANGLE";
     : POKE 36,69
     : PRINT "RATE";
     : POKE 36,79
     : PRINT "RATE";
     : POKE 36,91
     : PRINT "RATE";
     : POKE 36,100
     : PRINT "DEFLECTION";
---------------------
1610  POKE 36,114
     : PRINT "DEFLECTION";
     : POKE 36,127
     : PRINT "DEFLECTION"
---------------------
1620  POKE 36,25
     : PRINT "(G)";
     : POKE 36,35
     : PRINT "(DEG)";
     : POKE 36,47
     : PRINT "(DEG)";
     : POKE 36,58
     : PRINT "(DEG)";
     : POKE 36,67
     : PRINT "(DEG/SEC)";
     : POKE 36,77
     : PRINT "(DEG/SEC)";
     : POKE 36,89
     : PRINT "(DEG/SEC)";
     : POKE 36,102
     : PRINT "(DEG)";
---------------------
1630  POKE 36,116
     : PRINT "(DEG)";
     : POKE 36,129
     : PRINT "(DEG)"
---------------------
1640  PRINT
     : PRINT
---------------------
1650  FOR J = 1 TO N4
---------------------
1660     POKE 36,25
     :   PRINT AN(J);
     :   POKE 36,35
     :   PRINT AE(J);
     :   POKE 36,47
     :   PRINT BE(J);
     :   POKE 36,58
     :   PRINT F(J);
     :   POKE 36,69
     :   PRINT PE(J);
     :   POKE 36,79
     :   PRINT QE(J);
     :   POKE 36,91
     :   PRINT RE(J);
     :   POKE 36,102
     :   PRINT DS(J);
     :   POKE 36,116
     :   PRINT DR(J);
```

```
1670    POKE 36,129
    :   PRINT DA(J)
1680  NEXT
1690  PRINT
    : PRINT
    : POKE 36,23
    : PRINT "NOTE: LOAD FACTOR IS IN STABILITY AXES"
1700  PRINT D$
    : PRINT D$;"PR#0"
    : PRINT D$;"IN#0"
1710  PRINT
    : INPUT "ANOTHER CONDITION (Y/N)? ";A$
    : IF A$ = "Y" THEN 1040
1720  GOTO 90
1730  END
1740  PRINT
    : INPUT "STORAGE RECORD YOU WANT TO START AT";R
1750  INPUT "ENTER THE ORDER OF DESIRED AMAT --> ";N
1760  Z1 = 100000
1770  GOTO 210
1780  PRINT D$
    : PRINT D$;"PR#1"
    : PRINT CHR$ (15)
    : PRINT CHR$ (12)
1790  PRINT D$;"OPEN A7-D,L20,D2"
1800  FOR I = 1 TO N
1810    FOR J = 1 TO N
1820      PRINT D$;"READ A7-D,R";R
    :     INPUT A(I,J)
    :     R = R + 1
    :   NEXT
    : NEXT
1830  FOR I = 1 TO N
1840    FOR J = 1 TO 3
1850      PRINT D$;"READ A7-D,R";R
    :     INPUT B(I,J)
    :     R = R + 1
    :   NEXT
    : NEXT
1860  PRINT D$;"CLOSE A7-D"
```

```
1870  PRINT
    : PRINT
    : PRINT
    : PRINT
    : PRINT
    : PRINT
1880  POKE 36,15
    : PRINT "   ALTITUDE : ";C(0)
1890  POKE 36,15
    : PRINT "       MACH : ";C(1)
1900  POKE 36,15
    : PRINT "     WEIGHT : ";C(9)
1910  POKE 36,15
    : PRINT "         CG : ";C(8)
1920  POKE 36,15
    : PRINT "LOAD FACTOR : ";AN
1930  PRINT
    : PRINT
1940  POKE 36,6 * N
    : PRINT "A-MATRIX"
    : PRINT
    : PRINT
1950  I = 1
1960  FOR J = 1 TO N
1970    AM(I,J) = FN R(A(I,J))
1980    POKE 36,12 * J
    :   PRINT AM(I,J);
    : NEXT
1990  PRINT
2000  IF I = N THEN PRINT
  * : PRINT
  * : GOTO 2020
2010  I = I + 1
    : GOTO 1960
2020  POKE 36,24
    : PRINT "B-MATRIX"
    : PRINT
    : PRINT
2030  I = 1
2040  FOR J = 1 TO 3
2050    BM(I,J) = FN R(B(I,J))
```

```
2060     POKE 36,12 * J
     :   PRINT BM$(I,J);
     : NEXT
2070  PRINT
2080  IF I = N THEN PRINT
   * : PRINT
   * : GOTO 2100
2090  I = I + 1
     : GOTO 2040
2100  PRINT D$
     : PRINT D$;"PR#0"
     : PRINT D$;"IN#0"
2110  INPUT "ANOTHER CONDITION (Y/N)? ";A$
     : IF A$ = "Y" THEN 1740
2120  GOTO 90
2130  END
```

Eigenvector

This program uses the numerator method to compute eigenvectors from transfer functions. The magnitude and phase angle of each component of the eigenvectors are also computed.

EIGENVECTOR

```
1     D$ = CHR$ (4)
2     HOME
    : PRINT CHR$ (12)
    : PRINT
10    REM  CALCULATES EIGENVECTORS USING NUMERATOR METHOD
20    REM
30    REM  BY JEFFREY R. RIEMER
40    REM  26 DECEMBER 1983
50    D$ = CHR$ (4)
    : REM  CTRL-D
60    PRINT D$;"PR#3"
70    PRINT CHR$ (12)
    : PRINT
80    INPUT "ENTER SYSTEM ORDER --> ";N
90    DIM RE(N,15),IM(N,15),Z(N + 1),G(N + 1),GK(N + 1),AR
        (N,N),AI(N,N),ER(N,N),EI(N,N)
91    B = 1
100   PRINT
110   PRINT "ENTER THE VALUE OF THE ROOT BEING USED TO EVA
        LUATE THE NUMERATORS"
120   PRINT
    : PRINT "REAL,IMAGINARY  ";
130   INPUT RE(0,0),IM(0,0)
140   PRINT
145   IF Q = 1 THEN GOTO 1100
150   PRINT "ENTER THE NUMBER OF THE NUMERATOR BEING EVALU
        ATED"
160   PRINT
    : PRINT "NUMERATOR NUMBER  ";
170   INPUT G(B)
175   G = G(B)
176   P = G
180   PRINT
```

```
131   PRINT "ENTER THE NUMERATOR GAIN"
----------
182   PRINT
    : PRINT "NUMERATOR GAIN  ";
----------
183   INPUT GK(B)
    : PRINT
----------
185   GK = GK(B)
----------
190   PRINT "ENTER THE NUMBER OF ZEROES IN THIS NUMERATOR"
----------
195   PRINT
    : PRINT "HOW MANY ZEROES  ";
----------
200   INPUT Z(B)
----------
210   PRINT
    : PRINT "ENTER THE VALUE OF EACH ZERO"
----------
220   PRINT
    : PRINT "          REAL, IMAGINARY"
----------
230   PRINT
----------
240   FOR I = 1 TO Z(B)
----------
250     PRINT "  Z(";G;",";I;")= ";
----------
260     INPUT RE(G,I),IM(G,I)
----------
270   NEXT
----------
280   PRINT
----------
290   INPUT "ARE ALL ENTRIES CORRECT (Y/N)? ";A$
----------
300   IF A$ = "N" THEN 210
----------
305   MR = 1
    : MI = 0
----------
310   GOSUB 2000
----------
417   PRINT
----------
420   INPUT "DO YOU WANT TO EVALUATE ANOTHER NUMERATOR (Y/
        N)?  ";A$
----------
430   IF A$ = "N" THEN 999
----------
435   PRINT
----------
440   INPUT "DO YOU WANT TO USE THE SAME ROOT (Y/N)?  ";A$
----------
450   IF A$ = "N" THEN 470
----------
460   B = B + 1
    : GOTO 150
----------
```

```
470   GOSUB 1000
---------------------
480   GOTO 110
---------------------
999   GOSUB 1000
    : END
---------------------
1000  PRINT
    : PRINT
---------------------
1005  INPUT "WHICH MODE IS THIS EIGENVECTOR FOR?  ";B$
    : PRINT
---------------------
1006  PRINT D$;"PR#5"
---------------------
1010  PRINT "THE EIGENVECTOR FOR THE ";B$;" MODE"
    : PRINT
---------------------
1020  PRINT "ELEMENT";
    : POKE 36,15
    : PRINT "REAL";
    : POKE 36,30
    : PRINT "IMAGINARY"
---------------------
1030  PRINT
---------------------
1040  FOR I = 1 TO N
---------------------
1050     PRINT "    ";I;
    :    POKE 36,15
    :    PRINT "(";ER(1,I);")";
    :    POKE 36,27
    :    PRINT "+ J(";EI(1,I);")"
---------------------
1060  NEXT
---------------------
1061  PRINT D$;"PR#3"
---------------------
1062  Q = 1
    : PRINT
---------------------
1063  RETURN
---------------------
1065  PRINT
---------------------
1070  END
---------------------
1100  REM
---------------------
1105  FOR B = 1 TO P
---------------------
1106     MR = 1
    :    MI = 0
---------------------
1110     G = G(B)
    :    GK = GK(B)
---------------------
1120     GOSUB 2000
---------------------
1140  NEXT
```

```
1145  GOSUB 1000
1146  INPUT "DO YOU WANT TO EVALUATE ANOTHER ROOT?  ";A$
1147  IF A$ = "N" THEN END
1148  GOTO 110
1150  END
2000  REM  COMPLEX ALGEBRA
2010  FOR I = 1 TO Z(B)
2020     AR(G,I) = RE(0,0) - RE(G,I)
2030     AI(G,I) = IM(0,0) - IM(G,I)
2040     NR = MR * AR(G,I) - MI * AI(G,I)
2050     NI = MR * AI(G,I) + MI * AR(G,I)
2060     MR = NR
2070     MI = NI
2080  NEXT
2090  ER(1,G) = MR * GK
2100  EI(1,G) = MI * GK
2110  RETURN
```

Other Programs

The other programs were used to support this thesis. A fortran program to obtain eigenvectors using the IMSL routine EIGFR [Ref 13]. The program used to obtain the transfer functions was "Control" [Ref 6].

Appendix E

General Aircraft Information

Table E1

GENERAL AIRCRAFT INFORMATION

The dimension and design data were extracted from LTV Report No. 253320/8R-8089.

GENERAL DIMENSIONS

Length (not including test boom)	46.18 ft
Height over highest part of tail (static)	16.06 ft
Wing:	
Area	375 ft^2
Span	38.73 ft
Span, wings folded	23.77 ft
Aspect ratio	4.0
Taper ratio	0.25
Sweep of 1/4 chord	35 deg
Geometric twist	0 deg
Dihedral	-5 deg
Incidence	-1 deg
Root chord	15.49 ft
Tip chord	3.87 ft
Mean geometric chord length[1]	10.84 ft
Trailing Edge Flaps:	
Type	Single slotted
Area, each	21.74 ft^2

[1]Mean geometric chord (MGC) and mean aerodynamic chord (MAC) are used interchangeably.

Maximum deflection	40 deg
Chord	22.55-pct wing chord
Leading Edge Flaps:	
Area	
Inboard sections	18.36 ft^2
Outboard sections	18.88 ft^2
Chord	
Inboard section	1.01 ft
Outboard section	8-pct MAC
Ailerons:	
Type	Plain sealed
Spanwise range (inboard/outboard)	59.69 to 90.34 pct semispan
Chord	25-pct wing chord
Area, total	19.94 ft^2
Deflections	±25 deg
Spoilers:	
Spanwise range	28.94 to 43.46 pct semispan
Chord (inboard/outboard)	0.839/0.804 ft
Area (both sides)	4.60 ft^2
Deflection	60 deg TEU
Vertical Stabilizer, Not Including Dorsal:	
Area (root chord at WL 97)	115.2 ft^2
Span	12.86 ft
Mean geometric chord length	10.20 ft

Tail Length (25-pct wing MGC to 25-pct tail MGC)	13.49 ft
Rudder:	
Type	Plain sealed
Area	15.04 ft^2
Deflections	
Flaps up	±6 deg
Flaps down	±24 deg
Horizontal Stabilizer:	
Area (including 37.56 ft^2 in fuselage)	93.75 ft^2
Span	18.14 ft
Aspect ratio	3.50
Taper ratio	0.148
Sweepback of 1/4 chord	45 deg
Dihedral	5.42 deg
Mean geometric chord length	6.12 ft
Tail length (25-pct wing MGC to 25-pct tail MGC)	16.18 ft
Deflections	
TEU	26.5 deg
TED	6.75 deg
Speed Brake:	
Hinge point	Fuselage station 368.0 Waterline 58.25
Area	25 ft^2
Deflection	60 deg

Fuselage:

Length	46.18 ft
Max cross-sectional area	30.81 ft^2
Outside height	7.20 ft
Outside width	4.88 ft

Store Stations:

Number	Fuselage Station*	Baseline*	Capacity (lb)	Wet
1 & 8	473.3	136.6	3,500	Yes
2 & 7	443.5	97.2	3,500	No
3 & 6	434.4	61.2	2,500	Yes
4 & 5	384.2	40.4	500	No

*Fuselage station and baseline are at cg of Mark 29 IC Sidewinder missile.

Table E2

PARAMETER RANGE AND RESOLUTION

Parameters Recorded on Magnetic Tape	Range	Resolution
Angle of attack - nose boom vane (deg)	-10 to +30	.039
Angle of sideslip - nose boom vane (deg)	±20	.039
Roll attitude (deg)	±175	.342
Pitch attitude (deg)	±85	.166
Roll rate (deg/sec)	±250	.488
Pitch rate (deg/sec)	±60	.117
Yaw rate (deg/sec)	±20	.039
Normal acceleration - cg (g)	- 5 to +10	.015
Longitudinal stock force (lb)	±60	.117
Lateral stick force (lb)	±40	.078
Rudder pedal force (lb)	0 to ±200	.39
Rudder position (deg)	±25	.049
Aileron position (deg)	±26	.051
Unit horizontal tail position (deg)	27 TEU 7 TED	.033
Event mark		

Parameters Displayed in Cockpit (Flight Test)	Range
Airspeed - nose boom (kt)	40 to 650
Altitude - nose boom (ft)	0 to 50,000
Machmeter - nose boom	0.5 to 1.5
Engine high pressure rotor speed (rpm)	0 to 110 pct
Normal acceleration - cockpit (g)	-5 to +10
Speed brake position (deg)	0 to 60
Time correlation counter	- - -
Maneuver light	- - -
Calibrate light	- - -
Tape record light	- - -

Appendix F

Bode Plots

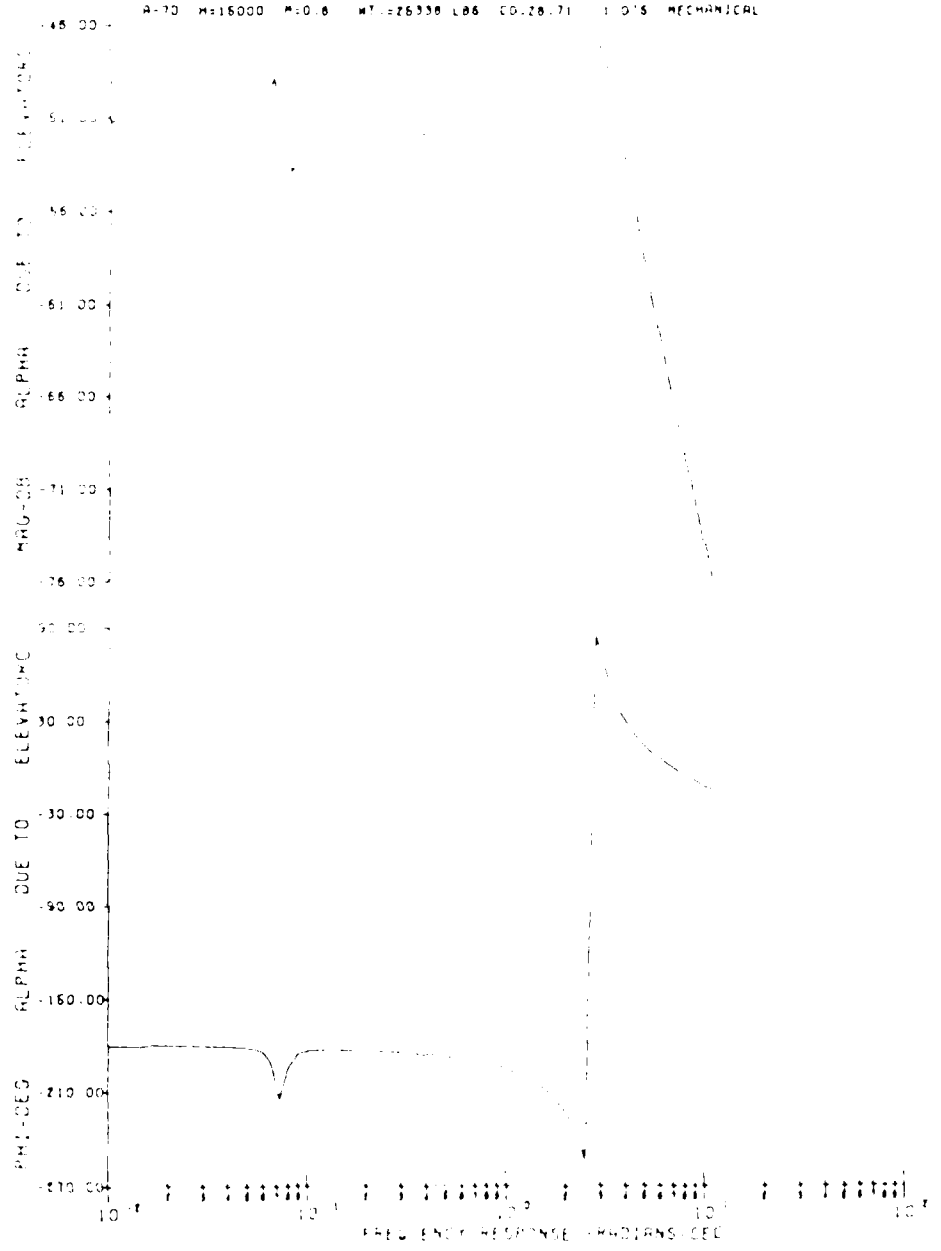

Figure 51. IG Mechanical Code Plot for Alpha due to Pilot Elevator Input

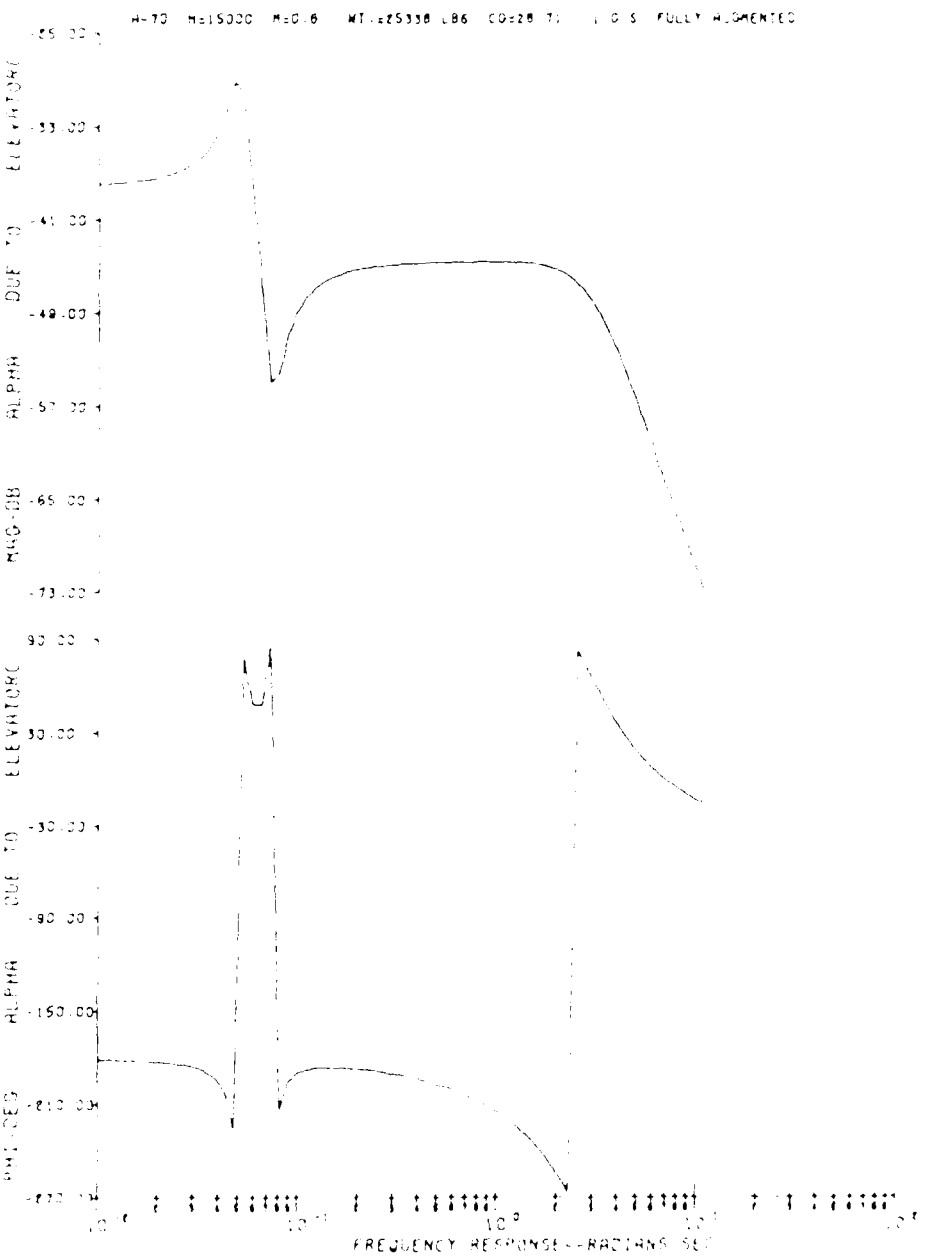

Figure F2. IG Fully Augmented Bode Plot for Alpha due to Pilot Elevator Input

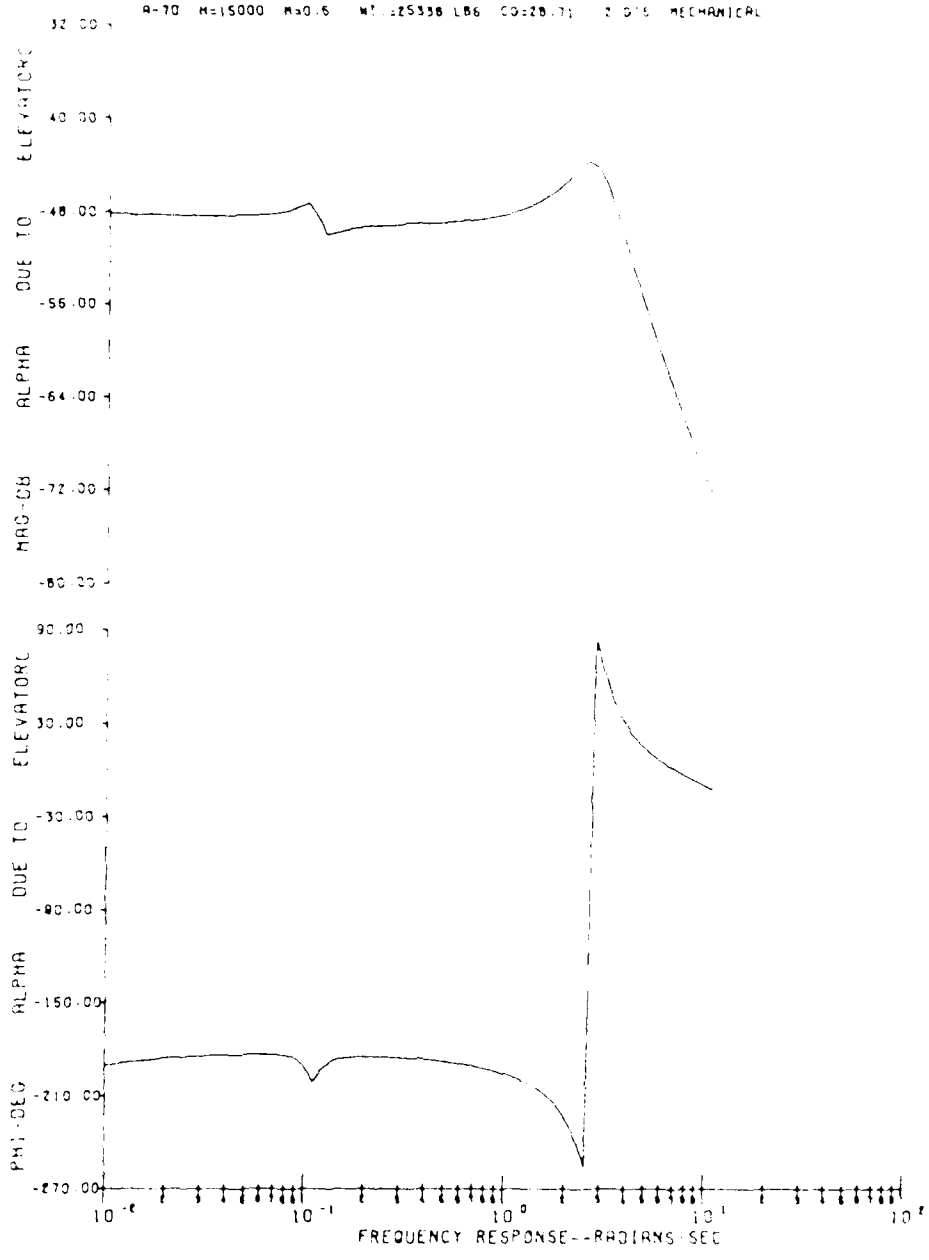

Figure F3. 2G Mechanical Bode Plot for Alpha due to Pilot Elevator Input

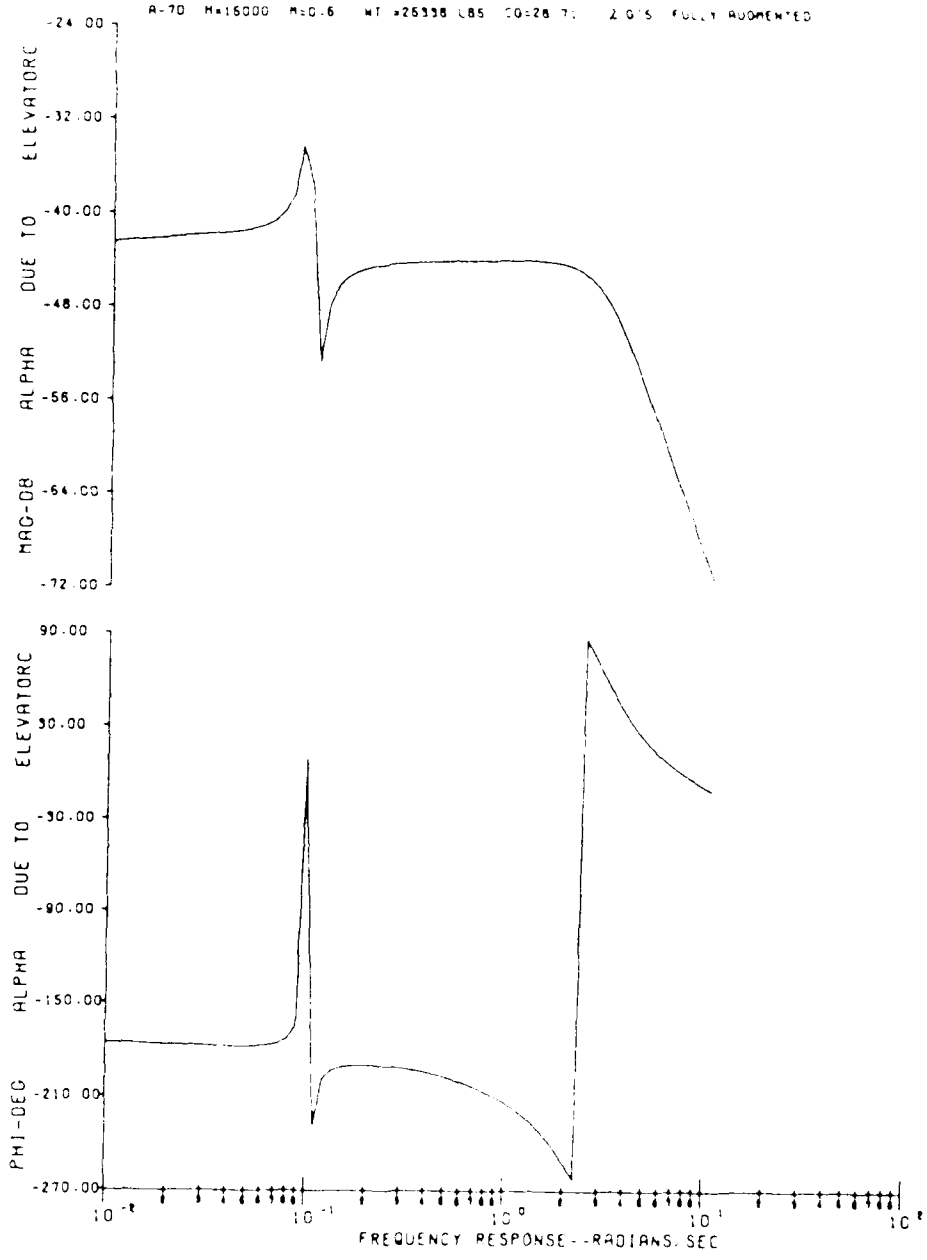

Figure F4. 2G Fully Augmented Bode Plot for Alpha due to Pilot Elevator Input

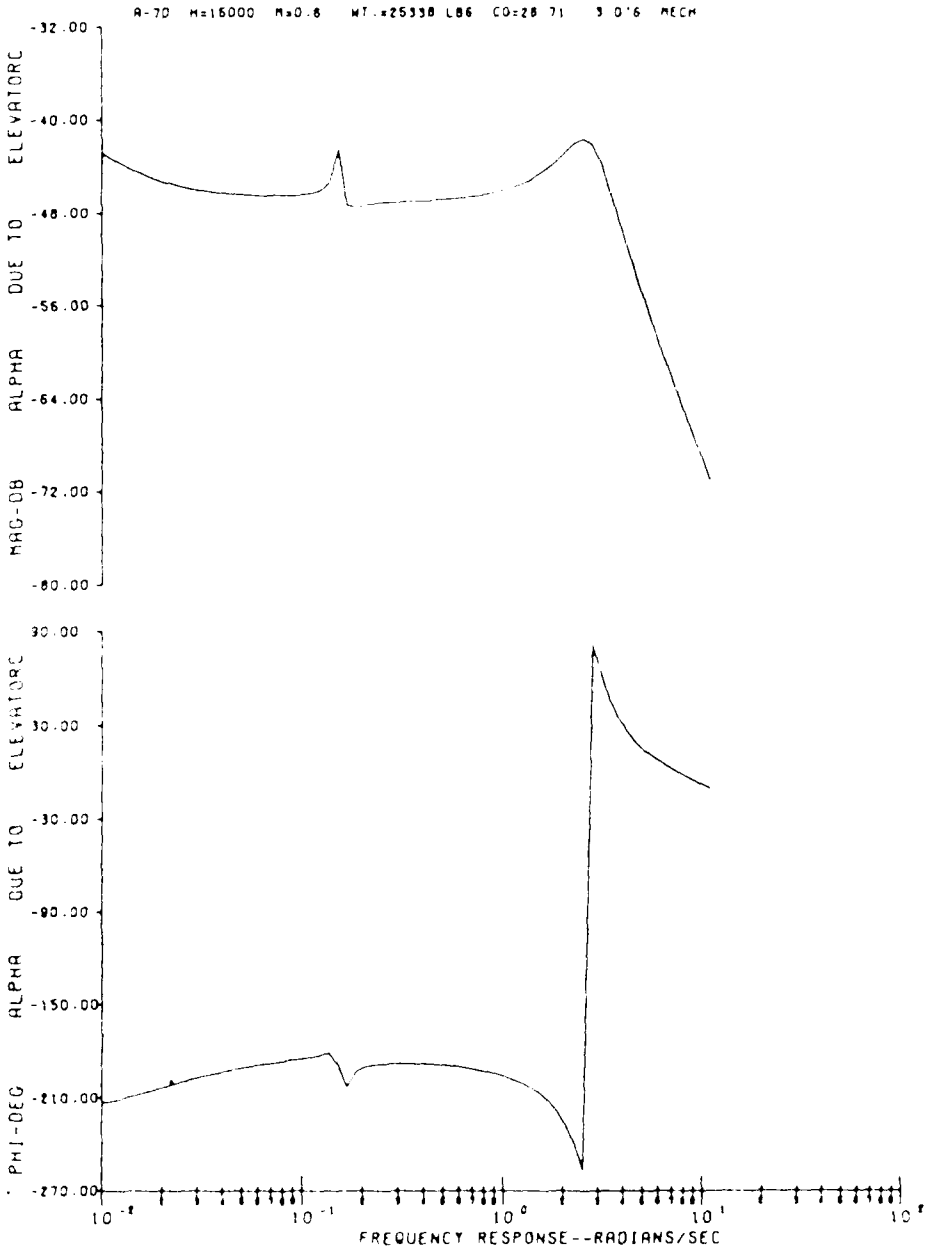

Figure F5. 3G Mechanical Bode Plot for Alpha due to Pilot Elevator Input

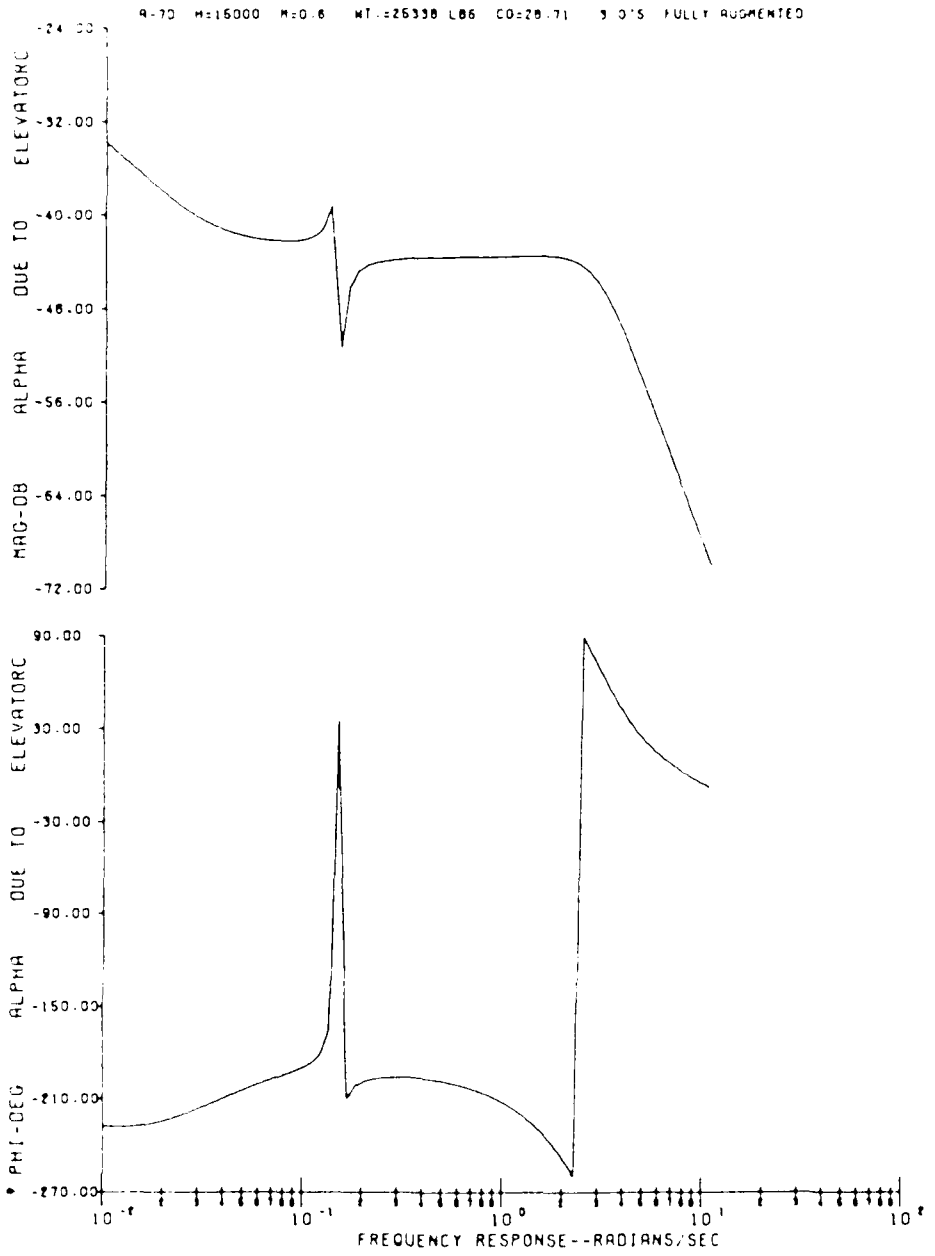

Figure F6. 3G Fully Augmented Bode Plot for Alpha due to Pilot Elevator Input

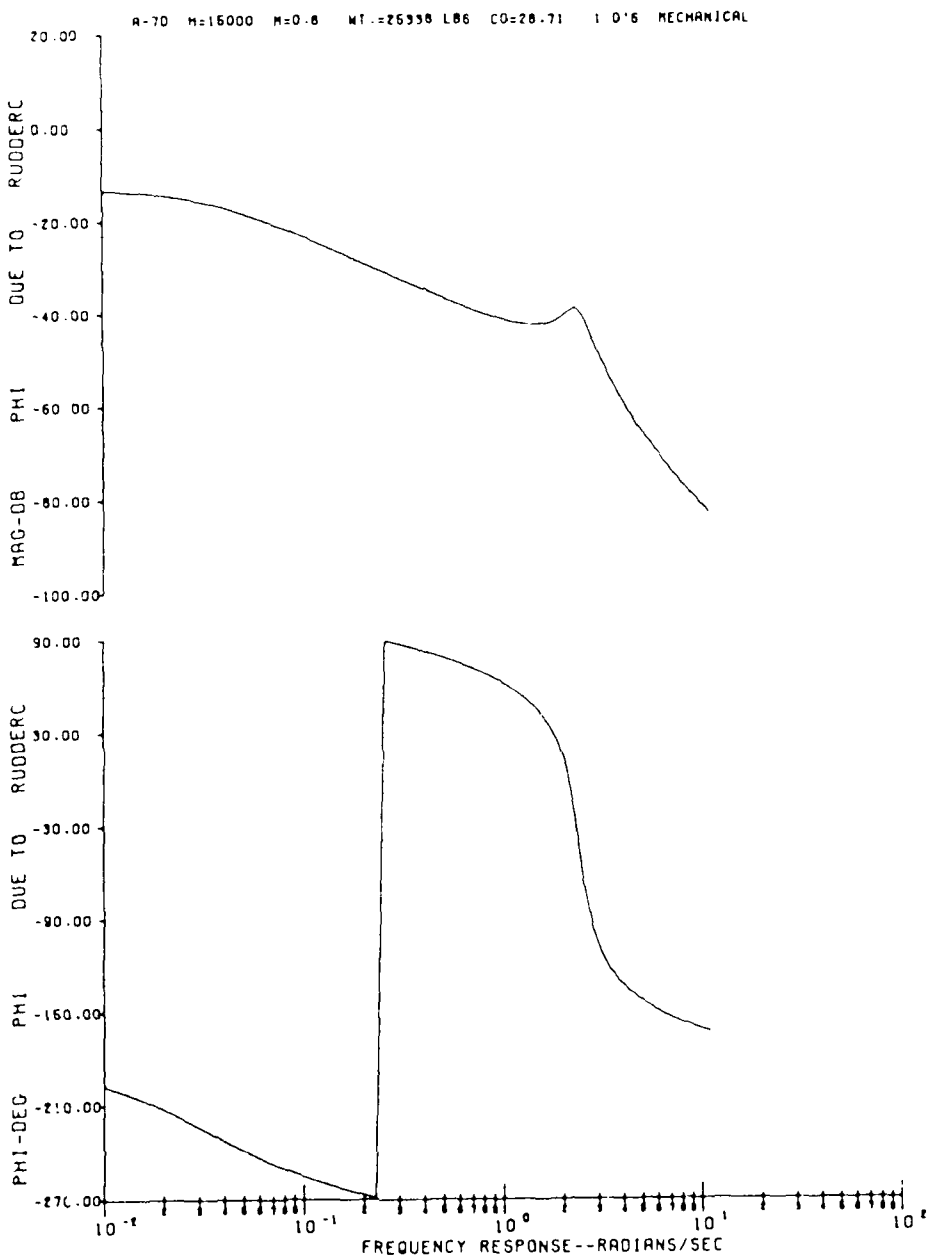

Figure F7. 1G Mechanical Bode Plot for Phi due to Pilot Rudder Input

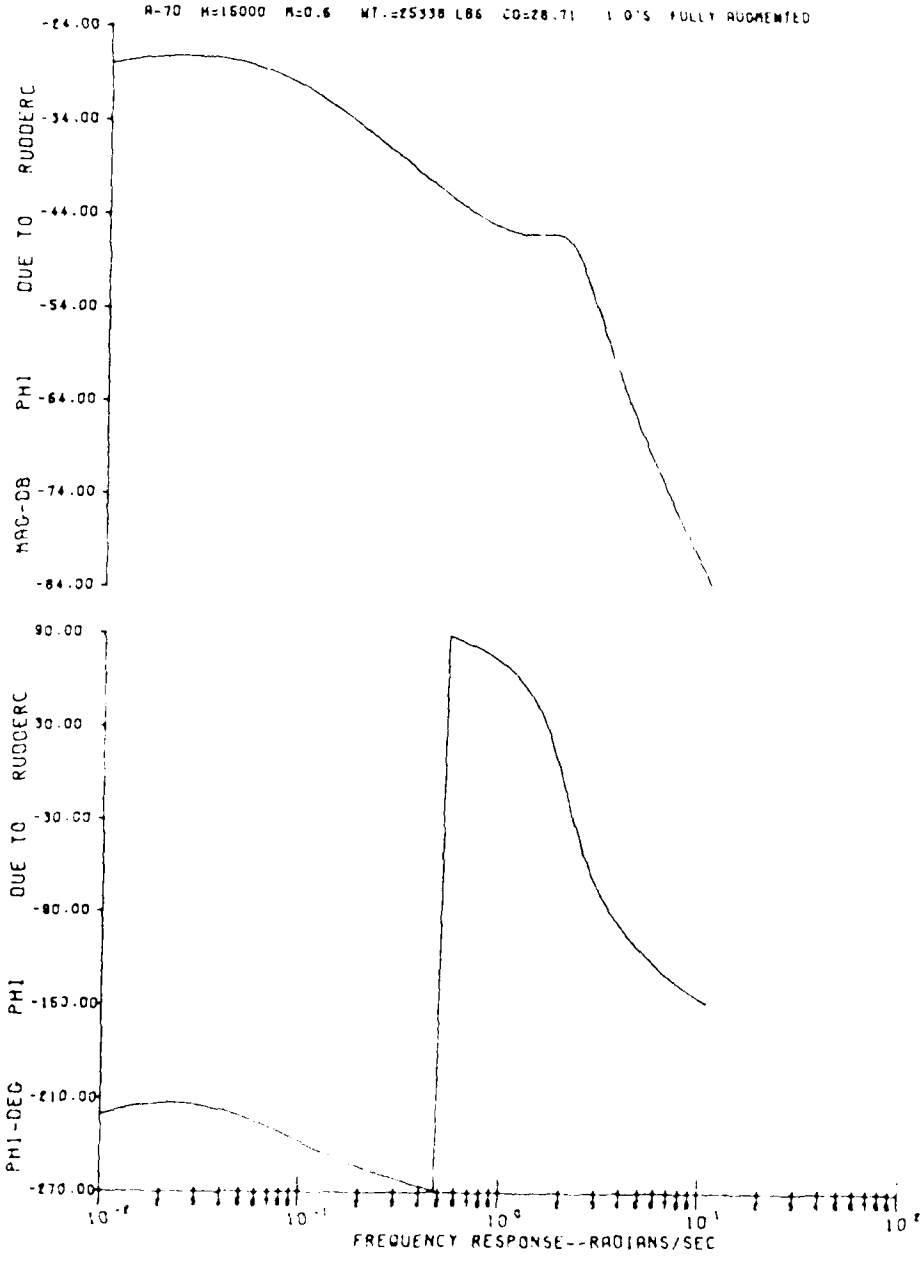

Figure F8. 1G Fully Augmented Bode Plot for Phi due to Pilot Rudder Input

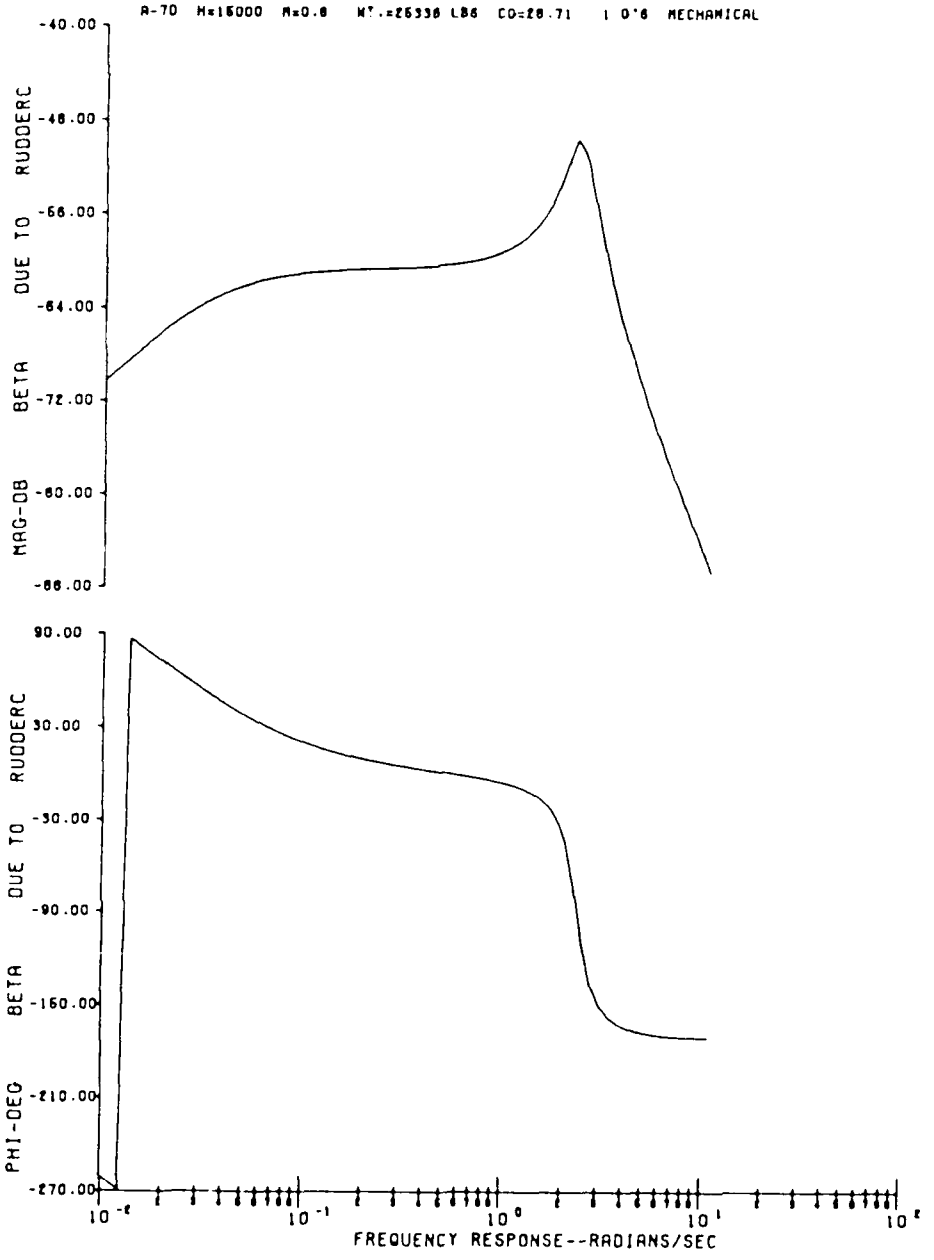

Figure F9. 1G Mechanical Bode Plot for Beta due to Pilot Rudder Input

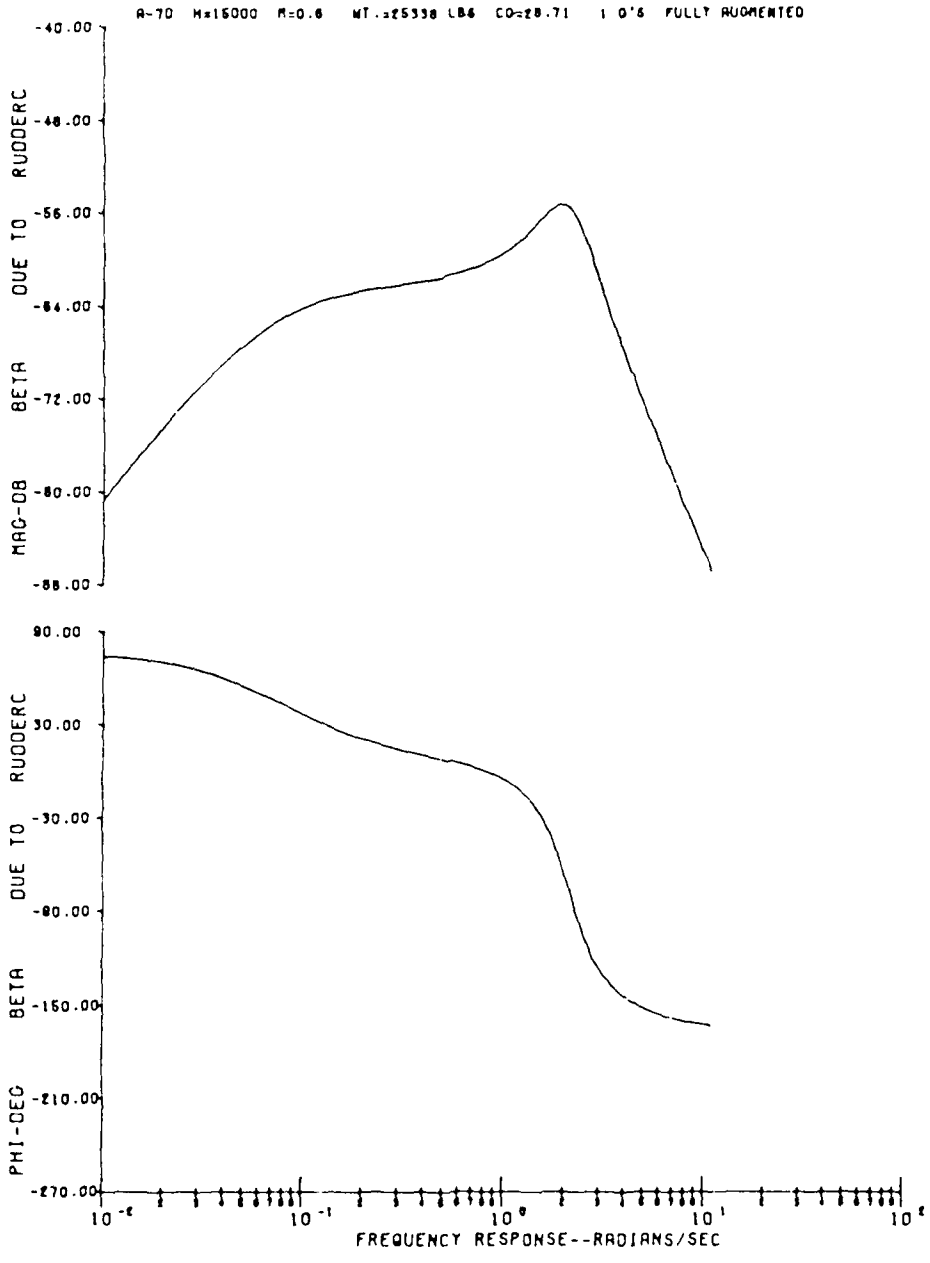

Figure F10. 1G Fully Augmented Bode Plot for Beta due to Pilot Rudder Input

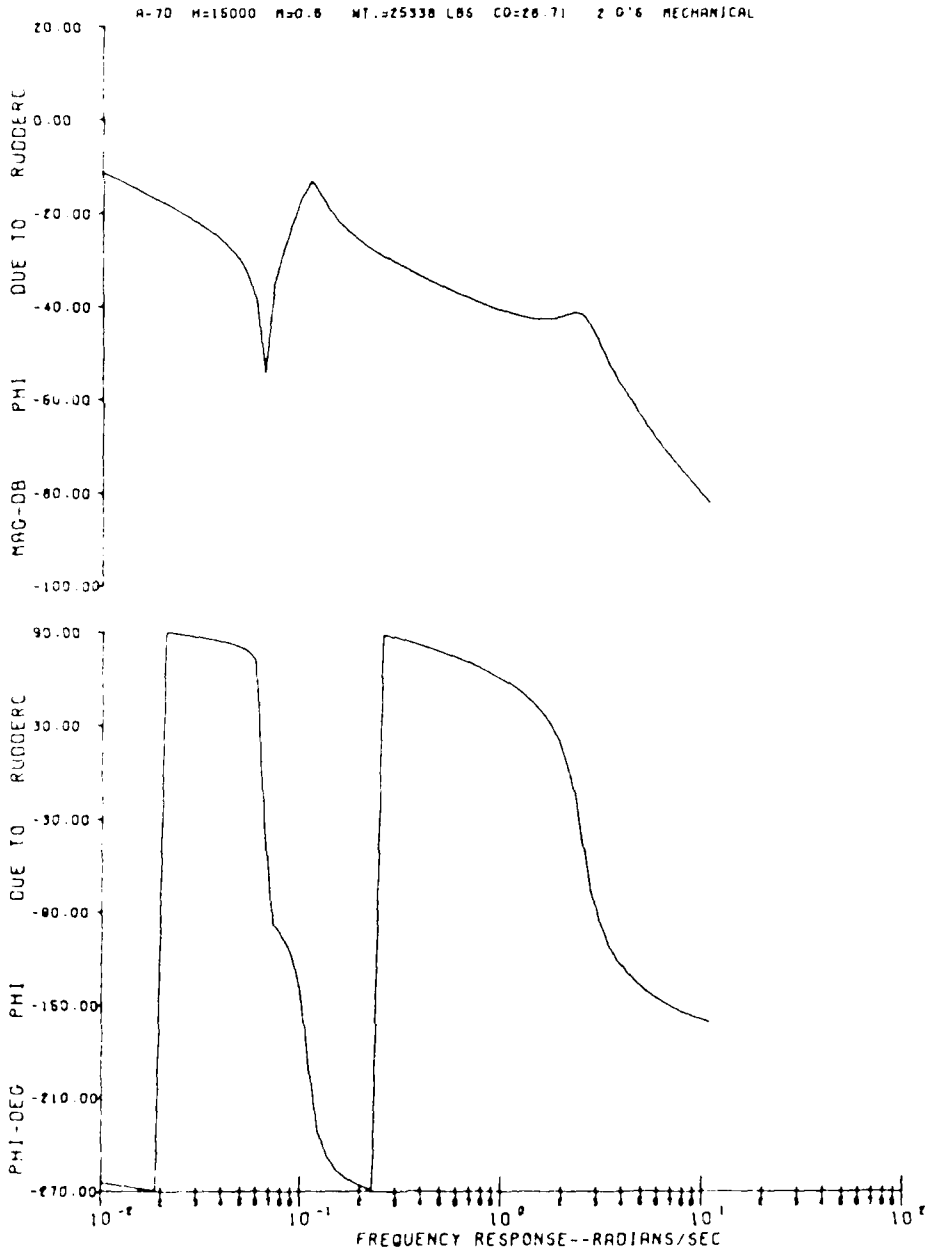

Figure F11. 2G Mechanical Bode Plot for Phi due to Pilot Rudder Input

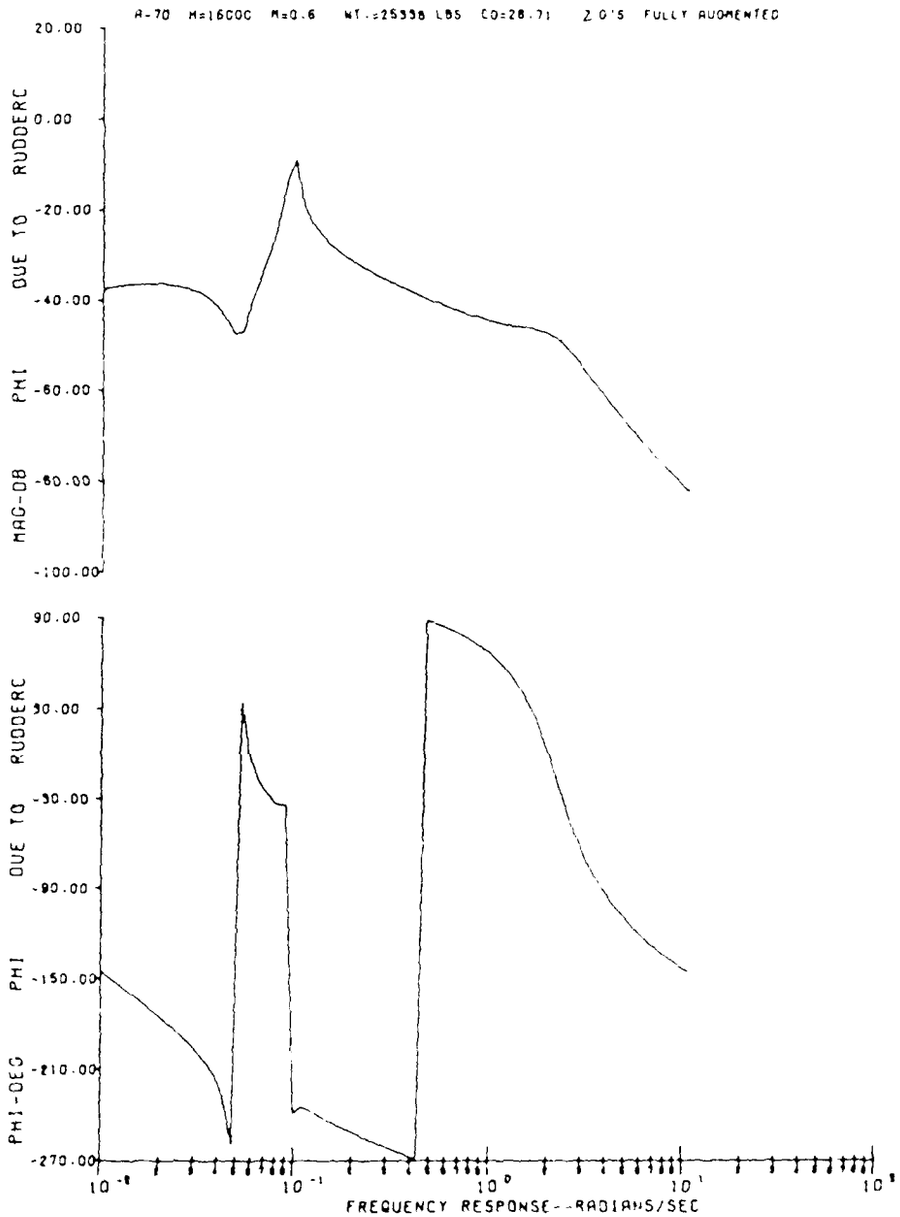

Figure F12. 2G Fully Augmented Bode Plot for Phi due to Pilot Rudder Input

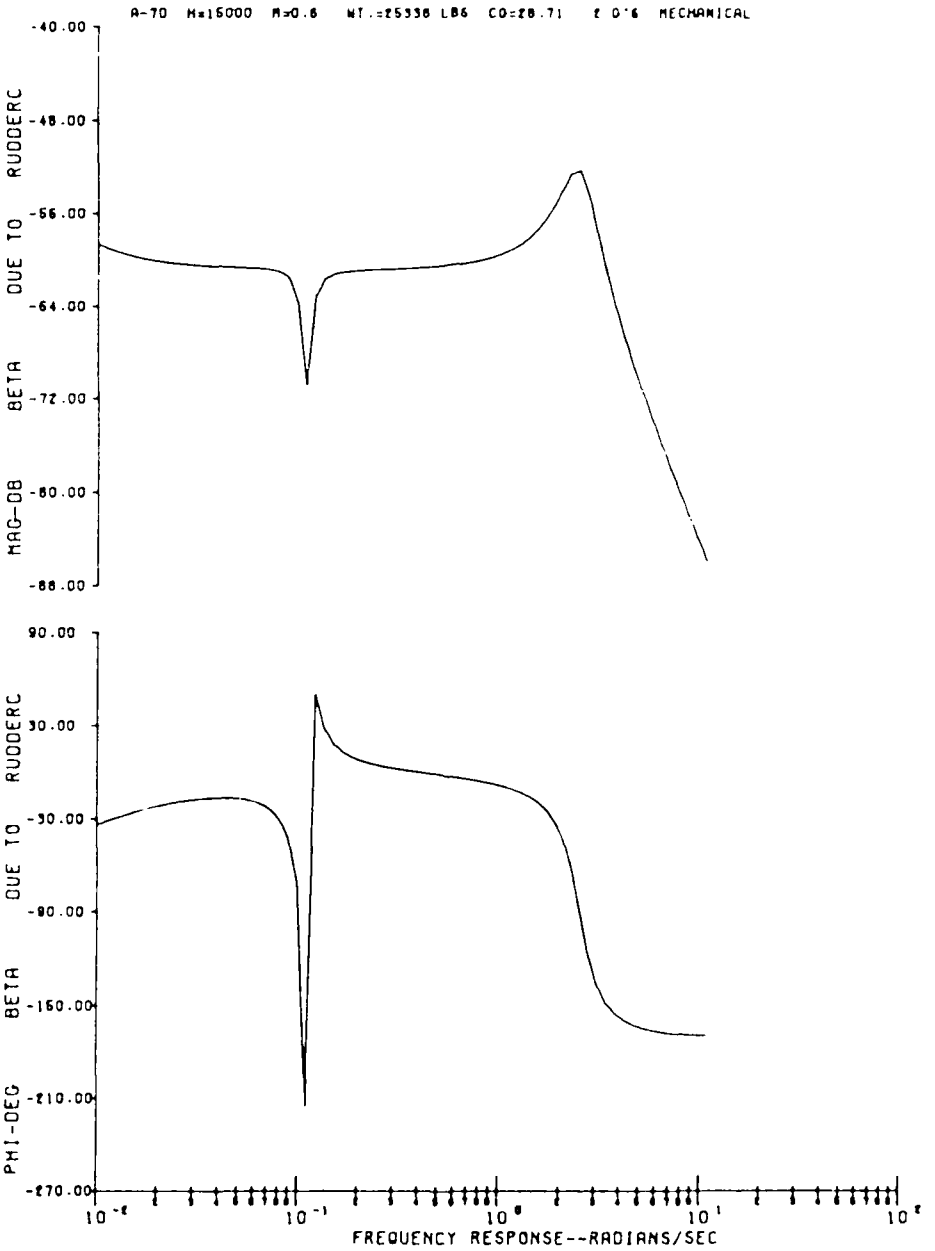

Figure F13. 2G Mechanical Bode Plot for Beta due to Pilot Rudder Input

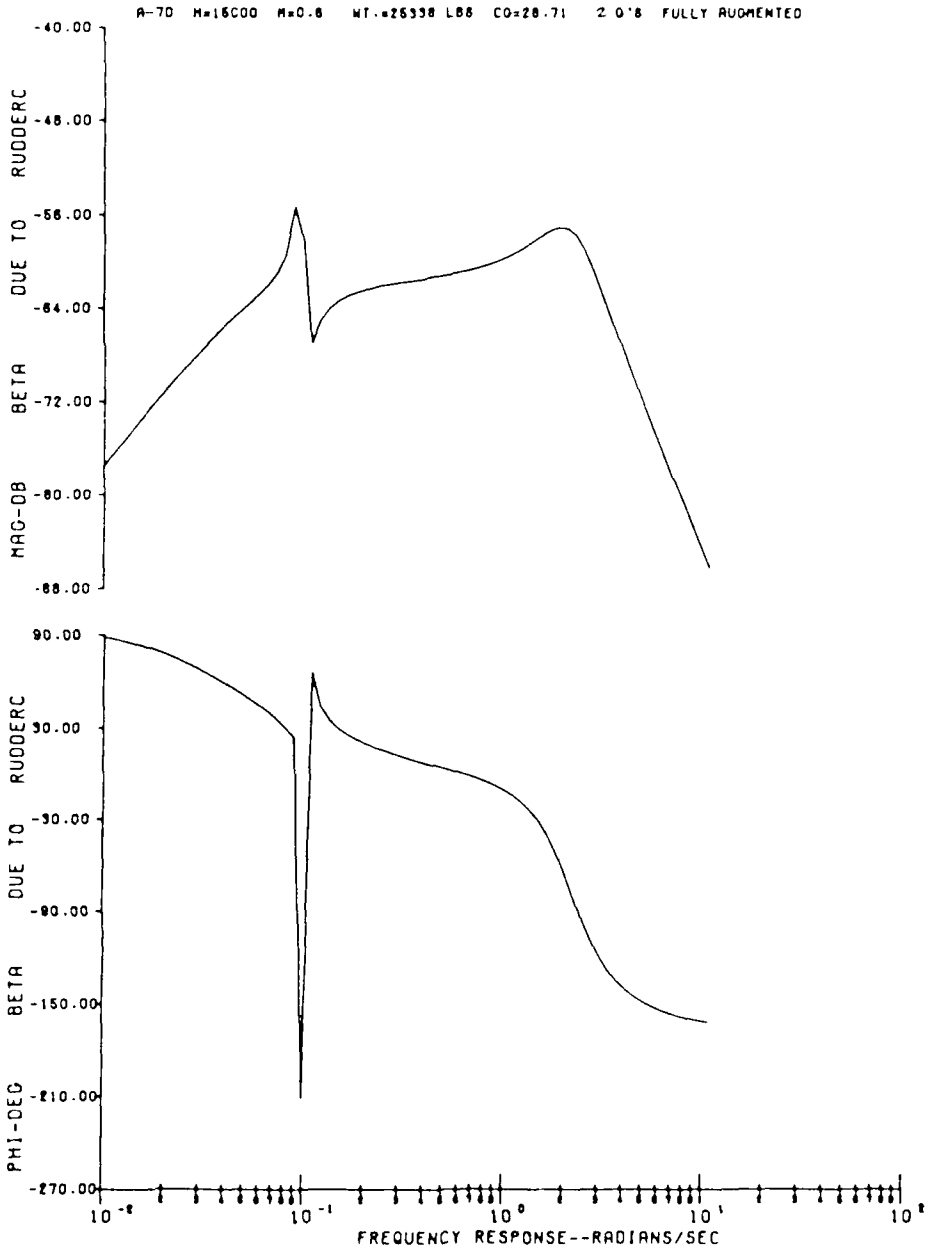

Figure F14. 26 Fully Augmented Bode Plot for Beta due to Pilot Rudder Input

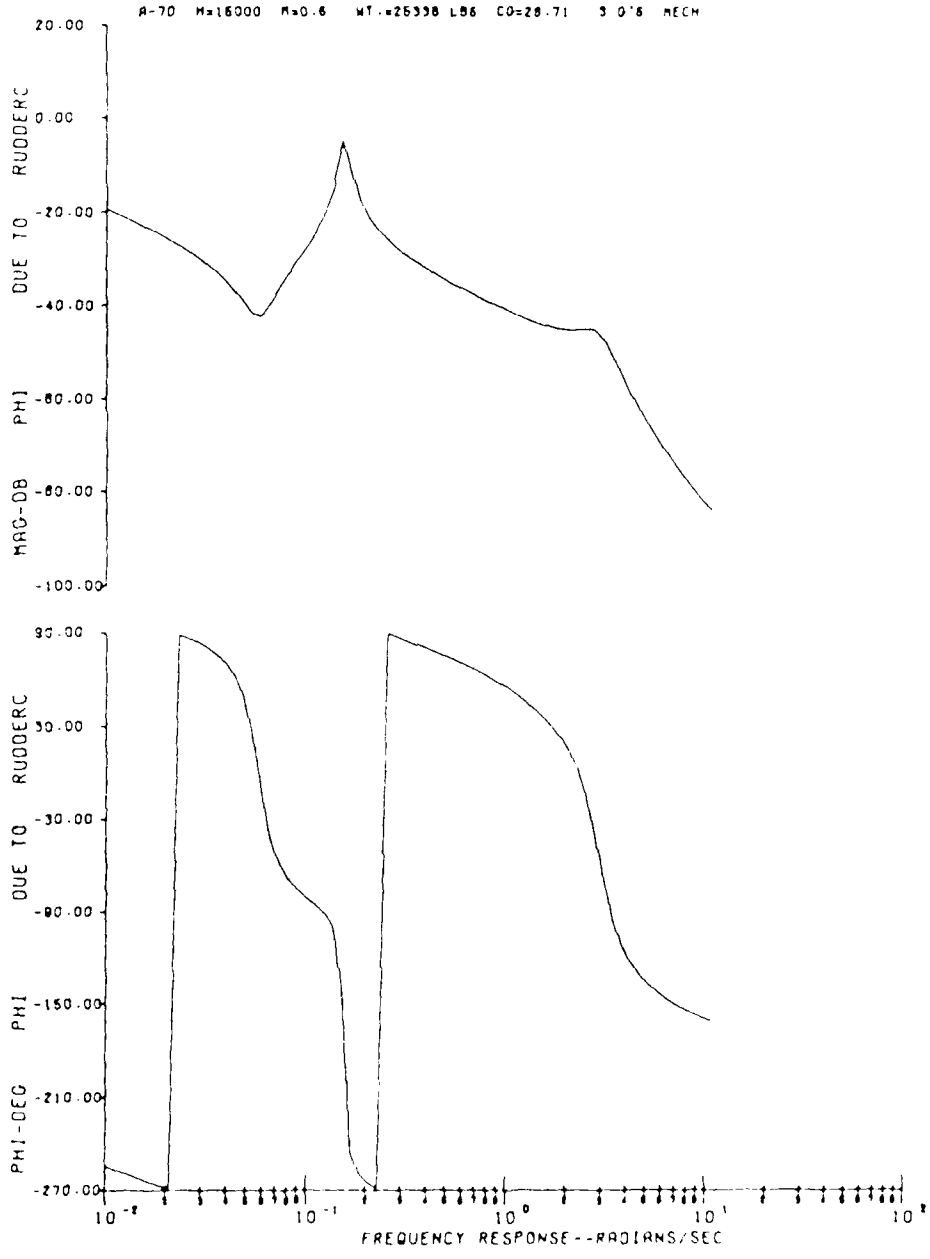

Figure F15. 3G Mechanical Bode Plot for Phi due to Pilot Rudder Input

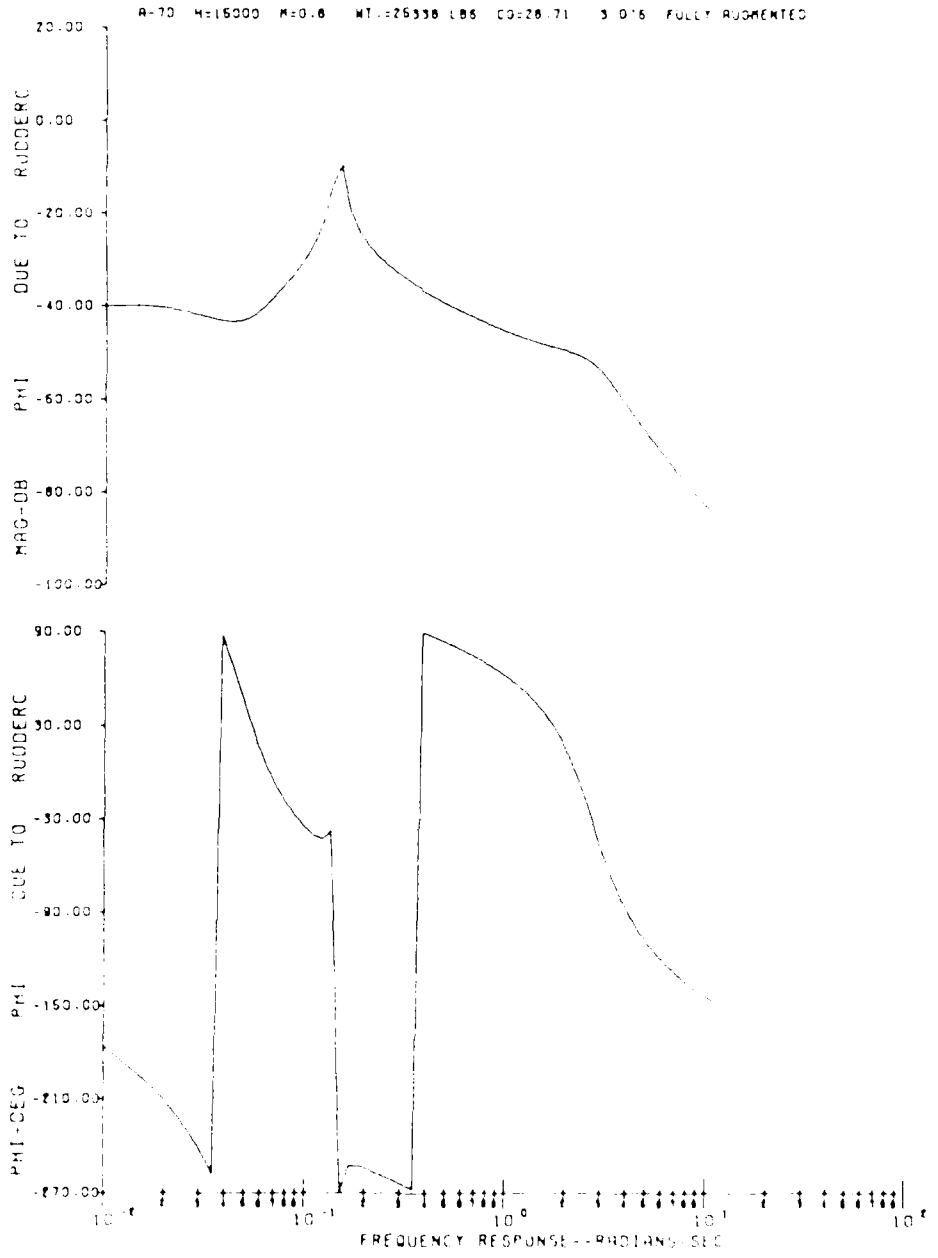

Figure FIG. 36 Fully Augmented Bode Plot for Phi due to Pilot Rudder Input

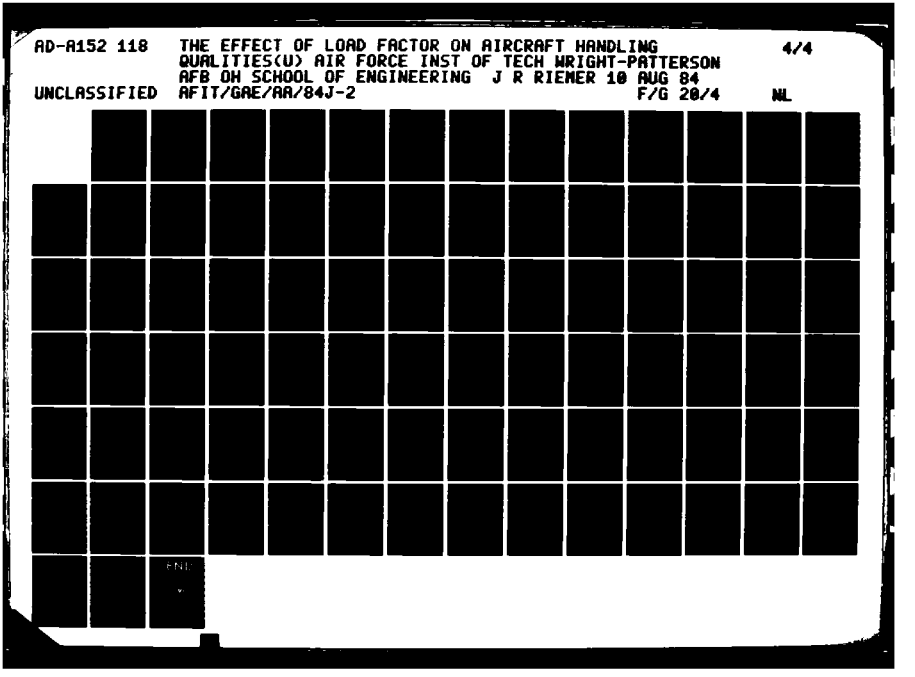
AD-A152 118
THE EFFECT OF LOAD FACTOR ON AIRCRAFT HANDLING QUALITIES(U) AIR FORCE INST OF TECH WRIGHT-PATTERSON AFB OH SCHOOL OF ENGINEERING J R RIEMER 10 AUG 84
4/4
UNCLASSIFIED
AFIT/GAE/AA/84J-2
F/G 20/4
NL

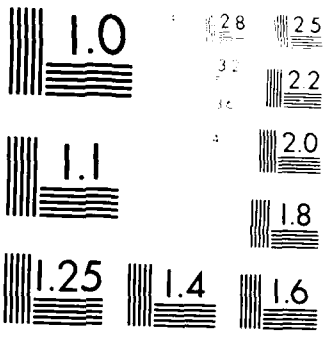

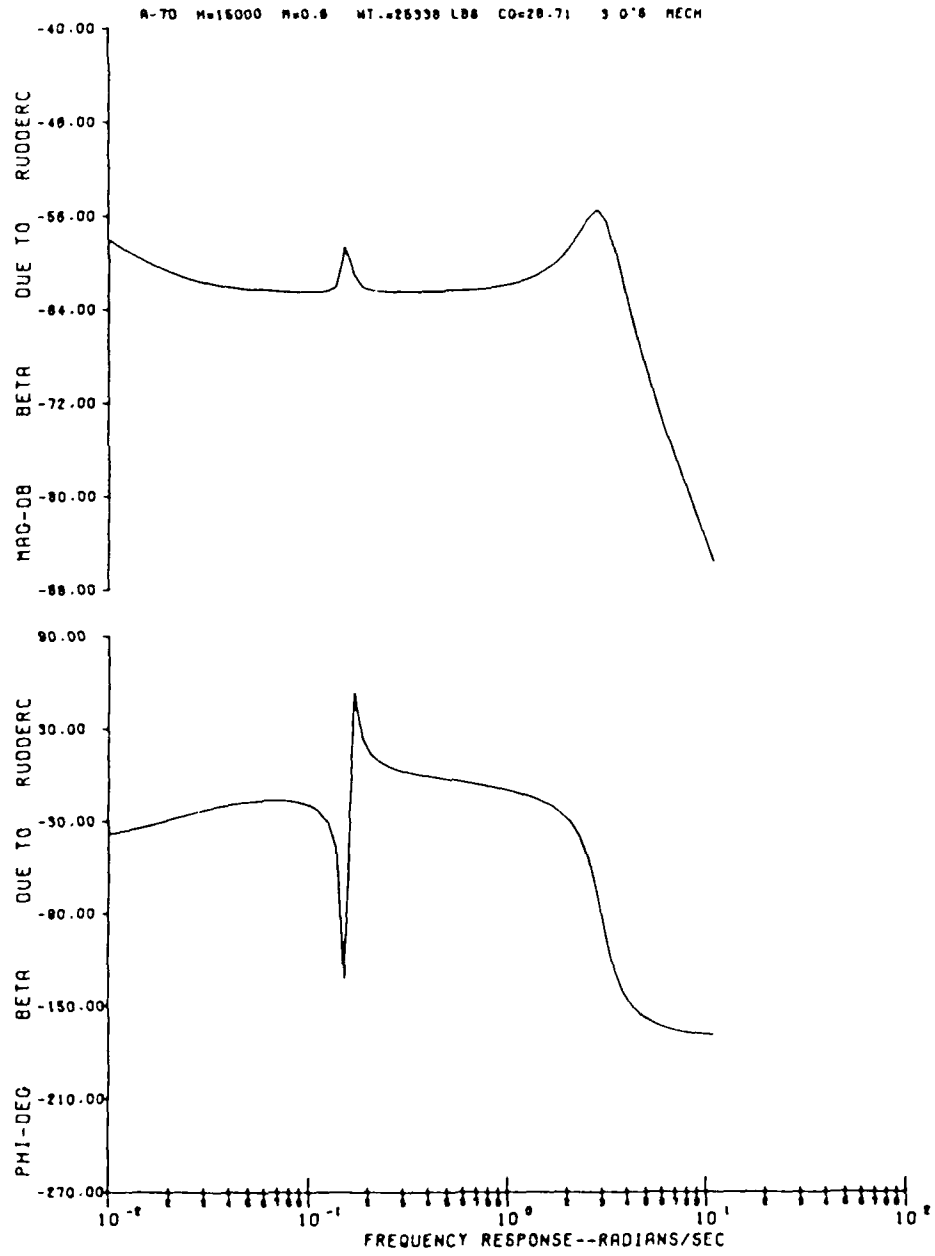

Figure F17. 3G Mechanical Bode Plot for Beta due to Pilot Rudder Input

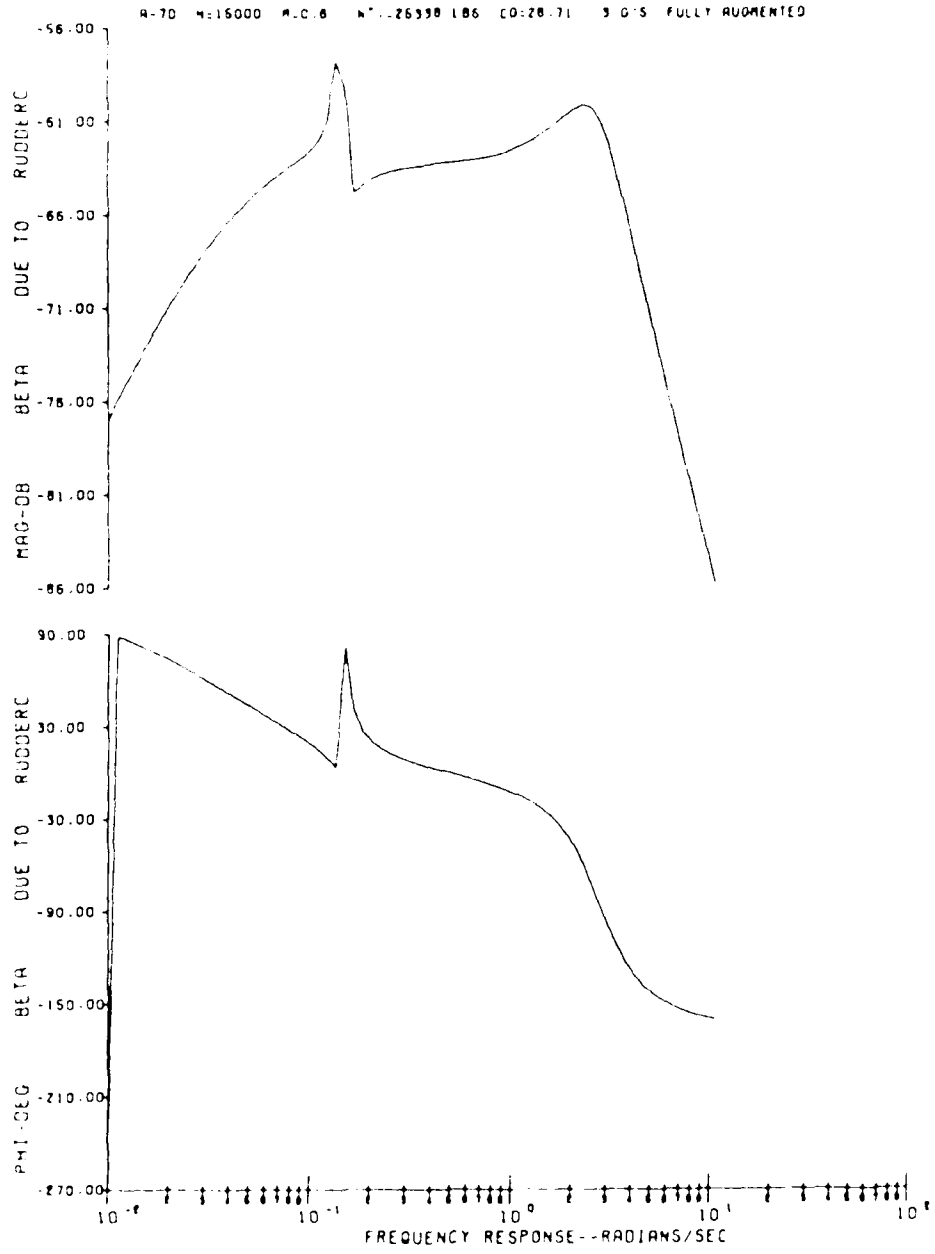

Figure F18. 3G Fully Augmented Bode Plot for Beta due to Pilot Rudder Input

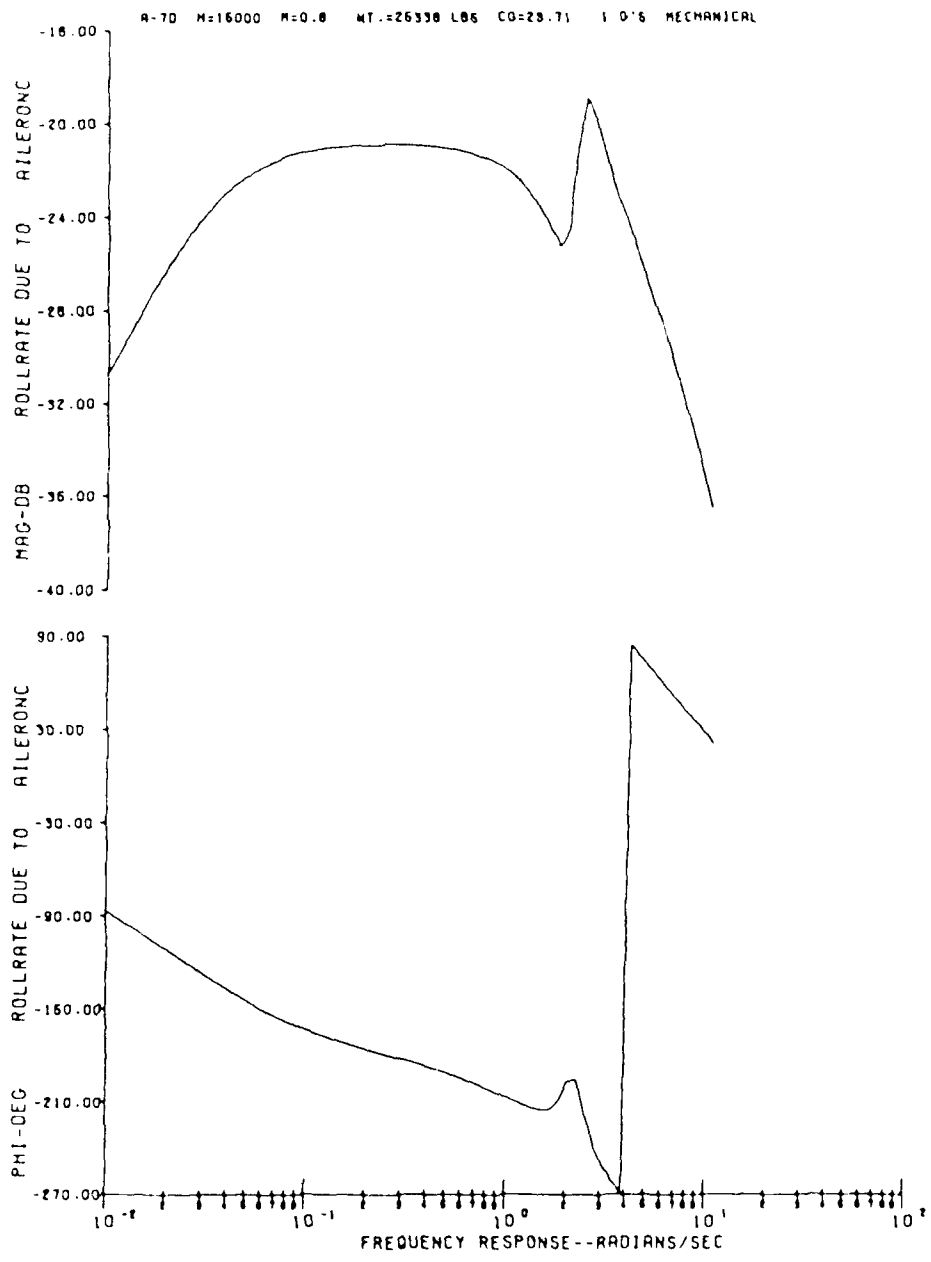

Figure F19. 1G Mechanical Bode Plot for Roll Rate due to Pilot Aileron Input

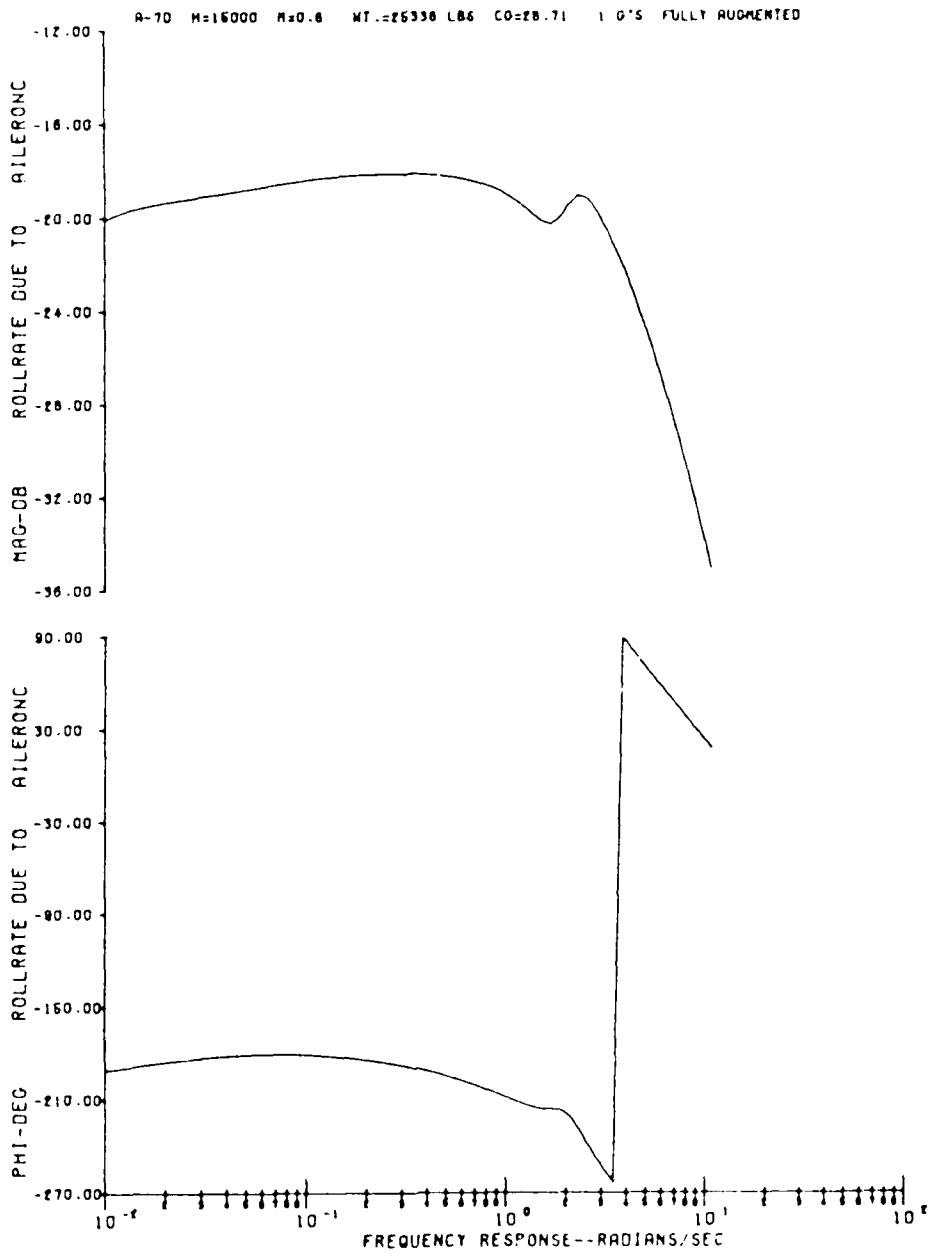

Figure F20. 1G Fully Augmented Bode Plot for Rol' Rate due to Pilot Aileron Input

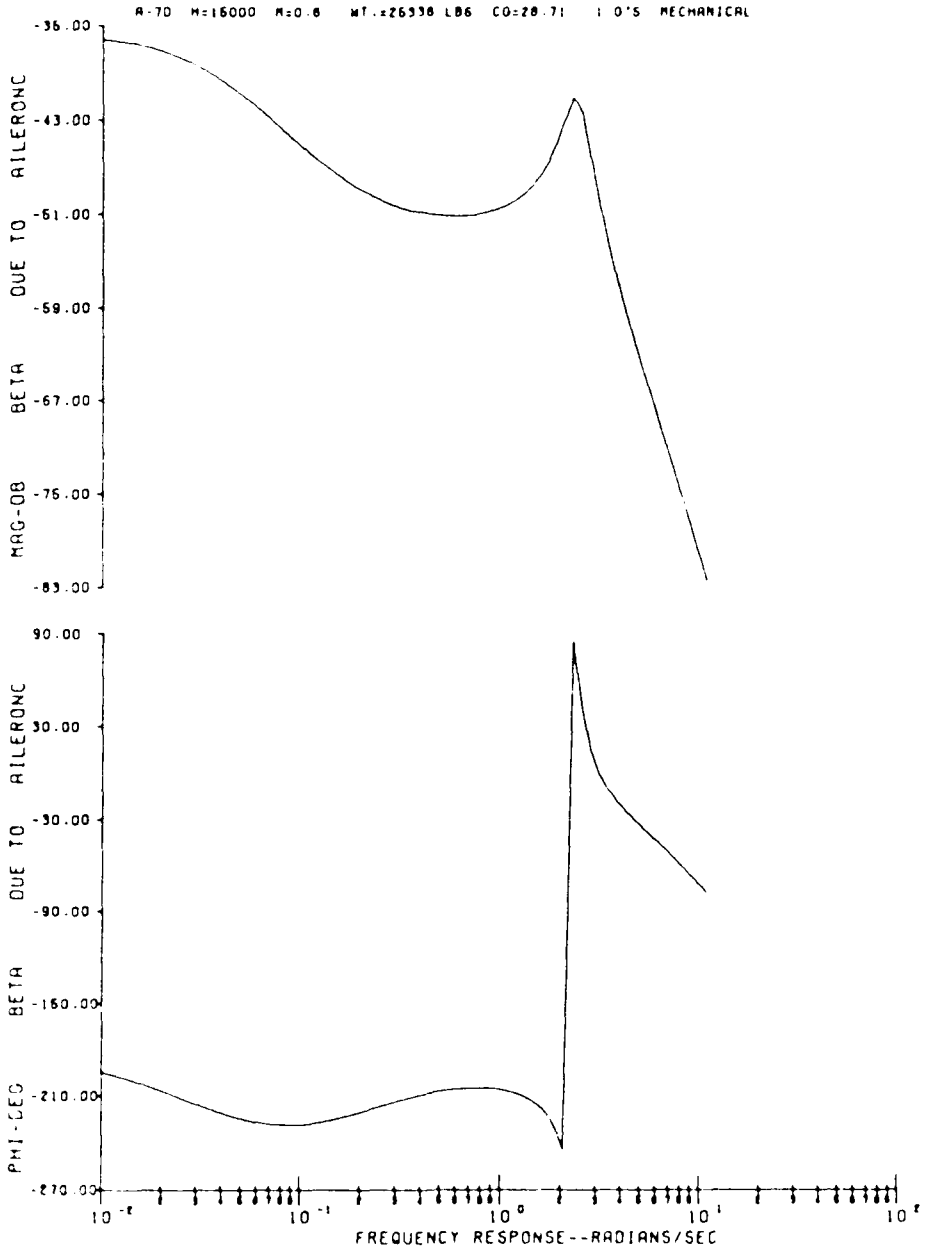

Figure F21. 1G Mechanical Bode Plot for Beta due to Pilot Aileron Input

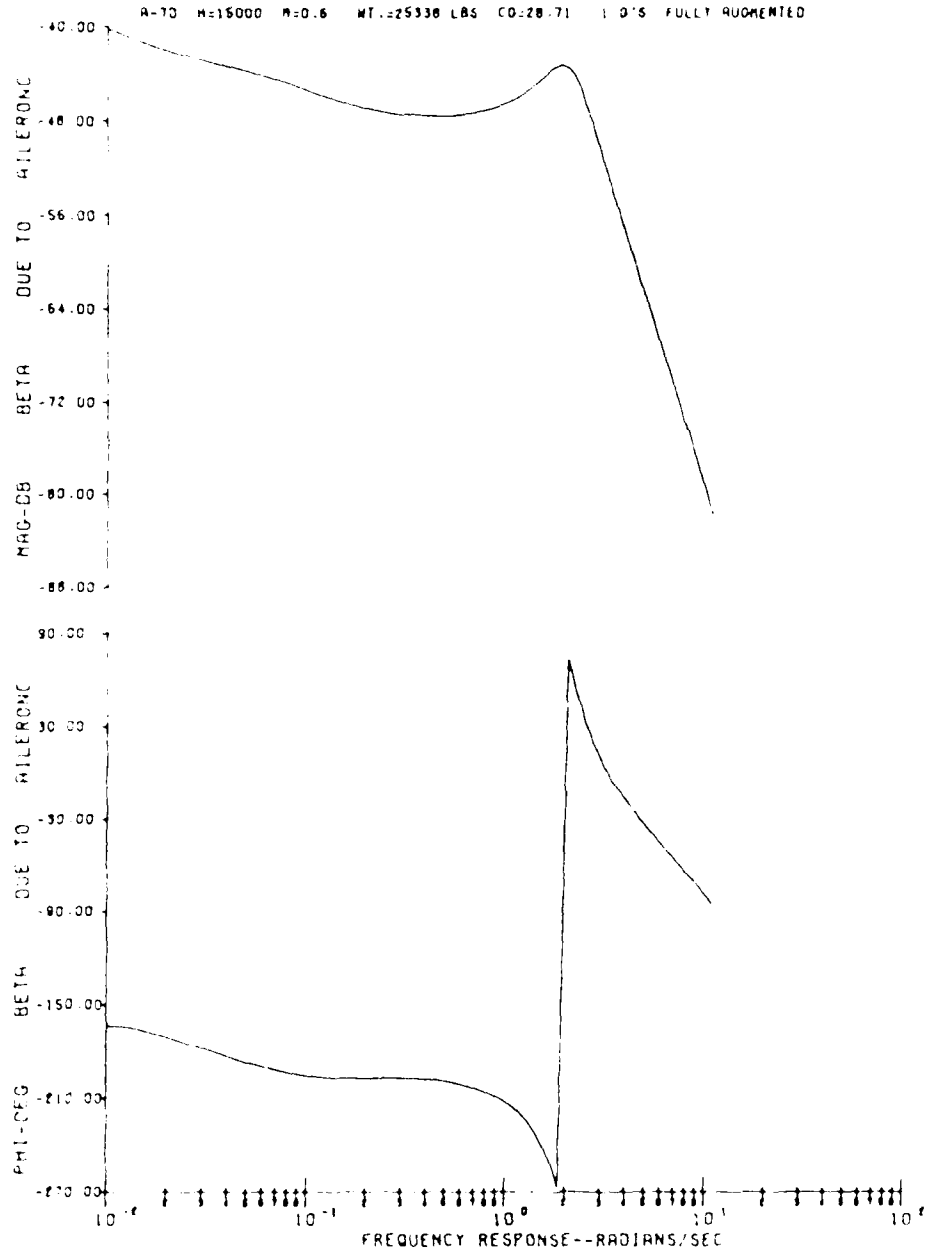

Figure F22. 1G Fully Augmented Bode Plot for Beta due to Pilot Aileron Input

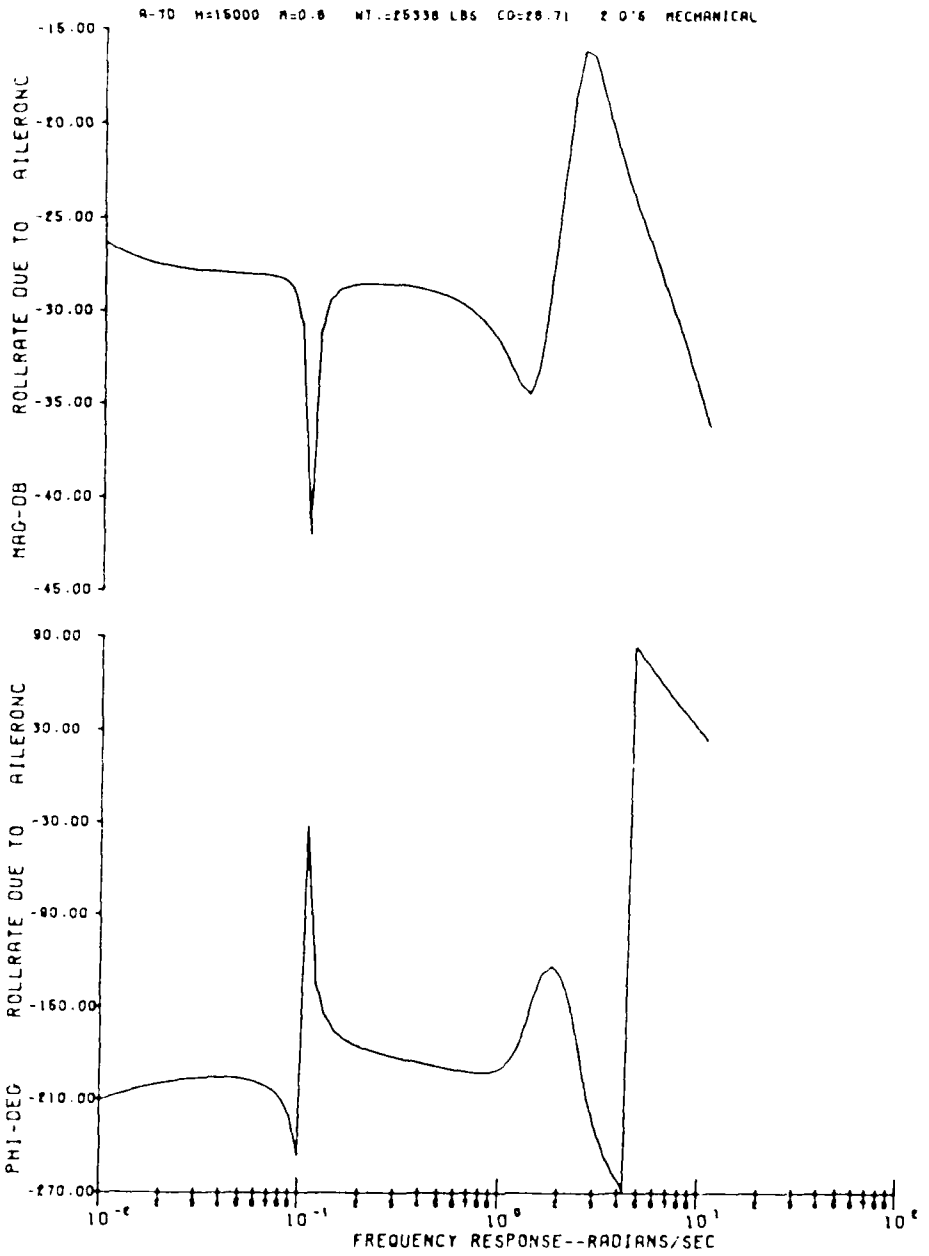

Figure F23. 2G Mechanical Bode Plot for Roll Rate due to Pilot Aileron Input

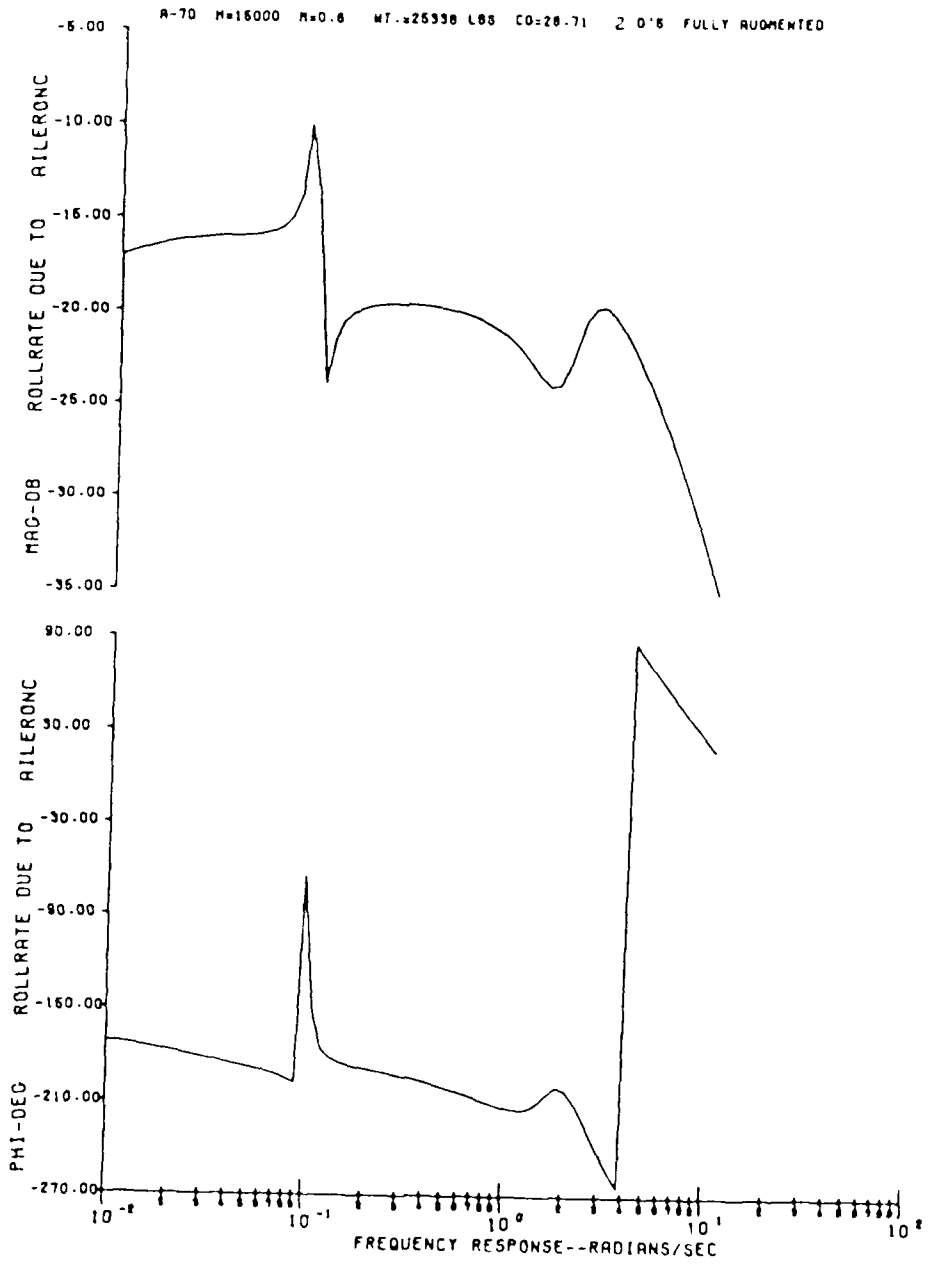

Figure F24. 2G Fully Augmented Bode Plot for Roll Rate due to Pilot Aileron Input

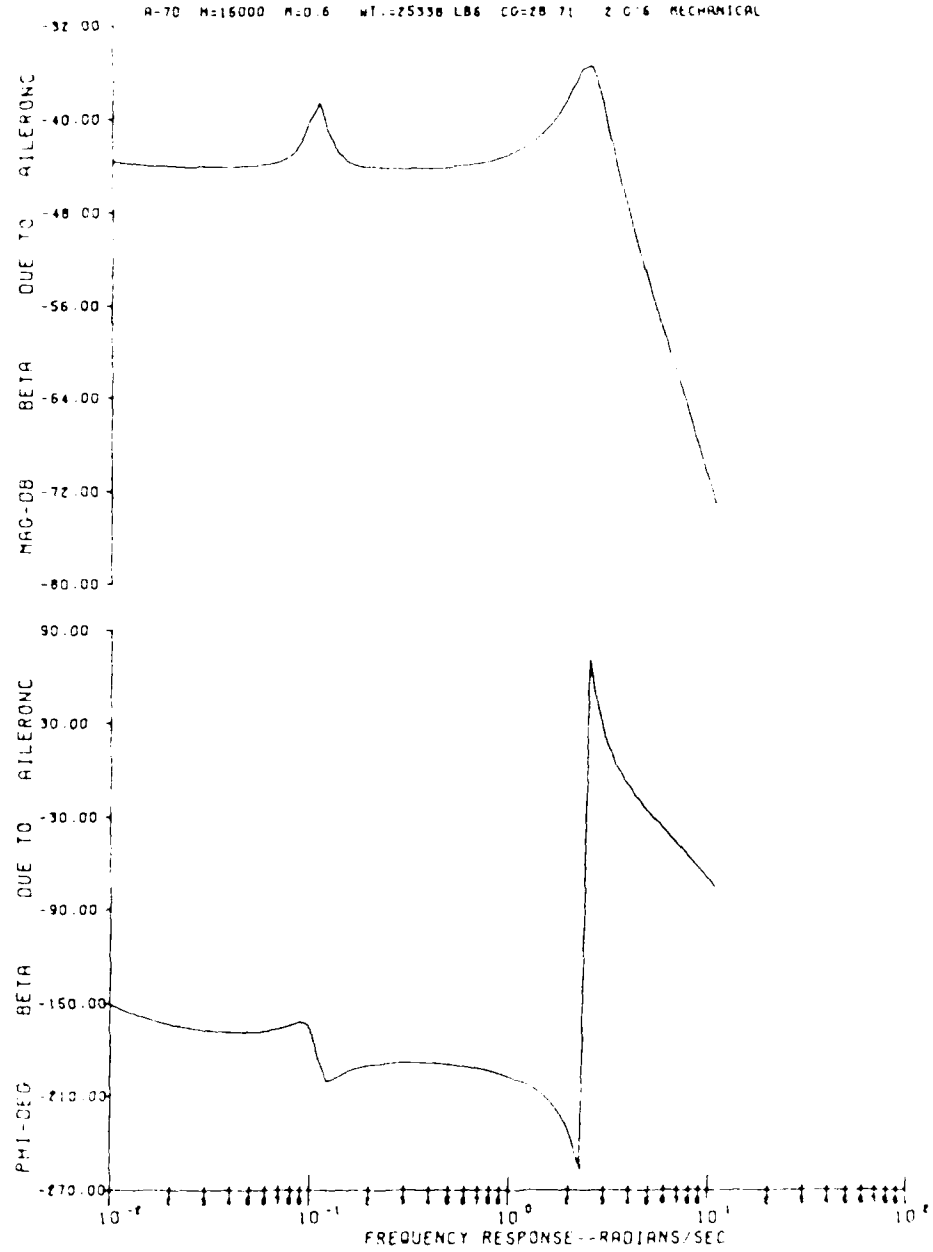

Figure F25. 2G Mechanical Bode Plot for Beta due to Pilot Aileron Input

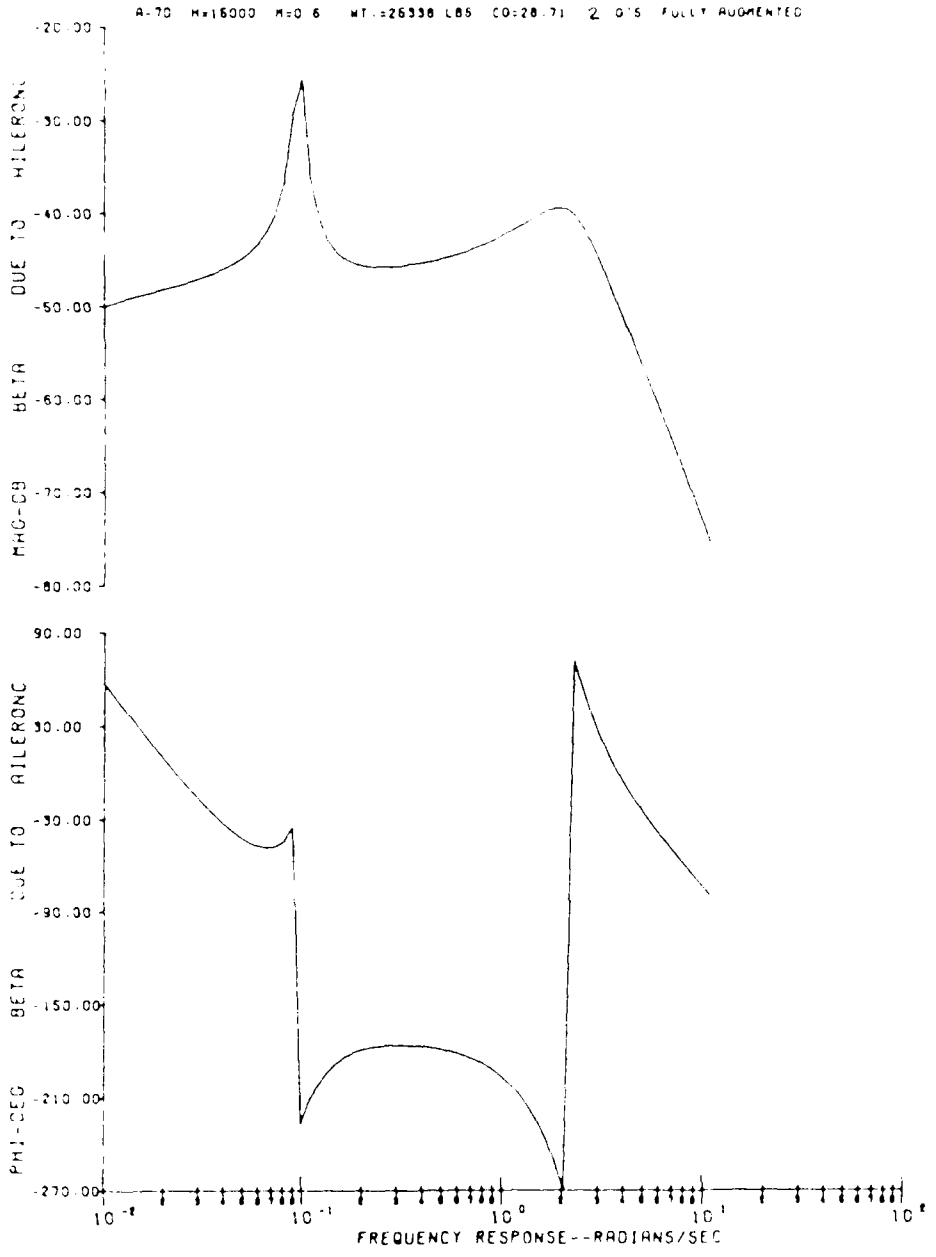

Figure F26. 2G Fully Augmented Bode Plot for Beta due to Pilot Aileron Input

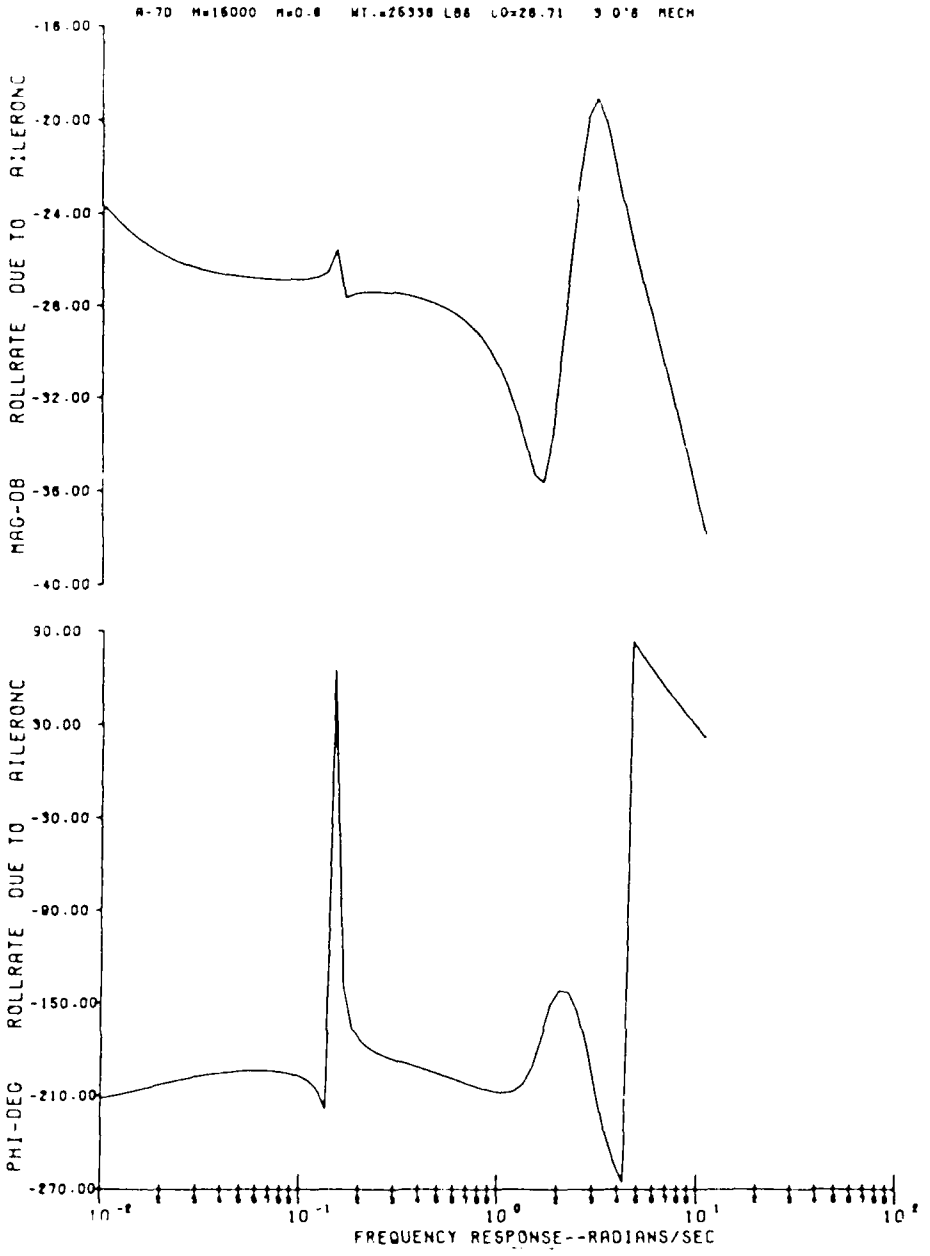

Figure F27. 3G Mechanical Bode Plot for Roll Rate due to Pilot Aileron Input

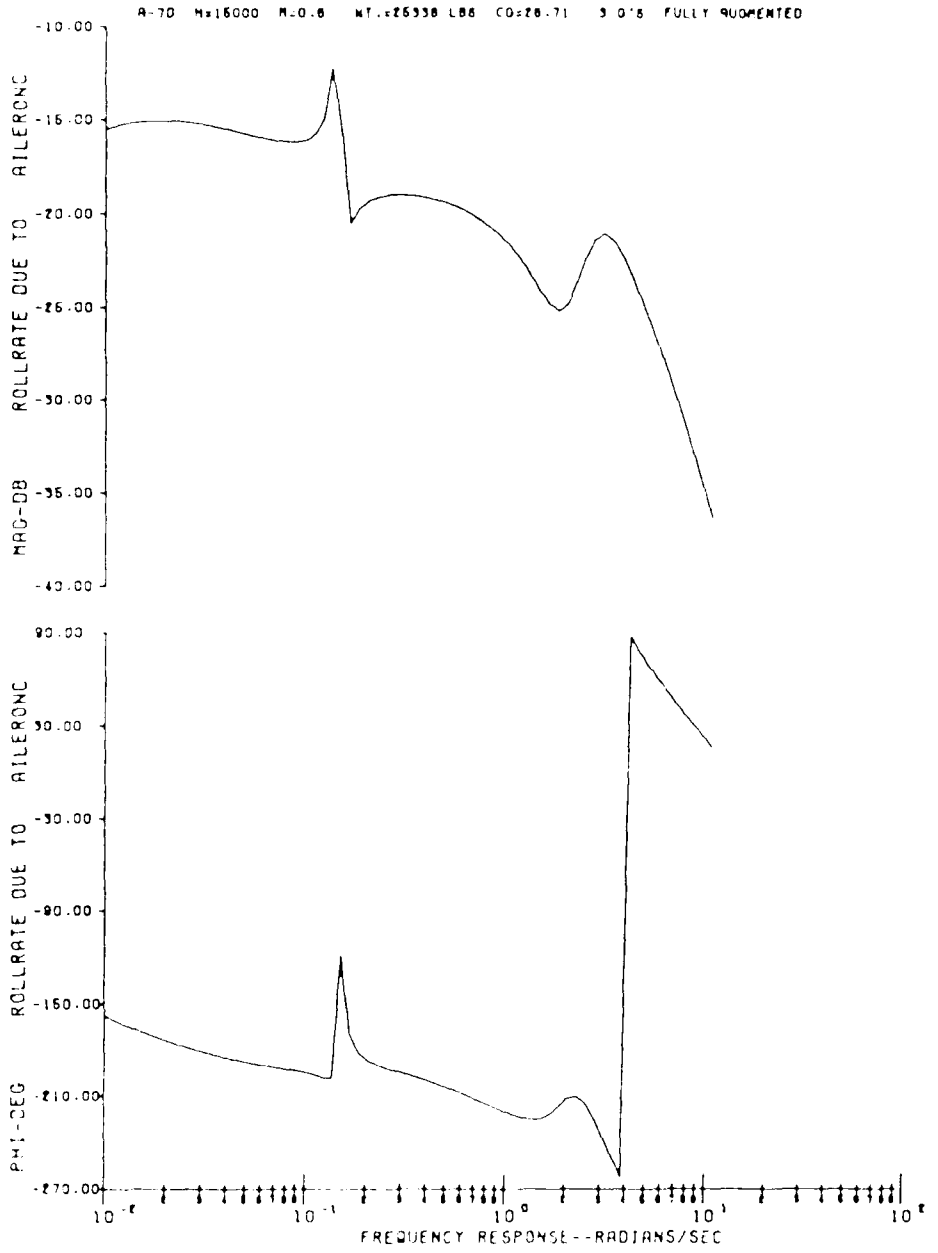

Figure F28. 65 Fully Augmented Bode Plot for Roll Rate due to Pilot Aileron Input

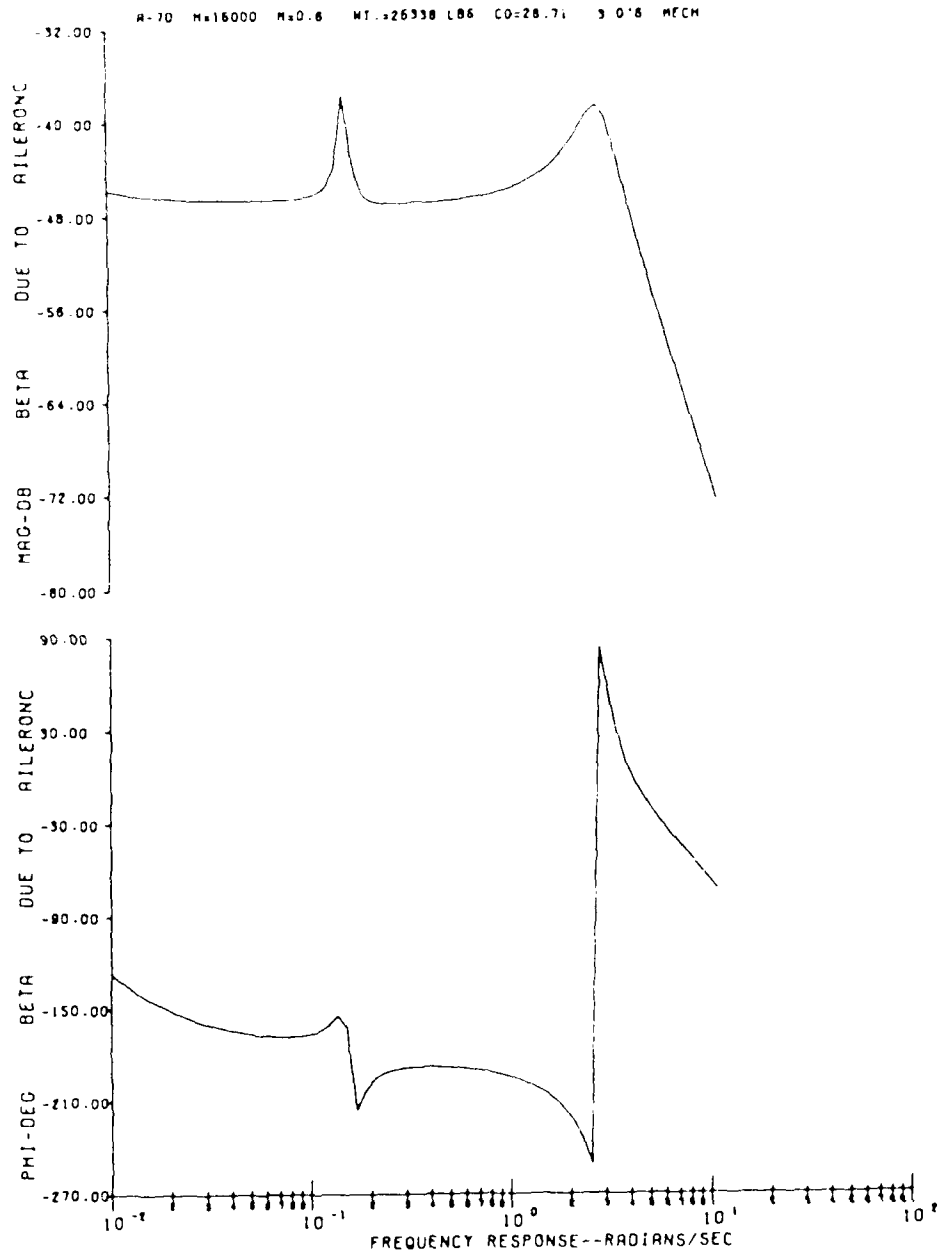

Figure F29. 3G Mechanical Bode Plot for Beta due to Pilot Aileron Input

Figure F30. 3G Fully Augmented Bode Plot for Beta due to Pilot Aileron Input

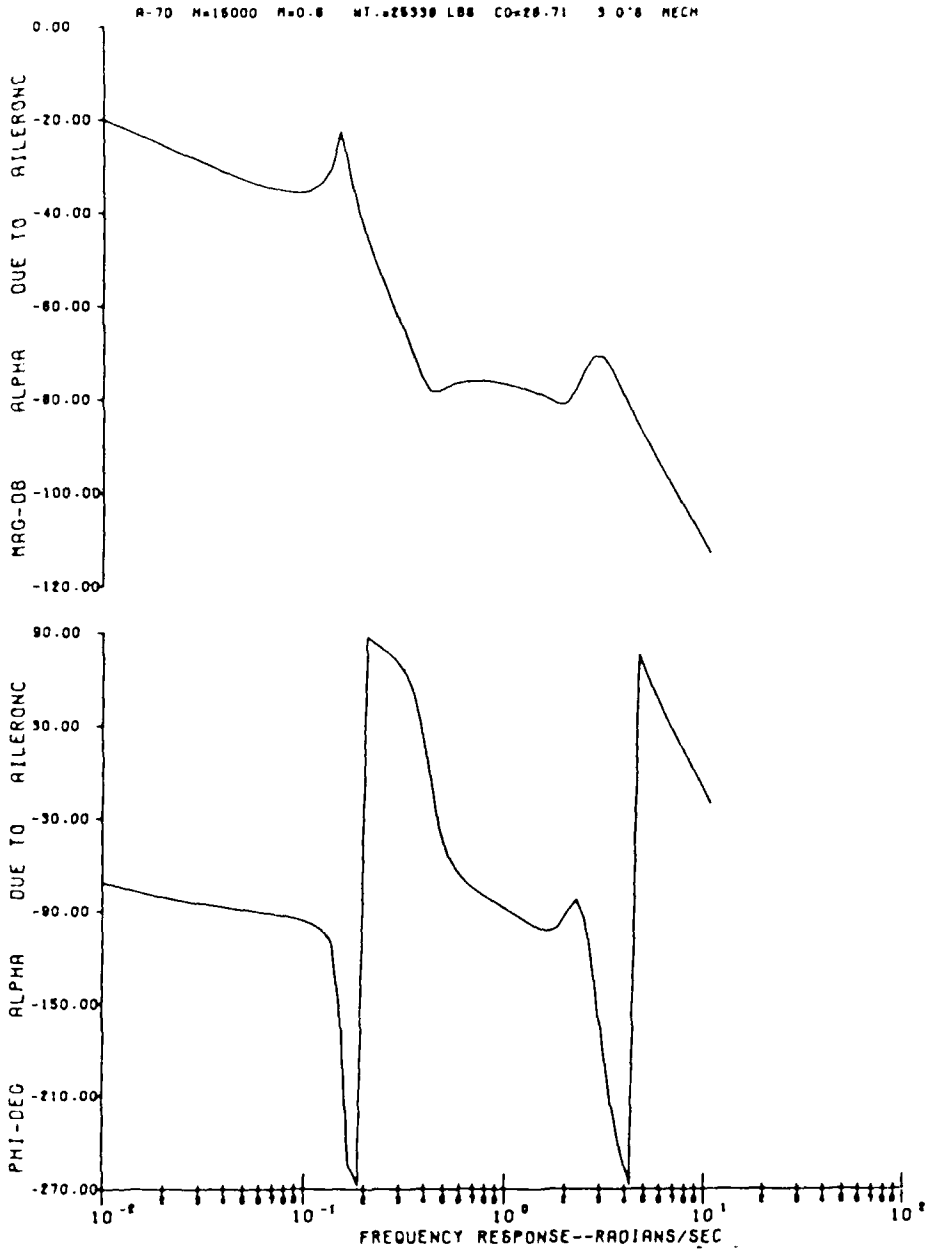

Figure F31. 3G Mechanical Bode Plot for Alpha due to Pilot Aileron Input

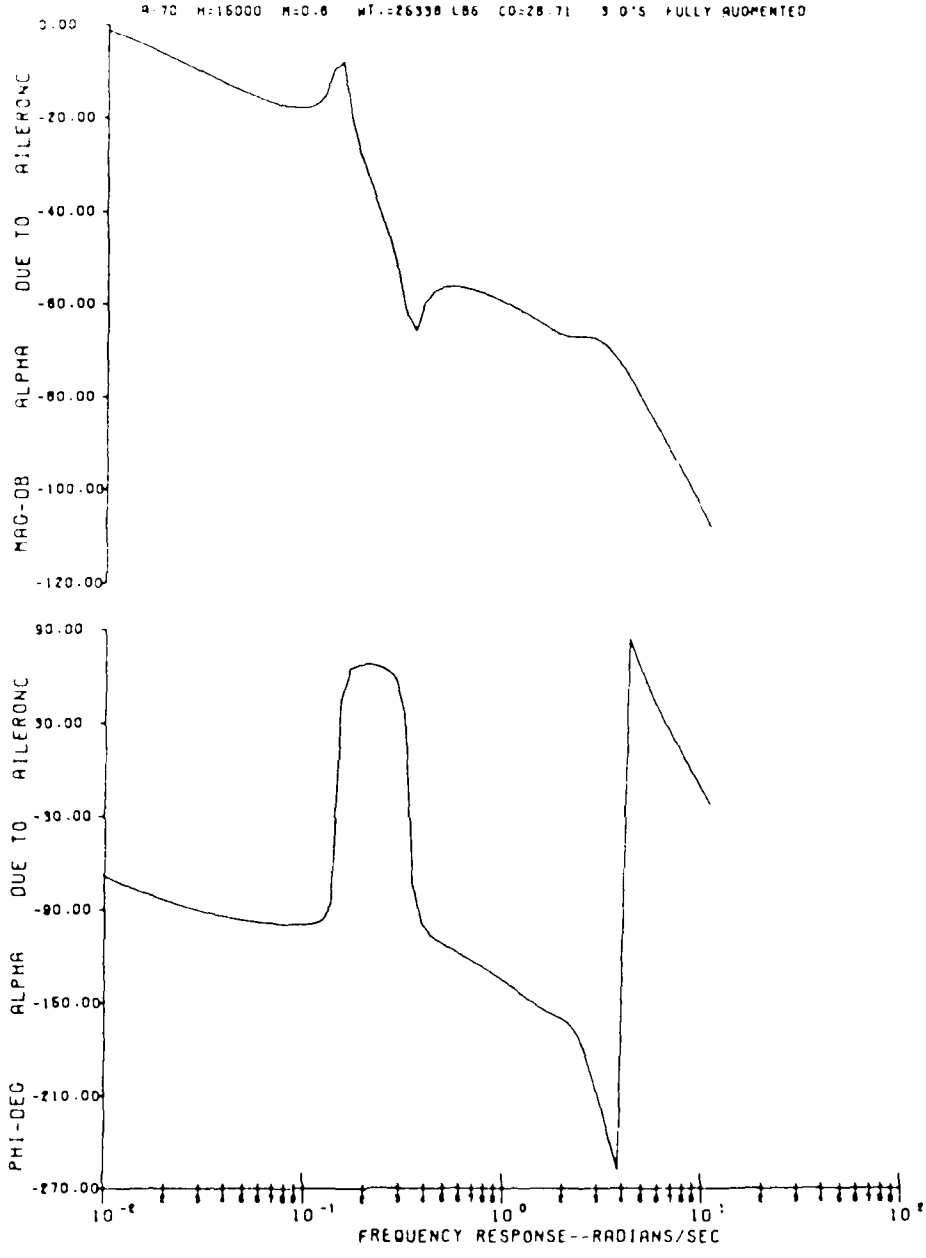

Figure F32. 3G Fully Augmented Bode Plot for Alpa due to Pilot Aileron Input

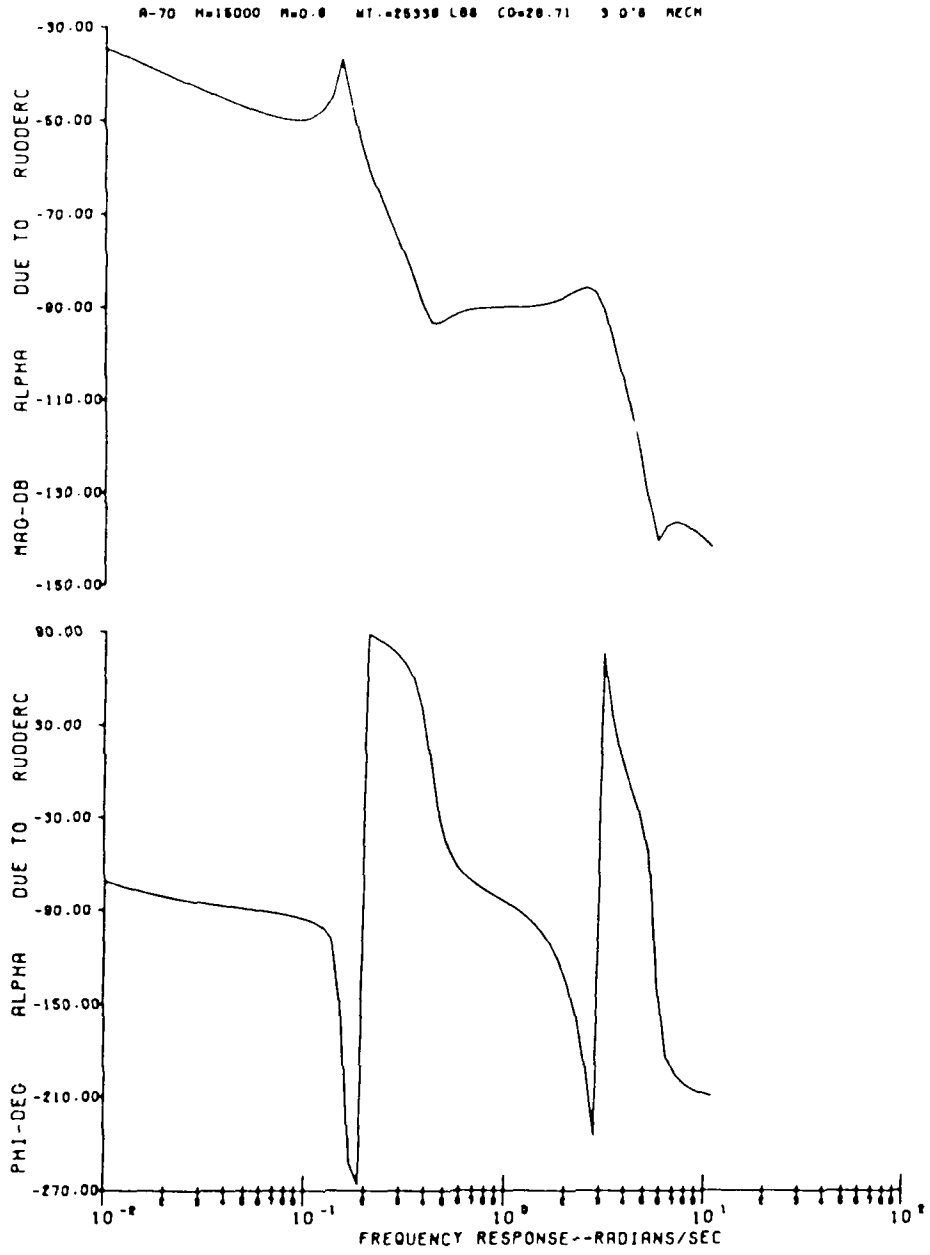

Figure F33. 3G Mechanical Bode Plot for Alpha due to Pilot Rudder Input

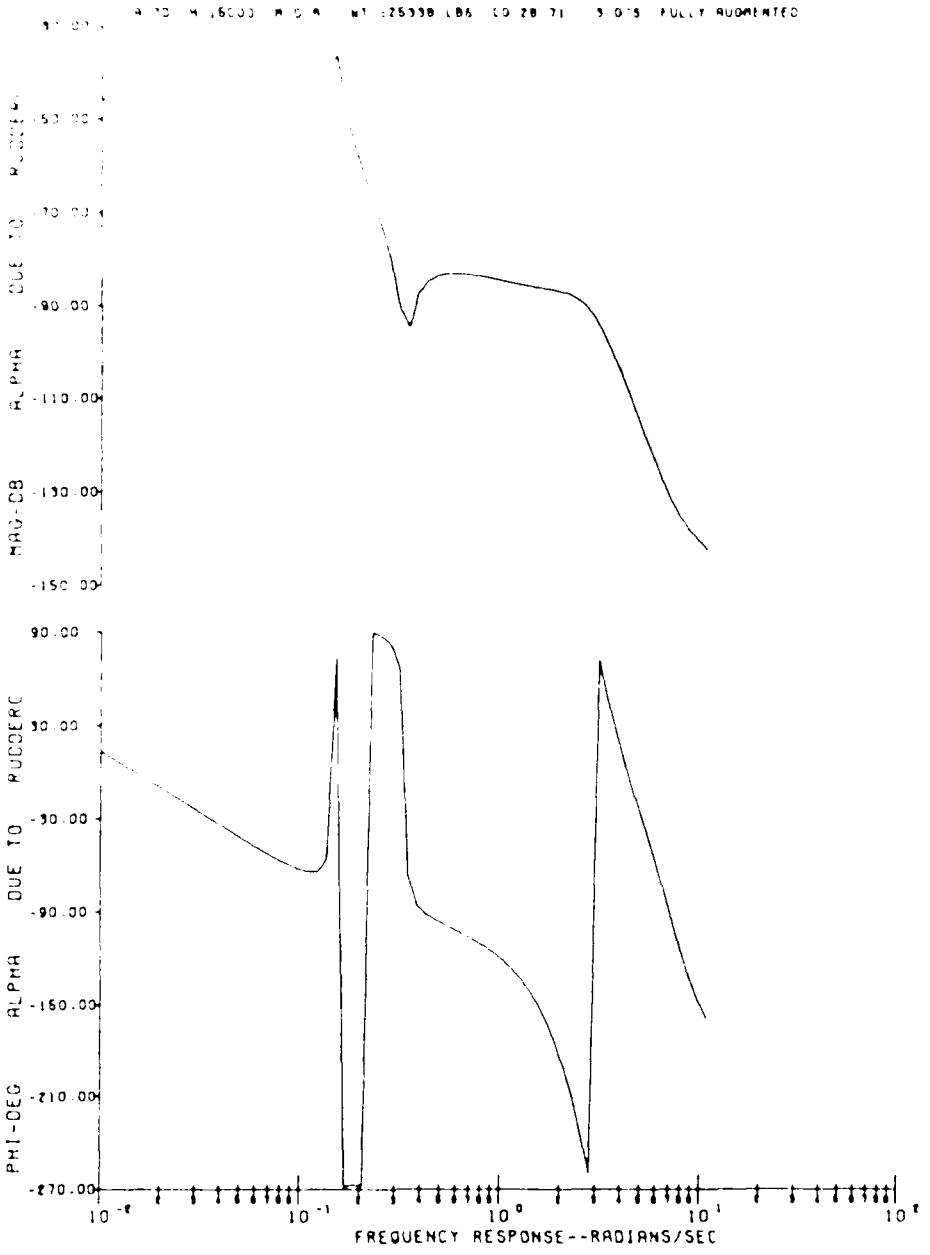

Figure F34. 3G Fully Augmented Bode Plot for Alpha due to Pilot Rudder Input

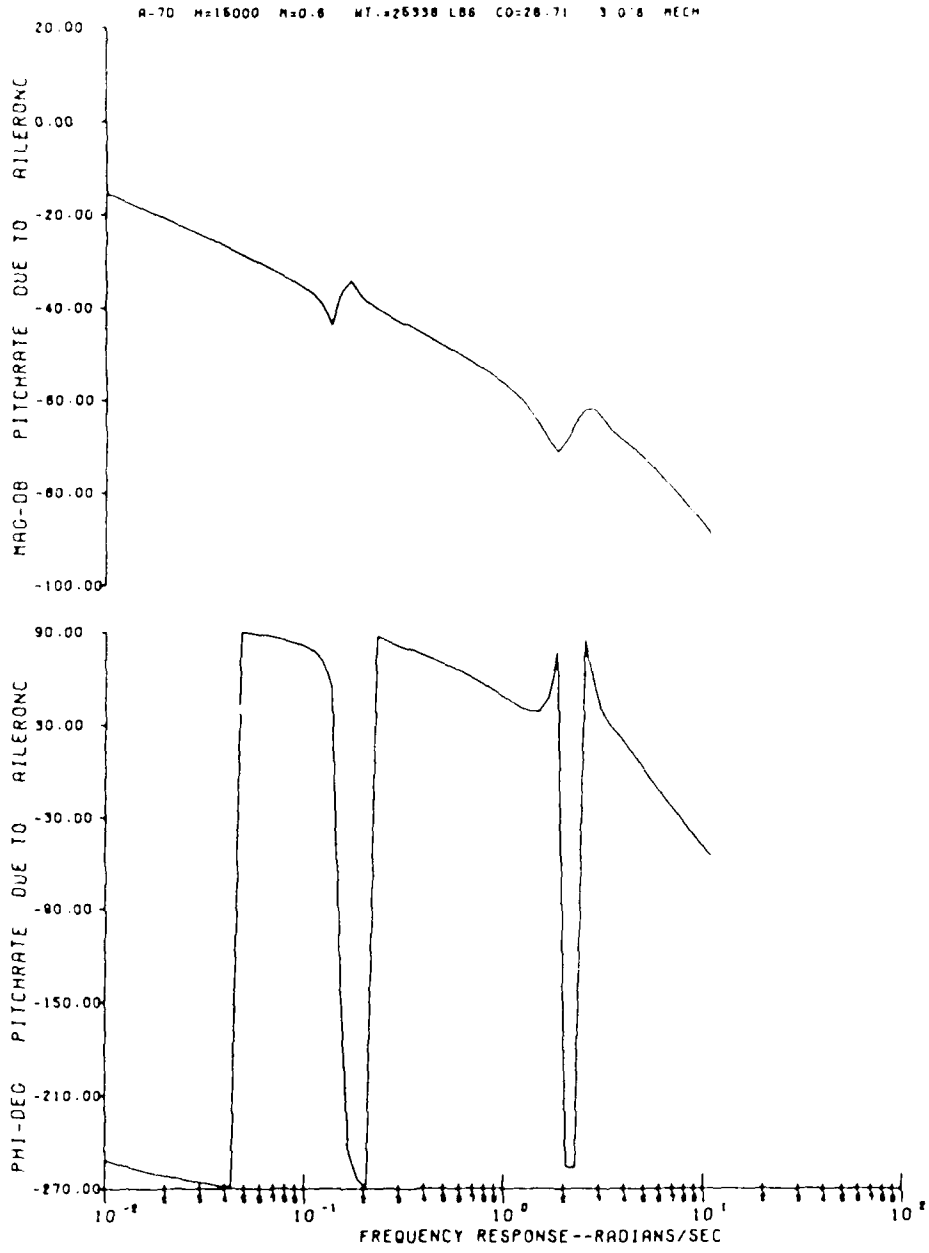

Figure F35. 3G Mechanical Bode Plot for Pitch Rate due to Pilot Aileron Input

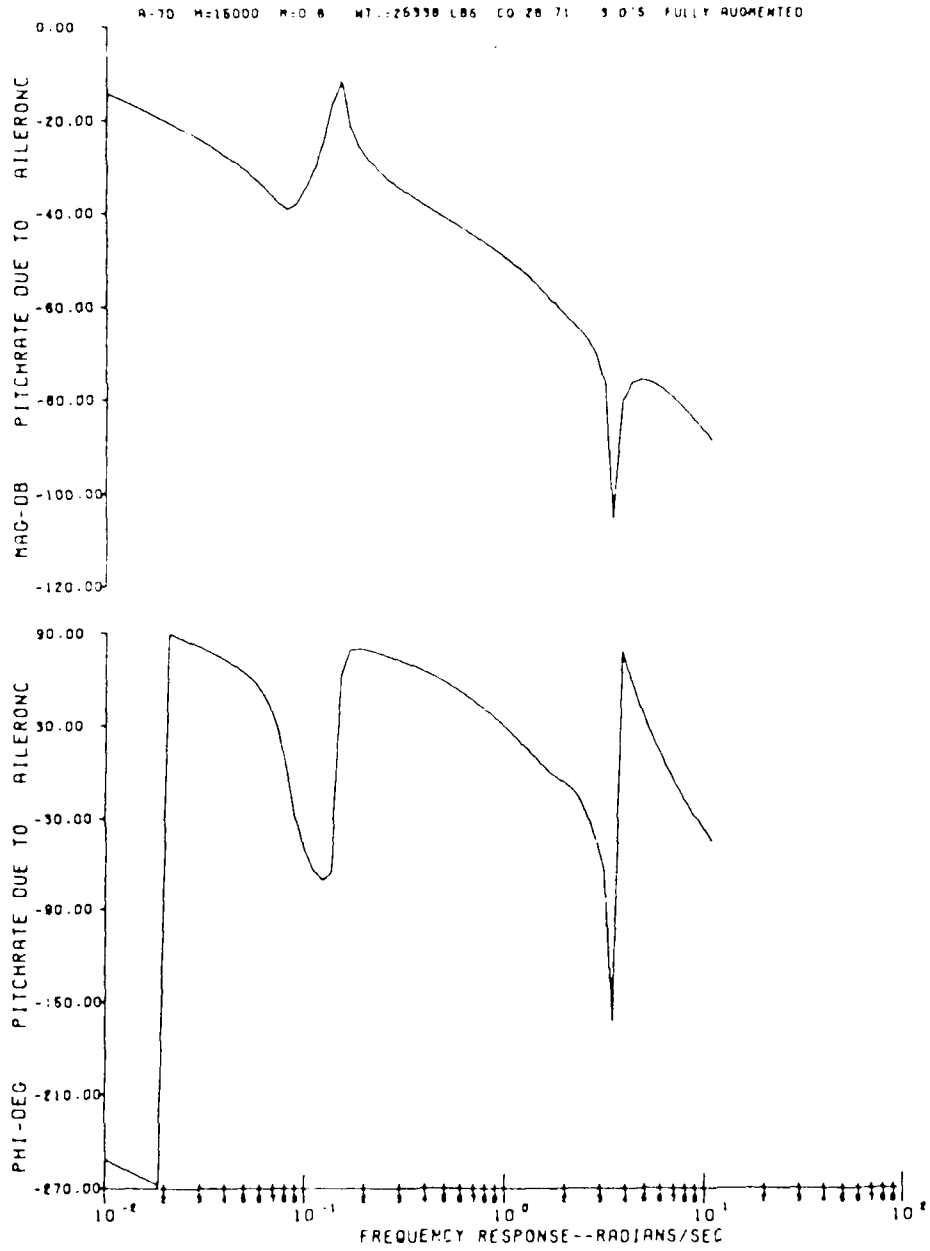

Figure F36. 3G Fully Augmented Bode Plot for Pitch Rate due to Pilot Aileron Input

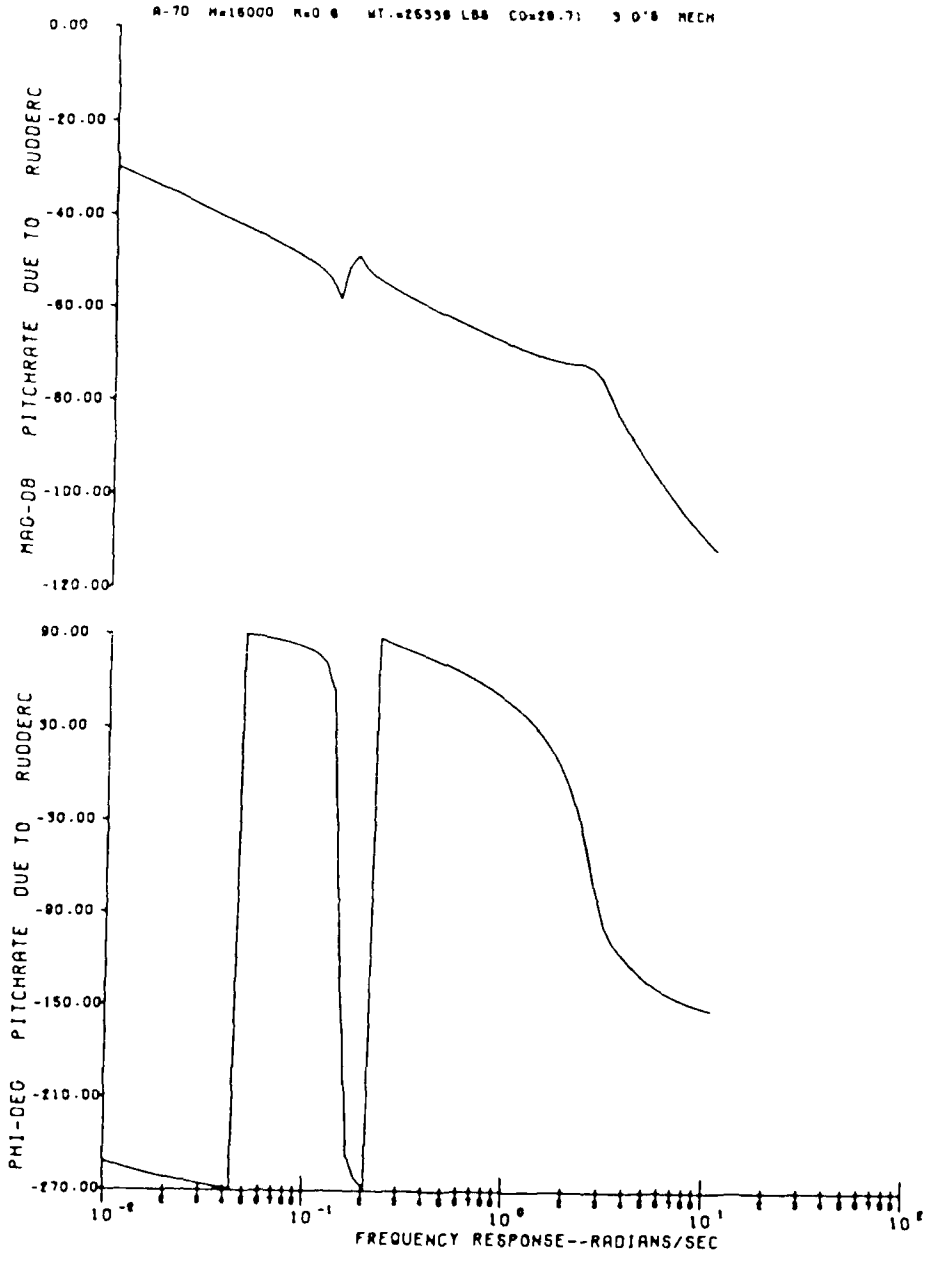

Figure F37. 3G Mechanical Bode Plot for Pitch Rate due to Pilot Rudder Input

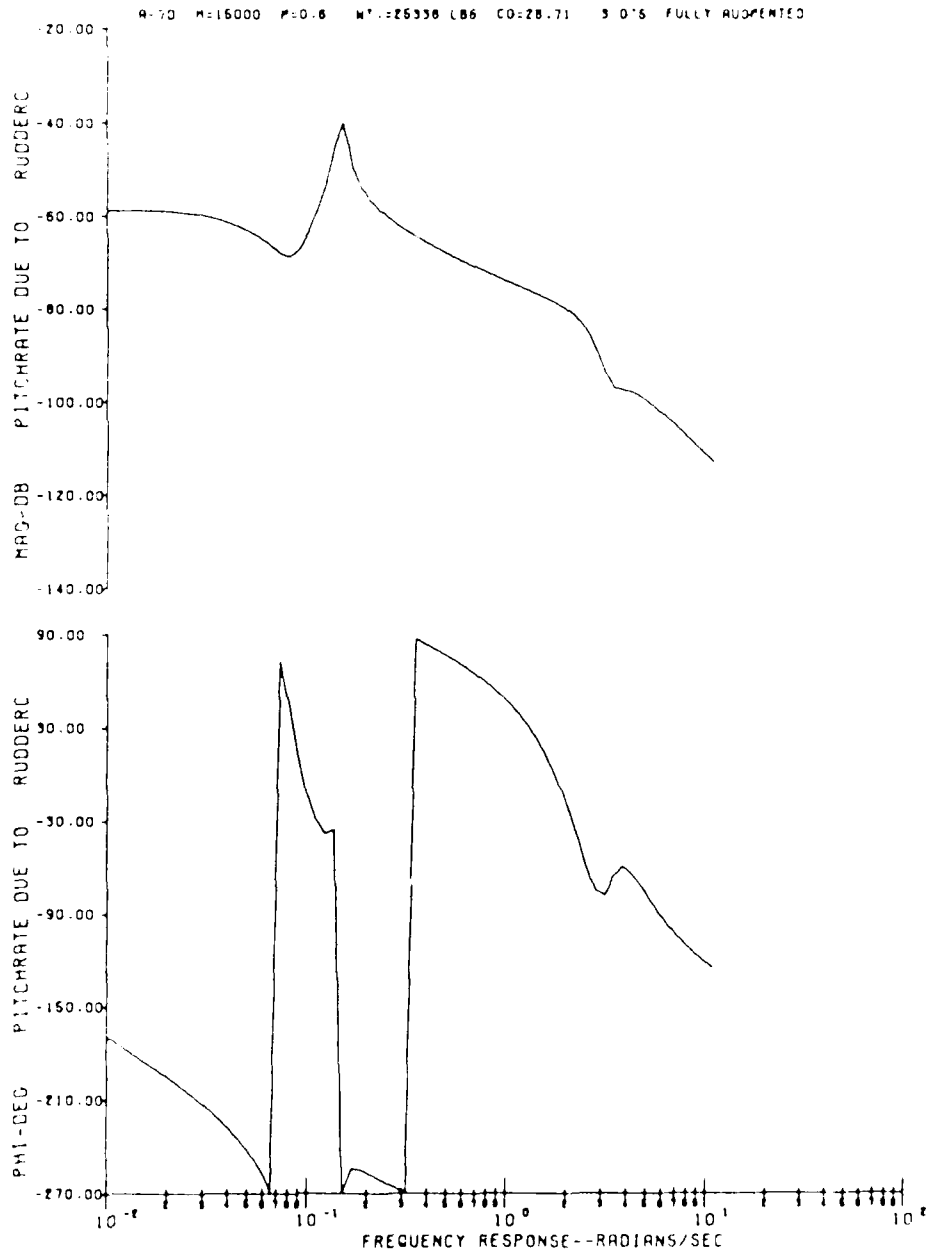

Figure F38. 3G Fully Augmented Bode Plot for Pitch Rate due to Pilot Rudder Input

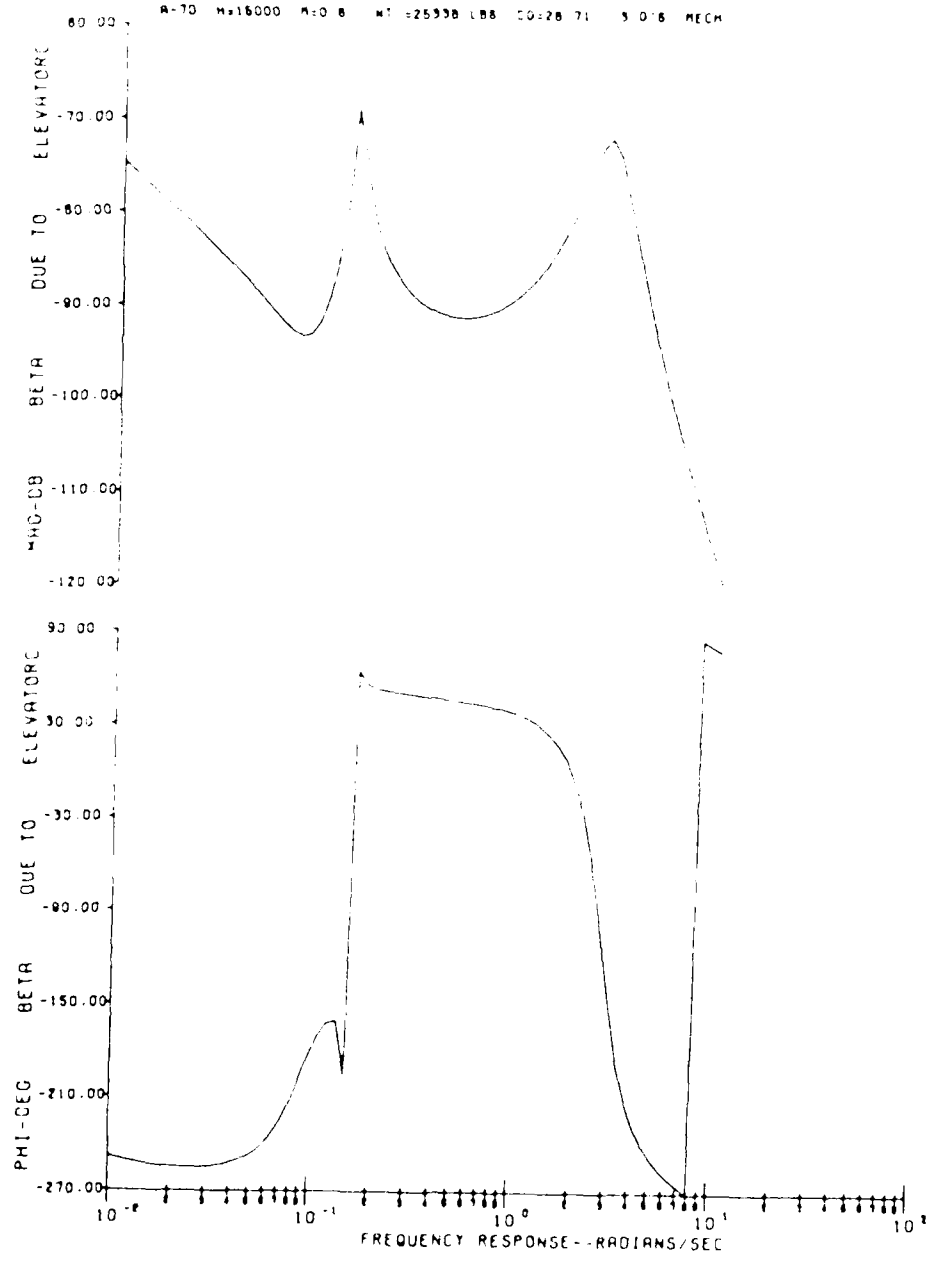

Figure F39. 3G Mechanical Bode Plot for Beta due to Pilot Elevator Input

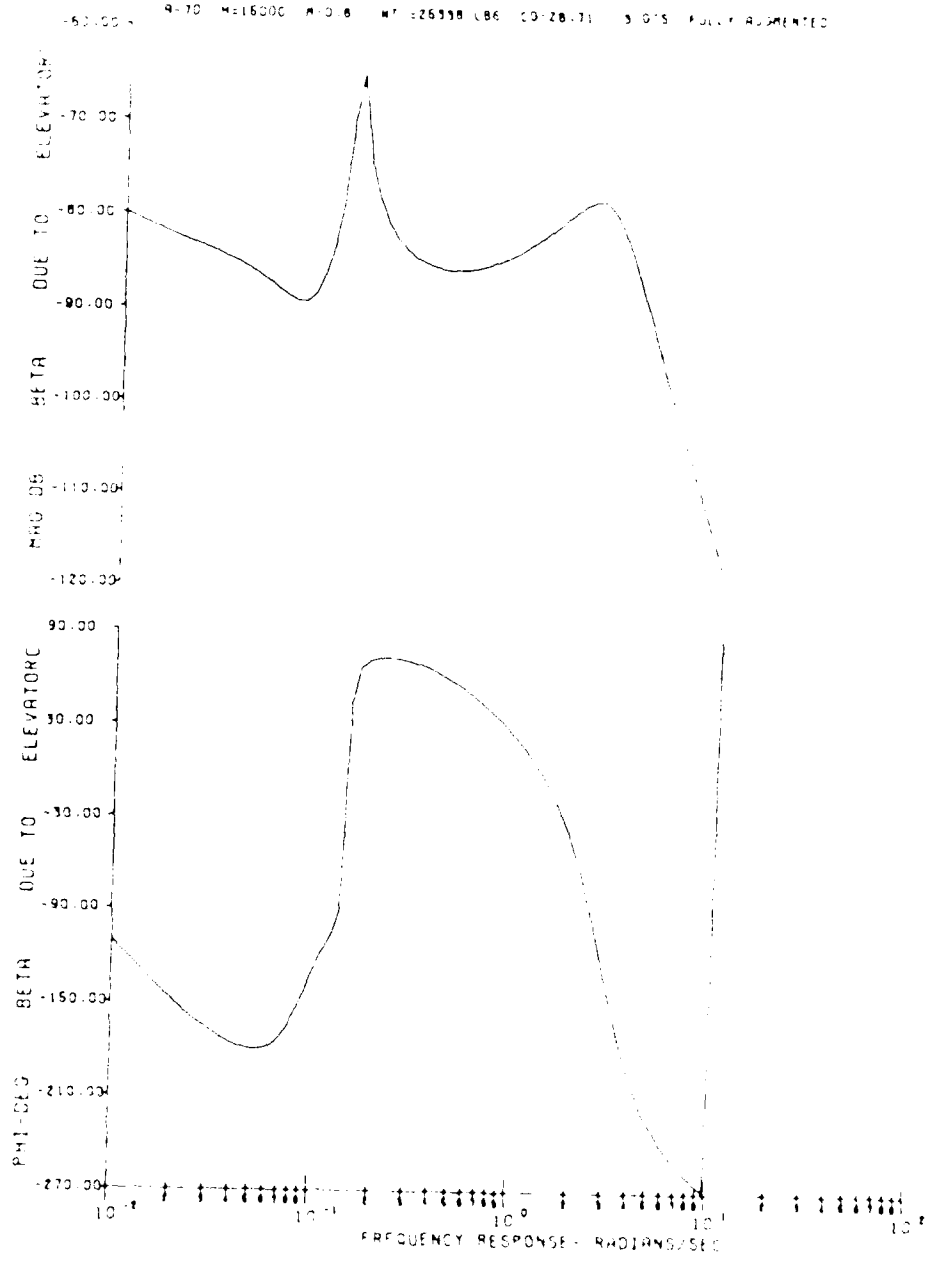

Figure F40. 3G Fully Augmented Bode Plot for Beta due to Pilot Elevator Input

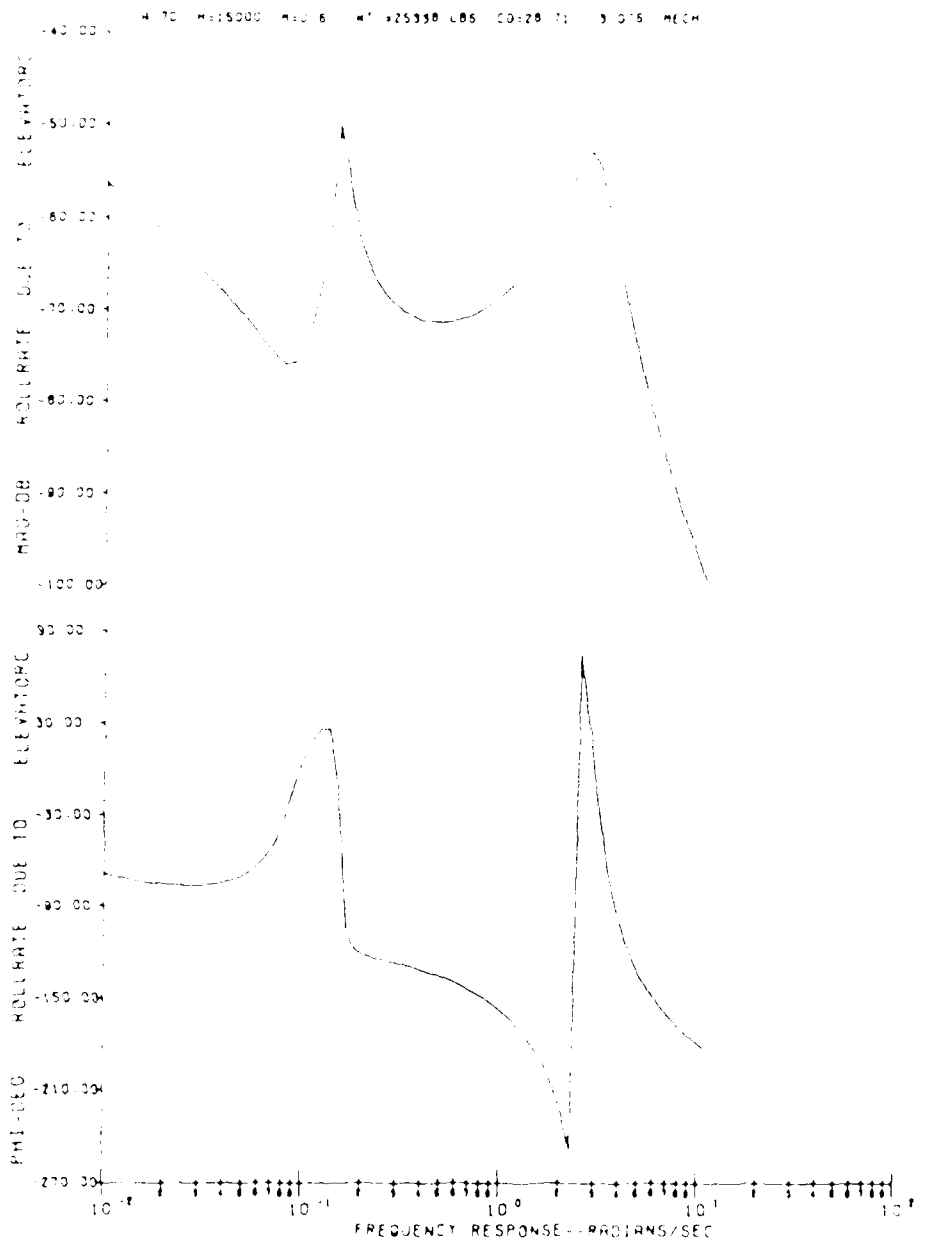

Figure F41. 3G Mechanical Bode Plot for Roll Rate due to Pilot Elevator Input

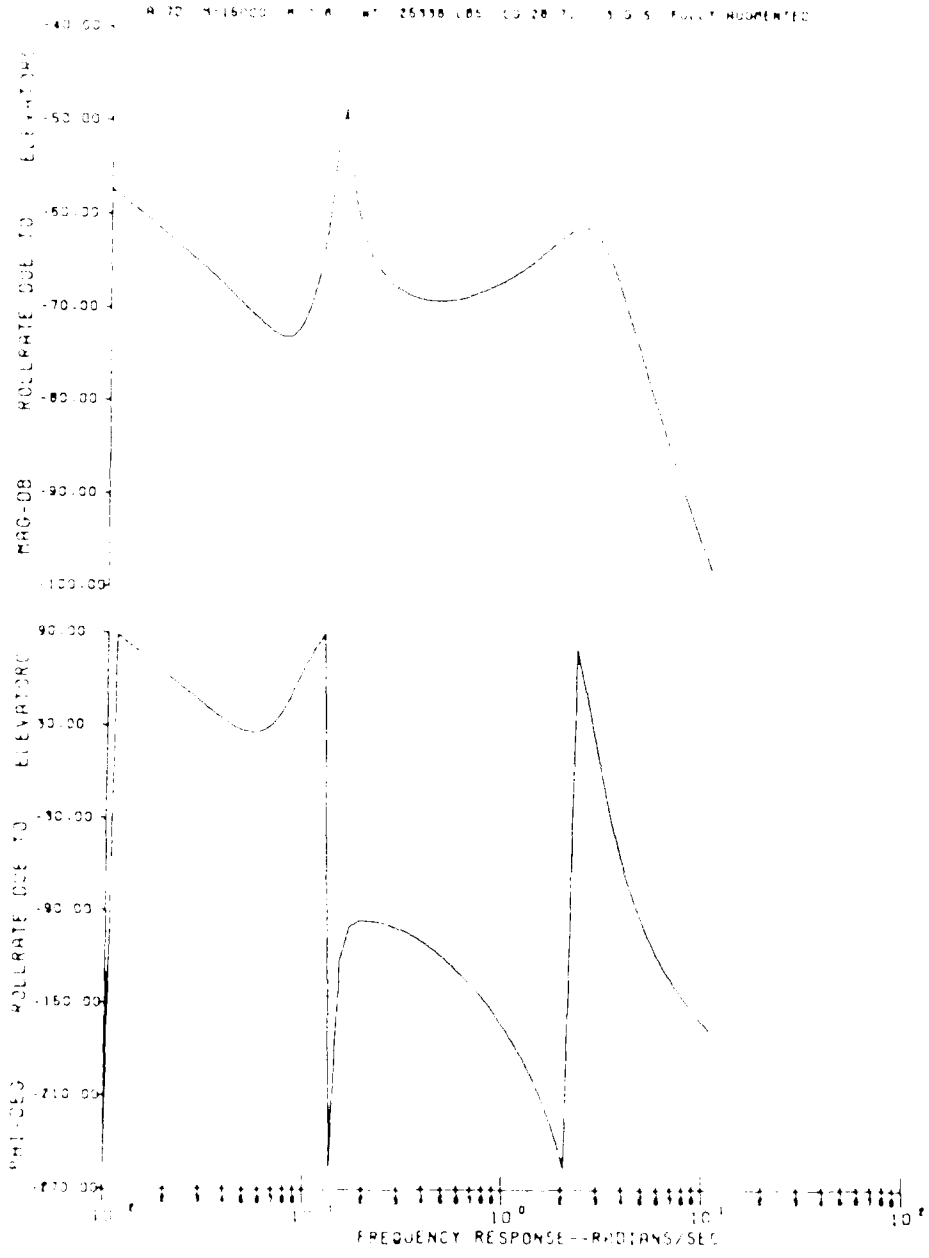

Figure F12. 76 Fully Augmented Bode Plot for Roll Rate due to Pilot Elevator Input

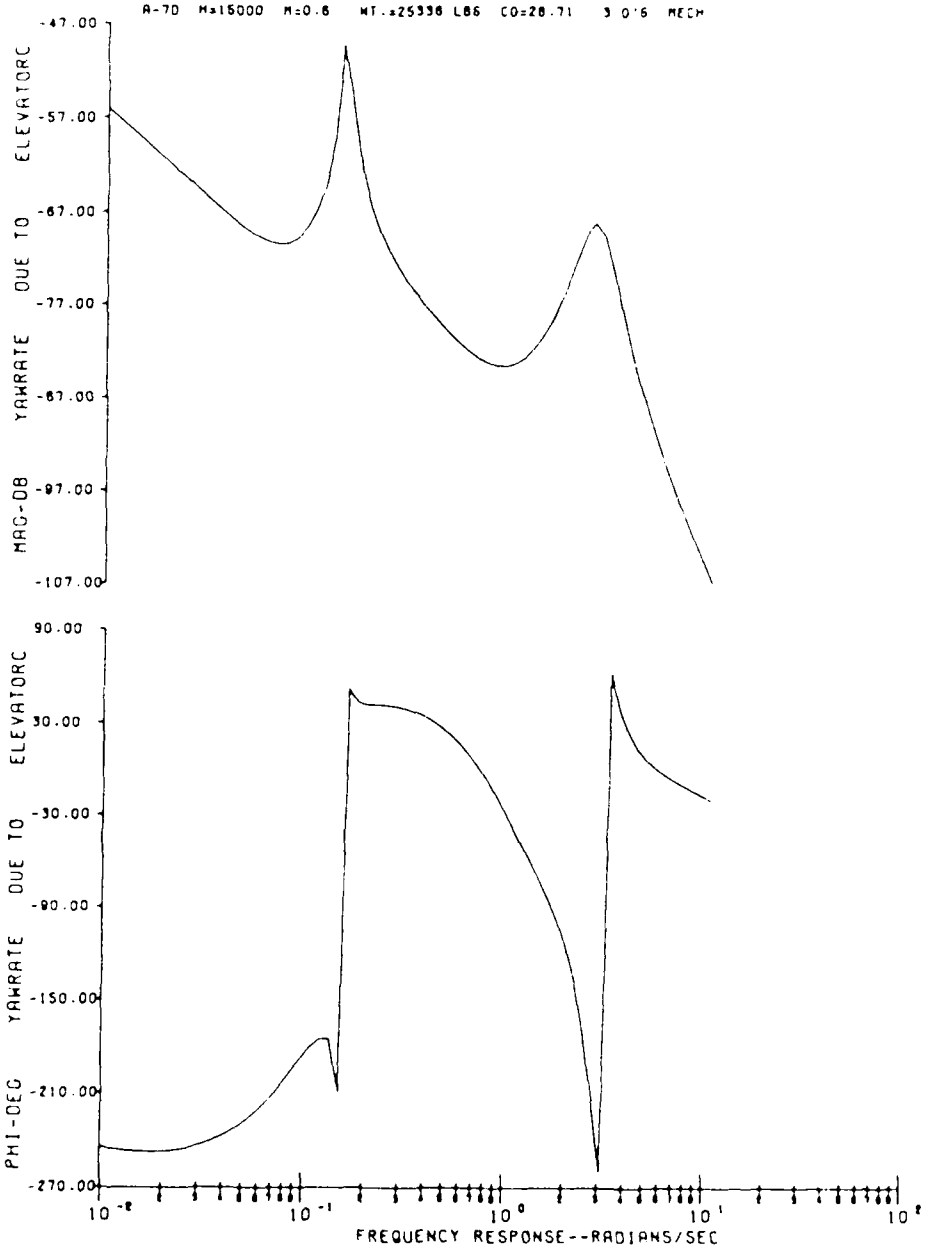

Figure F43. 3G Mechanical Bode Plot for Yaw Rate due to Pilot Elevator Input

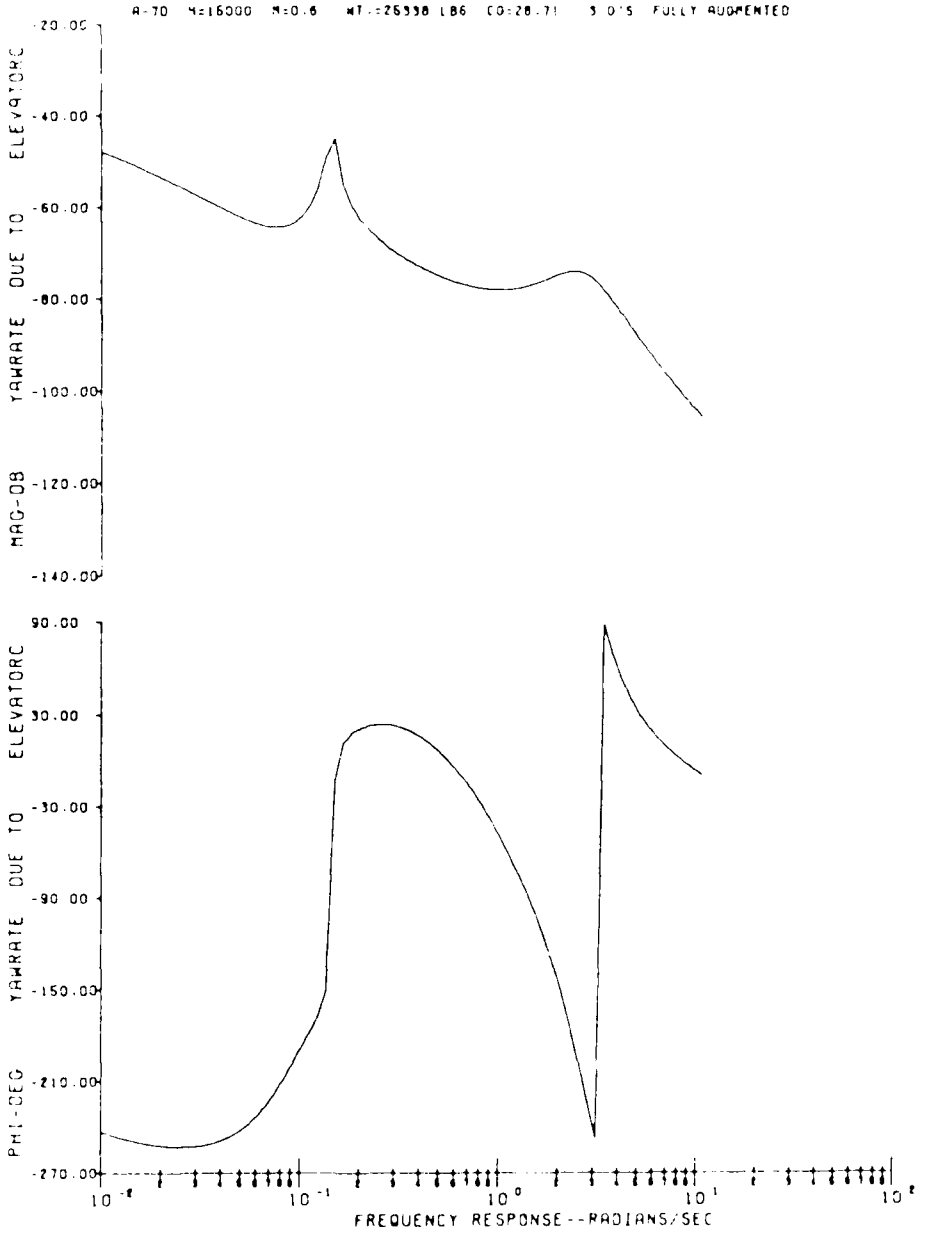

Figure F44. 3G Fully Augmented Bode Plot for Yaw Rate due to Pilot Elevator Input

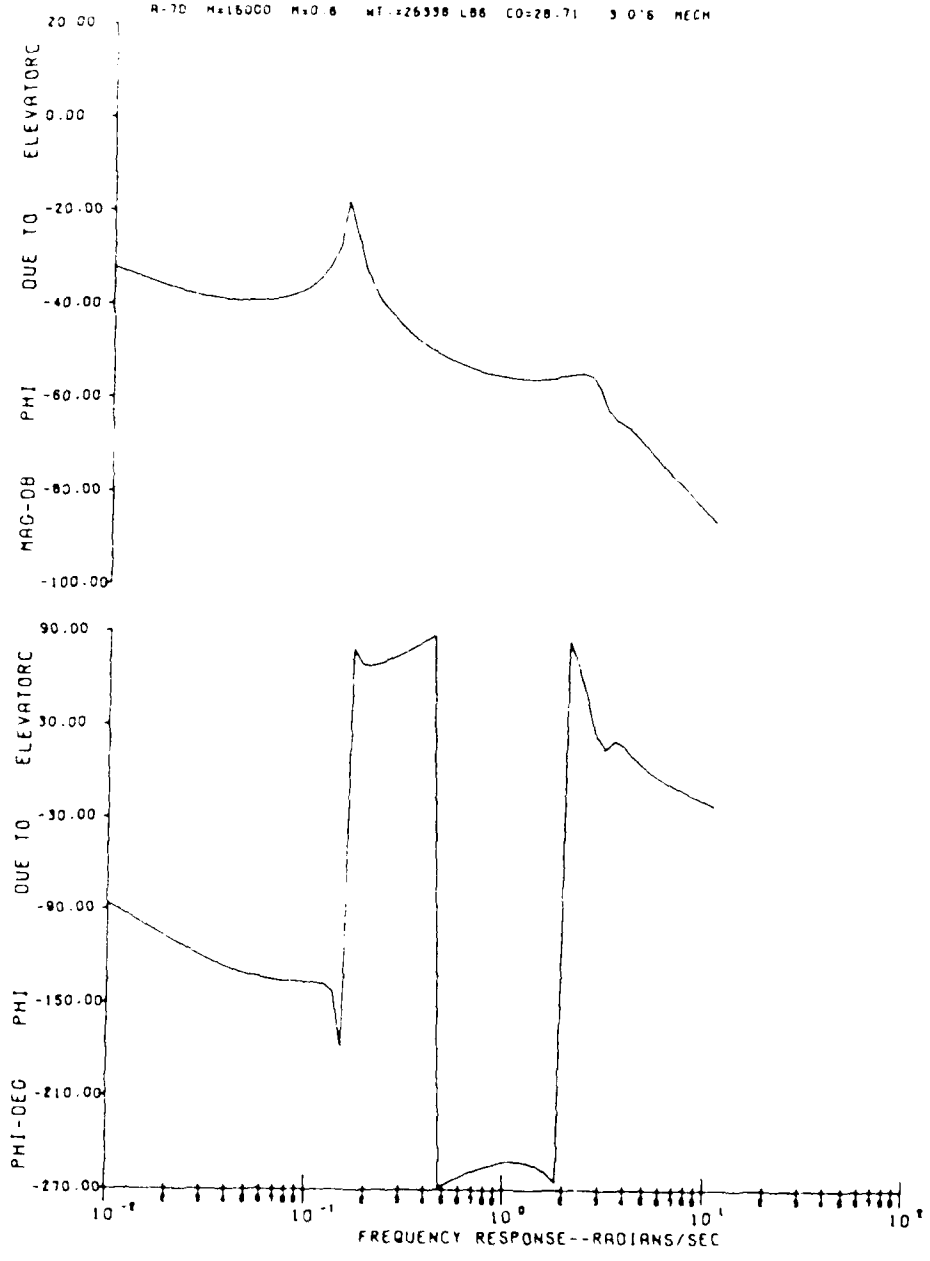

Figure F45. 3G Mechanical Bode Plot for Phi due to Pilot Elevator Input

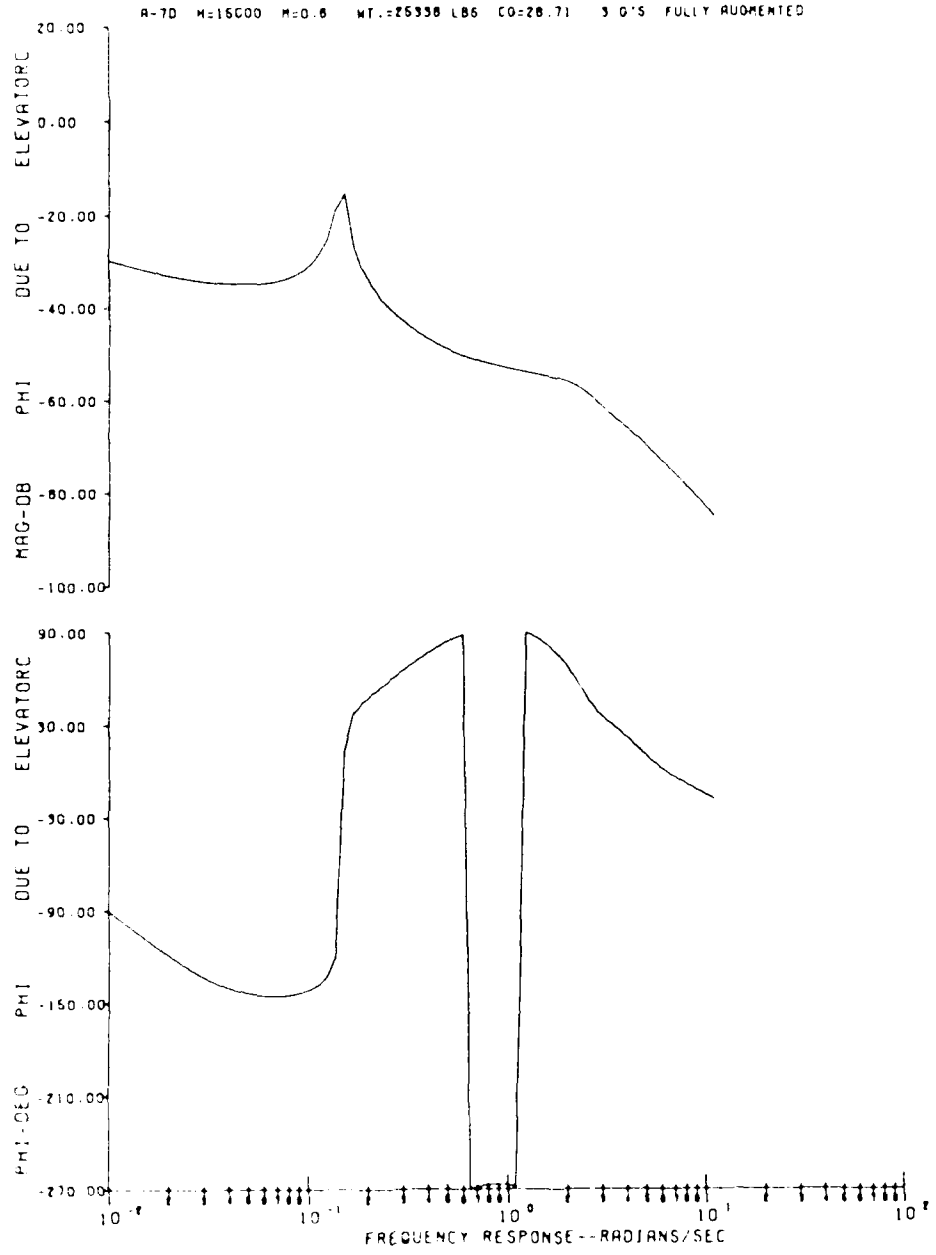

Figure F46. 3G Fully Augmented Bode Plot for Phi due to Pilot Elevator Input

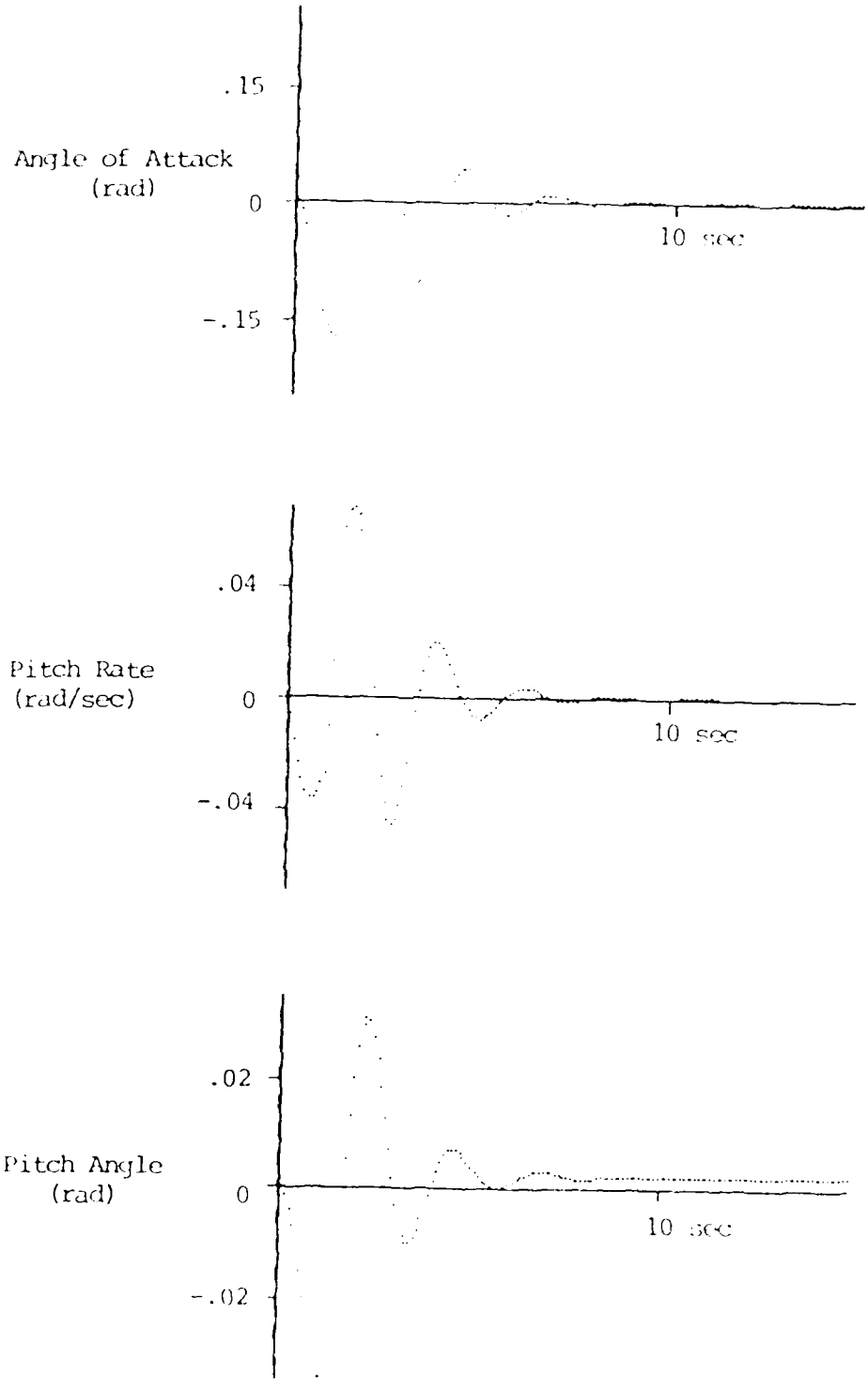

Figure 61. Simulated XG Mechanical Time Response to 5 lb Elevator Doublet

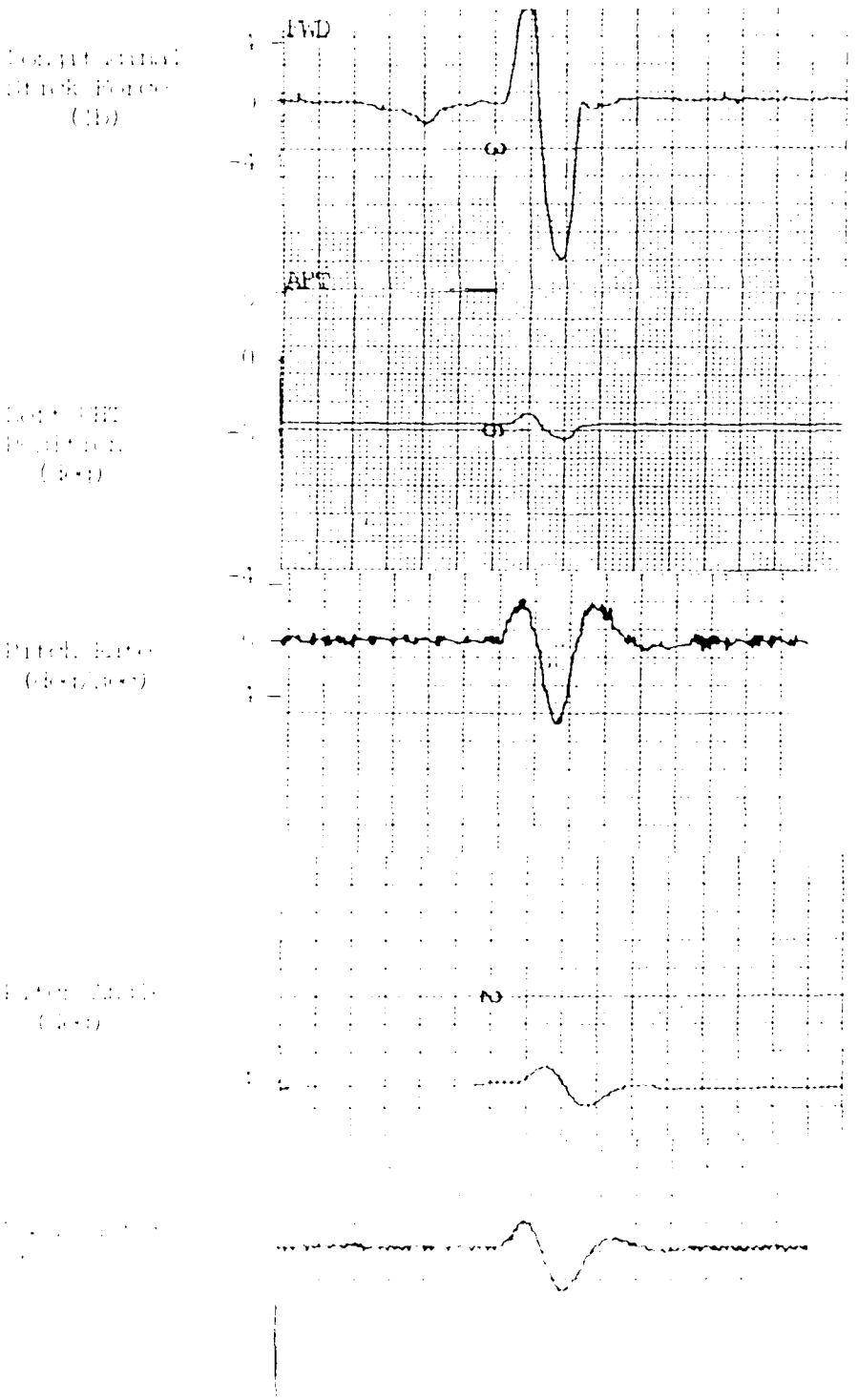

Fig. [illegible] Mechanical Time Histories
for Elevation Load Set

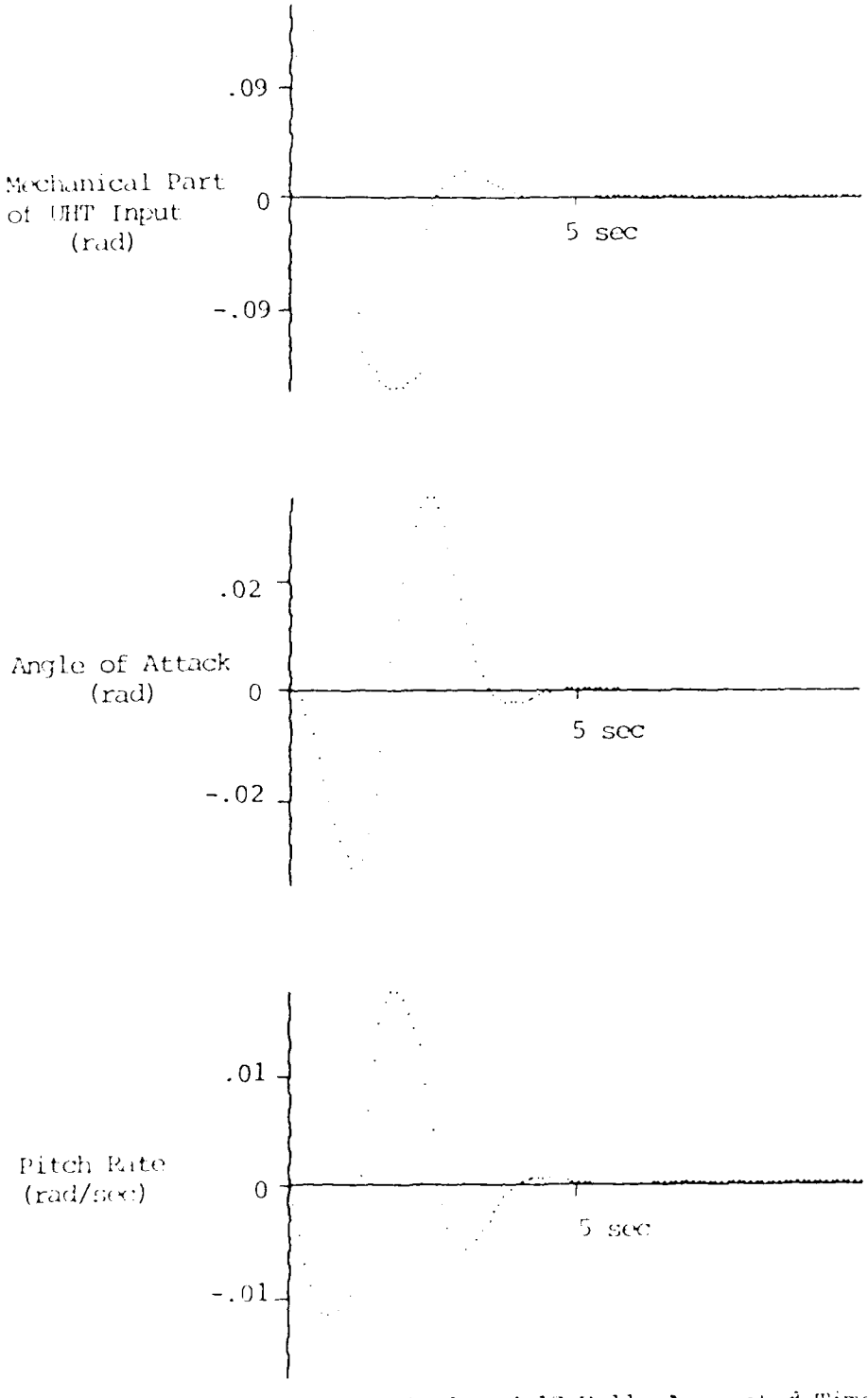

Figure G3. Simulated 1G Fully Augmented Time Response to 5 lb Elevator Doublet

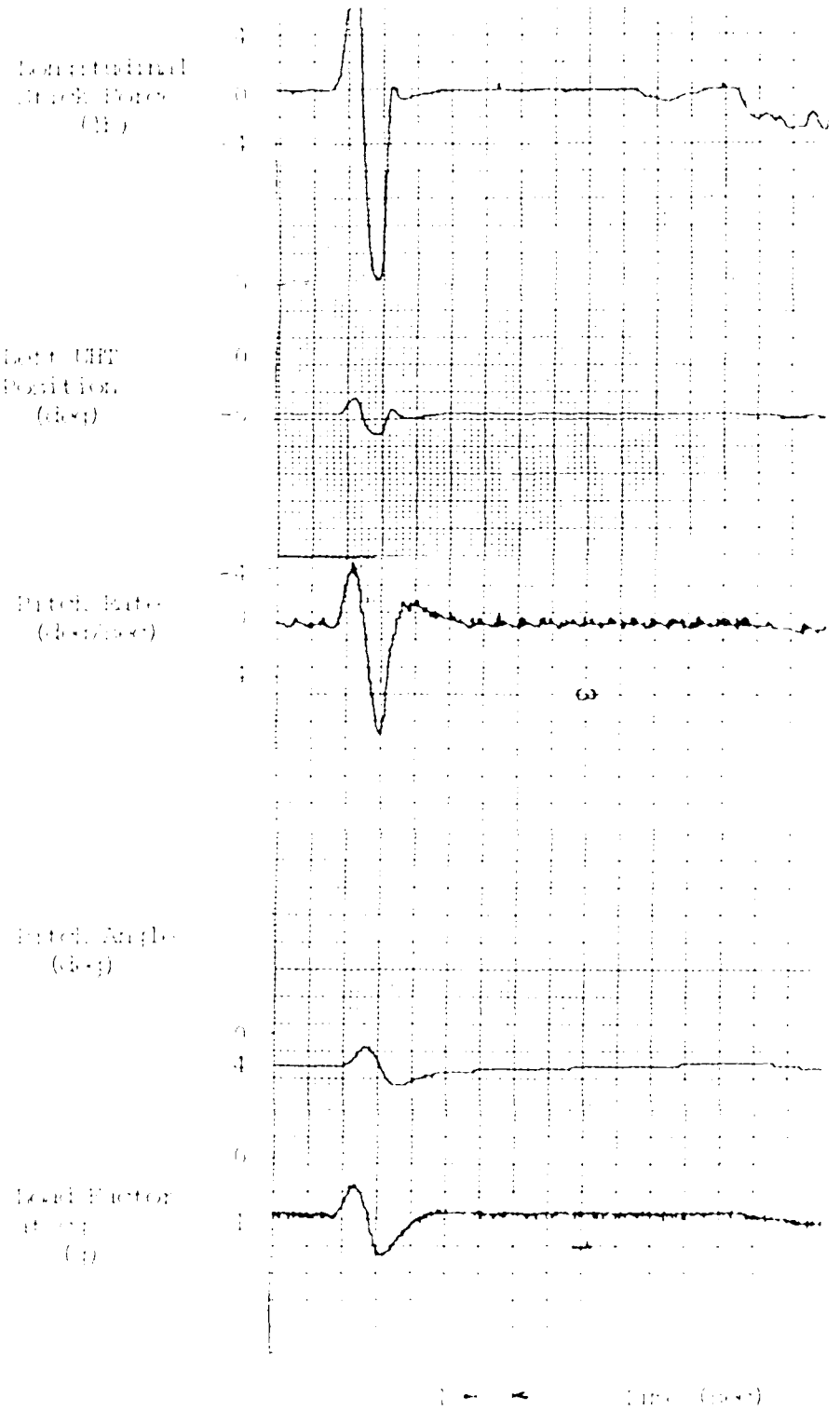
Longitudinal
Stick Force
(lb)
Left VHT
Position
(deg)
Pitch Rate
(deg/sec)
Pitch Angle
(deg)
Load Factor
(g)
Time (sec)

Figure 81. [illegible]

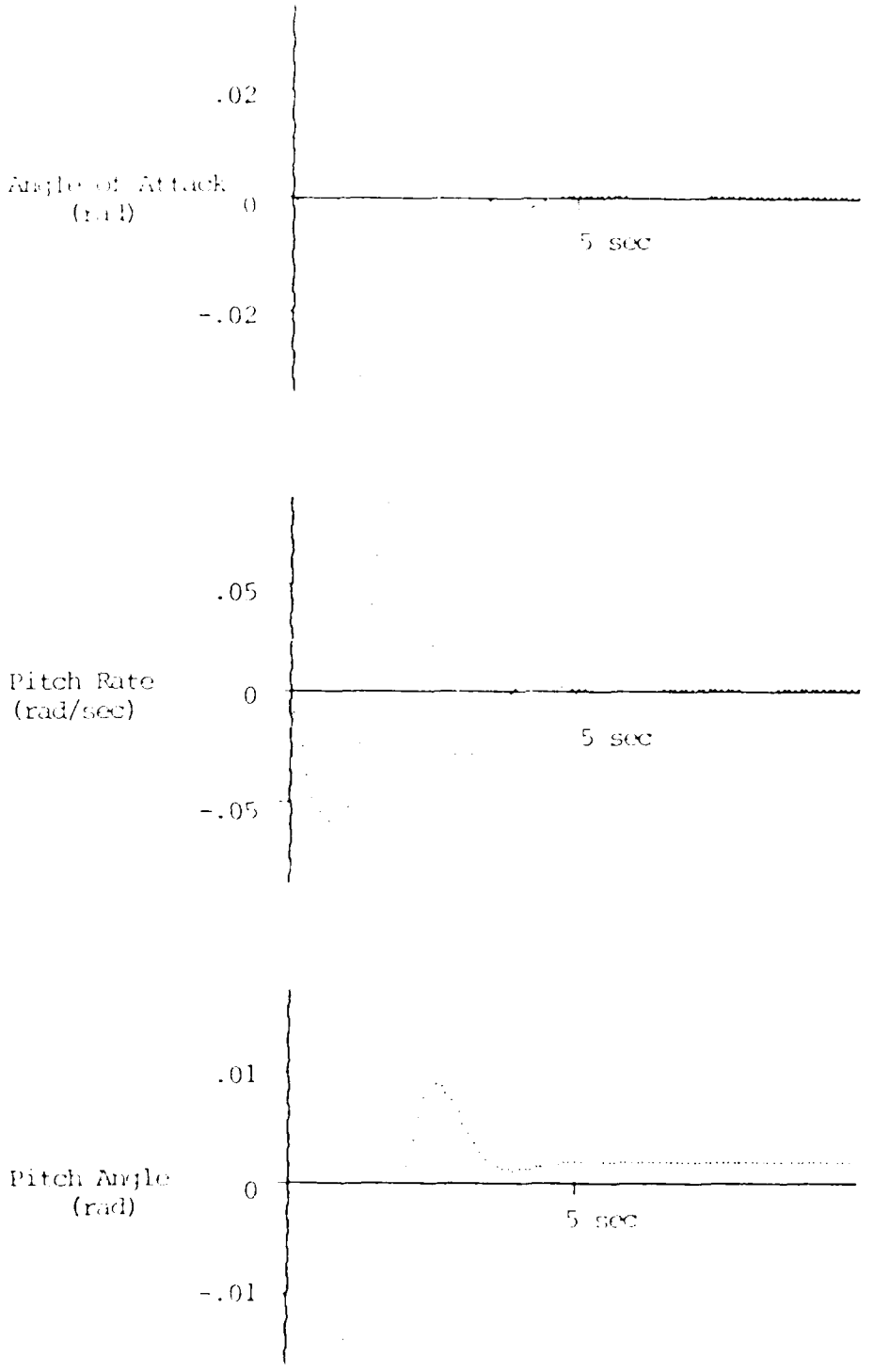

Figure 65. Simulated X3 Fully Augmented Time Response to 5 lb Elevator Doublet

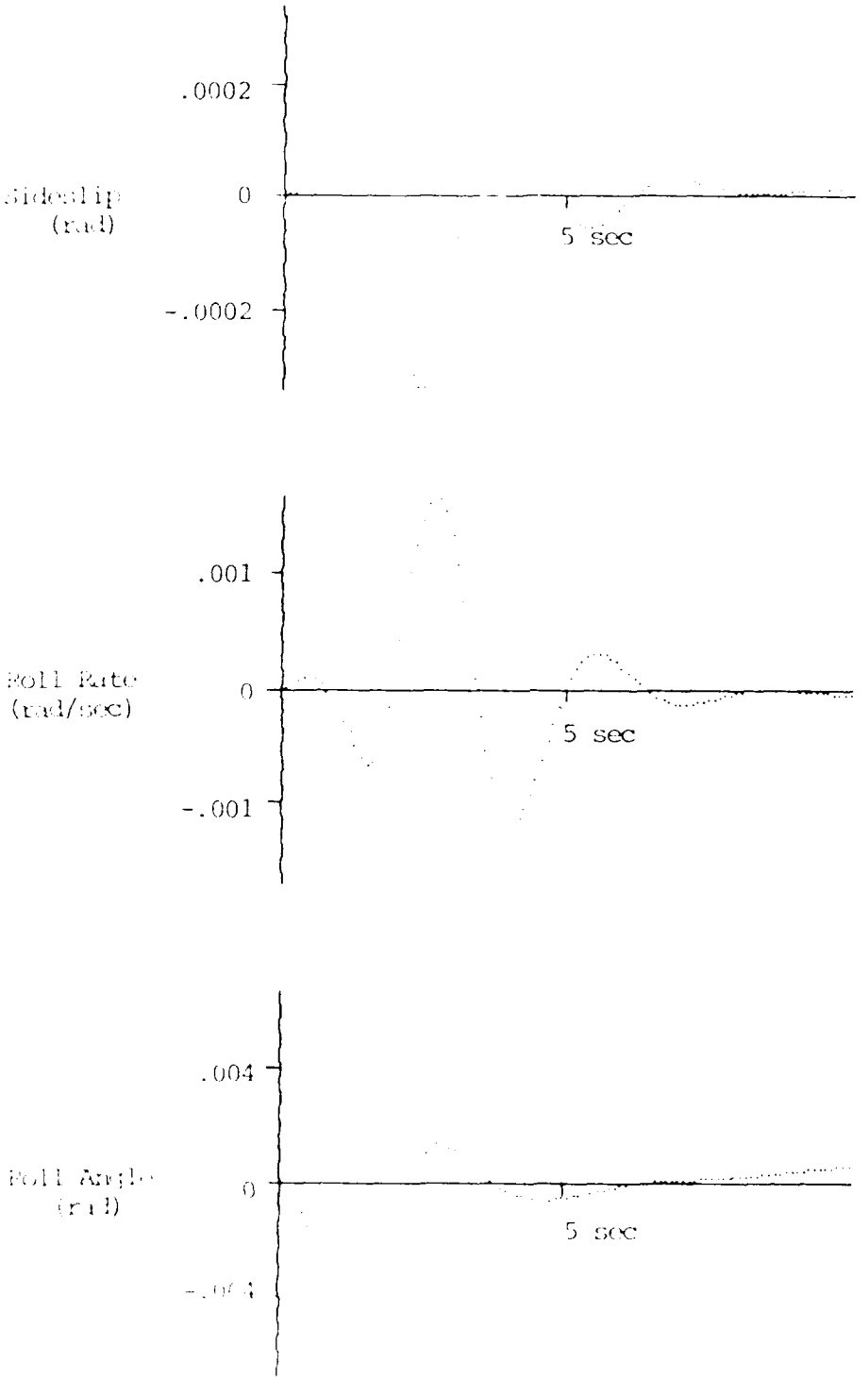

Figure 66. Simulated 25 Fully Augmented Time Response to 5 lb Elevator Doublet (Cross Coupling)

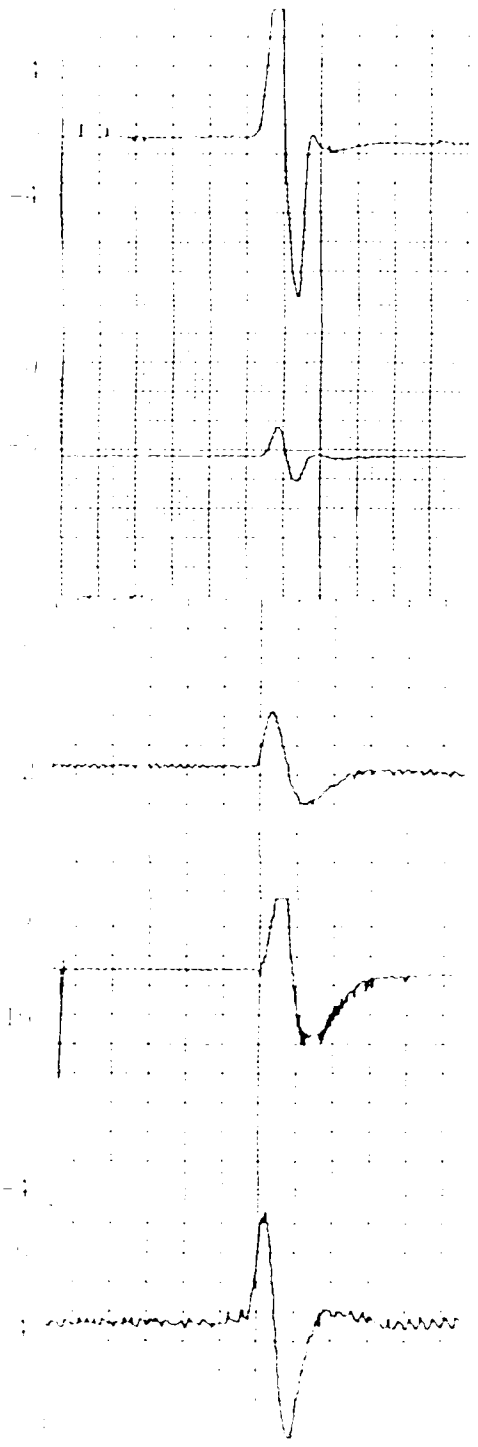

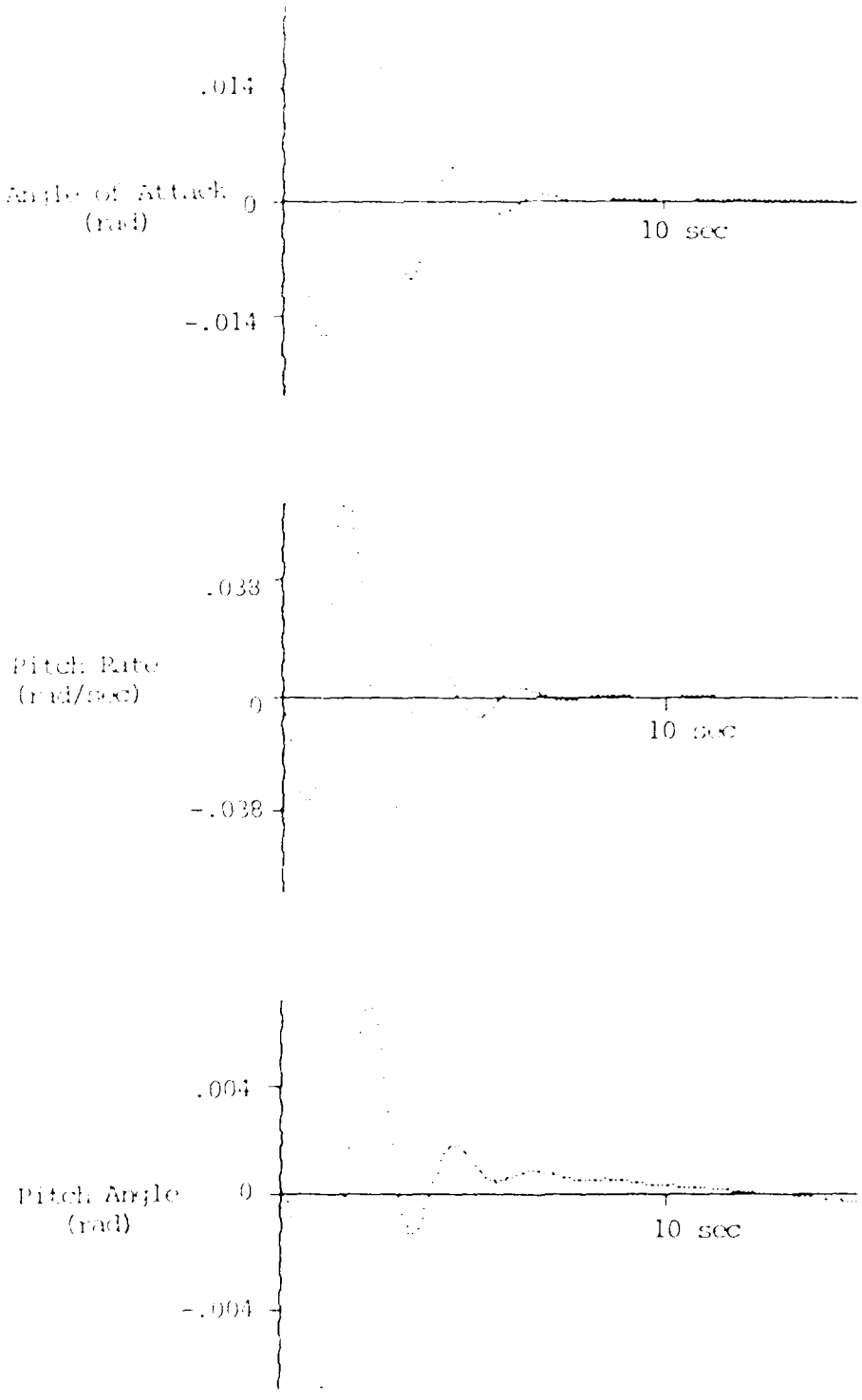

Figure 68. Simulated 5% Mechanical Time Response to 5 lb Elevator Doublet

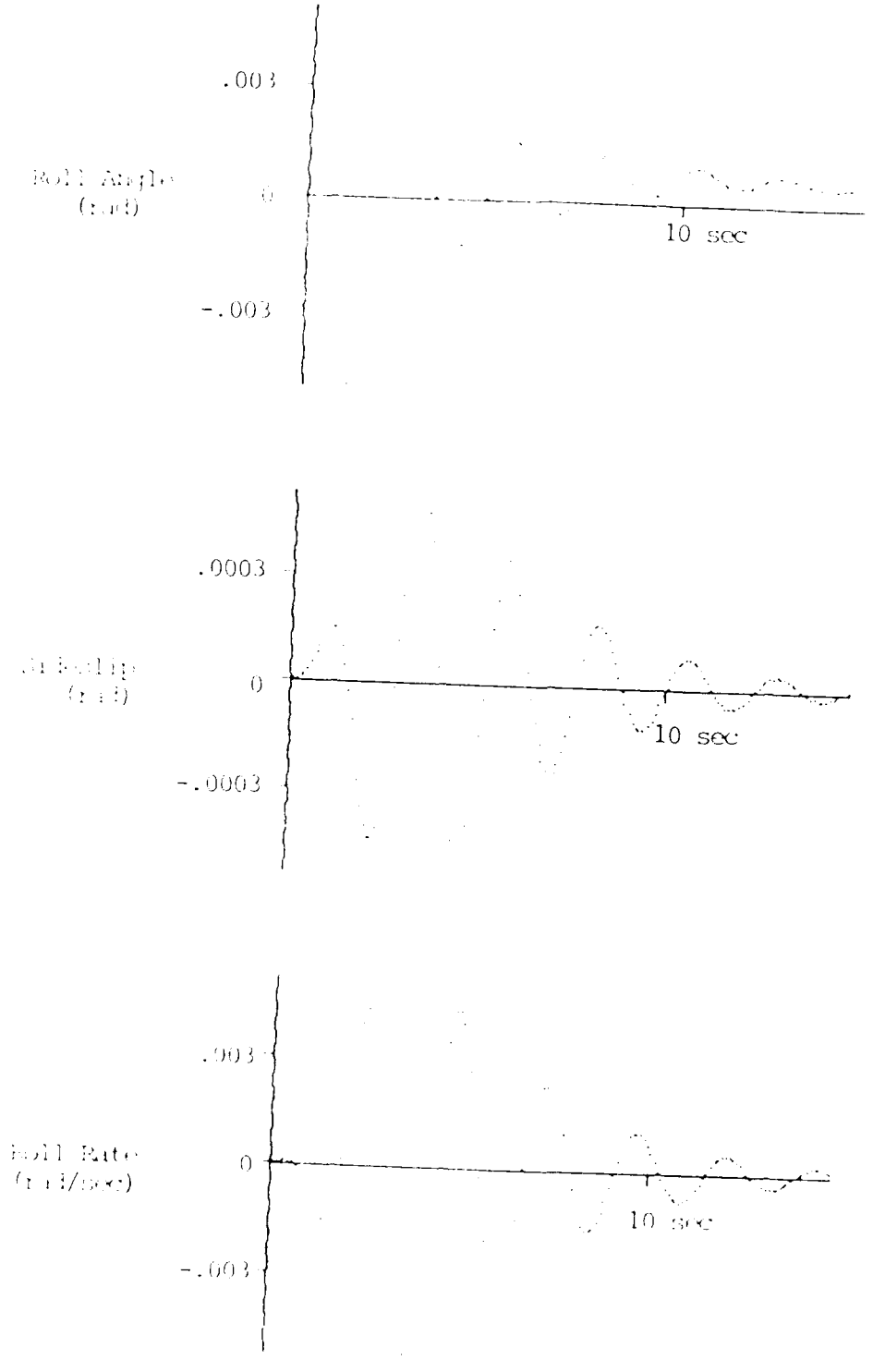

Figure [illegible]. Simulated 6 Mechanical Time Responses to 5 lb Elevator Doublet

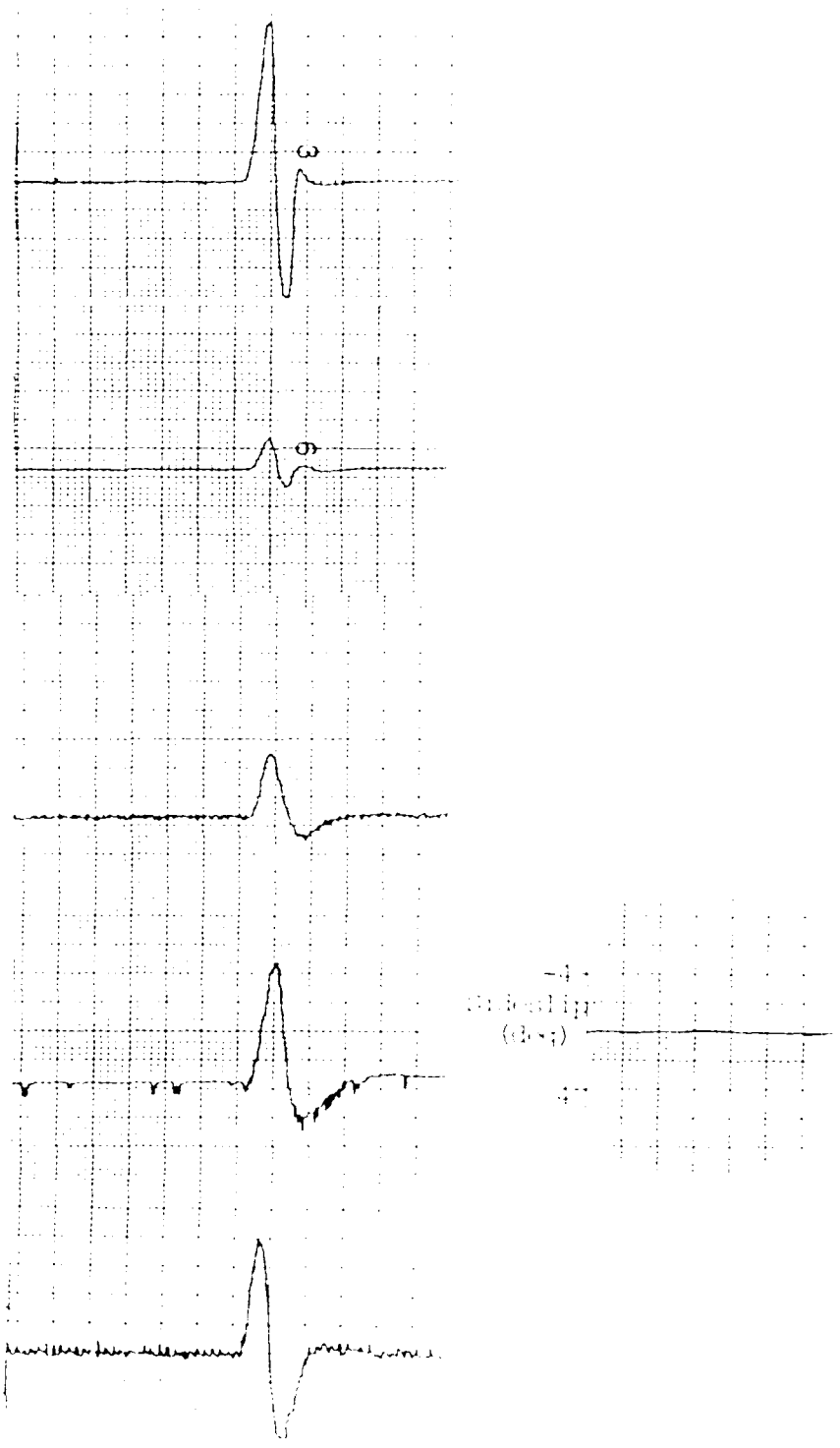

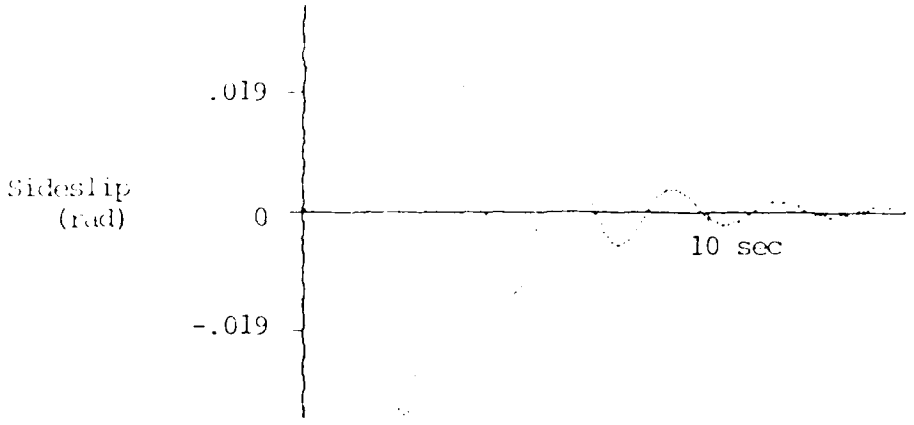

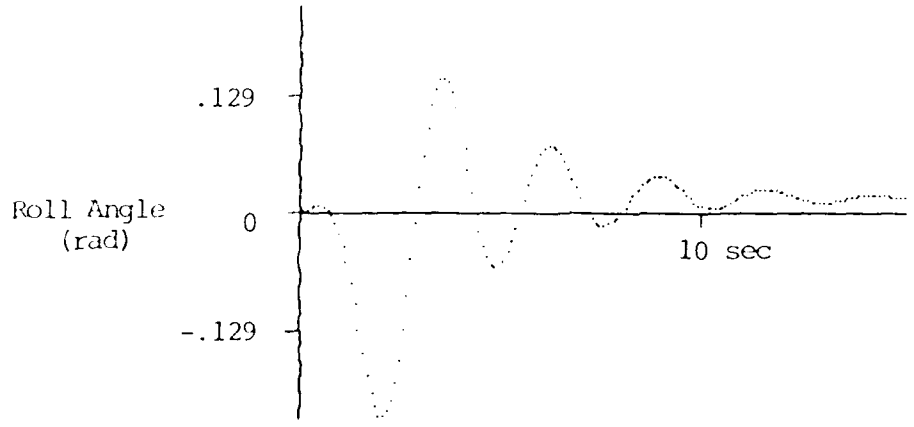

Figure G11. Simulated 1G Mechanical Time Response to 20 lb Rudder Doublet

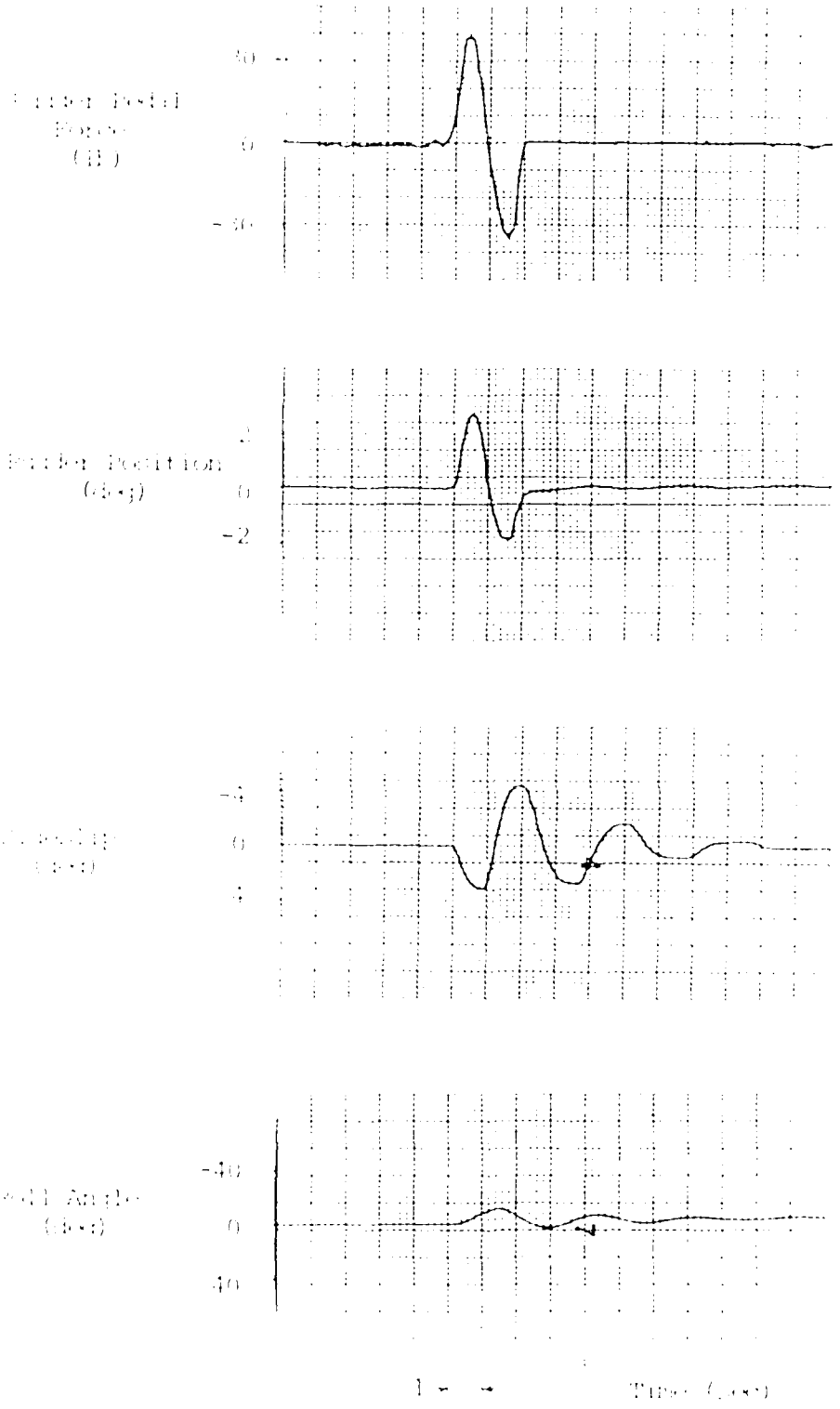

Figure 6.12. 95 Mechanical Tire Response to Pulse Loading

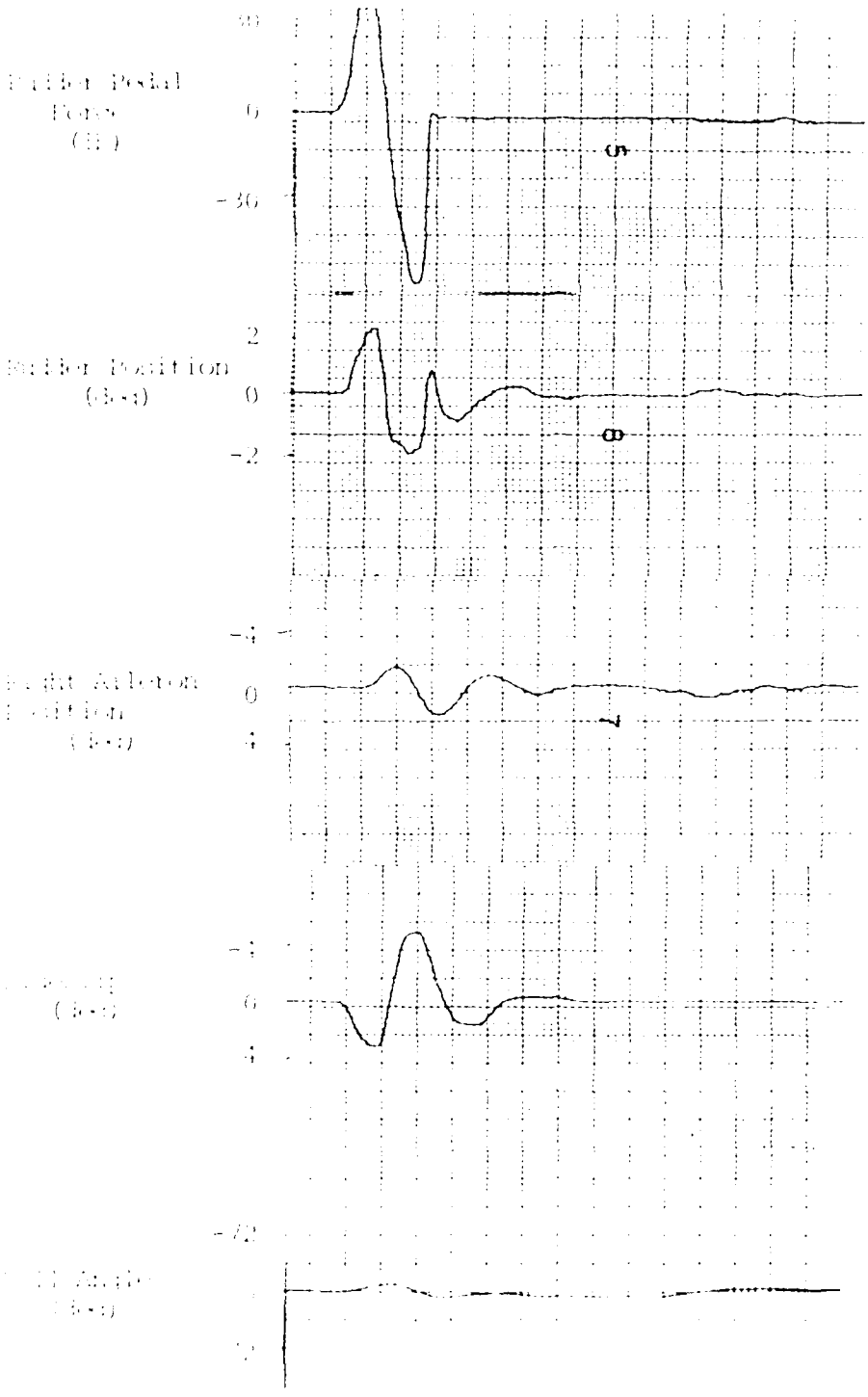
Rudder Pedal Force (lb)
Rudder Position (deg)
Right Aileron Position (deg)
(deg)
(deg)
6
-36
2
0
-2
-4
0
4
-4
0
4
-12
2

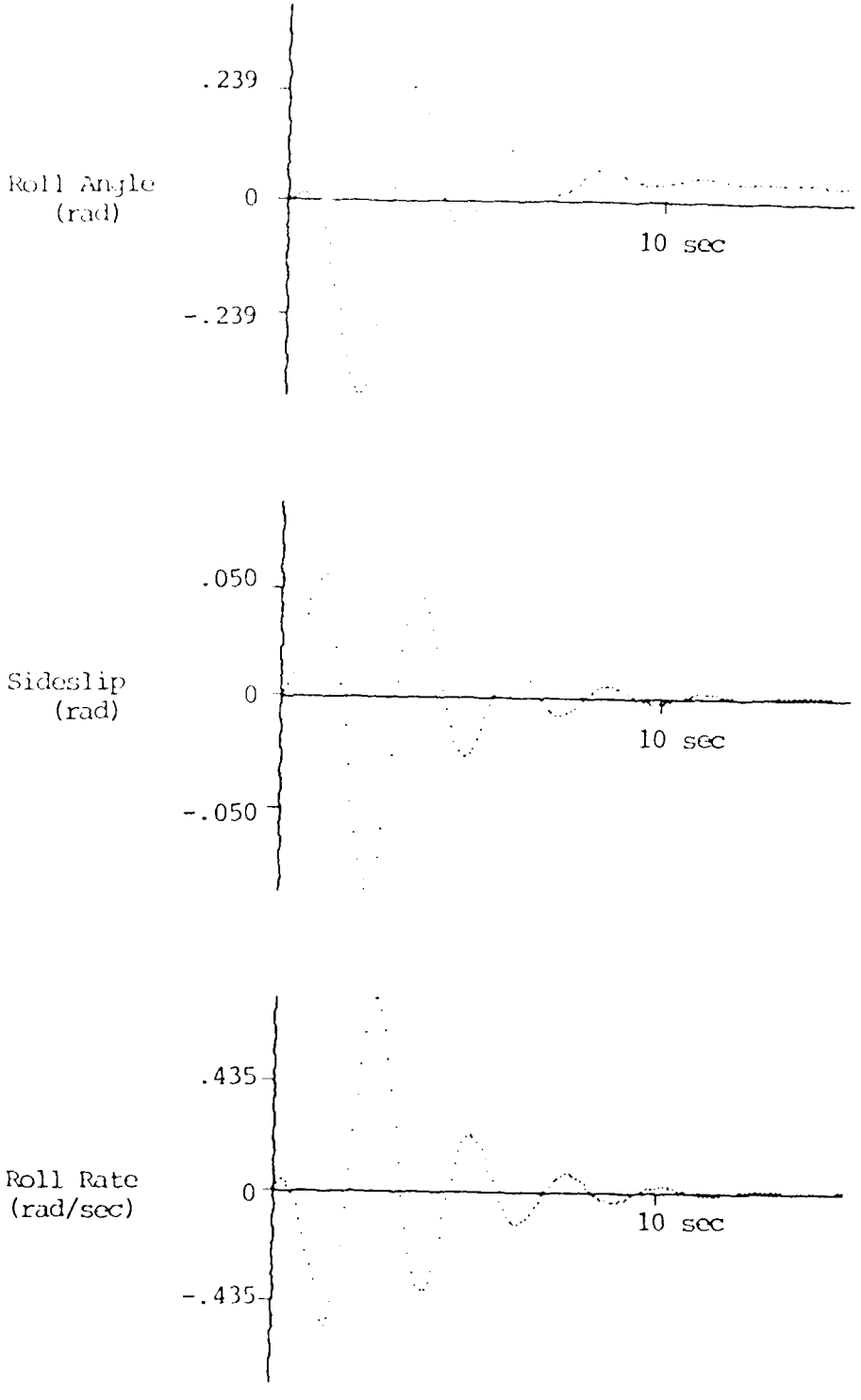

Figure G14. Simulated 2G Mechanical Time Response to 40 lb Rudder Doublet

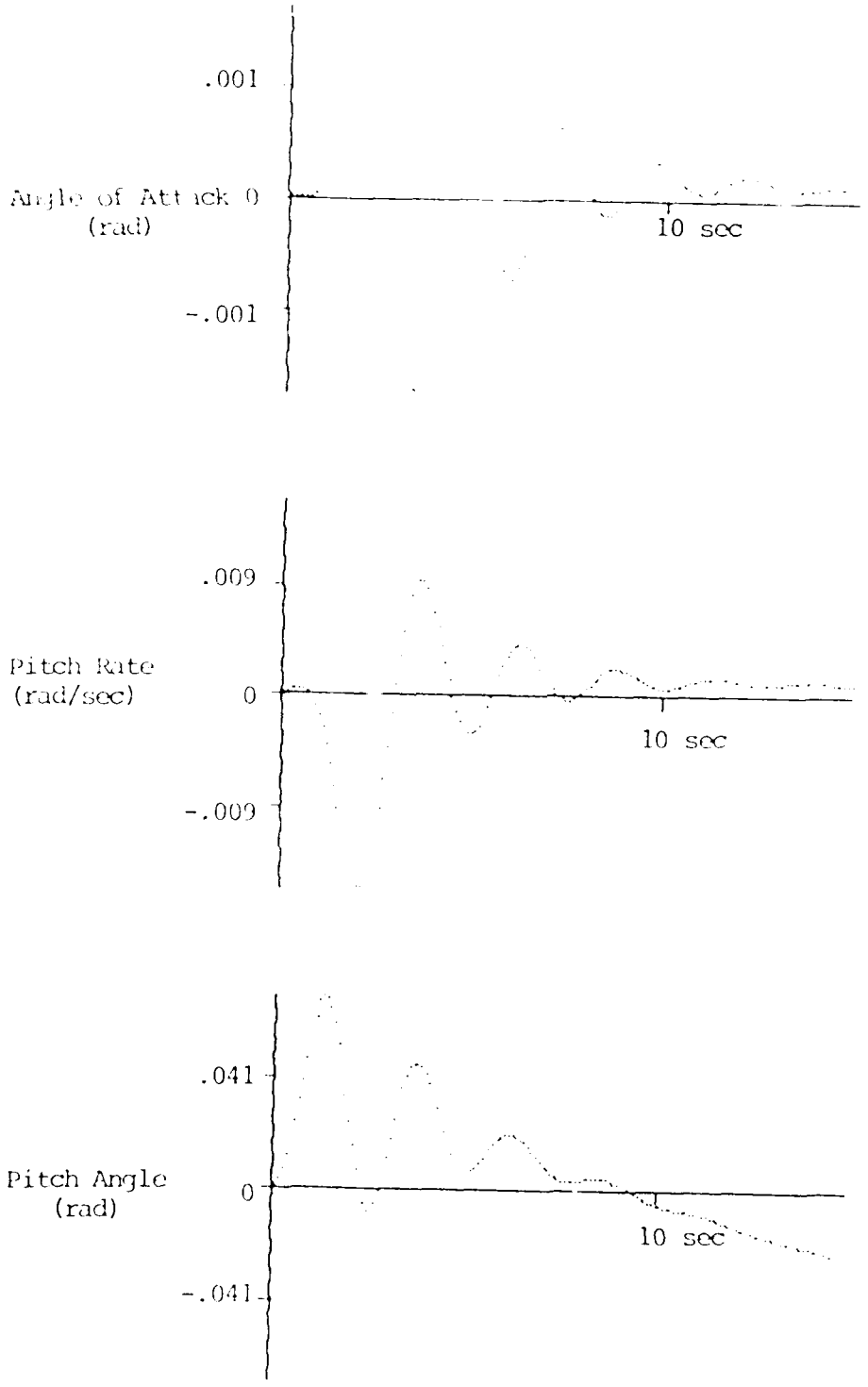

Figure G15. Simulated 2G Mechanical Time Response to 40 lb Rudder Doublet (Cross Coupling)

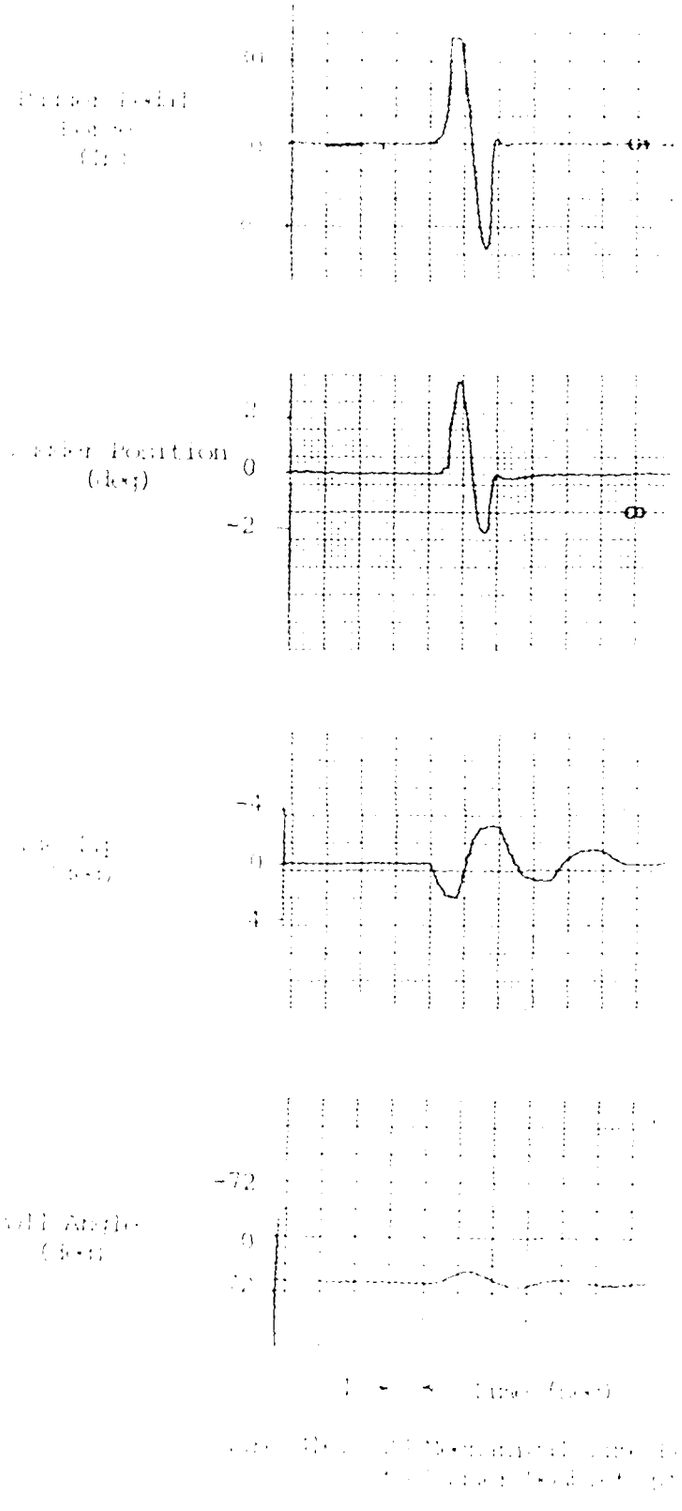

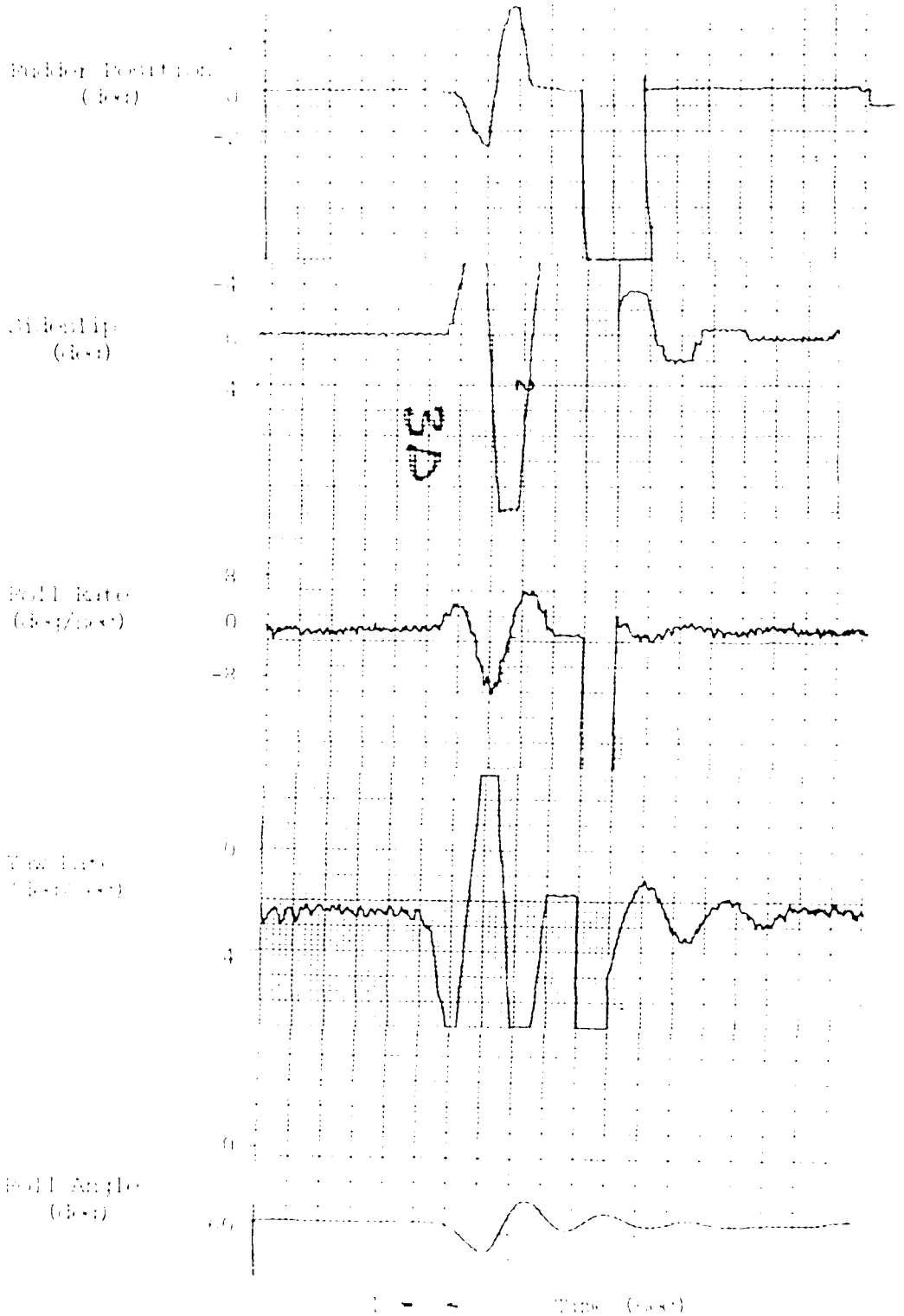

Figure 6.12 Pilot Response Time History for Pilot Induced Oscillation (Case II)

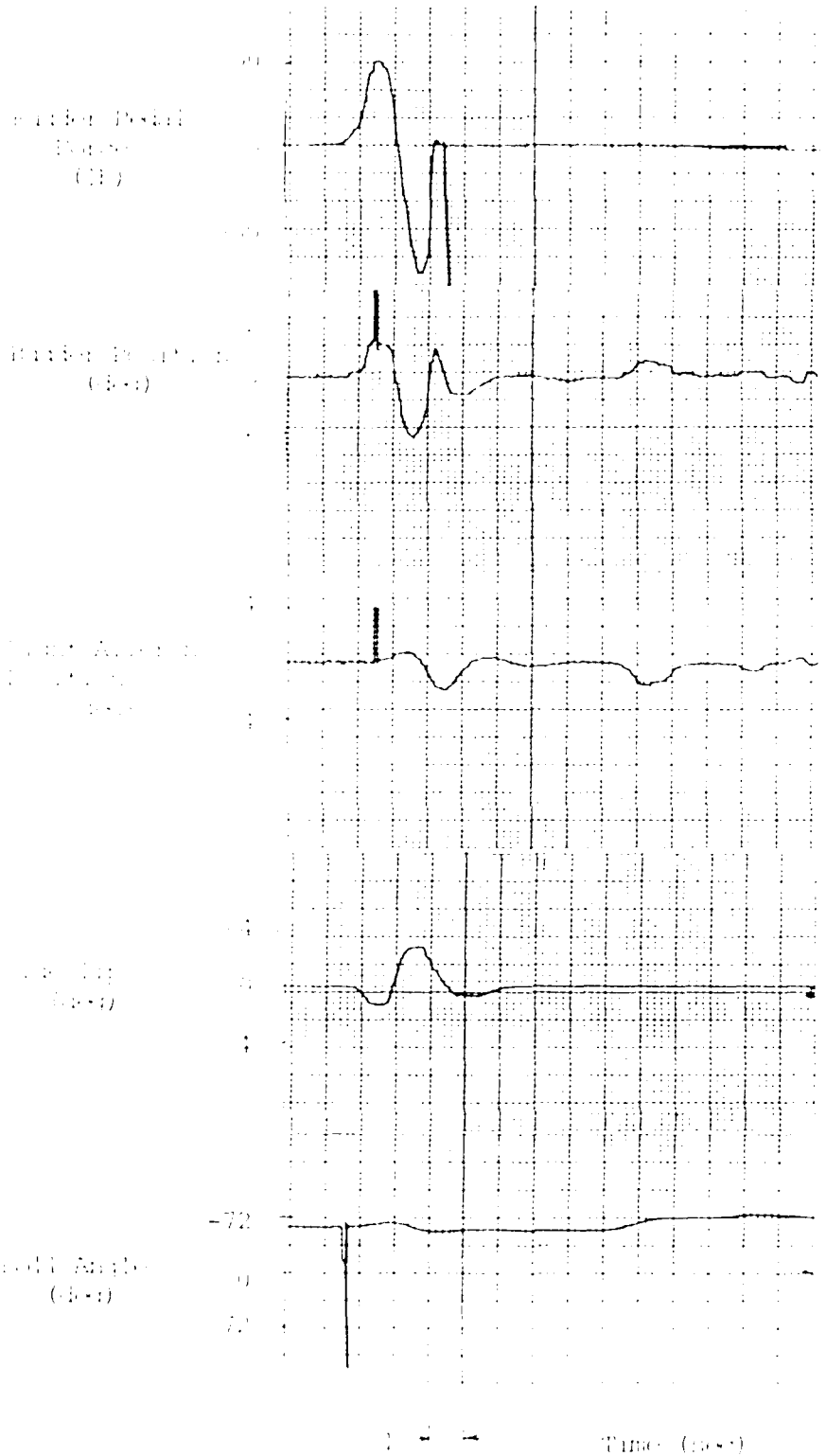

Time (sec)

Fully augmented Time Response
to Rubber Doublet

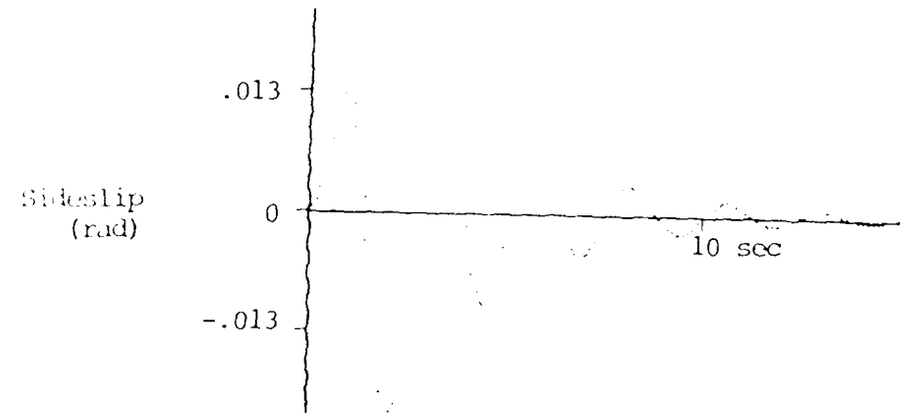

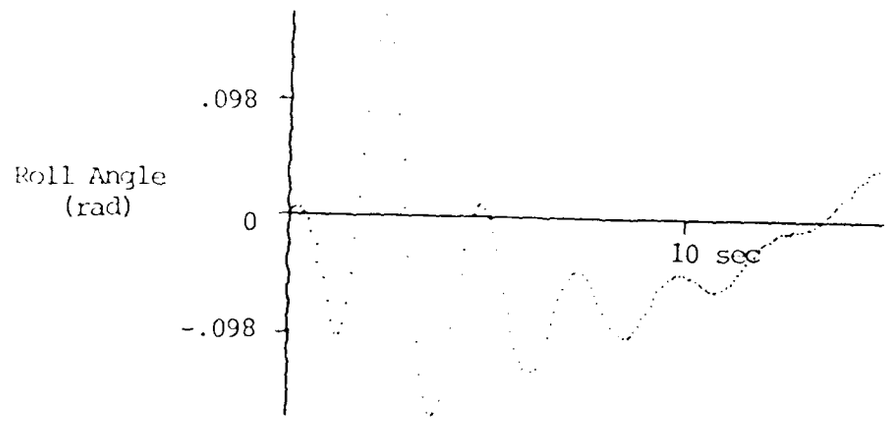

Figure G19. Simulated 3G Mechanical Time Response to 20 lb Rudder Doublet

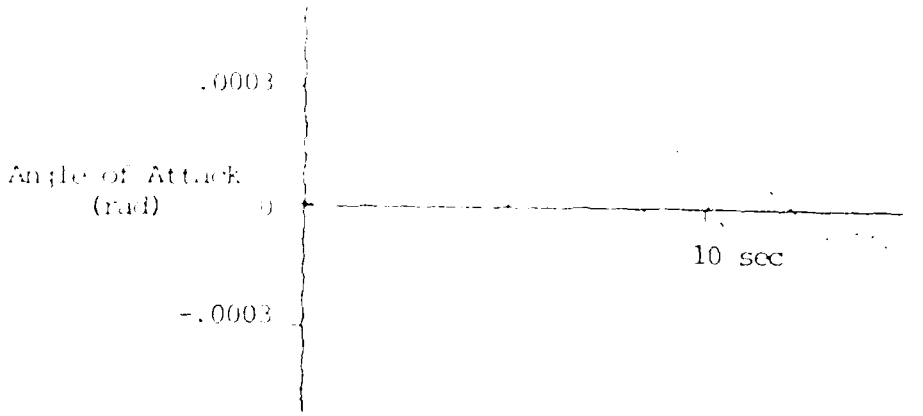

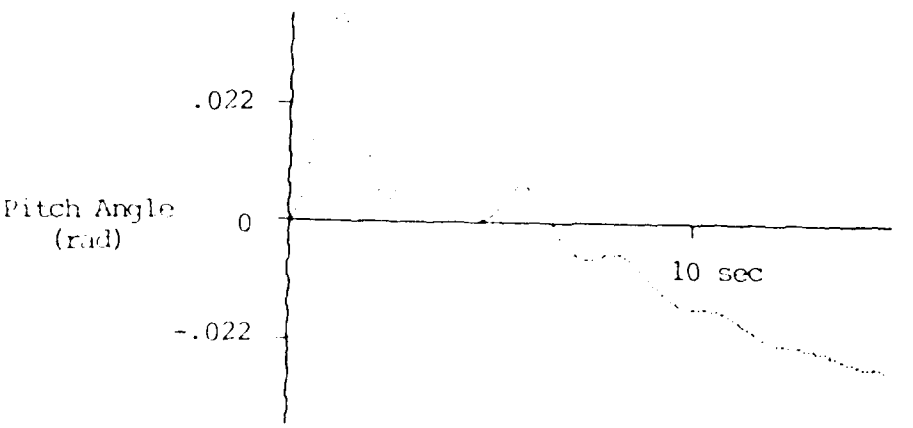

Figure G20. Simulated 3G Mechanical Time Response to 20 lb Rudder Doublet (Cross Coupling)

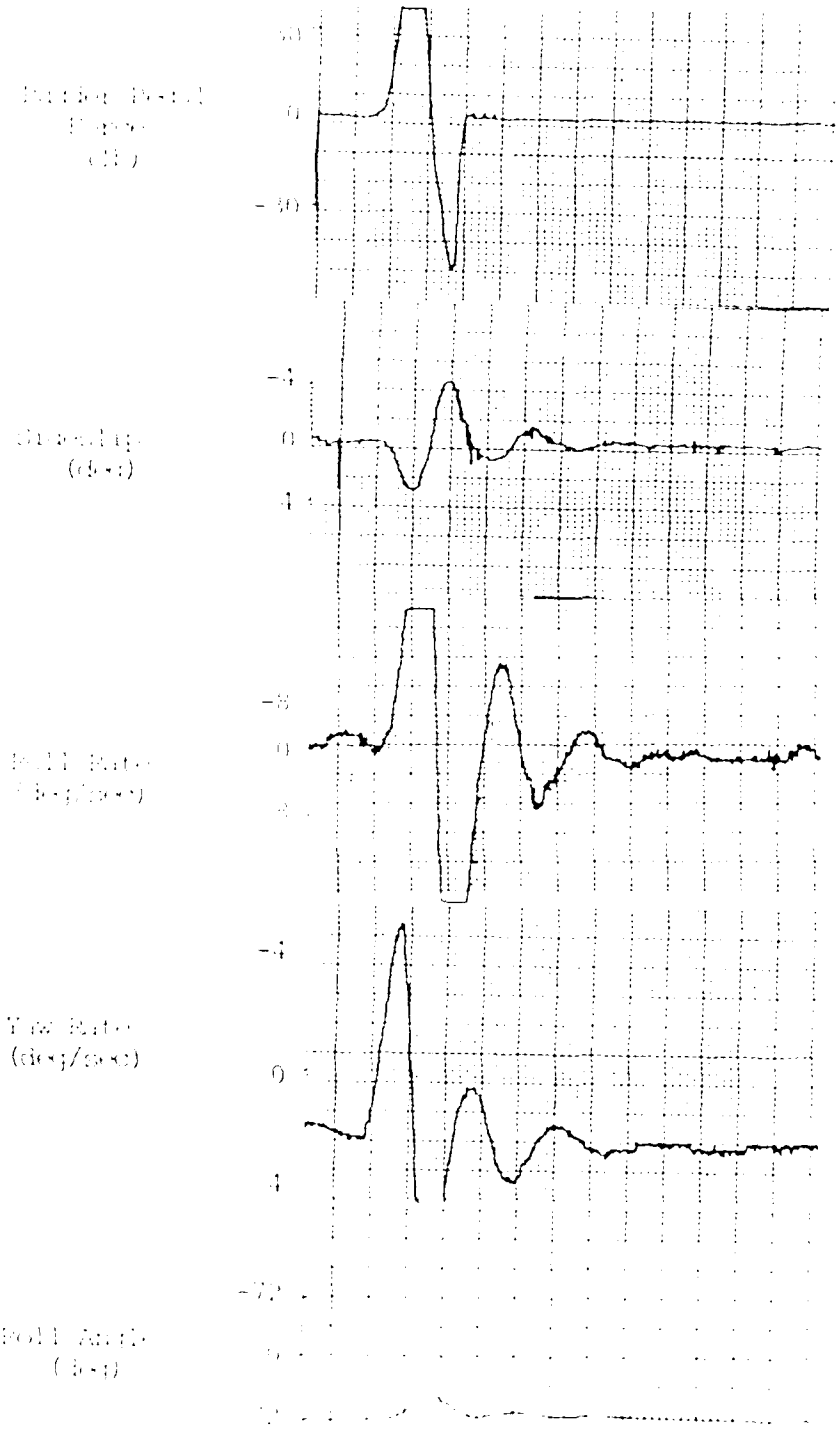

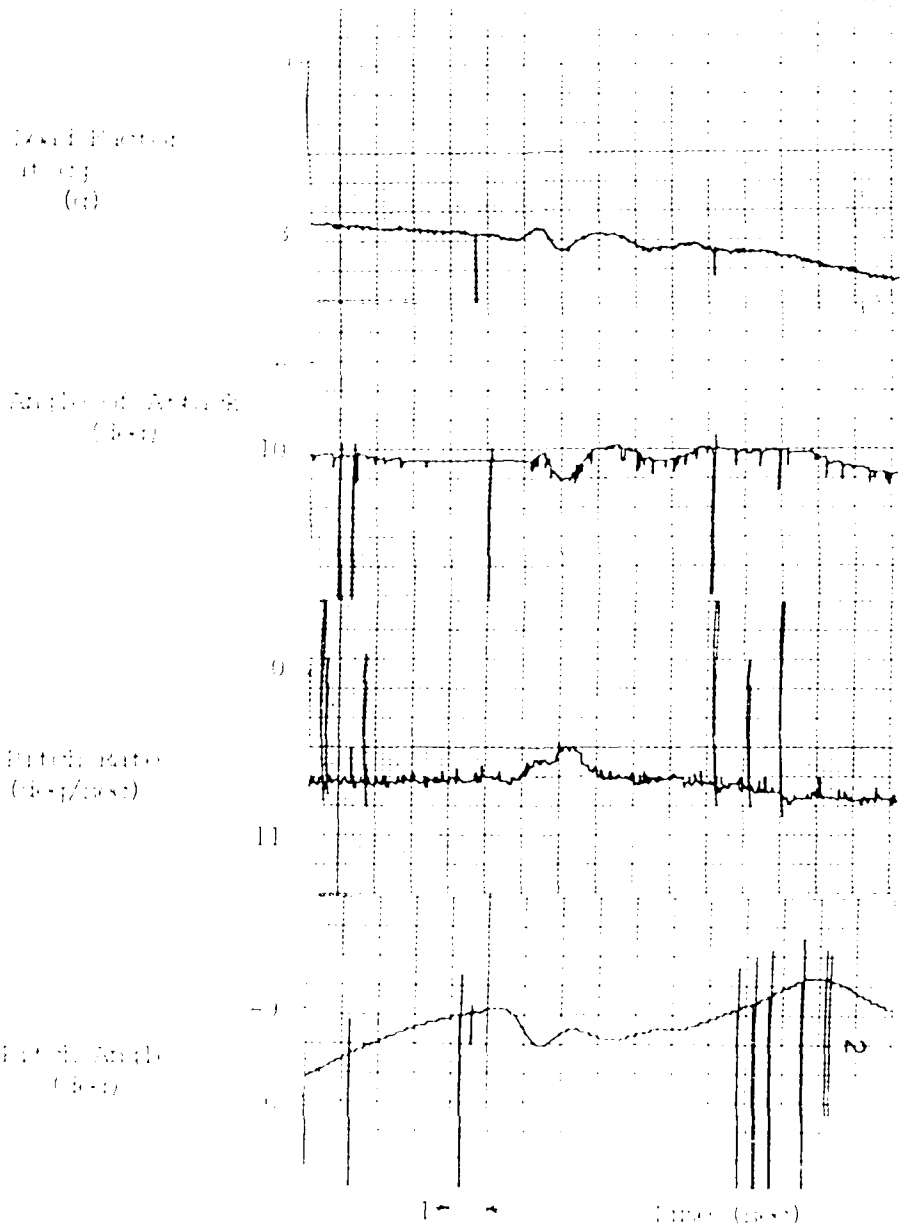

[illegible] 3 Mechanical Time Response to
Pulse Inputs (Cross-Coupling)

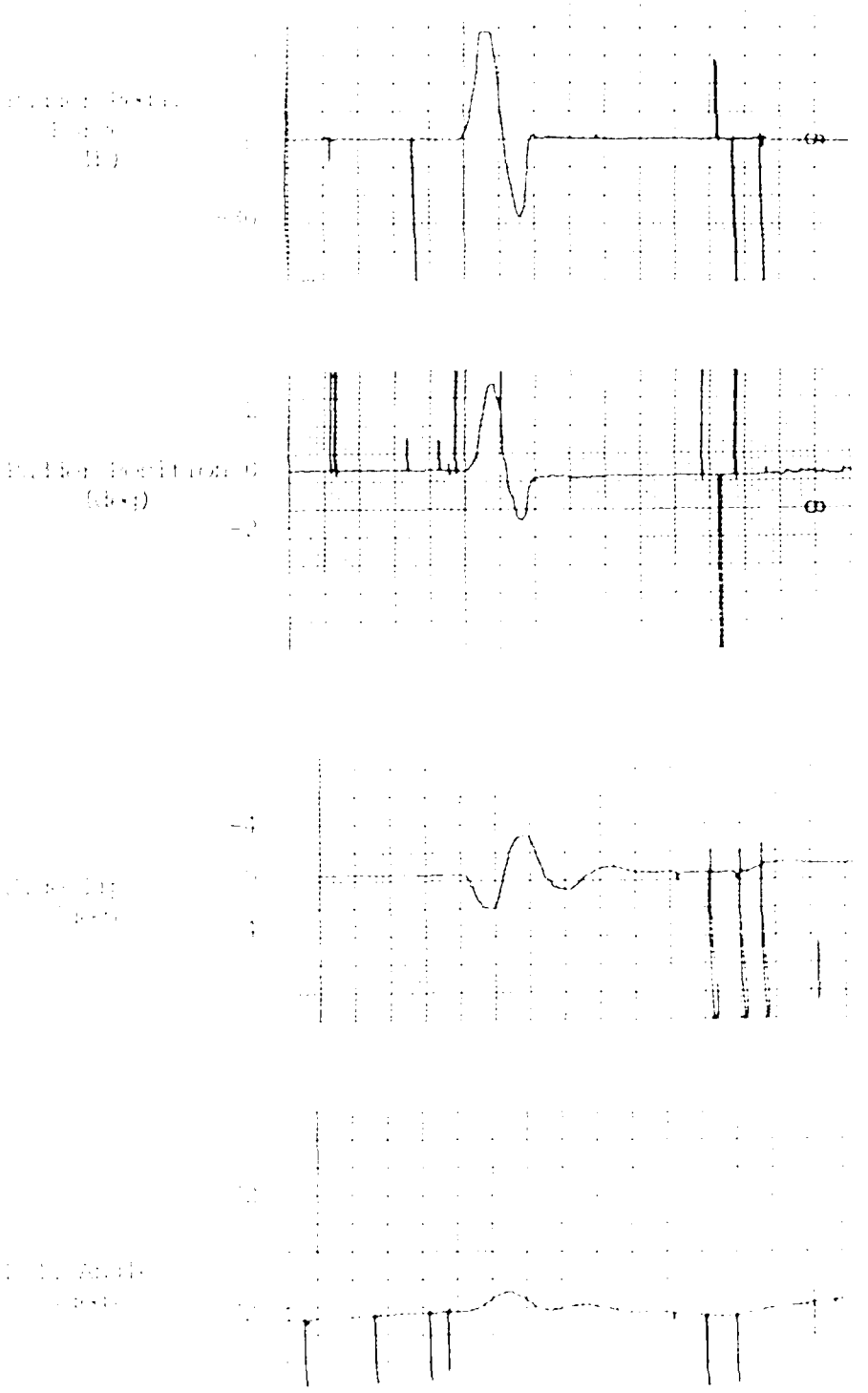

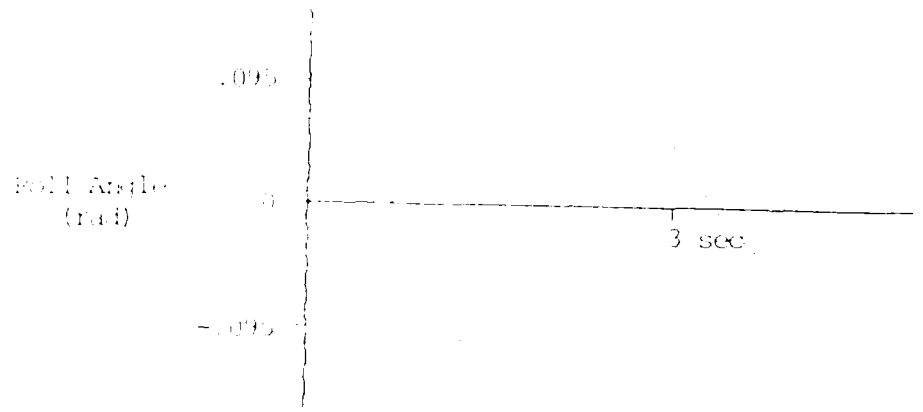

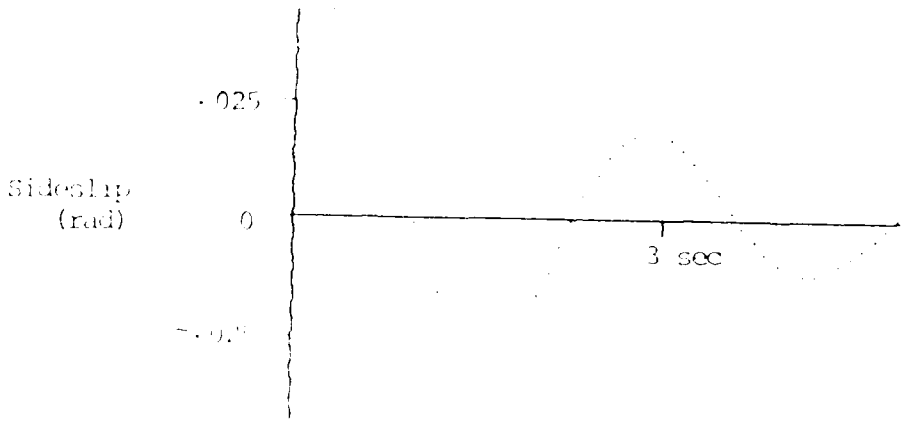

Figure [illegible] Aperiodic Tire Response
(Step Roll Disturbance for 1°)

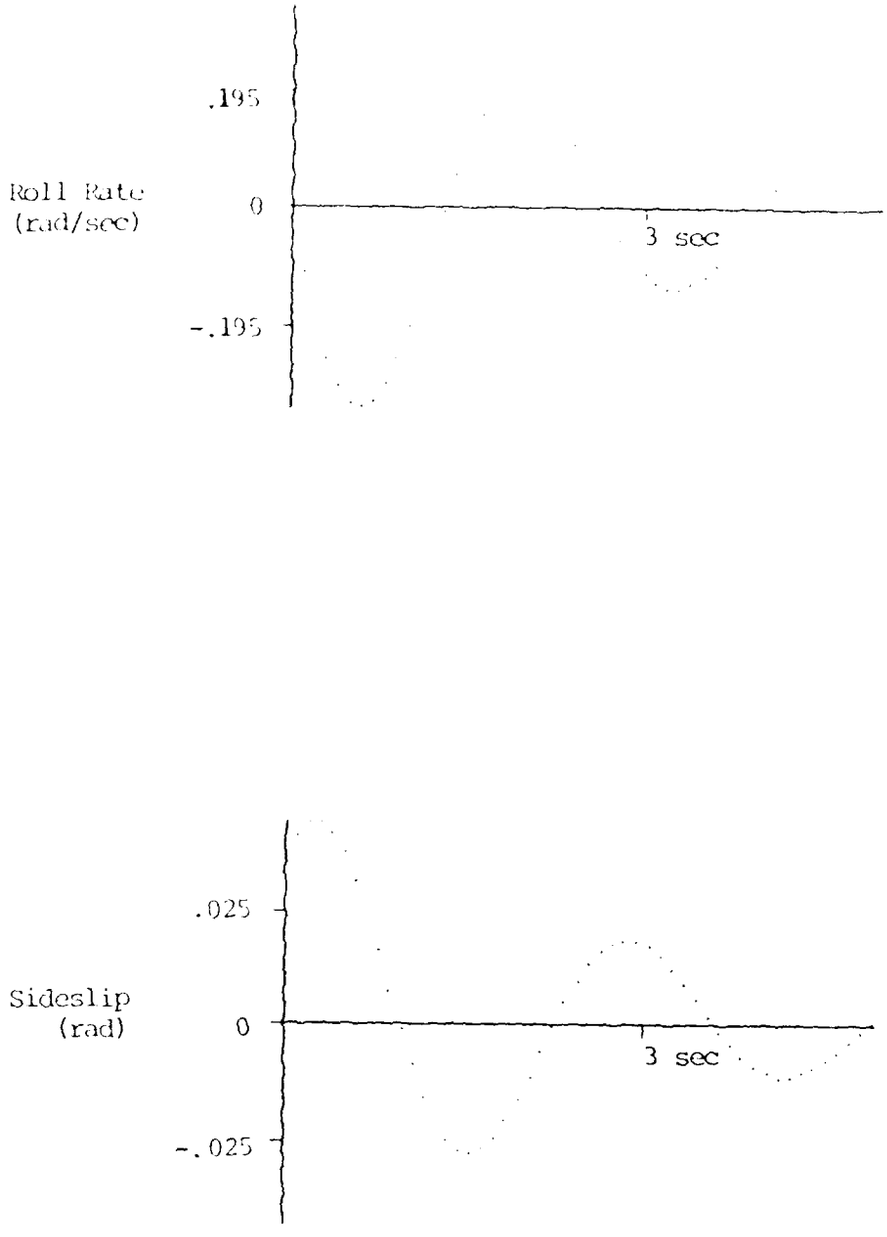

Figure G25. Simulated 1G Mechanical Time Response to Impulse (Dutch Roll Eigenvector for IC) (Part II)

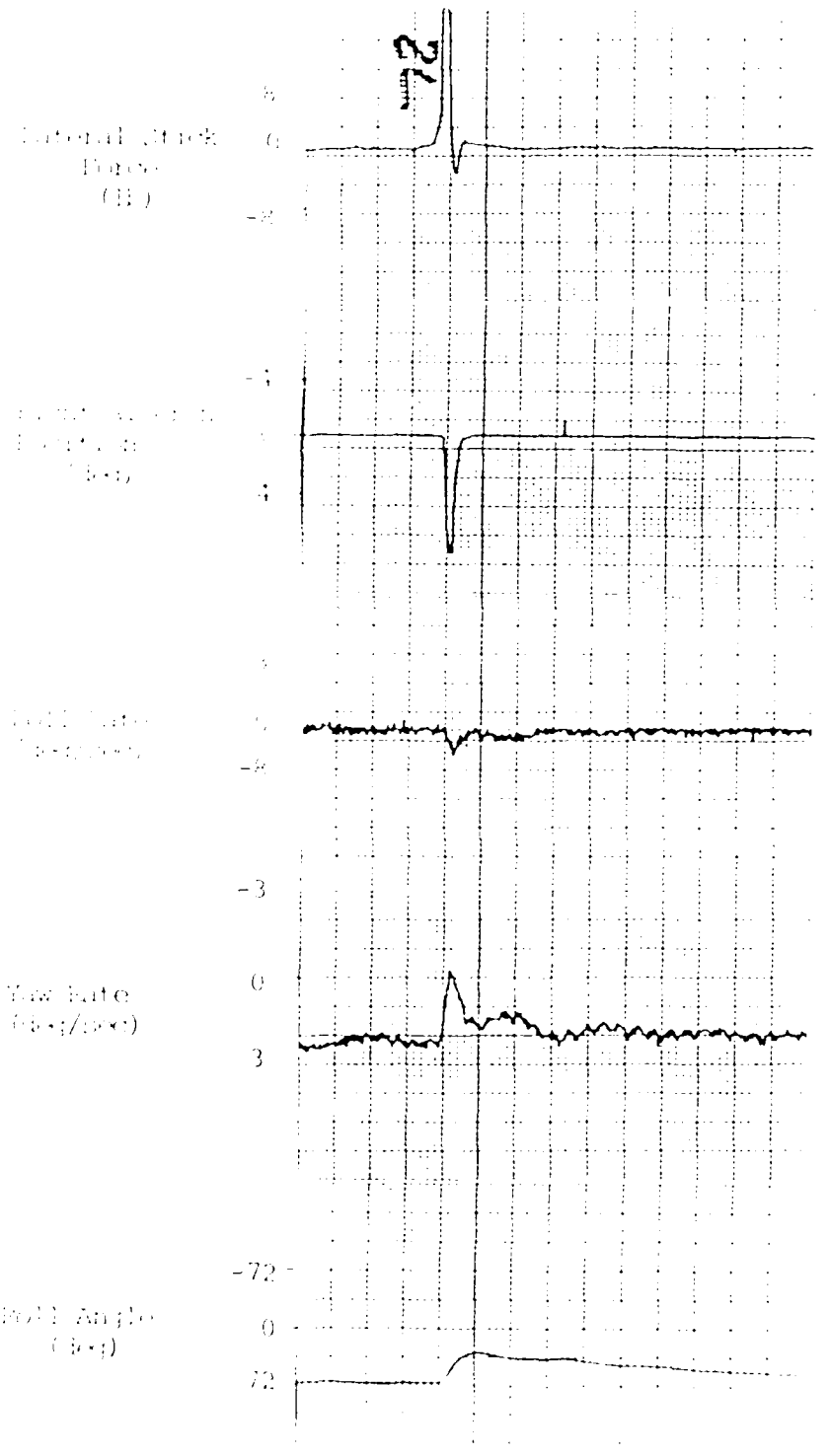

Figure 626. F/T Mechanical Time Response to Aileron Input

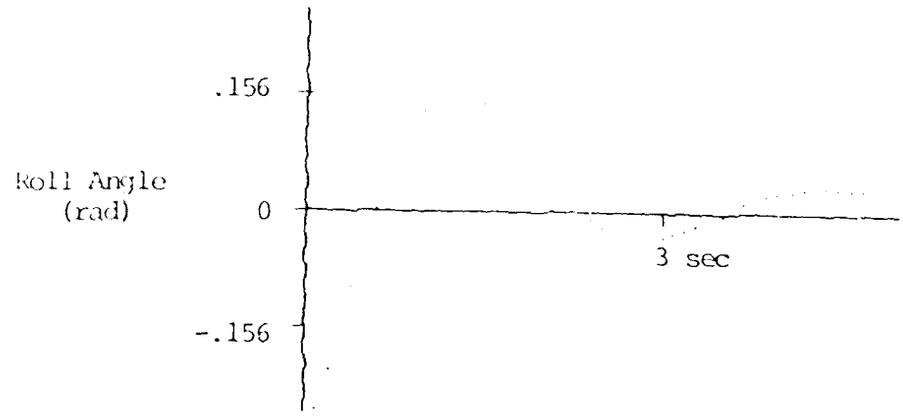

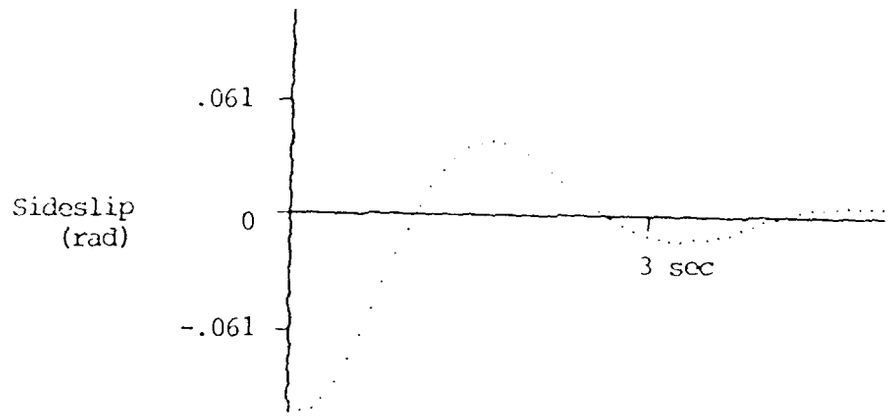

Figure G27. Simulated 1G Fully Augmented Time Response to Impulse (Dutch Roll Eigenvector for IC) (Part I)

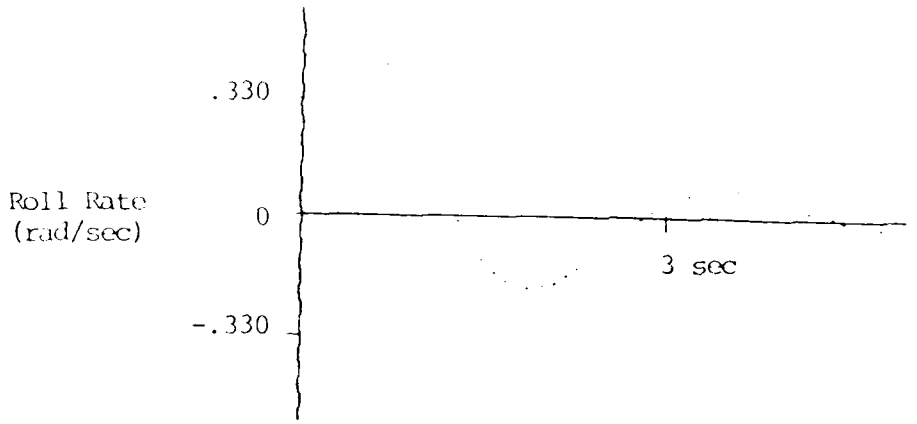

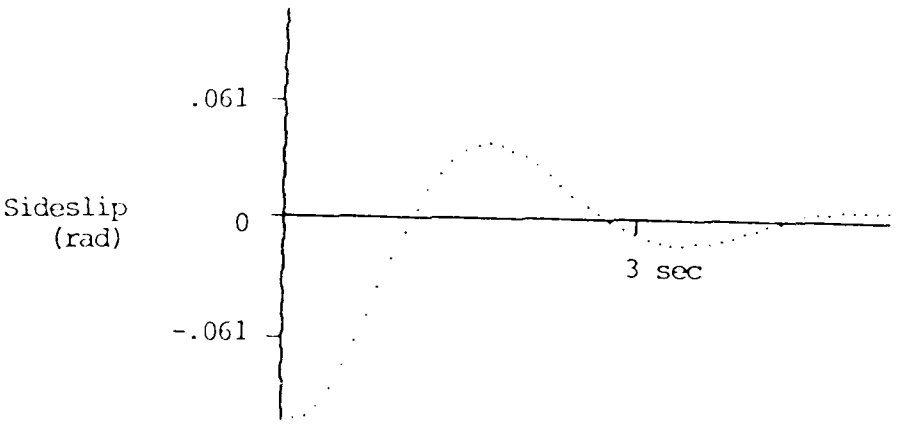

Figure G28. Simulated 1G Fully Augmented Time Response to Impulse (Dutch Roll Eigenvector for IC) (Part II)

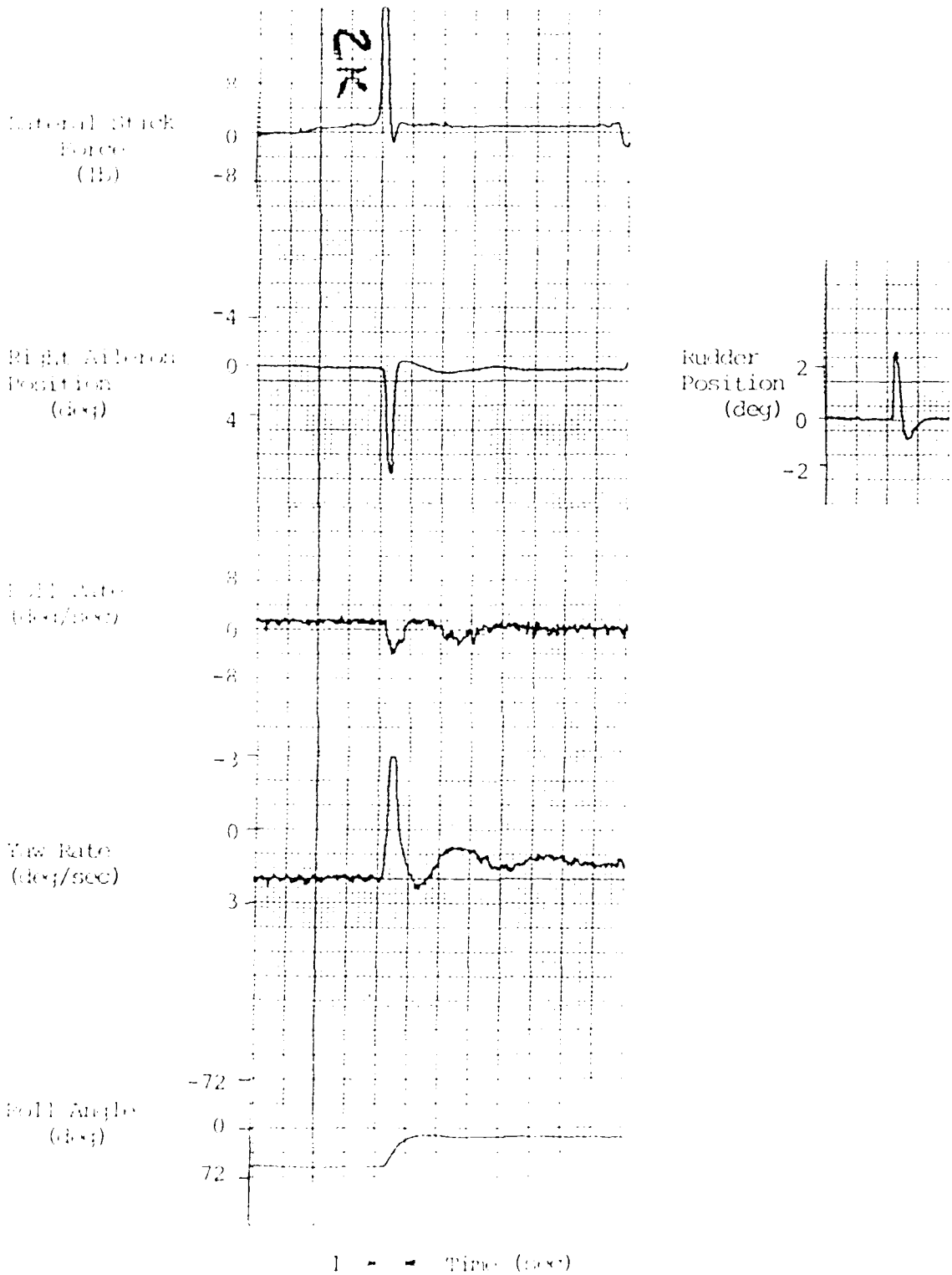

Figure 629. 1G Fully Augmented Time Response to Aileron Impulse

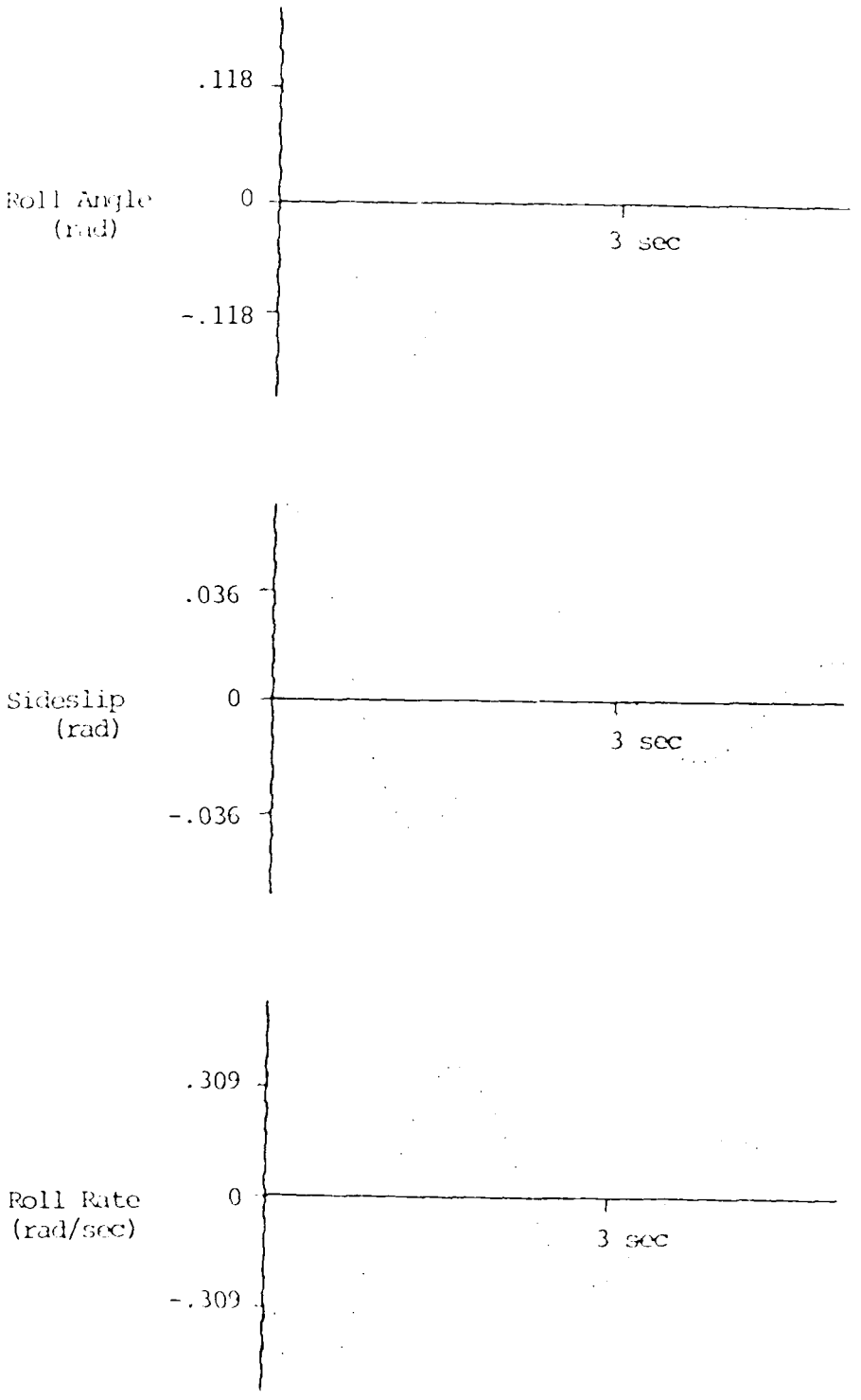

Figure G30. Simulated 3G Mechanical Time Response to Impulse (Dutch Roll Eigenvector for IC) (Part I)

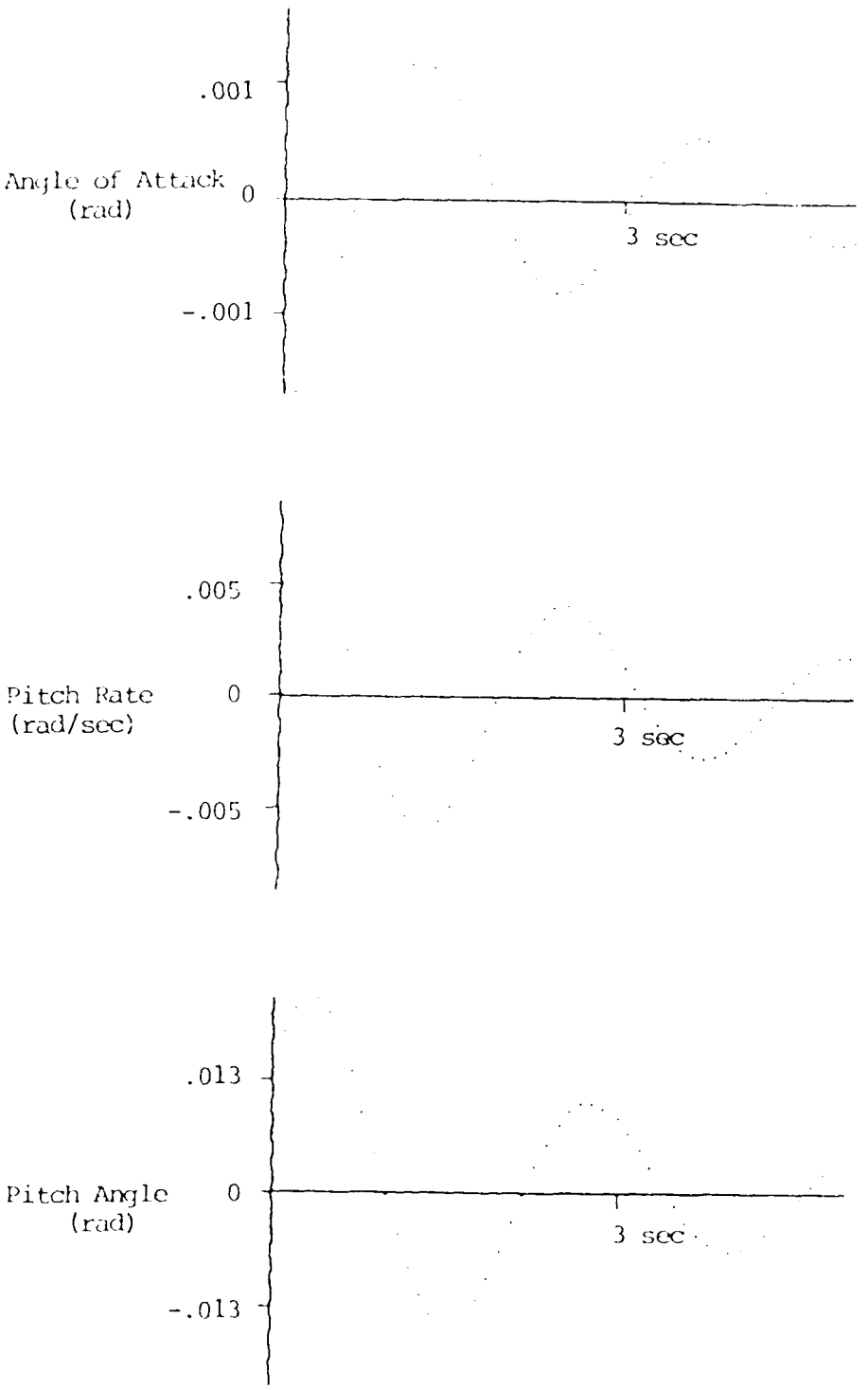

Figure G31. Simulated 3G Mechanical Time Response to Impulse (Dutch Roll Eigenvector for IC) (Part II)

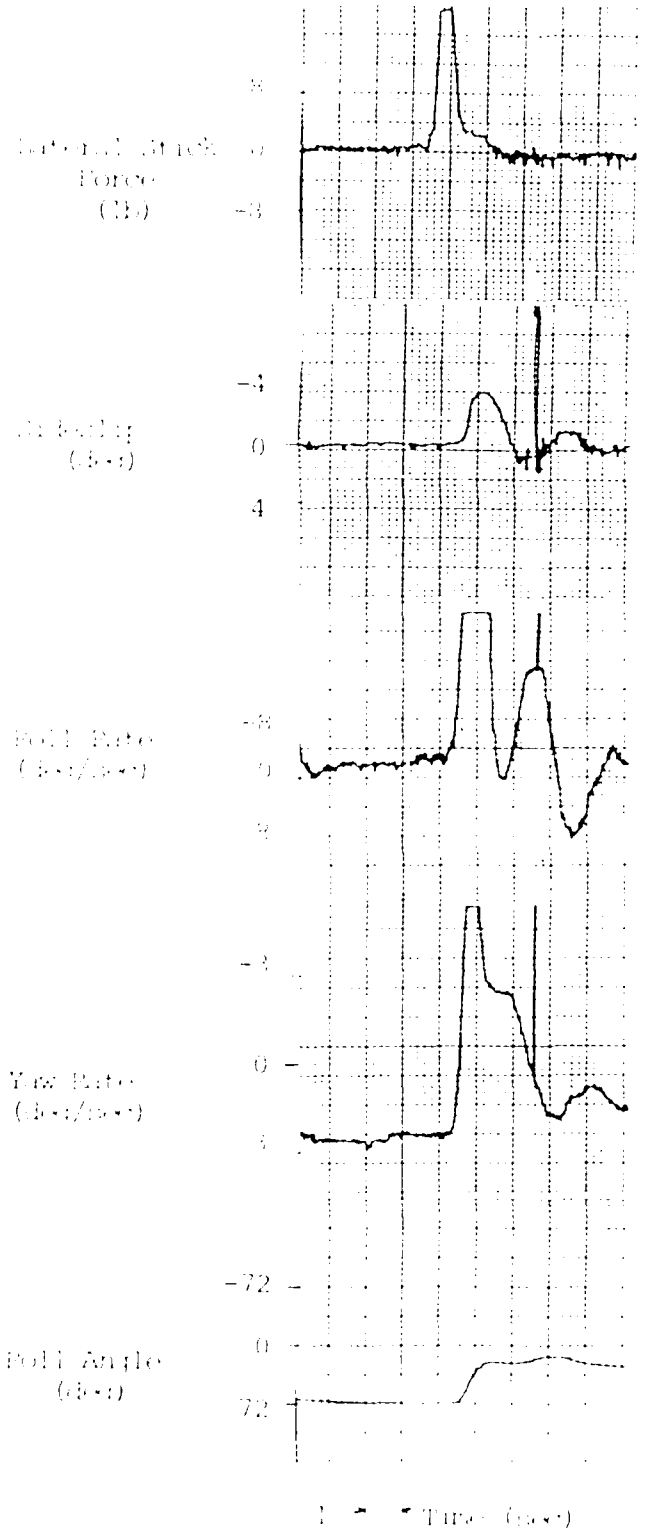

Figure 6.... Maneuver Time Histories for Aileron Input

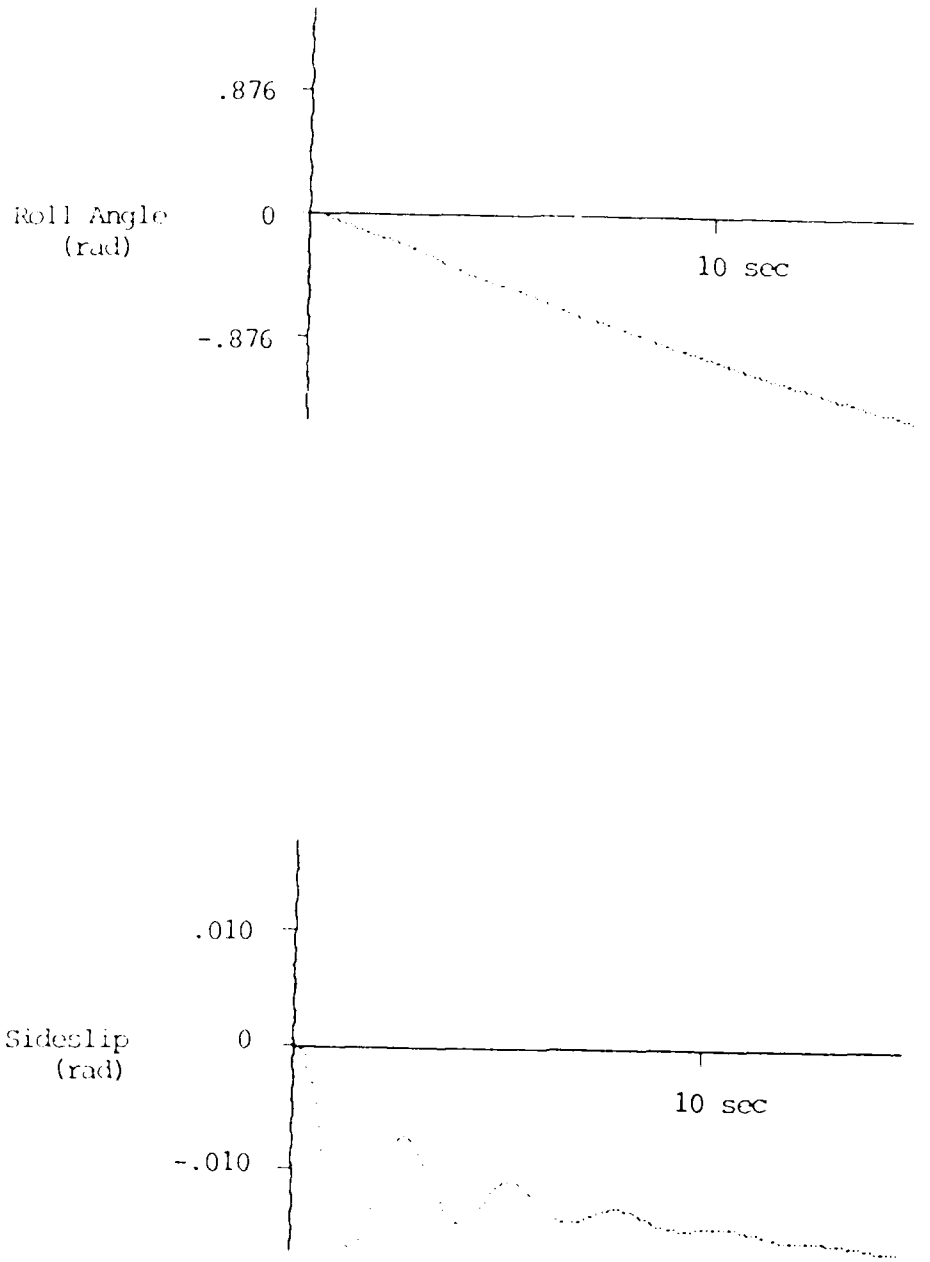

Figure G33. Simulated 1G Mechanical Time Response to 5 lb Aileron Step (Part I)

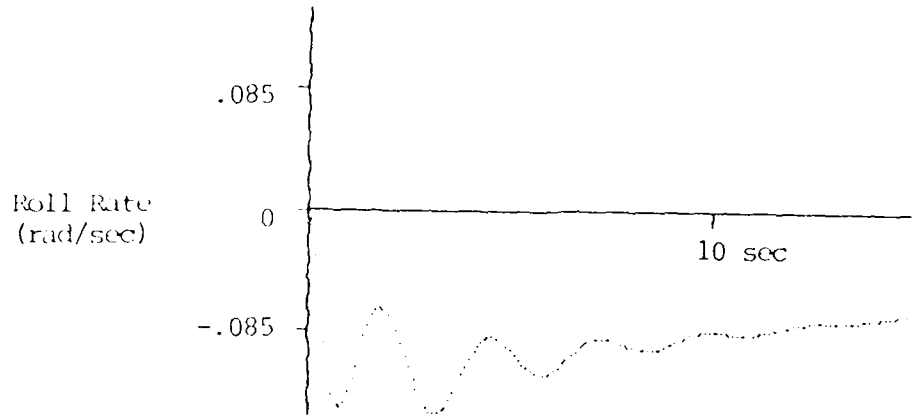

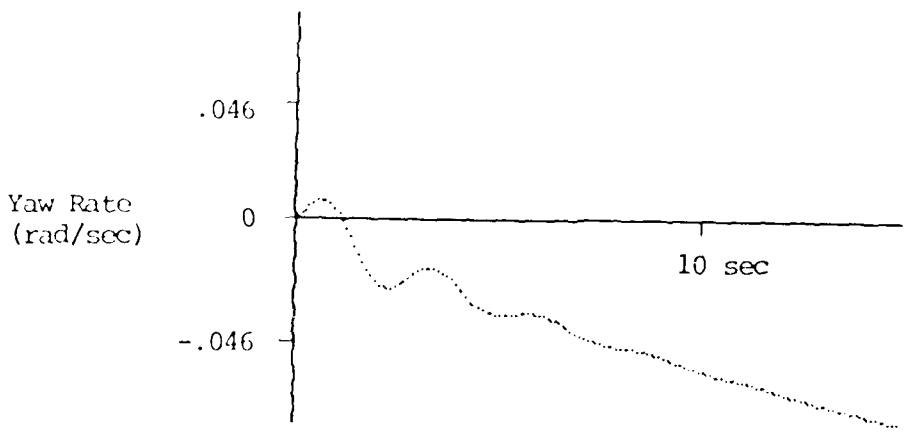

Figure G34. Simulated 1G Mechanical Time Response to 5 lb Aileron Step (Part II)

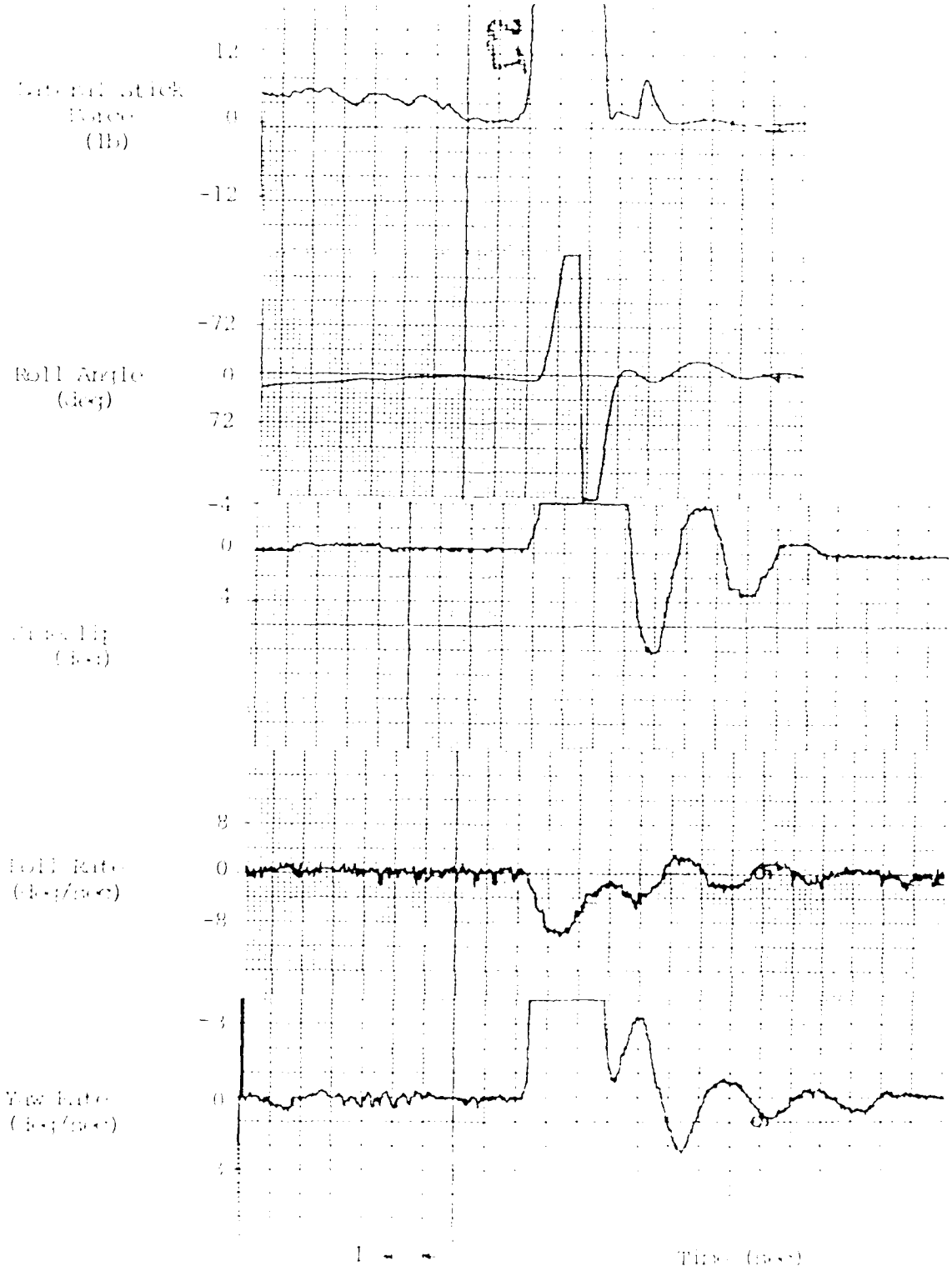

Figure C35. 16 Mechanical Time Responses to
Roll Aileron Step

Figure G36. Simulated 1G Fully Augmented Time Response to .2 In Aileron Step (Part 1)

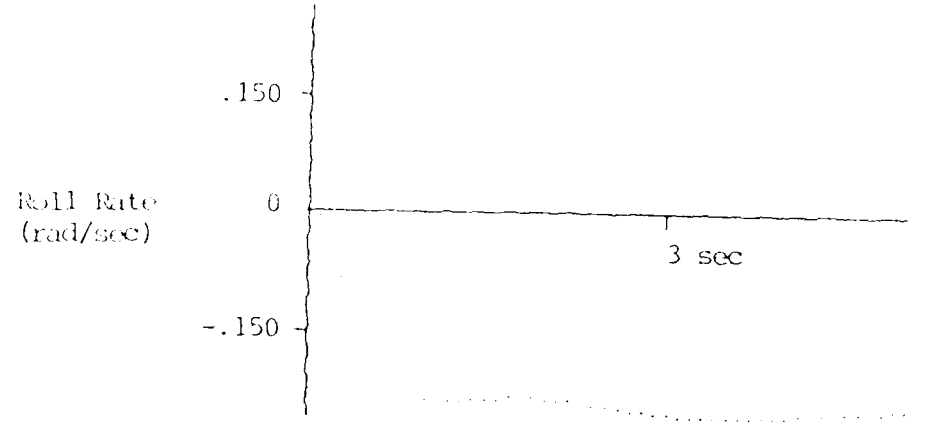

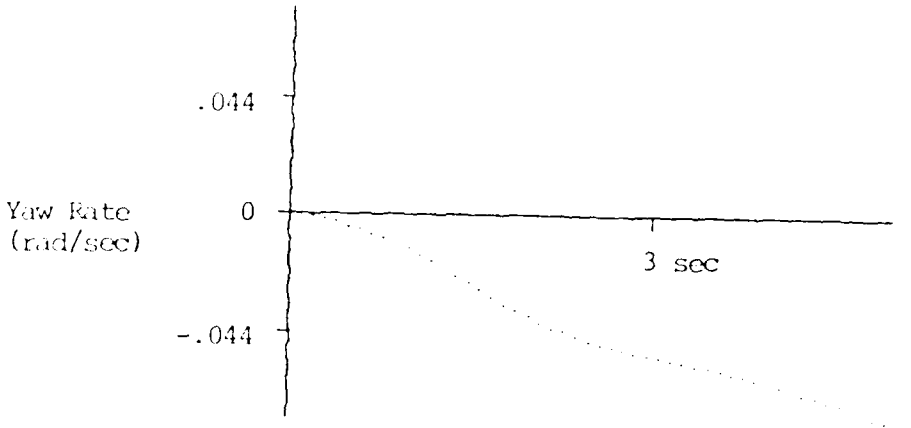

Figure G37. Simulated 1G Fully Augmented Time Response to 2 lb Aileron Step (Part II)

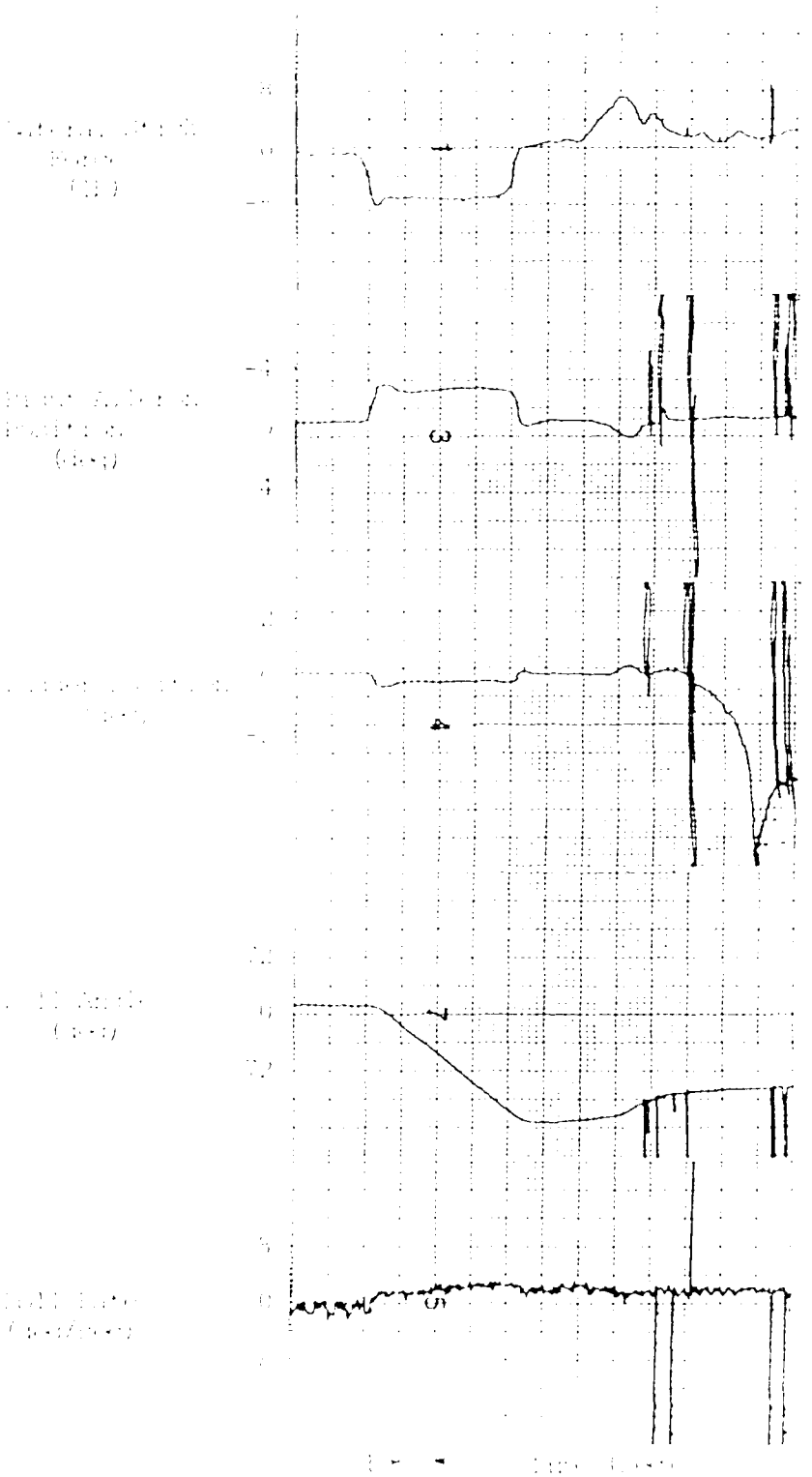

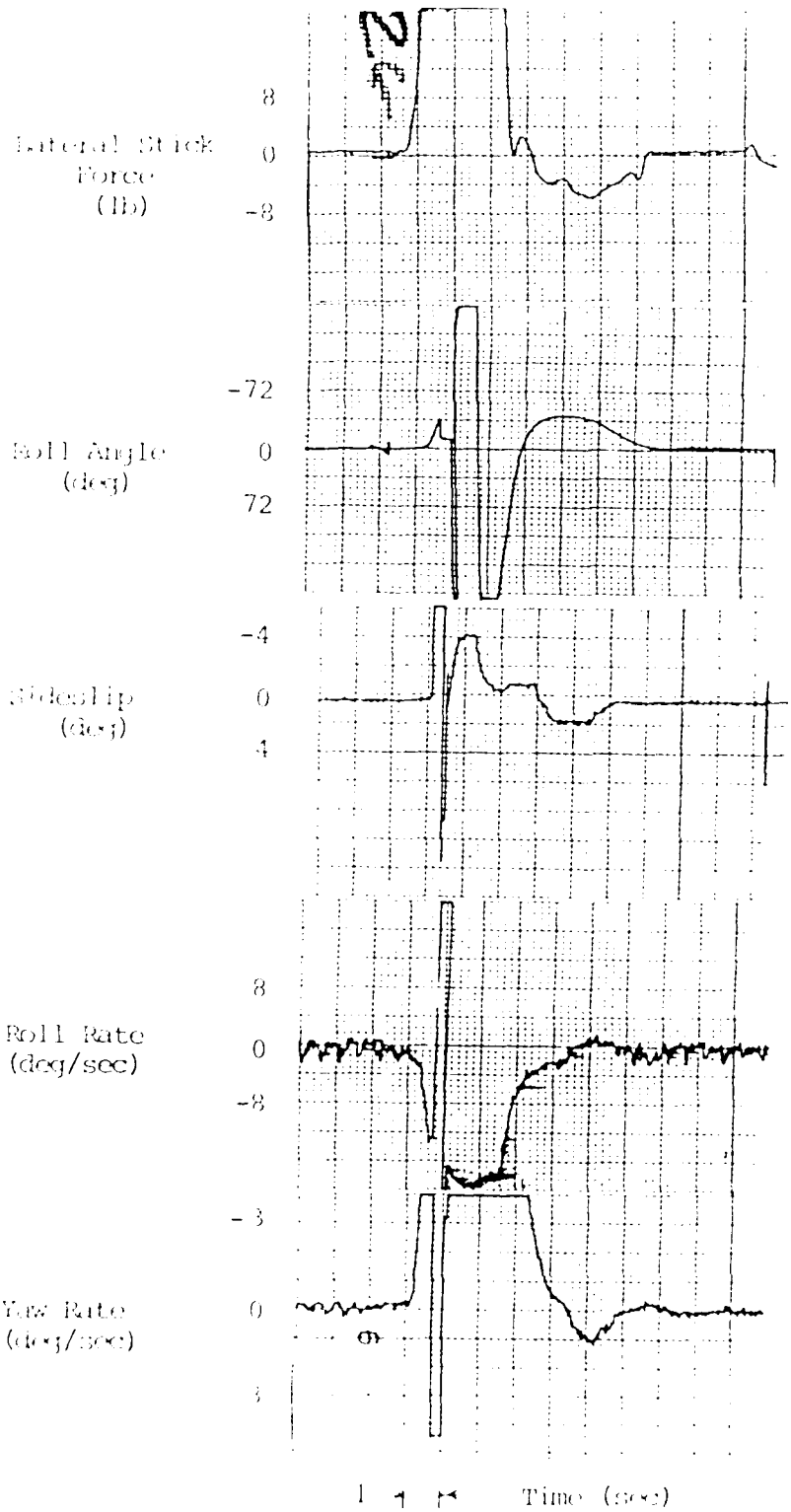

Figure G39. 1G Fully Augmented Time Response to Full Aileron Step

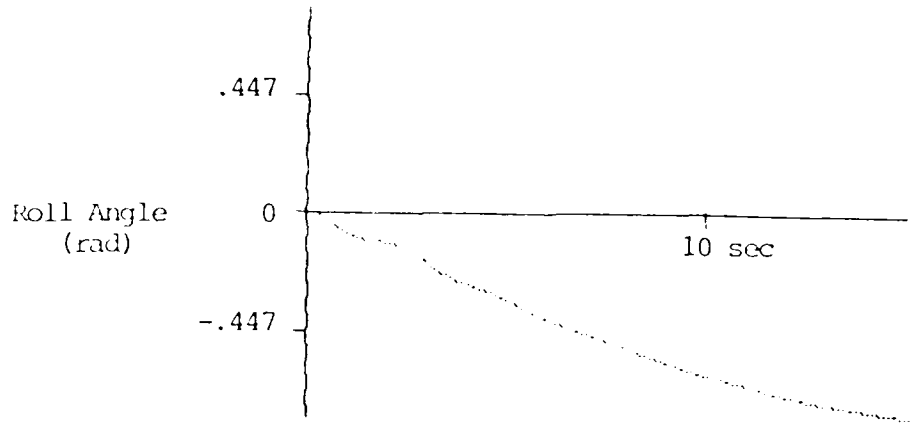

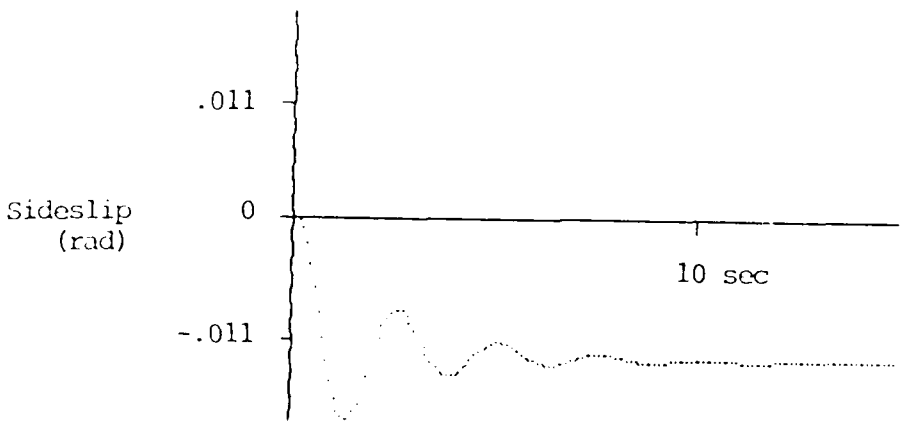

Figure G40. Simulated 2G Mechanical Time Response to 5 lb Aileron Step (Part I)

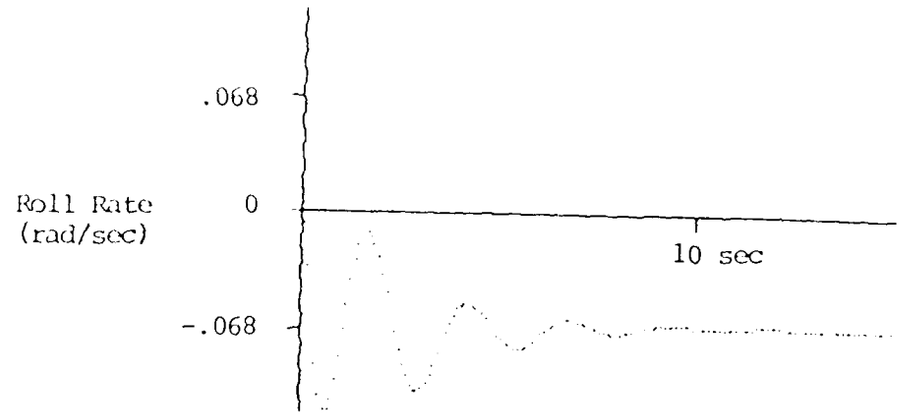

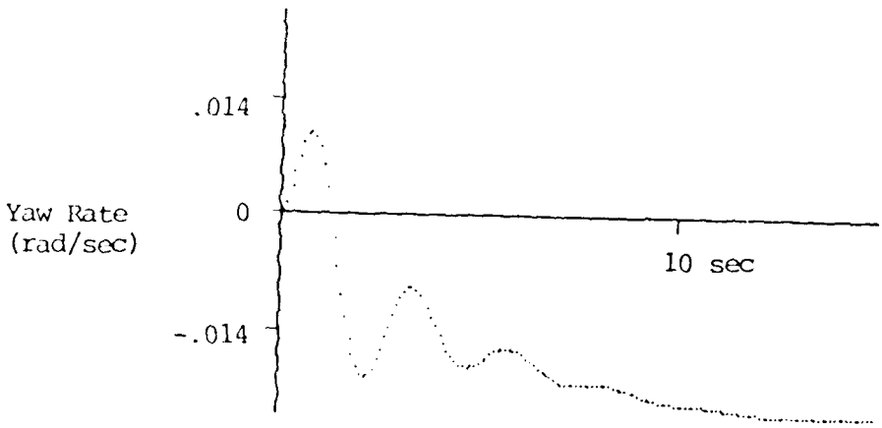

Figure G41. Simulated 2G Mechanical Time Response to 5 lb Aileron Step (Part II)

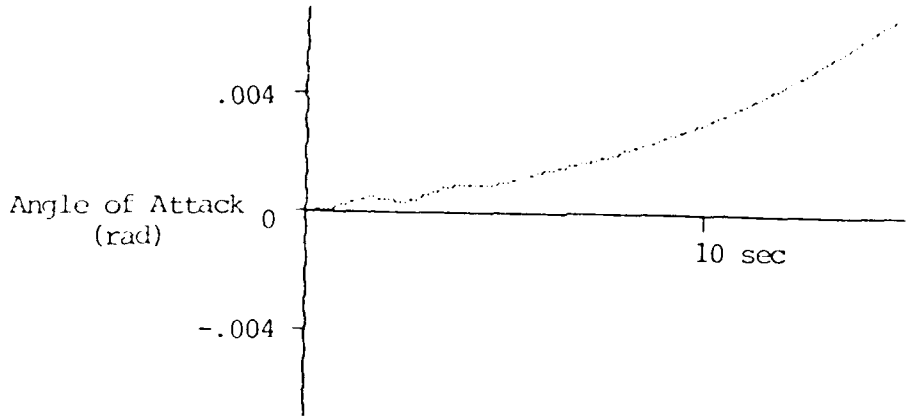

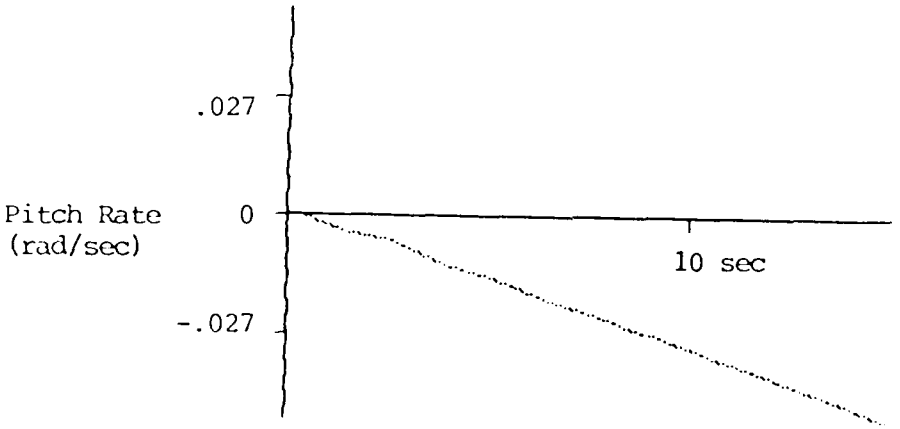

Figure G42. Simulated 2G Mechanical Time Response to 5 lb Aileron Step (Part III Cross Coupling)

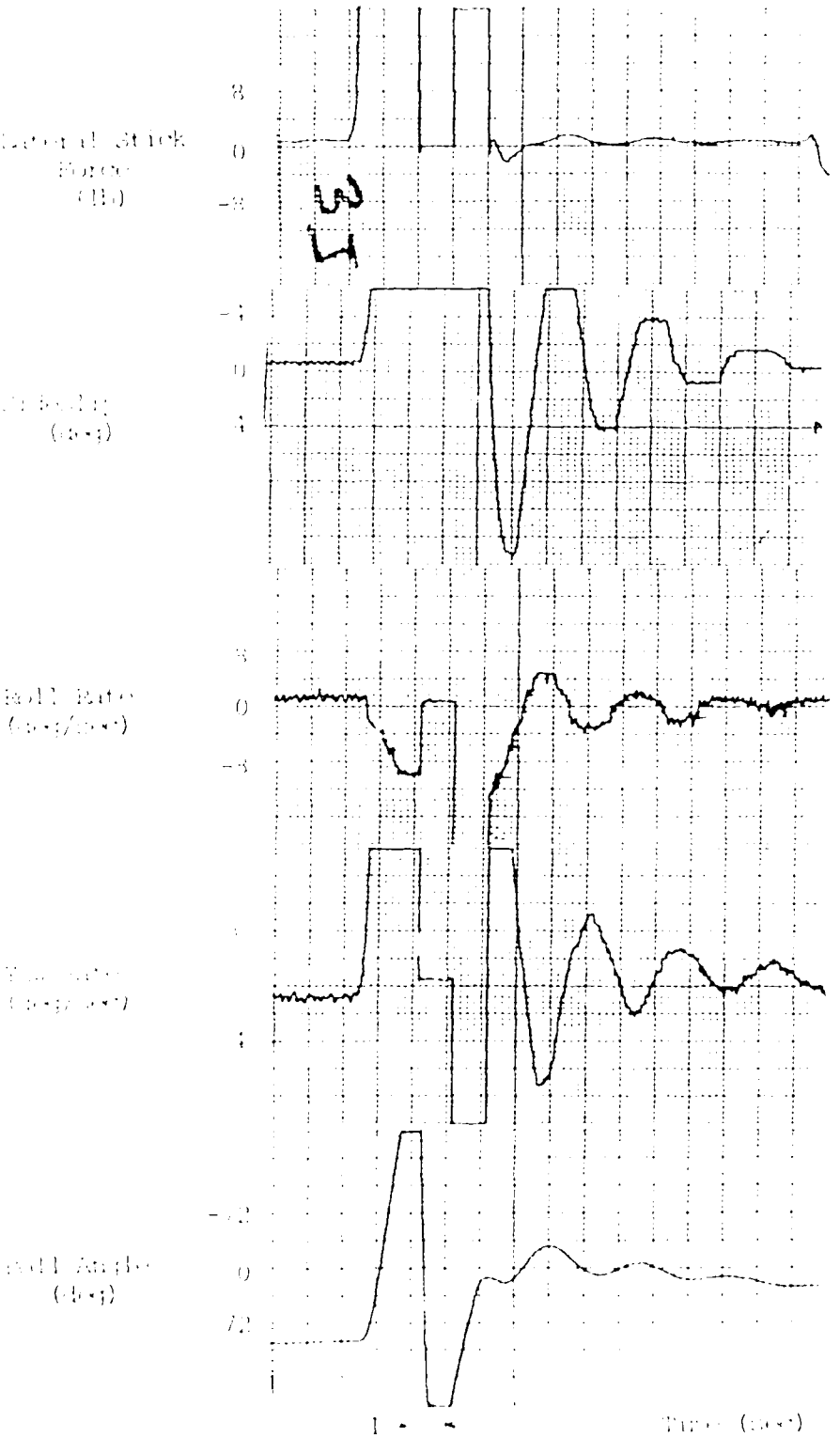

Figure G13. 2G Mechanical Fire Response to Full Aileron Step

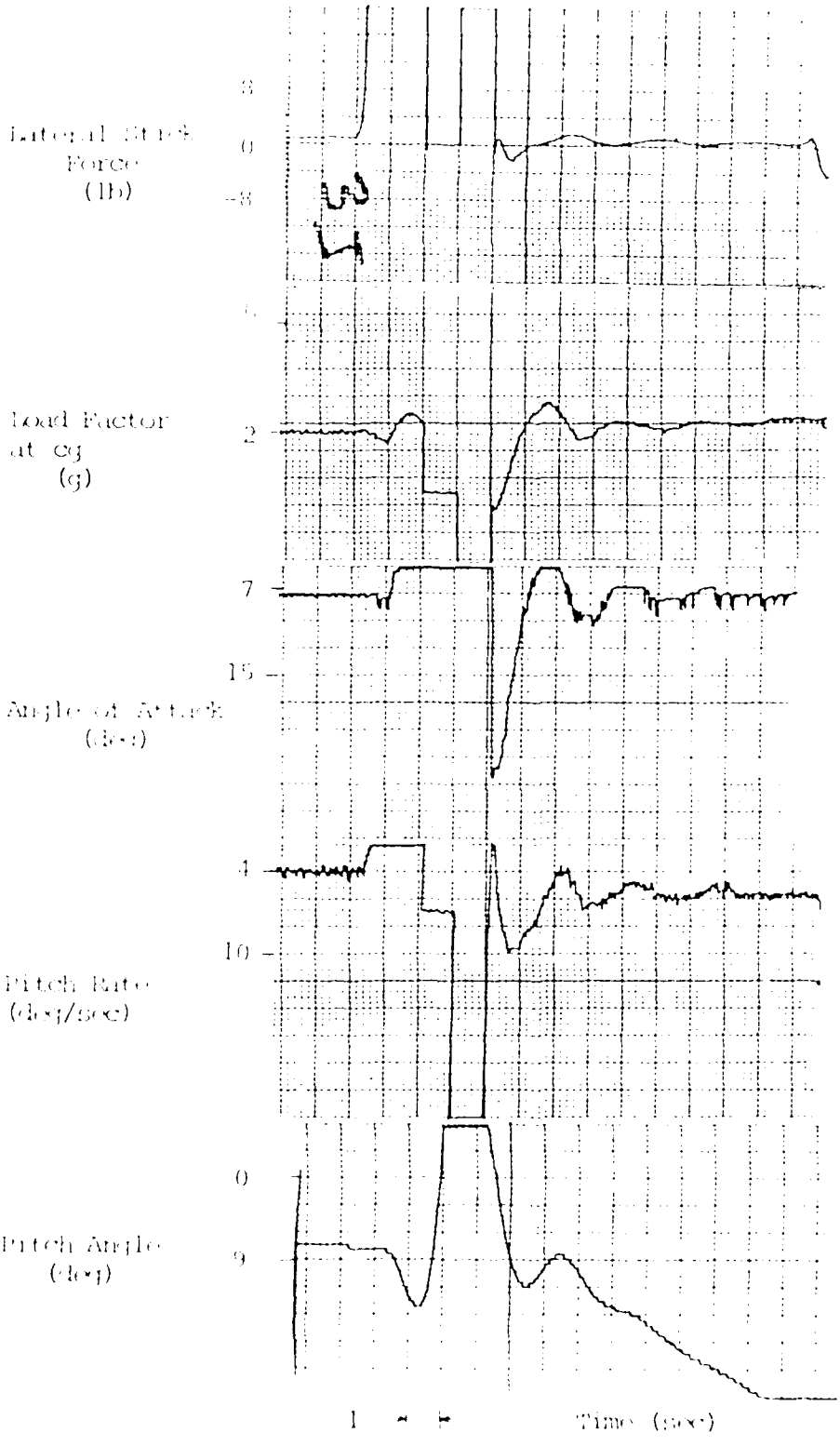

Figure 644. Mechanical Time Response to Full Aileron Step (Cross Coupling)

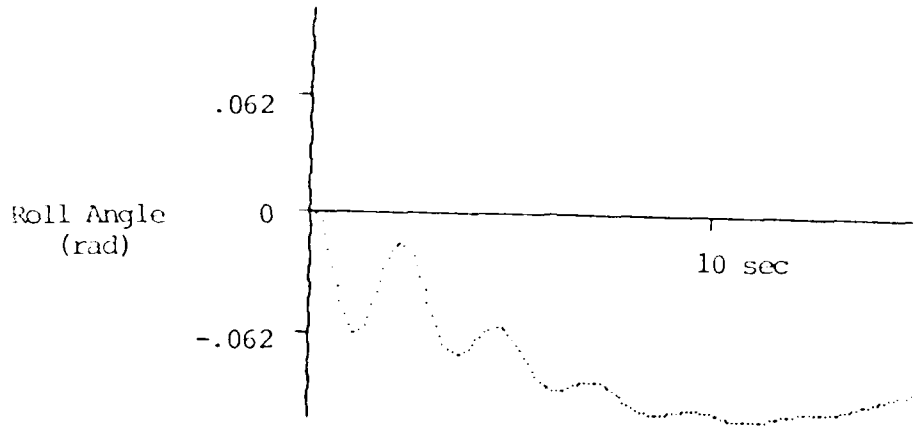

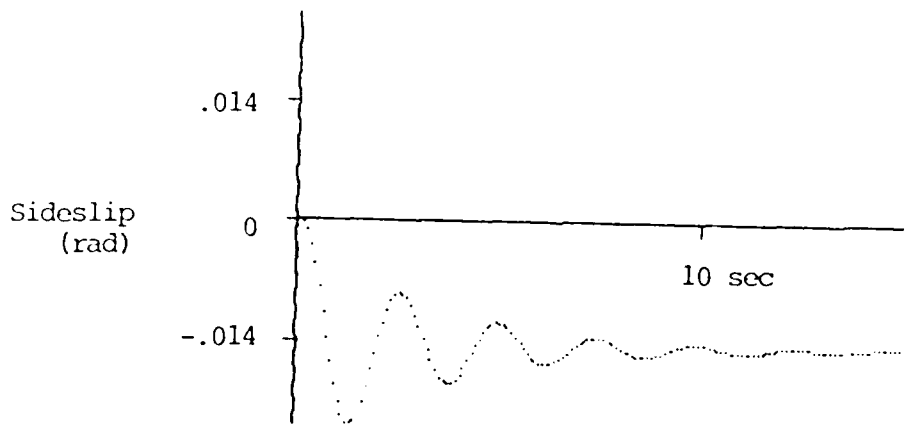

Figure G45. Simulated 3G Mechanical Time Response to 2lb Aileron Step (Part I)

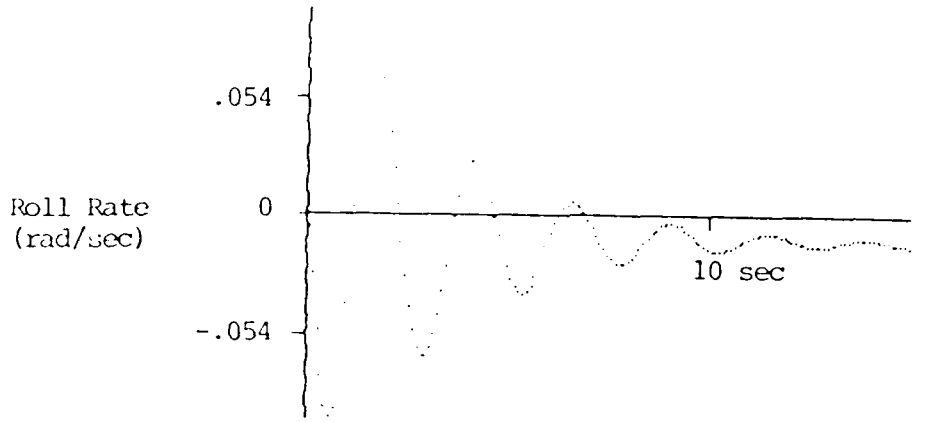

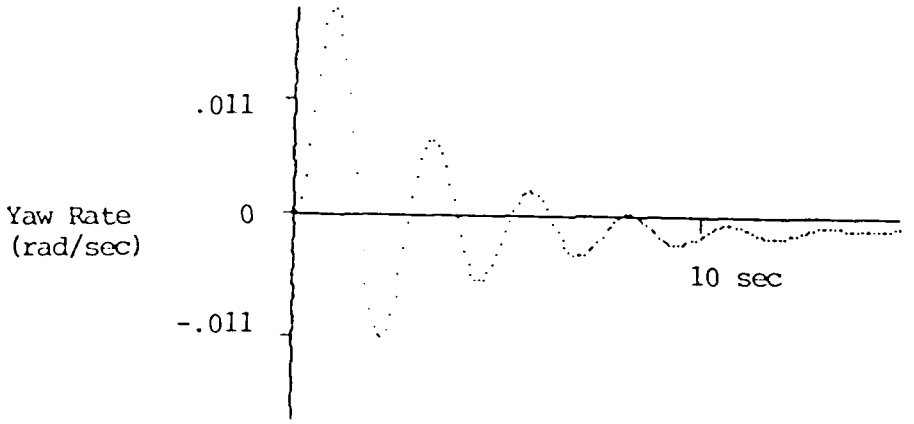

Figure G46. Simulated 3G Mechanical Time Response to 2lb Aileron Step (Part II)

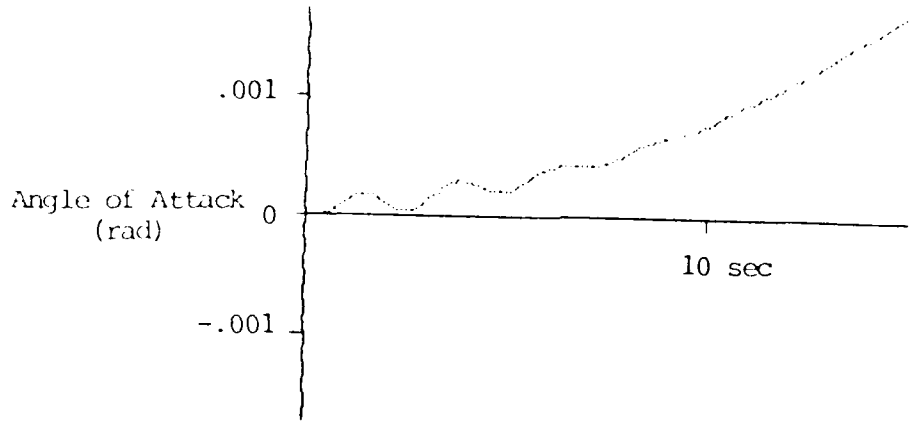

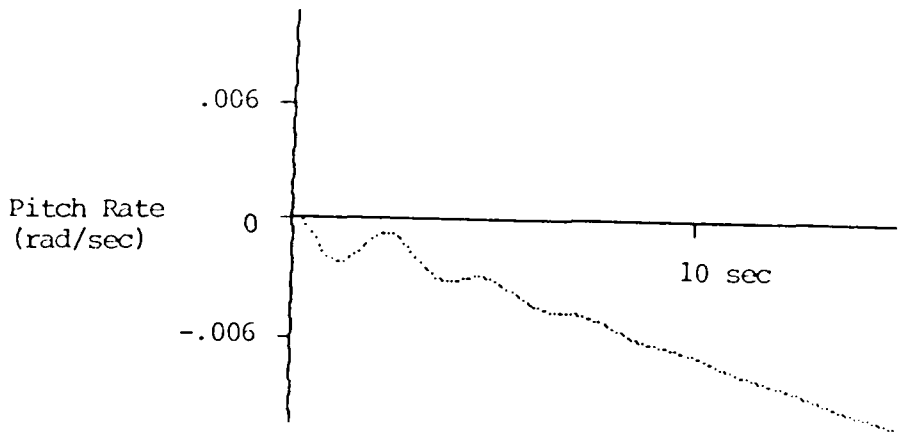

Figure G47. Simulated 3G Mechanical Time Response to 2 lb Aileron Step (Part III Cross Coupling)

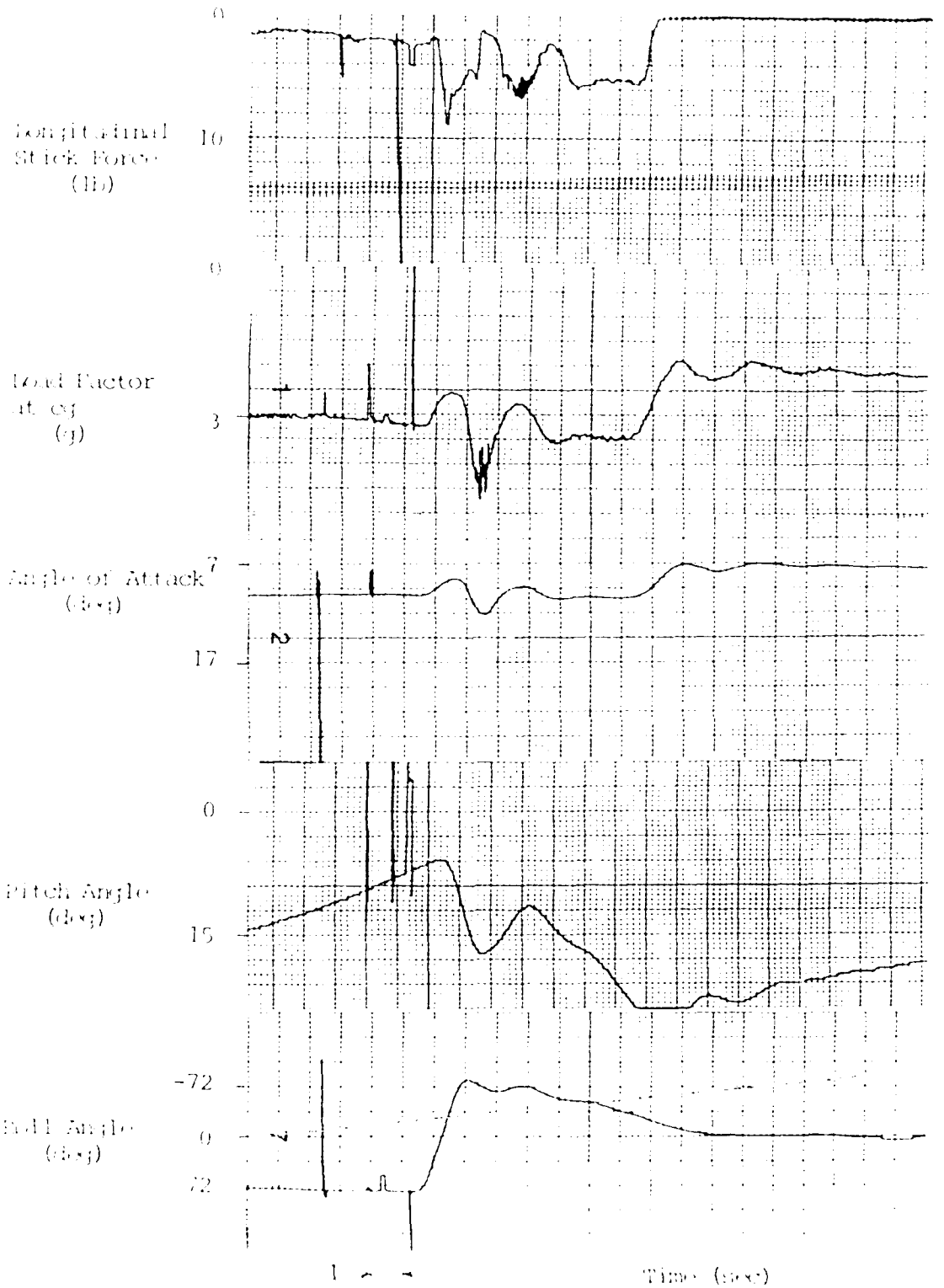

Figure G18. XG Mechanical Time Response to Full Aileron Step With Zero Att Stick

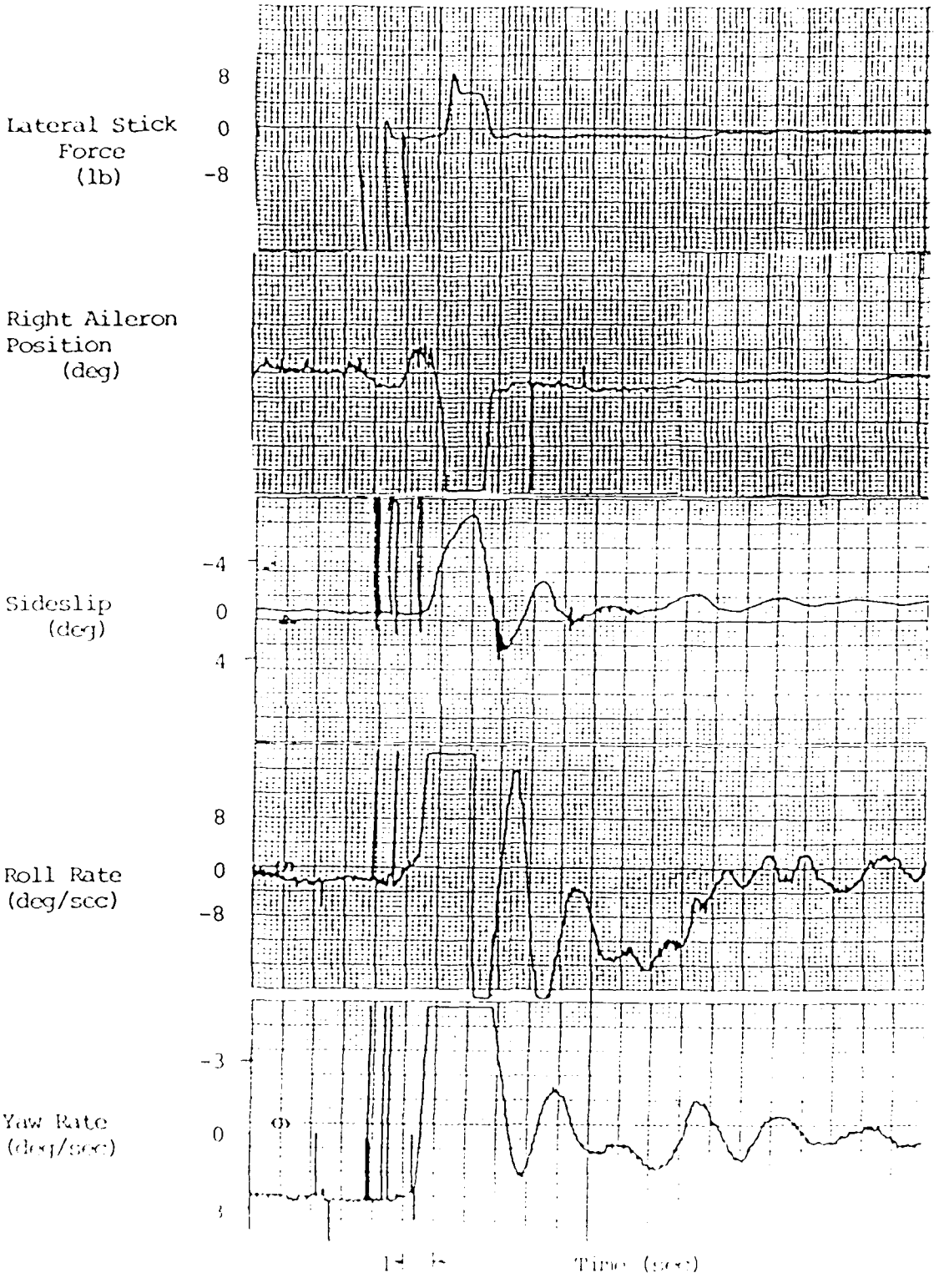

Figure C-10. Mechanical Time Response to ½ Aileron Step

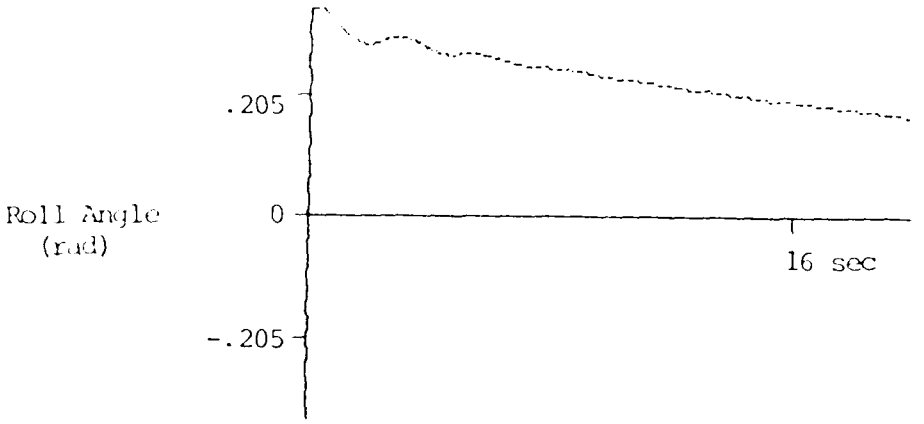

Mechanical Path

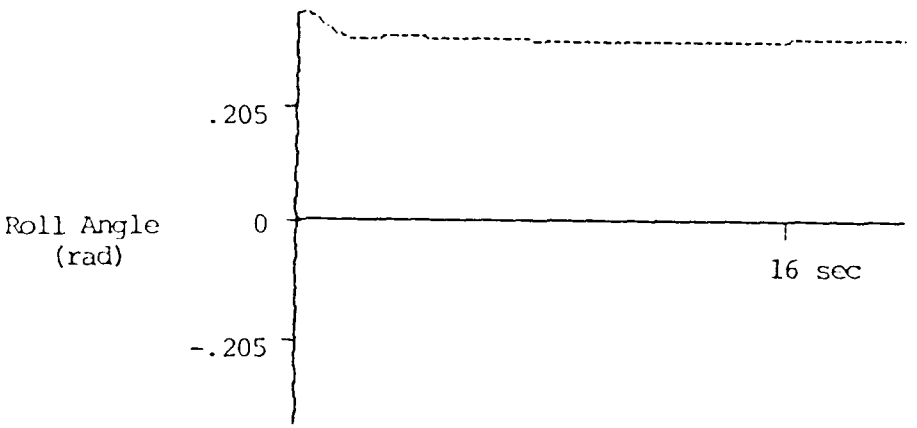

Fully Augmented Path

Figure G50. Simulated 1G Time Response to 20° (.349 rad) Roll Angle IC

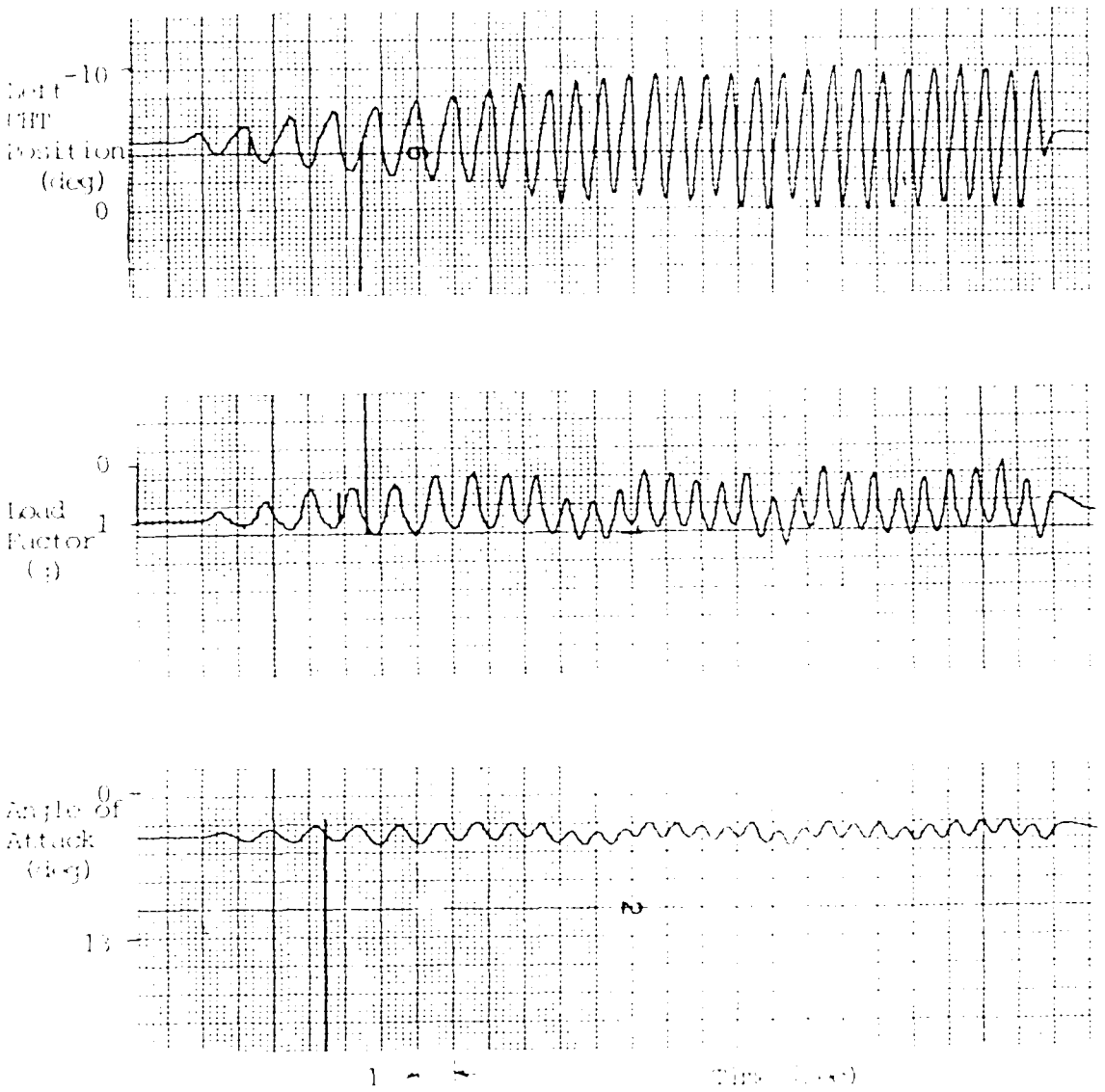

Figure 6.1. 1G Fully Augmented α Loop

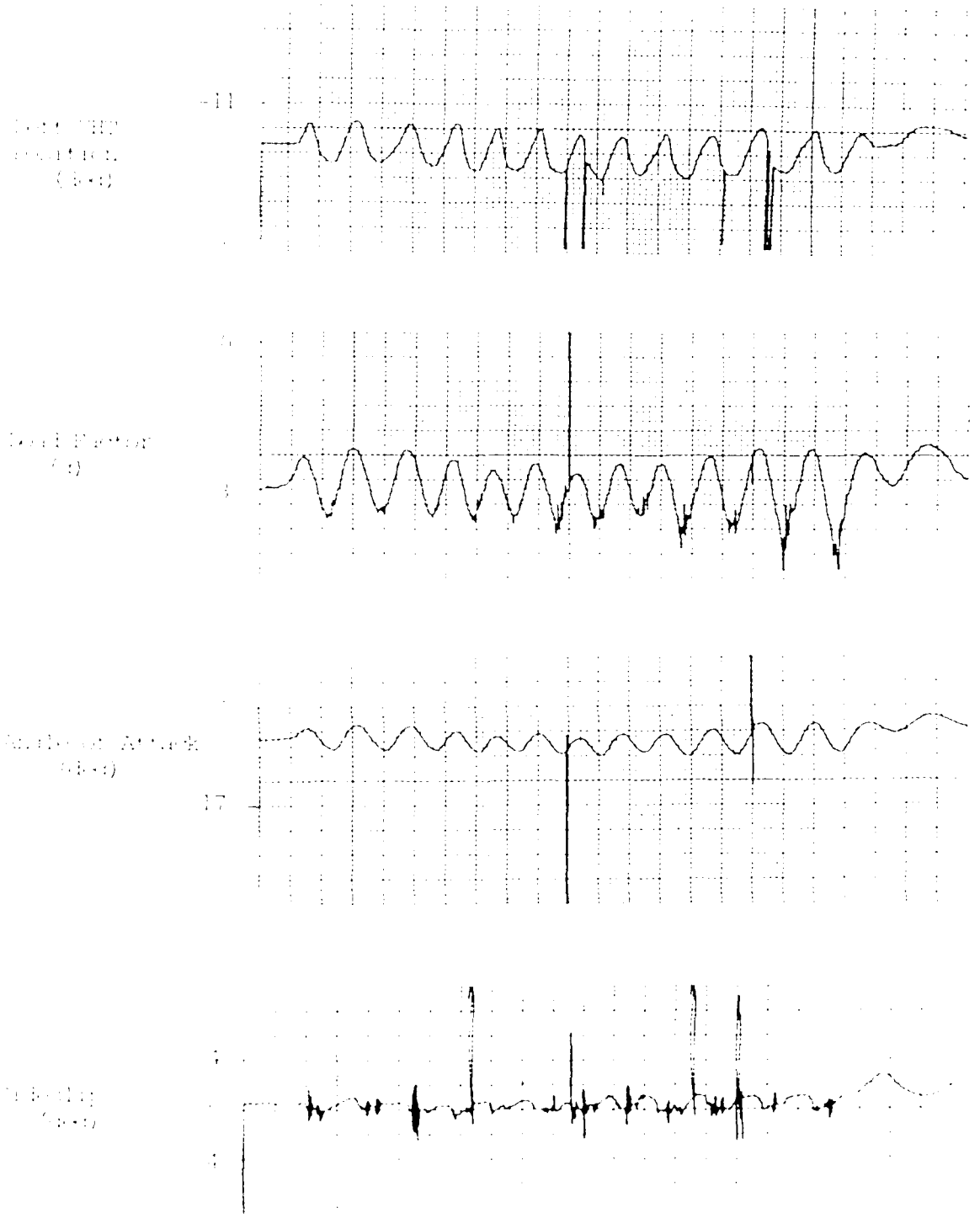

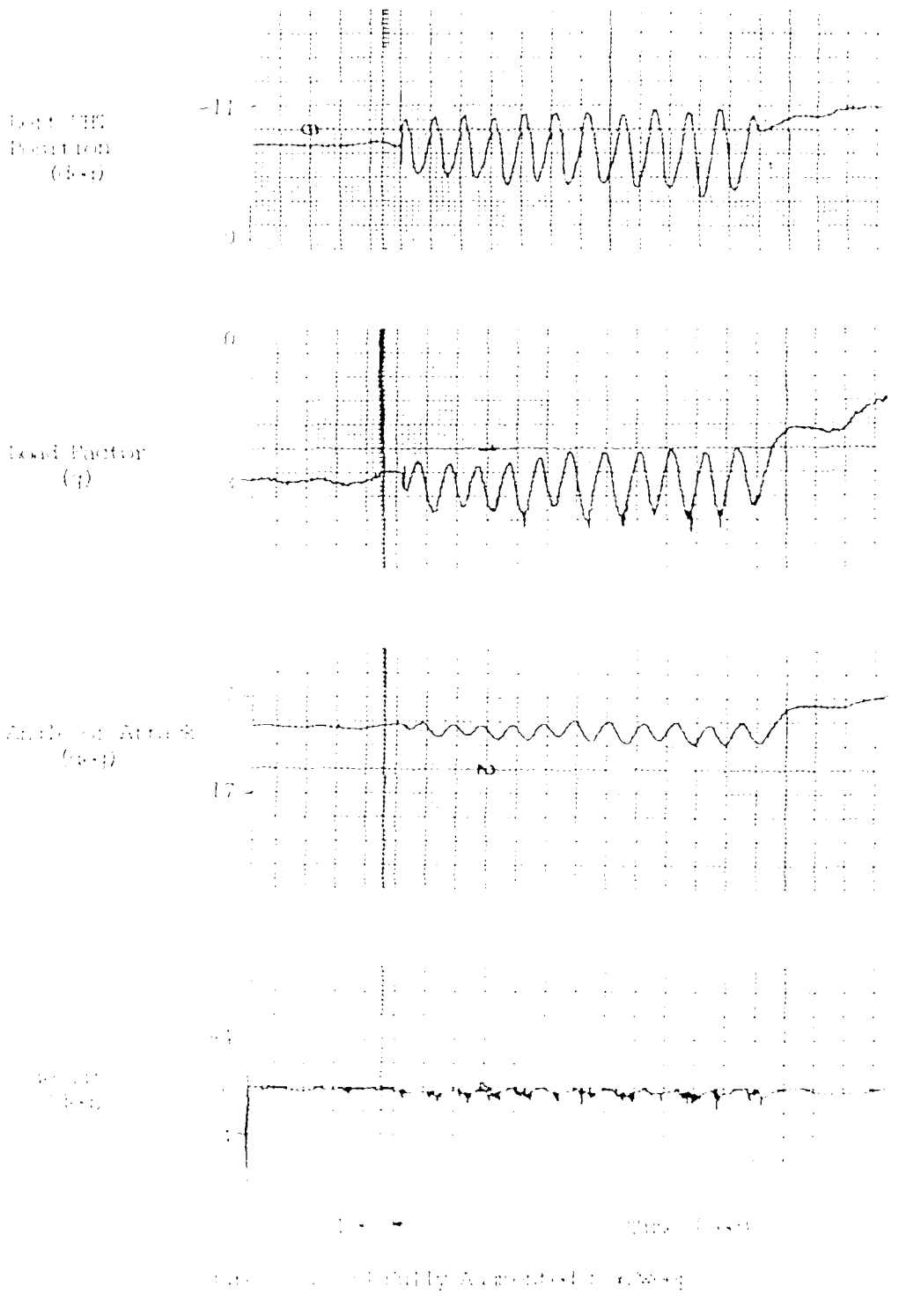

VITA

Captain Jeffrey R. Riemer was born 26 August 1951 in South Haven, Michigan. He graduated in 1969 from Leto Comprehensive High School in Tampa, Florida. He attended St. Petersburg Junior College for his associates degree and continued his undergraduate education at the University of Florida, which culminated in his receiving a Bachelor of Science Degree in Aerospace Engineering and a commission in the USAF through the ROTC program. He graduated from pilot training at Webb AFB, Big Spring, Texas in December 1975 where he received recognition as an Outstanding Graduate, and recipient of the Military Training Award, and ATC Commander's Trophy. Follow-on training in the F-4C at Luke AFB, Phoenix, Arizona lead to his first operational assignment as a F-4C Wild Weasel Pilot with the 67th Tactical Fighter Squadron, Kadena AB, Okinawa, Japan from February 1977 to August 1978. He followed this assignment as a T-37 Instructor Pilot at Columbus AFB, Columbus, Mississippi from September 1978 to May 1981. During this time he attended Squadron Officer's School in residence, and distinguished himself as a Top Graduate of the Pilot Instructor Training Course and Instructor Pilot of the Year 1980. His next assignment was as F-16 Acceptance Test Pilot with Air Force Plant Representative Office, General Dynamics in Fort Worth, Texas from April 1981 to May 1982, from which he was selected for the Joint Air Force Institute of Technology/ Test Pilot School program. The AFIT course work was completed in June 1983 with graduation from Test Pilot School as a Distinguished Graduate in June 1984.

END

FILMED

5-85

DTIC